

Spring 5-2000

Retention of Ionizable Compounds in HPLC

Rosario LoBrutto
Seton Hall University

Follow this and additional works at: <https://scholarship.shu.edu/dissertations>

 Part of the [Analytical Chemistry Commons](#)

Recommended Citation

LoBrutto, Rosario, "Retention of Ionizable Compounds in HPLC" (2000). *Seton Hall University Dissertations and Theses (ETDs)*. 1240.
<https://scholarship.shu.edu/dissertations/1240>

Retention of Ionizable Compounds in HPLC

By:

Rosario LoBrutto

Dissertation submitted to the Department of Chemistry of
Seton Hall University in partial fulfillment of the
requirements for the degree of

DOCTOR OF PHILOSOPHY

in

Chemistry

May, 2000

South Orange, New Jersey

Abstract

Retention of Ionizable Compounds in HPLC

The use of high performance liquid chromatography for the analysis of ionizable compounds has become of increasing importance over the last 2 decades. Initially, separations were carried out on native silica columns and later on chemically modified silicas. In this work, we investigate the effect of mobile phase modifiers on the retention of ionogenic species in the reversed phase mode. The effect of pH on the analyte ionization and its HPLC retention for basic and acidic compounds were investigated. It was shown that the pH of the aqueous/organic mobile phases was dependent upon the type and amount of organic eluent. This had led to an apparent shift in the analyte pK_a . The effects of type and concentration of counteranion of the acidic modifier on the retention of ionized basic analytes was studied. The retention of these solutes was shown to increase at increasing counteranion concentration. This was attributed to the decrease of the analyte solvation. A model based on the Langmuir approach is suggested to describe the effect of desolvation of the protonated basic analyte as a function of concentration.

It was shown that thermodynamically correct determination of the column void volume is needed for consistent theoretical description of observed effects. The void volume was measured by three different methods (pycnometry, minor disturbance and retention of isotopically labeled components). The effect of temperature on the column void volume was also studied.

Organic components of commonly used eluent systems of reversed phase HPLC exhibit specific interactions with hydrophobic stationary phases. This leads

to the accumulation (excess adsorption) of the organic solvent eluent components onto the reversed phase surface which was measured. The interpretation of these measurements allow the estimation of the degree of possible penetration of organic molecules into the bonded layer. The adsorbent geometry (surface area, pore volume) and column geometry (void volume, exclusion volume) are essential for correct measurement and interpretation of the excess adsorption isotherms. The effect of chain length and type of organic solvent on the void volume and exclusion volume was studied. Also, determination of the adsorbent geometry of various silicas was performed with LTNA and a novel discontinuous Headspace method.

We certify that we have read this thesis and that, in our opinion, it is adequate in scope and quality as a dissertation for the degree of Doctor of Philosophy.

APPROVED



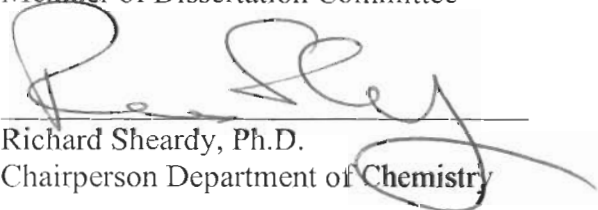
Yuri V. Kazakevich, Ph.D.
Research Mentor



Nicholas H. Snow, Ph.D.
Member of Dissertation Committee



Stephen Kelty, Ph.D.
Member of Dissertation Committee



Richard Sheardy, Ph.D.
Chairperson Department of Chemistry

Acknowledgements

During my graduate school career, I have had the opportunity to **develop myself** as a research scientist. This would not have been possible without the support of my employer Merck, for giving me the time I needed to obtain my degree. I would also like to give special thanks to my advisor Dr. Kazakevich for his encouragement, his expertise of mostly everything, and most of all his friendship.

I would also like to acknowledge the Snow and Kazakevich research group at Seton Hall University and several faculty members who helped me throughout the doctoral process. The faculty members to whom I would like to give special appreciation for all their help during my Ph.D. residency include: Dr. Snow, Dr. Kelty, Dr. Sowa, Dr. Murphy and Dr. Maloy. The research group members I would especially like to thank for all their help with the experimental work and for being great friends are Fred Chan and Alan Jones. I would also like to thank Keith Flood for all his helpful suggestions and for the extra time and effort he has given me.

The Merck colleagues I would like to especially thank include Tao Wang and Richard Egan for all their encouragement throughout the Ph.D. process. I would also like to acknowledge the support of my colleagues: Nelu Grinberg, Lili Zhou and Neil McGachy. I would also like to express my gratitude to Merck & Co., Inc. once again for allowing me this chance of a lifetime to pursue my life long goal of becoming a Ph.D. scientist.

On the non-academic side I would like to express my thanks to all my family members, my fiancée's family and my friends. I would like to give special thanks to my sister, Calogera, for all her help and always being there for me. I also would like to thank

my parents for all their support and encouragement over the last 20 years of education. Most of all I would like to thank my fiancée, Ginny, for all her patience and understanding while I was obtaining my Ph.D. Her comfort, support and encouragement will never be forgotten.

Table of Contents

	Page
Abstract	ii
Acknowledgments:	v
Table of Contents:	vii
List of Figures	xvi
List of Tables:	xxvi
Thesis Structure	1
Chapter 1. History and Current State of the Art	
Overview	4
Ion-Exchange Chromatography	5
Salt or Buffer Type	6
Column Type	7
Normal Phase Chromatography	7
Analyte Ionization	11
Applications	15
Ionization and HPLC Retention in Reversed Phase HPLC	23
Effects in Region A	26
Effects in Region B	27
Effects in Region C	27
Modes of Reversed Phase	28
Ion Suppression	28
Ion-Interaction	29
Ion-Interaction Models for the Process of Retention	29
Ion Pair Formation in the Mobile Phase	29

Dynamic Ion Exchange	31
Dynamic Complex Exchange	33
pH and Ion Interaction	35
Ion-Interaction Reagent Concentration	36
Effect of Salt, Buffer Concentration and Ionic Strength	42
Applications of Ion-Interaction Chromatography	42
Effect of Organic in Reversed Phase and Ion-Interaction Chromatography	46
Summary	52
Chapter 2. Effect of Organic Solvent on the pK_a of Ionogenic Solutes	
Summary	58
Historical	58
Change in Dielectric Constant	67
Effect of Analyte Structure on pK _a	77
Methods Used to Determine Ionization Constants	81
Determination of pH Values in Aqueous/Organic Mixtures	82
Method 1	83
Method 2	84
Determination of the pK _a Using HPLC	93
Acid Error	95
Experimental	98
Instrumentation	98
Chemicals	98
Chromatographic Conditions	99
Results and Discussion	100

Influence of Type of Acidic Modifiers on Ionogenic Analyte pK_a Shift	100
Eluent Composition Influence on the pK_a	100
Effect of Analyte Structure and Type of Organic Solvent	113
Reproducibility	115
Effect of Changing Concentration of Organic and type of Buffer System	118
Basic Analytes	118
Acidic Analytes	129
Conclusion	129
Chapter 3. Effect of the Eluent pH, Type and Concentration of Acidic Modifiers on the HPLC Retention of Basic Analytes	134
Summary	134
Introduction	135
Historical	135
Hydrophobicity of the Counteranion	135
Concentration of the Counteranion of the Acidic Modifier	137
Analyte Structure	137
Analyte Solvation and Secondary Interactions	138
Comparison of Retention Models	138
Ion-Pair Formation Versus Ion Association	140
Experimental	146
Apparatus	146
Chemicals	147
Chromatographic Conditions	147

Results and Discussion	148
Comparison of the effect of acidic modifiers on retention using 10 mM sodium hydrogen phosphate buffer	148
Phosphoric Acid	148
Trifluoroacetic Acid and Perchloric Acid	150
Comparison of Modifiers	156
Chaotropic Effect	159
Comparison of Trifluoroacetic Acid, Phosphoric and Perchloric Acid Without Addition of Buffer	168
pH versus Concentration Effects	173
Comparison of Using Different Starting Phosphate Buffer Concentrations	183
Effect on Acidic, Neutral, and Zwitterionic Components	191
Advantages of Using Chaotropic Agents	194
Peak Shape	194
Resolution	194
Selectivity	195
Specific Applications (Beta Blockers)	200
Conclusion	205
Chapter 4. Development of Model for Analyte Desolvation/ Solvation Process	211
Summary	211
Introduction	212
Experimental	216
Apparatus	216
Chemicals	217
Chromatographic Conditions	217

Results and Discussion	218
Analyte Desolvation/Solvation Model	218
Influence of Type of Counteranion on Solvation Parameter	223
Effect of Type of Eluent on the Solvation Parameter	231
Effect of Concentration of Organic Solvent on the Solvation Parameter	232
Effect of Temperature on the Solvation Parameter	248
Effect of pH on the Retention of Basic Analytes Using This Model	250
Effect of Type and Organic Composition at Different Concentrations of Perchlorate Anion	255
Conclusion	260
Chapter 5. Geometry of Chemically Modified Silica and Its Relation to Retention Mechanism in Reversed Phase HPLC	264
Summary	264
Introduction	265
Silica	265
Chemically Modified Phases	269
Stationary Phases and Properties	270
Bonded Phases	270
Picket Fence	277
Solvated Hydrocarbon Chains Models	279
Collapsed Configuration	281
Bonded Phase Stability	283
Effect of Chain Length	284

Void Volume	285
Definition of the Void Volume	286
Static Methods	286
Inorganic Salts	288
Organic Compounds	289
Isotopically Labeled Components	290
Radioactively Labeled Compounds	290
Deuterated Compounds	291
Minor Disturbance Method	293
Void and Pore Volume Relationship	295
Experimental	299
Adsorbents and Columns	299
Low Temperature Nitrogen Adsorption (LTNA)	299
HPLC Systems	300
Reagents and Chemicals	303
Results and Discussion	305
Analysis of the Geometrical Parameters of Modified Silicas	305
Pore Volume	305
Bonded Layer Thickness and Bonding Density	311
Determination of the Void Volume	316
Determination of Column Exclusion Volume and Packing Density	321
Comparison of the Column Void Volume with the Adsorbent Pore Volume	328

Relationship of the Column Void and Exclusion Volume with the Adsorbent Pore Volume	333
Surface Area of Alkyl-Modified Adsorbents	334
Determination of Void Volumes of Eight Other Columns	337
Effect of Temperature on Void Volume	340
Excess Adsorption	353
Measurement of Excess Adsorption	358
Determination of Excess Amount Using Labeled Components	359
Determination of Excess Amount Using Minor Disturbance Method	359
Comparison of Minor Disturbance Method and Labeled Components	360
Excess Adsorption Determined Using Minor Disturbance and Deuterated Components	361
Adsorbed Layer Thickness	378
Filling of Adsorption Layer	380
Adsorption-Partitioning Model	384
Summary	387
Addendum	393
Chapter 6. Discontinuous Head-Space Desorption Method For Characterization of Adsorbents	409
Summary	409
Introduction	410
Characterization of Adsorbents	410
Surface Area	410

Capillary Condensation and Capillary Evaporation Region	414
Pore Volume	415
Headspace Techniques for Measurement of Adsorption/Desorption Isotherms	416
Overview of Static Headspace Technique	416
Overview Headspace-GC with Multiple Adsorbate Extraction (HS-MHE)	417
Experimental	418
Sample Preparation	418
Low Temperature Nitrogen Adsorption (Static Mode)	419
Headspace Methods	419
Discontinuous Headspace Desorption (DHD) Experiments	421
Measurement of the Desorption Isotherm From a Single Vial	423
System Calibration and Desorption Calculation Procedure	425
System Calibration	425
Isotherm Calculations	427
Determination of Pore Volume	430
Pore Size Distribution Calculations	432
Results and Discussion	432
Surface Area of Chemically Modified Adsorbents	436
Comparison of Surface Area Measurements	441
Comparison of the Pore Volume and Pore Size Distribution Measurements	441
Surface Area of Nonporous Material	445

Effect of Different Analytes	448
Conclusions	451
Chapter 7. Overall Conclusions	452

List of Figures

<u>Figure</u>		<u>Page</u>
1.1.	Separation of Basic Compounds on Bare Silica by Ion Exchange	10
1.2.	Theoretical Retention For Acidic and Basic Compounds as a Function of pH	13
1.3.	Acidic Analyte Solvation	14
1.4.	Analyte Solvation With Eluent Components	16
1.5.	Effect on Retention of Strongly Solvated Small Hydrophobic Basic Compounds	18
1.6.	Retention of Benzoic Acid at 70/30 MeCN/H ₂ O, pH=6 on Prodigy ODS 2 Column	19
1.7.	Effect of the Organic Eluent Component on the Solvation of Acidic Components and their Peak Shape	21
1.8.	Effect of Analyte Ionization as a Function of pH	22
1.9.	General Retention Dependence of Basic Analytes on the Mobile Phase pH	24
1.10.	General Retention Dependence of Acidic Analytes on the Mobile Phase pH	25
1.11.	Effect of pH and Ion-Interaction Reagent on the Basic Analyte Retention	37
1.12.	The Sorption of Ion Pair Reagent As Function of Concentration of Reagents of Increasing Hydrophobicity	39
1.13.	Log k Data of Adrenaline Versus the Stationary Phase Concentration, (P _s), of BuSO ₃ Na, HexSO ₃ Na and OctSO ₃ Na in Eluents With Changing and Constant Sodium Concentration	41
1.14.	Effect of the Mobile Phase pH and Ion-pair Reagent Concentration on the Retention of Different Bile Acids	44

1.15.	Effect of Ion-Interaction Reagent Octyl Sulfate on the Retention of Acidic, Basic and Neutral Analytes	45
1.16.	Effect of the Addition of Tetrabutyl Ammonium Iodine (TBAI) on Retention of Acidic, Basic and Neutral Analytes	47
1.17.	Retention Volume Versus Carbon Number For a Homologous Series of Alkylbenzenes at Various Organic Composition	48
1.18.	Effect of Analyte Hydrophobicity and Organic Eluent Composition in Reversed Phase Chromatography	49
1.19.	Influence of Methanol and Acetonitrile on the Retention of Benzene and Anionic Solutes in Ion-Pair Chromatography	51
2-1.	Plot of pK_a Versus Increasing Ethanol Concentration of Three Aniline Structurally Related Basic Compounds	60
2-2.	Plot of pK_a Versus Increasing Methanol Concentration of 3 Aniline Structurally Related Basic Compounds	62
2-3.	Absorbance Spectra of Identical Concentrations of Two Basic Analytes	64
2-4.	Plots of the UV Absorbance Against the pH	66
2-5.	Comparison of pK_a determined Values Using Potentiometric Methods and Theoretical Approach	72
2-6.	Carboxylic Acids pK_a Values Versus Mole Fraction of Acetonitrile, X_{AN} , in Acetonitrile-Water Mixtures	74
2-7.	Plot of pK_a Values (Protonated Amino Group) of Selected Quinolones Versus the Reciprocal of the Relative Permittivity of Solvent Mixtures	76
2-8.	pH(s) Versus Percent Acetonitrile For Eight Different Buffer Systems	89
2-9.	Variation of pK_a Values of Polyprotic Acids With the Methanol-Water Composition	91
2-10.	Comparison of pH meter Efficiency in a Low pH Region	97

2-11.	Dependence of the Retention Factor of Aniline and N-methylaniline on the Mobile Phase pH.	101
2-12.	Retention Factor Versus pH For a Series of Pyridines of Increasing Hydrophobicity	102
2-13.	Retention Factor Versus pH For an Isomeric Series of Dimethylpyridines	103
2-14.	Retention Factor Versus pH For an Isomeric Series of Benzylamines	104
2-15.	Comparison of Retention Factor For 4-ethylpyridine Obtained With Three Different Acidic Mobile Phase Modifiers	105
2-16.	Comparison of Retention Factor For N-methylaniline Obtained With Three Different Acidic Mobile Phase Modifiers	106
2-17.	Retention Factor Versus pH at Different Organic Compositions (pH Shift)	109
2-18.	Graphical Representation of the pH Shift For Acidic Modifiers	111
2-19.	Comparison of pH Shift and pK_a Shift	112
2-20.	Structures and pK_a 's of Some of the Basic Compounds Studied	120
2-21.	Effect of pH on the Retention of Basic Analytes of Varied pK_a	122
2-22.	Retention Factor Versus pH of the Aqueous Phase Adjusted With Acetic Acid	123
2-23.	Structures of Acidic Analytes	126
2-24.	Retention of Acidic Compounds as a Function of Mobile Phase pH	128
3-1.	Schematic of Ion-Pairing	141
3-2.	Schematic of Conductance Versus Dielectric Constant	144

3-3.	Retention Factor Versus pH For an Isomeric Series of Dimethylpyridines	149
3-4.	pH Dependence of the Retention of 4-ethylpyridine	151
3-5.	The Effect of TFA (pH Adjustment) on Retention of 4-ethylpyridine	152
3-6.	Effect on Retention of Aniline When Perchloric Acid Was Used as the Acidic Modifier Throughout pH Region 1.3 - 7.1	157
3-7.	Comparison of Retention Factors of 4-ethylpyridine as a Function of pH With Three Different Acidic Modifiers	158
3-8.	pH Dependence of Ionization of Acidic Modifiers	162
3-9.	Comparison of the Chaotropic Effect on 3,4 dimethylpyridine Caused by Trifluoroacetate, Dihydrogenphosphate and Perchlorate Counteranions Plotted Against Mobile Phase pH	169
3-10.	Comparison of the Chaotropic Effect on 2-propylpyridine Caused by Perchlorate and Trifluoroacetate Counteranions Plotted Against Mobile Phase pH	170
3-11.	Effect of Counteranion of H_2PO_4^- Against Retention Factor	172
3-12.	Retention Factor of 2-ethylpyridine and 4-ethylpyridine Versus Concentration of Perchlorate Anion	174
3-13.	Retention Factor of Basic Analytes Versus Concentration of Perchlorate Anion	176
3-14.	Increase in Retention of Basic Compound at Increasing Perchlorate Concentrations at a Variable pH	178
3-15.	Increase in Retention of Basic Compound at Increasing Perchlorate Concentrations at a Variable pH of Potassium Phosphate Buffer	179
3-16.	Increase in Retention of Basic Compound Observed With Increased Concentration of Perchlorate at Constant pH	180

3-17.	Effect of Retention Factor Versus Concentration of Perchlorate Anion on Basic Analyte	181
3-18.	Effect of Total Ionic Strength on the Retention of Pyridinal Compound	184
3-19.	Effect of Perchlorate Anion Concentration on the Retention Factor of Lactic Acid	185
3-20.	Retention Factor Versus Phosphate Not Corrected For Ionic Strength	186
3-21.	Retention Factor Versus Total Ionic Strength	188
3-22.	Retention Factor Versus Concentration of Dihydrogen Phosphate and Total Ionic Strength (2 n-propyl and 4 n-propyl pyridine)	189
3-23.	Retention Factor Versus Concentration of Dihydrogenphosphate and Total Ionic Strength (4-ethylpyridine and 2,4 Lutidine)	190
3-24.	Effect of Initial Phosphate Buffer Concentration Followed by Adjustment With Perchloric Acid	192
3-25.	Plot of Acids and Zwitterionic Components at Different Perchlorate Concentrations at pH=2.0	193
3-26.	Effect of Eluent pH Adjusted With Perchloric Modifier For a Series of Substituted Pyridines	196
3-27.	Effect of Eluent pH Adjusted With Perchloric Acid For an Isomeric Series of Disubstituted Pyridines	197
3-28.	Decrease in Retention of o-chloroaniline is Governed by Ionization While Increase in Retention of Phenylethylamine is Governed by Chaotropicity	199
3-29.	Effect of Perchlorate Concentration on Retention on Beta Blockers, Theophylline and 4-ethylpyridine	201
3-30.	Effect of Perchlorate Concentration on Retention of Beta Blockers, Caffeine and Phenylethylamine	203
3-31.	Effect of Perchlorate Concentration on Retention of Beta Blockers and o-chloroaniline	204

4-1.	Theoretical Dependence of Retention Factor Versus Concentration of Acidic Modifier Counteranion	222
4-2.	Change of the Retention of Basic Analytes at Low pH With the Increase of the Concentration of Dihydrogenphosphate Counteranion	224
4-3.	Change of the Retention of Basic Analytes at Low pH With the Increase of the Concentration of Perchlorate Counteranion	228
4-4.	Retention Factor versus Perchlorate Concentration at 90%Aqueous :10%Acetonitrile	233
4-5.	Retention Factor versus Perchlorate Concentration at 90%Aqueous:10%Methanol	234
4-6.	Retention factor Versus Concentration, 35°C For Pyridinal and Benzlyamine Compounds	235
4-7.	Retention Factor of 2-6 dimethylpyridine Versus Concentration at Different Mobile Phase Compositions, 35°C	236
4-8.	Retention Factor of 4-ethylpyridine Versus Concentration at Different Mobile Phase Compositions, 45°C	245
4-9.	Solvation Parameter, K, Dependence as a Function of Organic Concentration, 35°C	246
4-10.	Retention Factor Versus Concentration at Different Mobile Phase Compositions, 45°C	247
4-11.	Influence of the Solvation Parameter as a Function of Inverse Temperature	249
4-12.	Retention Factor Versus Concentration of Perchlorate	252
4-13.	Retention Factor of Basic Compounds Versus Concentration of Perchlorate	253
4-14.	Retention Factor of Aniline and N-methylaniline Versus Concentration at two pH's: 2.6 and 2.9	254

4-15.	Effect of Acetonitrile Content on the Retention of 2-picoline, and 4-picoline at Varying Perchlorate Concentrations	256
4-16.	Effect of Acetonitrile Content on the Retention of benzylamine, R-methylbenzylamine, at Varying Perchlorate Concentrations	257
4-17.	Effect of Acetonitrile Content on the Retention of 4-ethylpyridine, and 3,5-dimethylpyridine at Varying Perchlorate Concentrations	258
4-18.	Effect of Methanol Content on the Retention of Basic Analytes at Varying Perchlorate Concentrations	259
5-1.	Active Surface Groups on Silica Gel	267
5-2.	Reaction Scheme of Monofunctional Bonding of Ligands to the Silica Surface	272
5-3.	Pore Model of Bonded Phases Illustrating the Steric Hindrance Effect Originating From Pore Curvature and Phase Length	275
5-4.	Schematic of the Picket Fence Conformation	278
5-5.	Schematic of the 'Fur' Conformation of the Stationary Phase	280
5-6.	Schematic of the Stacked Conformation of the Stationary Phase	282
5-7.	Decrease of the Adsorbent Pore Volume With Increase of the Chain Length of the Bonded Ligands	297
5-8.	Nitrogen Adsorption Isotherms on Bare Silica and on the C ₁₈ Modified Adsorbent	301
5-9.	Representative Dependencies of the Minor Disturbance Peaks For Different Eluent Types on C ₁ Columns and C ₁₈ Columns	304
5-10.	Comparison of the Molecular Volumes of Bonded Ligands With That Calculated From Density of Corresponding Liquid	310

5-11.	Comparison of the Molecular Volumes of Bonded Ligands With The Molecular Volumes of Liquid n-alkanes	312
5-12.	Comparison of Experimental Bonded Layer Thickness Dependence on the Number of Carbon Atoms With Theoretical Calculated for All-Trans Alkyl Chains Conformation	313
5-13.	Bonded Layer Thickness Versus Carbon Number	314
5-14.	Comparison of the Retention Volumes Obtained Using Deuterated Components and Minor Disturbance Method on Nomo Set 1-C ₁₈	318
5-15.	Decrease of the Column Void Volume With the Increase of the Alkyl Modifier Chain Length Bonded on the Silica Surface	322
5-16.	Schematic Representation of the Position of Different Polymer Molecules on the Outer Surface of Silica Particles	324
5-17.	Decrease of the Retention Volume Due to the Molecular Size On C ₈ Modified Silica	326
5-18.	Dependence of the Void Volume and Exclusion Volume of the Column Versus Carbon Number	327
5-19.	Dependence of the Pore Volume Ratio (LTNA/HPLC)	331
5-20.	Measured and Corrected Surface Area Values of Studied Adsorbents	338
5-21.	Dependencies of the Minor Disturbance Peaks For the Same Eluent at Different Temperatures (Prodigy ODS-2 Methanol/Water)	343
5-22.	Dependencies of the Minor Disturbance Peaks For the Same Eluent at Different Temperatures (Prodigy ODS-2 MeCN/Water)	345
5-23.	Dependencies of the Minor Disturbance Peaks For the Same Eluent at Different Temperatures (Prodigy ODS-2 Benzene/Water)	347

5-24.	Comparison of the Void Volumes Determined for Prodigy ODS-2 with Three Different Eluent Systems Using the Minor Disturbance Method	349
5-25.	Dependencies of the Minor Disturbance Peaks Across the Entire Concentration Range of Acetonitrile at Different Temperatures	350
5-26.	Determination of the adsorbate Molecular Area From the Excess Adsorption Isotherm For Monomolecular Adsorption Model	363
5-27.	Overlay of all Excess Adsorption Isotherms of Acetonitrile From Water at 25°C Versus Mole/L MeCN	370
5-28.	Overlay of all Excess Adsorption Isotherms of Acetonitrile From Water at 25°C Versus Mole Fraction Acetonitrile	371
5-29.	Overlay of all Excess Adsorption Isotherms of Methanol From Water at 25°C Versus Mole/L MeOH	372
5-30.	Overlay of all Excess Adsorption Isotherms of THF From Water at 25°C Versus Mole /L THF	373
5-31.	Excess Adsorption Isotherms Obtained Using Minor Disturbance Peaks and Deuterated Components, C ₁₈	375
5-32.	Excess Adsorption Isotherms Obtained Using Minor Disturbance Peaks and Deuterated Components, C ₁₂	376
5-33.	Excess Adsorption Isotherms Obtained Using Minor Disturbance Peaks and Deuterated Components, C ₈	377
5-34.	The relationship Between Increasing Carbon Number and Thickness of the Adsorbed Layer	381
5-35.	Comparison of the Bonded Layer and Adsorbed Layer Thickness	382
5-36.	Filling of the Adsorbed Layer on a Reversed Phase Surface	385
5-37.	A schematic representation of the Bonded Layer , the Adsorbed Layer and the Pumped Mobile Phase Composition	388

5-38.	A Schematic of the Pore and Bonded Layer Dimensions (Thickness of the Bonded Layer Corrected for the Surface of Curvature)	389
5-39.	A Schematic of the Pore, Bonded Layer and Adsorbed Layer Dimensions (Thickness of Adsorbed Layer Corrected for the Surface of Curvature)	391
6-1.	Typical IV Adsorption and Desorption Isotherms	412
6-2.	GC-Head-space System Used For Desorption Experiments	420
6-3.	Headspace Experimental Profile For Benzene Desorption From Spherisorb Silica	424
6-4.	System Calibration Curves For Benzene and Cycloheptane	428
6-5.	Benzene Desorption Isotherm Measured by Discontinuous Headspace Desorption Method on Spherisorb Silica	431
6-6.	Benzene Desorption Isotherm Measured by DHD on Prodigy-Si and Full Nitrogen Sorption Isotherm on the Same Adsorbent	433
6-7.	Benzene Desorption Isotherm Measured With DHD System and Full Nitrogen Isotherm on Prodigy-ODS2	435
6-8.	Theoretical and Experimental Dependencies of the Surface Area of Chemically Modified Adsorbents Versus the Number of Carbon Atoms of Alkyl Chains Attached to the Silica Surface	438
6-9.	Pore Size Distribution Measured With LTNA and DHD Methods on Prodigy-Si Adsorbent	442
6-10.	Pore Size Distribution Measured With LTNA and DHD Methods on Prodigy-ODS2	443
6-11.	Benzene Desorption Isotherm From Spherical Nonporous Silica Particles	447
6-12.	Desorption Isotherm and Pore Size Distribution of Spherisorb-Si Measured by DHD of Cycloheptane at 60°C	449

List of Tables

<u>Table</u>		<u>Page</u>
2-I	pK _a Values Determined in Hydroorganic Mixtures For Acidic and Basic Compounds	61
2-II	UV Absorbance 255nm For Pyridine and UV Absorbance 259 nm For 2,4-dimethylpyridine	65
2-III	pK _a Values Determined by Using Theoretical Approach Based on Preferential Solvation and on Methanol-Water Interaction	71
2-IV	pK _a Values of Some Common Acids	78
2-V	Slope of Change of the pH(s) Per Percent of Acetonitrile For Eight Different Buffers	90
2-VI	Change in the pK _a of Common HPLC Acidic Modifiers Per Ten Percent Methanol	92
2-VII	Chromatographic Versus Titration pK _a Values	107
2-VIII	The Effect of pH Shift and pK _a Shift	114
2-IX	Effect of Methanol on Shift of pK _a	116
2-X	Reproducibility of Chromatographically Determined pK _a Using Perchloric Acid as Acidic Modifier	117
2-XI	Effect of Changing Organic Composition on the Analyte pK _a Value of Basic Analytes (Zorbax XDB-C ₁₈ column)	119
2-XII	Effect of Changing Organic Composition on the pK _a Value of Basic Analytes (Prodigy ODS-2 column)	121
2-XIII	Effect of Organic Content on the Analyte pK _a and Reproducibility	124
2-XIV	Chromatographically Determined pK _a of Acids	127
3-I	Increase in Symmetry Factor For 4-ethylpyridine With Decrease in pH	153
3-II	Retention Factor at Each pH Adjustment With Trifluoroacetic Acid	154
3-III	Retention Factor at Each pH Adjustment With Perchloric Acid	155

3-IV	Single-Ion Free Energies of Transfer, $\Delta G^{\circ t}$ From Water to Methanol and Water to Acetonitrile	166
3-V	Retention Factors of the Basic Compounds Obtained at Increasing Perchlorate Concentrations	177
4-I	Retention Factors and Solvation Parameters Obtained Using Dihydrogen Phosphate as the Counteranion and Acetonitrile/Water Eluent on Zorbax Eclipse XDB-C18 Column	225
4-II	Retention Factors and Solvation Parameters Obtained Using Dihydrogen Phosphate as the Counteranion and Acetonitrile/Water Eluent on Luna-C ₁₈ Column	226
4-III	Retention Factors and Solvation Parameters Obtained Using Perchlorate as the Counteranion and Acetonitrile/Water Eluent on Zorbax Eclipse XDB-C18 Column	227
4-IV	Comparison of Solvation Parameters Obtained when Using Dihydrogenphosphate and Perchlorate Anions and Acetonitrile/Water Eluent on Zorbax Eclipse XDB-C ₁₈ Column	230
4-V	Retention Factors and Solvation Parameters Obtained Using Perchlorate as the Counteranion and Methanol/Water Eluent on Zorbax Eclipse XDB-C18 Column	237
4-VI	Retention Factor and Solvation Parameters Obtained Using Perchlorate as the Counteranion and MeCN/Water (50:50) Eluent on Zorbax Eclipse XDB-C18 Column at 35°C	239
4-VII	Retention Factor and Solvation Parameters Obtained Using Perchlorate as the Counteranion and MeCN/Water (40:60) Eluent on Zorbax Eclipse XDB-C18 Column at 35°C	240
4-VIII	Retention Factor and Solvation Parameters Obtained Using Perchlorate as the Counteranion and MeCN/Water (30:70) Eluent on Zorbax Eclipse XDB-C18 Column at 35°C	241
4-IX	Retention Factor and Solvation Parameters Obtained Using Perchlorate as the Counteranion and MeCN/Water (20:80) Eluent on Zorbax Eclipse XDB-C18 Column at 35°C	242
4-X	Retention Factor and Solvation Parameters Obtained Using Perchlorate as the Counteranion and MeCN/Water (10:90) Eluent on Zorbax Eclipse XDB-C18 Column at 35°C	243

4-XI	Retention Factor and Solvation Parameters Obtained Using Perchlorate as the Counteranion and MeCN/Water (10:90) Eluent on Zorbax Eclipse XDB-C18 Column at 25°C	244
5-I	Geometric Parameters of Bare Porous Silica and Alkylsililated Gels	307
5-II	Corrected Pore Volume and the Volume of Bonded Phase	308
5-III	Void Volume Values Measured With MeCN/Water, MeOH/Water and THF/Water and Labeled Component For 1 st Set of Columns	319
5-IV	Void Volume Values Measured With MeCN/Water, MeOH/Water and THF/Water, Pycnometry, Labeled Component For 2 nd Set of Columns	320
5-V	Column Exclusion Volumes and Packing Density	325
5-VI	Comparison of the Adsorbents Porosity Measured by LTNA and HPLC methods	330
5-VII	Correlation of the Calculated and Measured Mass of the Adsorbents in the Column	335
5-VIII	Void Volume Values of Six Commercial Columns	339
5-IX	Retention Volume Dependence For Methanol Disturbance Peaks From 5-28°C	344
5-X	Retention Volume Dependence For Acetonitrile Disturbance Peaks From 10-50°C	346
5-XI	Retention Volume Dependence For Benzene Disturbance Peaks From 5-55°C	348
5-XII	Retention Volume dependence For Acetonitrile Disturbance Peaks From 5-50°C	351
5-XIII	Characteristics of the Acetonitrile Adsorbed Layer	367
5-XIV	Characteristics of the Methanol Adsorbed Layer	368
5-XV	Characteristics of the Tetrahydrofuran Adsorbed Layer	369

5-XVI Comparison of Adsorbed Layer Thickness Obtained With V_R From Deuterated and V_R From Minor Disturbance Method	374
5-XVII Concentration of the Adsorbed Layer at Different MeCN/Water Compositions	386
A5-I MeCN/Water Minor Disturbance Retention Volumes For 1 st Set of Columns	393
A5-II Acetonitrile/Water Minor Disturbance Retention Volumes For 2 nd Set of Columns	394
A5-III Methanol/Water Minor Disturbance Retention Volumes For 1 st Set of Columns	395
A5-IV Methanol/Water Minor Disturbance Retention Volumes For 2 nd Set of Columns	396
A5-V THF/Water Minor Disturbance Retention Volumes For 2 nd Set of Columns	397
A5-VI Deuterated Retention Volumes For Nomo Set 1-C ₁₈	398
A5-VII Deuterated Retention Volumes For Nomo Set 1-C ₁₂	399
A5-VIII Deuterated Retention Volumes For Nomo Set 1-C ₈	400
A5-IX MeCN/Water Minor Disturbance Retention Volumes for Waters Symmetry C ₁₈ , Eclipse XDB-C ₁₈ and Luna C ₁₈ -2 Columns	401
A5-X MeCN/Water Minor Disturbance Retention Volumes for Kovalsil-C ₁₄ , Jupiter C ₁₈ and Luna C ₁₈ columns	402
6-I Benzene and Cycloheptane DHD Calibration Parameters	429
6-II Surface Area and Pore Volume of Prodigy-ODS2	440
6-III Pore Volume and Average Pore Radius of Prodigy-Si and Prodigy-ODS2 Adsorbents Measured With LTNA and DHD Methods	444
6-IV Surface Area and Porosity of Spherisorb-Si Calculated From DHD Experiments With Benzene and Cycloheptane	450

Thesis Structure

The work described in this thesis contains studies of different aspects of reversed phase chromatography. This section is provided for the reader to understand how these different aspects are related

Chapter 1 describes analyte ionization and the history of how these ionogenic species have been analyzed by various forms of chromatography. Different ion-interaction retention models and their various applications described in the literature are provided.

Chapter 2 describes the effect of organic solvent on basic and acidic analyte ionization. A comparison of chromatographically determined pK_a values versus titration pK_a values is given. The organic solvent has a strong effect on the analyte ionization and obviously would affect any ion-interaction mechanism as well as the chromatographic selectivity.

Chapter 3 provides a structured overview of various ion-interaction applications to which our experimental data are compared and contrasted. The results within this chapter **include** studies of the effects of various mobile phase modifiers on the ionized analyte **retention**. It was shown that the analyte solvation of the ionized species was greatly influenced by the type and concentration of the pH acidic modifier. The role of the eluent on the formation of ion-associated species including ion-pairs is discussed.

In Chapter 4, a theoretical description of a desolvation model based on the Langmuir approach is proposed. Theoretical retention factors for the completely solvated and desolvated forms of the analyte, as well as the analyte's solvation constant, were

determined. The influence of type of counteranion, temperature and organic composition upon the solvation constant has been studied.

Thermodynamically accurate determination of the void volume is necessary for theoretical description of HPLC retention process. We dedicated Chapter 5 to the discussion of the determination of void volume of various adsorbents by classical methods such as pycnometry, minor disturbance and retention of isotopically labeled components. The relationship of change of column void volume with temperature is also shown. A brief literature review is given along with our experimental determinations. Void volume is defined as the total volume of liquid phase in the column and is comprised of the exclusion and adsorbent pore volume. The determination of the pore volume of the silica and modified adsorbents of the same silica allows us to predict the conformation of alkyl chains bonded on the surface of porous silica. We compared the HPLC adsorbent porosity to that measured by classical low temperature nitrogen adsorption (LTNA). Also, we showed that organic components exhibit specific interactions with the hydrophobic stationary phases and are excessively adsorbed on the reversed phase surface. The second portion of Chapter 5 is a description of the general solute retention model in reversed phase chromatography. We used excess adsorption isotherms as a fundamental tool for investigation of the physical process involved in chromatographic retention. We provided a distinction of the partitioning and adsorption retention mechanisms as well as a description of the “partition-adsorption” model developed in our laboratory.

In Chapter 6, a headspace-GC (HSGC) method with multiple extractions from a single vial was developed for the measurement of desorption isotherms with any volatile organic component at any reasonable temperature. The geometric parameters of non-porous

silica, porous silica and chemically modified silica have been determined by this method. The methodology and instrumentation for the determination of porosity and surface areas of solids at various temperatures have been described. We also determined the pore volume and other geometric parameters of various reversed phase adsorbents using low temperature nitrogen adsorption (LTNA) under vacuum at 77K. A classical description of the adsorption and desorption isotherms measured with this technique is presented. On the basis of the desorption isotherms, the pore size distribution was calculated by the Barrett, Joyner Hallender (BJH) method where the pore shape was assumed to be cylindrical. The measurement of the total surface area was performed according to Brunauer- Emmett Teller (BET) theory. This discontinuous headspace desorption method could serve as a valuable tool for surface scientists to determine surface energies using analyte probes of different size and polarity.

**Due to large quantity of references incorporated within this thesis the references will be located at the end of each chapter rather than the conventional style at the end of the thesis.*

Chapter 1

History and Current state of the art

Overview

HPLC separation of ionic or ionizable components was first performed on the basis of ion-exchange mechanisms^[1-3]. In this process, the retention of ionic analytes is governed by their ionic interactions with ion-exchange sites embedded in the packing material^[4-5]. This process appears to be inflexible for the separation of organic ionizable compounds, which are usually weak acids or bases. Tools for adjusting the selectivity of separation are very limited in this mode. The separation of closely related organic bases or acids with small differences in chemical structure is nearly impossible to perform in an ion-exchange mode.

Further modification of the ion-exchange process was the introduction of ion-pair chromatography. This mode is a hybrid of the reversed-phase and ion exchange processes. The addition of ion-pairing agent (some form of surfactants) in the mobile phase causes the formation of ionic pairs with ionic analyte molecules. It is believed that these neutral pairs are retained in HPLC column according to regular reversed-phase process^[6-7].

Another concurrent effect in the ion-pair mode is the adsorption of ion-pairing agent on the surface of reversed-phase packing material. This causes a decrease of the available hydrophobic surface and its transformation into an ion-exchange type surface^[8-9].

Ion-pair HPLC mode is a superposition of two competitive processes; ion exchange and reversed-phase. Component retention is strongly dependent on the type of ion-pairing agent, its concentration and, most of all, on the history of the column used. The virgin reversed-phase (RP) column does show the hydrophobic selectivity in the ion-pair mode.

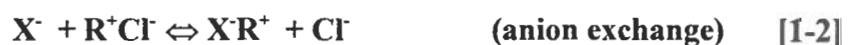
However, with time, the adsorbent surface can become covered with dense layer of adsorbed surfactant. This may irreversibly transform a RP column into an ion exchange one.

Ion-Exchange Chromatography

The first application involving chromatographic analysis for ionogenic compounds was Ion-Exchange Chromatography (IEC) [4]. Further developments in HPLC led to the analyses of these compounds by reversed phase and ion-pair reversed phase chromatography. Ion-exchange chromatography has been used for the analysis of acidic and basic compounds such as amino acids, peptides, nucleic acids, etc. Ion exchange chromatography (IEC) is applicable to the separation of almost any type of charged molecule, from large proteins to inorganic ions.

The columns used for ion exchange have charged groups covalently attached to the stationary phase where an anion exchange column carries a positive charge (usually a quaternary ammonium or amine group) and cation-exchange columns carry a negative charge (sulfonate or carboxylate groups). Cation exchange columns are used for the separation of cations such as protonated bases and anion exchange columns for anionic or acidic samples.

The retention in ion exchange chromatography can be represented as follows [1-1 and 1-2]:



where the stationary phase is represented by R^- for cation exchanger; R^+ for an anion exchanger and the sample by X^+ (cation) or X^- (anion). The counterion in the mobile phase for the cation exchange is assumed to be Na^+ and for the anion exchange Cl^- and the sample ion is univalent.

Typically, the effect of the counterion concentration on the analyte retention factor, k , has been generalized for a sample ion of charge z and a univalent counterion ^[10] as:

$$k = \frac{1}{(\text{CounteranionConc.})^z} \quad [1-3]$$

Therefore, an increase in the salt or buffer concentration in IEC will lead to decreased retention. This effect will be more pronounced for more highly charged species. The ionic strength of the mobile phase has been varied in order to control the sample retention. This effect will be prominent for species with different charges. For the separation of similarly charged components, the selectivity usually may not be adjusted by modifying the salt or buffer concentration. Due to the differences in analyte pK_a the adjustment of the eluent pH may be used to adjust the selectivity in these cases and may prove beneficial. For example, in ion-exchange chromatography, if a cation exchange column is used for the analysis of basic compounds a decrease in pH leads to greater sample ionization and increased retention. This is the opposite effect observed for reversed phase chromatographic retention.

Salt or Buffer type

The type of anions or cations present in buffered mobile phase may have a significant effect on the retention of ionizable solutes. A counterion that reduces the sample retention more than the same concentration of another counterion can be denoted as a stronger ionic displacer. Therefore, the stronger the ionic displacer (counterion), the greater the interaction strength with the ion exchange column which leads to greater desorption of the analyte of the same charge from the surface. In addition, more highly charged displacers are usually stronger ionic displacers.

The relative strength of different displacers in anion-exchange chromatography is ^[10-11]



The relative strength of different displacers in cation exchange chromatography is ^[12]



Column Type

There are generally four types of ion exchange columns: weak and strong cation exchangers (WCX and SCX, respectively) and weak and strong anion exchangers (WAX and SAX, respectively). For the strong ion exchangers the ionization state of the ionic groups do not change over a pH range of 2-12 since they may have very **low pK_a values**, such as $-\text{SO}_3^-$ for cation exchange or very high pK_a values, such as $-\text{N}(\text{CH}_3)_3^+$ groups for anion exchange. However, weak ion exchangers may lose their charge dependence on the pH of the mobile phase and this in turn will lead to the reduced retention of the ionized species in the mobile phase. For example, if a cation exchange column stationary phase has COO^- groups, the pK_a of the COOH is around 4 and at pH values below 4 the COO^- becomes more protonated. Interactions of a protonated basic compound will be reduced due to a lesser amount of negative charged surface. Weak ion exchangers are another effective means of changing selectivity or for reduced retention.

Normal Phase Chromatography

The use of normal phase chromatography for the separation of basic and acidic compounds had marked the beginning of a very important era that led to the further development of these separations in reversed phase chromatography. Normal phase chromatography is a mode of liquid chromatography that employs polar stationary phases and **non-polar** eluents. Retention is predominately governed by hydrogen bonding,

electrostatic interactions, and more specifically, dipole-dipole interactions. The stationary phases most typically used for normal phase are silica, alumina and chemically bonded phases, such as aminopropyl, cyanopropyl, nitrophenyl and diol. These include modified alumina, titania and zirconia, modified silica gels, impregnated silica gels and nitrophases. This form of chromatography though was not widely used since it did not give the chromatographer the flexibility to vary the analyte ionization since most applications were carried out in pure organic solvent.

However, some researchers had modified the surface of the silica with the use of adsorbed buffer salts prior to the chromatographic analysis of basic and acidic compounds. The pH of the buffer, concentration and the type of buffer to modify the silica surface had a significant effect upon the retention and peak shape of the analytes^[13-15].

It was found that at constant ionic strength in primarily methanolic eluents, eluent pH influences retention via ionization of surface silanols and protonation of basic analytes. A word of caution should be stated that the pH of the organic eluent does not correspond to the pH of a purely aqueous solution and this may pose problems when trying to justify the ionization state of the basic compound at a particular pH. However, for quaternary ammonium compounds e.g. (Emerpronium), only changes in the silanol ionization need to be considered since the increase in retention of these compounds with increasing pH is similar to the ionization profile of the silica silanols^[16]. At constant pH, the retention was found to be proportional to the reciprocal of the eluent ionic strength for fully protonated basic analytes and quaternary ammonium compounds.

The analysis of basic drugs of abuse have also been chromatographed on silica related to reversed phase conditions using a methanol-rich aqueous ammonium nitrate at high pH^[17].

A more detailed study of the use of these aqueous eluents with silica for the chromatography of bases at methanol compositions above 50% containing ammonium nitrate has been reported by Sugden et. al. ^[18]. They noticed a decrease in retention for the basic analytes using mildly basic to acidic mobile phase conditions and attributed this to the suppression of the interactions between protonated species and the silanol groups on the surface. The silanols groups were becoming less ionized at lower pHs. Law^[19], analyzed six highly basic compounds ($pK_a > 8$) on four different silica columns with a mobile phase composition of 90% methanol/(ammonium nitrate buffer, pH=9 to 10). The retention and elution order on all these columns were very similar: Figure 1-1 shows the lack of separation power in the normal phase mode for ionizable components.

The use of normal phase chromatography has proven to be somewhat successful for the analysis of basic and acidic compounds, however, sometimes the retention behavior has been unpredictable. The development of reversed phase supports including chemically modified silicas with alkylchlorosilanes has led to better separation of basic and acidic components since the analyte ionization state may be changed as a function of the eluent pH and more predictable retention mechanisms have been obtained.

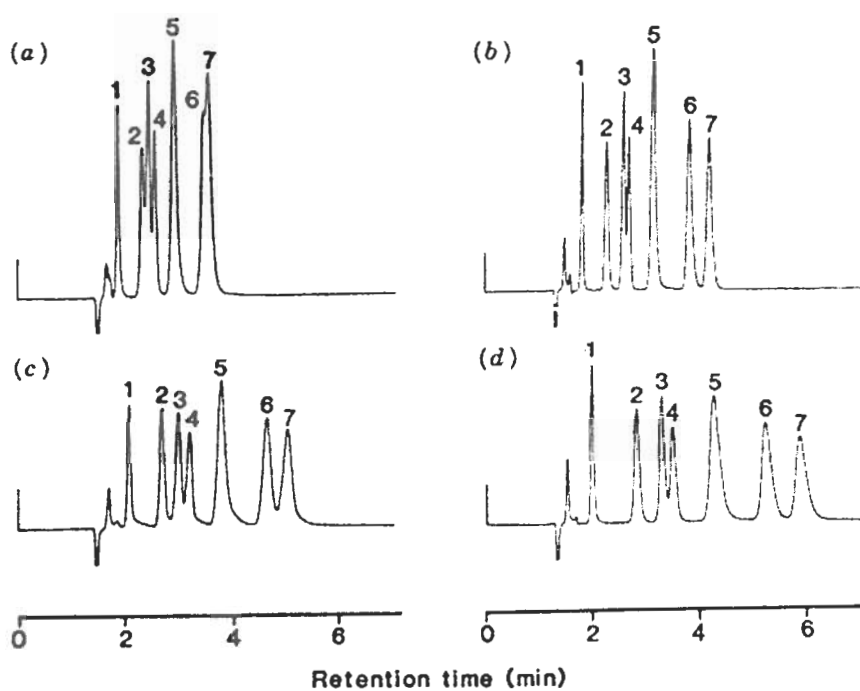


Figure 1-1. Separation of basic compounds on bare silica by ion exchange.^[19] Sample: 1, phendimetrazine; 2, phenylpropanolamine; 3, phentermine; 4, amphetamine; 5, morphine; 6, ephedrine; 7, methylamphetamine. Conditions: 25 x 0.5 cm columns of Hypersil (a), Spherisorb S5W (b), Nucleosil 50-5 (c), and Zorbax BP-Sil (d); mobile phase is 90% methanol-ammonium nitrate, pH: 10.1; flow rate: 2.0 mL/min; Temperature: ambient.

Analyte Ionization

Ionization of the analyte could be expressed by one of the following equilibria



Equilibrium constants are usually written in one of the following forms:

$$K_a = \frac{[\text{A}^-] \cdot [\text{H}^+]}{[\text{AH}]} \quad [1-6]$$

The larger the value of K_a , the stronger the acid. Strong acids that are virtually 100% ionized in water have $\log K_a$ values ≥ 0 because $[\text{HA}]$ is very small. For weak acids, as are most acidic HPLC analytes the predominant equilibrium [1-4] is toward the formation of HA, and $\log K_a$ values are less than 0. The general equation for the $\text{p}K_a$ is given:

$$\text{p}K_a = -\log K_a \quad [1-7]$$

The $\text{p}K_a$ is related to the pH by the Henderson-Hasselbalch equation:

$$\text{p}K_a = \text{pH} + \log \left(\frac{[\text{AH}]}{[\text{A}^-]} \right) \quad [1-8]$$

The product of the ionization constant for an acid and the ionization constant of its conjugate base is equal to the ion product constant of water where $K_a \times K_b = K_w$. From this relationship a similar expression could be written for bases.

$$\text{p}K_a = \text{pH} + \log \left(\frac{[\text{B}]}{[\text{BH}^+]} \right) \quad [1-9]$$

In the last twenty years, it was realized that all organic ionizable compounds do show certain specific hydrophobic interactions with reversed-phase stationary phases [20-22]. These relatively weak interactions offer significant HPLC selectivity in separation of even related compounds. pH is a primary tool for controlling selectivity through the change of the analyte ionization state.

Reversed phase retention is based on the competitive dispersive (hydrophobic) interactions of the analyte with the stationary phase. Therefore, a simplistic rule for the retention in reversed-phase HPLC, is the more hydrophobic the component, the more it is retained. By simply following this rule, one can conclude that any organic ionizable component will have longer retention in its neutral form than in the ionized form as shown in Figure 1-2. Ionization is a pH dependent process and the change of the mobile phase pH has a significant effect on the separation of complex organic mixtures containing basic or acidic components.

As mentioned before, a compound in its ionic form is more hydrophilic, tends to have less interaction with hydrophobic stationary phase, and tends to be more solvated with water molecules. Solvation is the association of the analyte with the solvent molecules primarily by the formation of hydrogen bonds, as shown in Figure 1-3. This also caused a significant decrease in retention of ionized components.

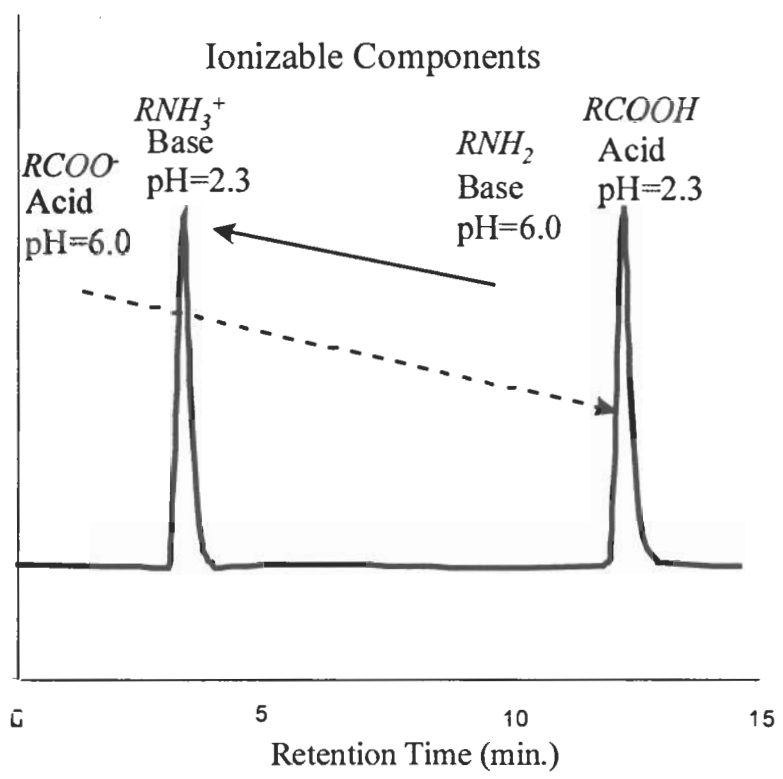
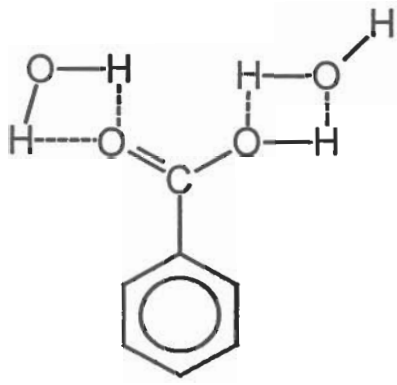
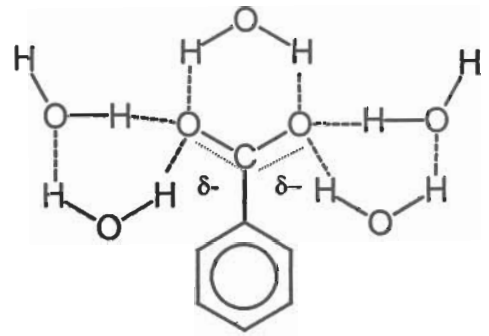


Figure 1-2. Theoretical retention for acidic and basic compounds as a function of pH.



Acid in its neutral form
More hydrophobic

A



Acid in its ionized form
Less hydrophobic

B

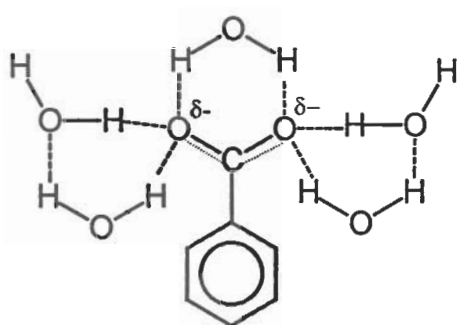
Figure 1-3. Acidic analyte solvation. A) An acid in its neutral form is more hydrophobic and will be retained longer compared to its more B) solvated ionized form.

However, not only can water solvate the ionized solutes but so could the organic portion of the mobile phase in the reversed phased system as shown in Figure 1-4. Methanol is able to participate in the analyte solvation via hydrogen bonding while acetonitrile may not. Solvation with methanol may form a partially hydrophilic shell that could be retained on the reversed phase adsorbent. Therefore, when considering an ion-interaction mechanism one should consider not only the analyte ionization state, but also probability of the analyte solvation with the aqueous and/or organic components of the eluent.

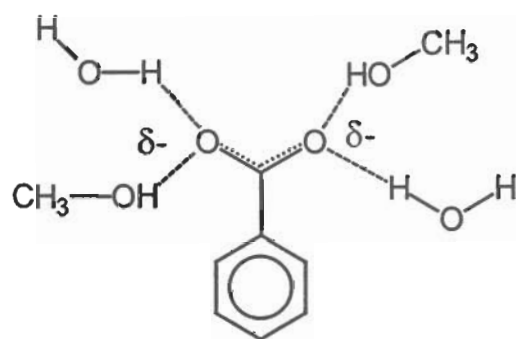
Applications

Typically, at low pH, the elution of the basic components is fast. This is advantageous to the chromatographer since the desired separation of their basic components may be obtained in the shortest possible time. However, this retention may be too low and analytes may elute before the void volume. The basic analytes in their cationic (protonated) form can be solvated and therefore are hydrophilic. The hydrophobic nature of protonated basic analytes and their solvation will affect the elution. Therefore, if a small basic analyte, which has small molecular size and low hydrophobicity, is strongly solvated, it may elute before the void volume.

Void volume can be defined as the total volume of the liquid phase inside the column. Highly solvated analytes form very hydrophilic molecular clusters, which may not penetrate into the hydrophobic space inside the reversed-phase adsorbent particles. This will cause the analytes fast elution primarily through the interparticle space with very low retention volume.



A



B

Figure 1-4. Analyte solvation with eluent components. A) Solvation of ionized benzoic acid in acetonitrile/water eluent, B) Solvation of ionized benzoic acid in methanol/water eluent.

For example, small basic analytes such as pyridine and 2-ethylpyridine may elute before the void volume, as shown in Figure 1-5. Other more hydrophobic analytes such as aniline and N,N-dimethylaniline at same experimental conditions were eluted after the void volume at the same experimental conditions [23].

The decrease of the organic content in the mobile phase from 80% acetonitrile to 10% acetonitrile, which usually significantly increases the analyte retention, does not have any effect on the elution of those excluded compounds. In these cases, some mobile phase additives which affect the analyte solvation may have to be employed to increase retention.

Typically, at a high pH, acidic components are ionized and highly solvated. Their retention is very low and often, they may elute before the void volume. Figure 1-6 shows one practical example of what could happen with acids at high pH. Acidic analytes in their anionic form are strongly solvated even stronger than protonated bases. An ionic exclusion effect may be seen when solvated analyte will not be able to penetrate inside the pore space of the packing material. This will cause the analyte's elution with a very low exclusion volume as if it would be a polymer. Figure 1-6 shows elution of benzoic acid at pH ~6.0 at 70/30 MeCN/Water on Prodigy-ODS2 column (150x4.6 mm). At this pH benzoic acid is fully ionized and eluted at 1.12 minutes while an average void volume for these type of columns are 1.7 ml.

There are also other drawbacks when weak acidic components are analyzed at high pH. Poor peak shapes may also be observed especially if the analyte is a small hydrophobic compound in which the hydrophobic part of the molecule is comparable to that of the acidic moiety. For larger hydrophobic acidic compounds this effect may not be prevalent.

Strongly Solvated Basic components

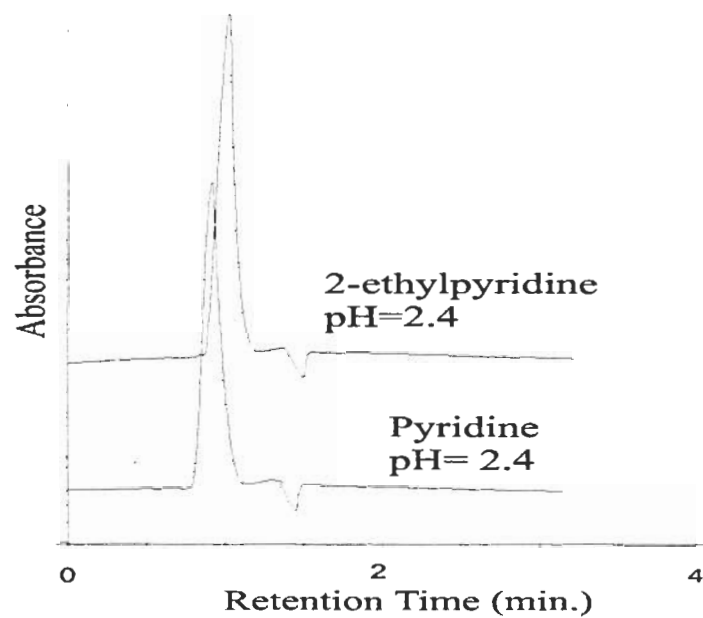


Figure 1-5. Effect on retention of strongly solvated small hydrophobic basic compounds. Column 15x0.46cm Zorbax XDB-C18 with void volume of 1.4 ml; mobile phase: Acetonitrile- Aqueous adjusted with phosphoric acid, pH=2.4 (80:20); flow rate, 1.0 ml/min; 25°C, UV, 254 nm; sample:1ul injection.

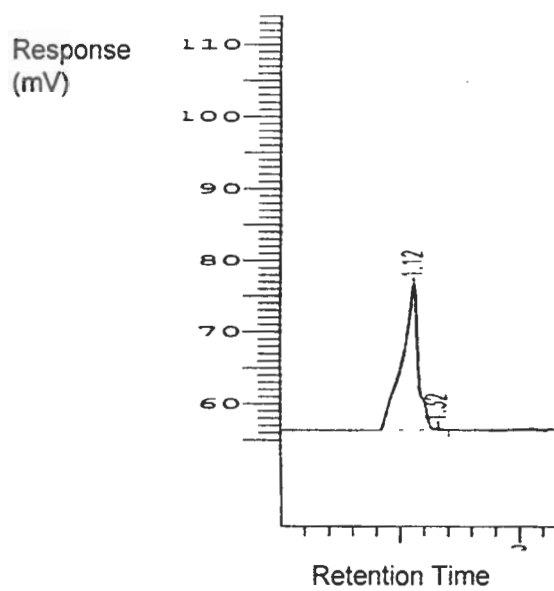


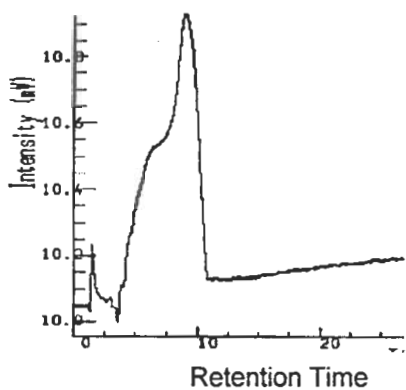
Figure 1-6. Retention of benzoic acid at 70/30 MeCN/H₂O, pH=6 on Prodigy ODS2 column. Column void volume is 1.7 ml.

The anionic form of the acidic compound is strongly solvated by water molecules. If the organic eluent modifier can participate in the analyte solvation, the solvation shell will possess some hydrophobicity and may actually increase the retention. Figure 1-7a illustrates this effect with a small hydrophobic acidic compound, benzoic acid. Similar effects have been observed for salicylic acid. Methanol may hydrogen bond and solvate the acidic analytes. Therefore, when methanol is used versus acetonitrile at higher pH's poor peak shapes may be obtained. As can be seen in Figure 1-7a, the benzoic acid peak front starts prior to the void volume and extends to 10 min. In order to improve peak shape, pH was decreased to 2.5, as seen in Figure 1-7b. Decrease of the pH suppresses the ionization of the acid. This increases its hydrophobicity and overall retention. This also makes peaks more narrow and symmetrical.

The pK_a is a characteristic constant of the specific analyte. From the Henderson Hasselbalch equation, one can conclude that relative amounts of neutral and ionic forms of the analyte could be easily adjusted by varying the mobile phase pH. Moreover, if the pH is about two units away from the component pK_a , more than 99% of the analyte will be in either ionic or neutral form, depending upon the direction of the pH shift as seen in Figures 1-8a and 1-8b for a typical acid and basic compound. The y axis denotes the percent of analyte ionization. The percentage ionized may be calculated with a given pK_a and pH for acids and bases using equations [1-10] and [1-11].

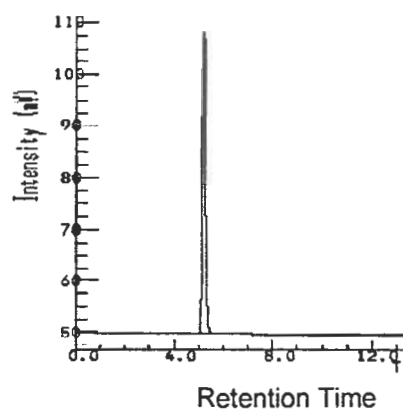
$$\% \text{ Ionized} = \frac{100}{1 + 10^{(pK_a - pH)}} \quad \text{Acids} \quad [1-10]$$

$$\% \text{ Ionized} = \frac{100}{1 + 10^{(pH - pK_a)}} \quad \text{Bases} \quad [1-11]$$



Benzoic acid in MeOH/H₂O
no buffer

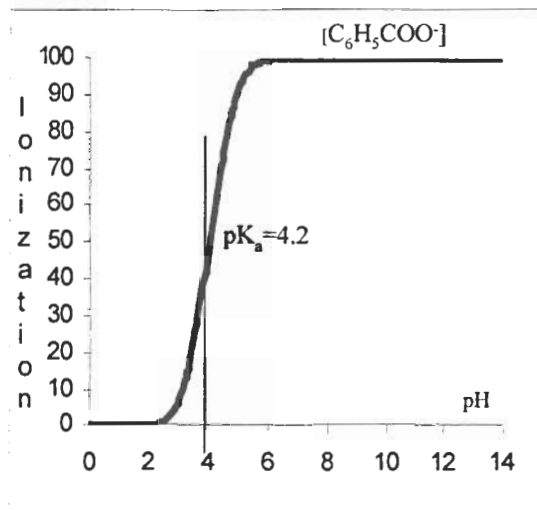
a



Benzoic acid in MeOH/H₂O
pH = 2.5

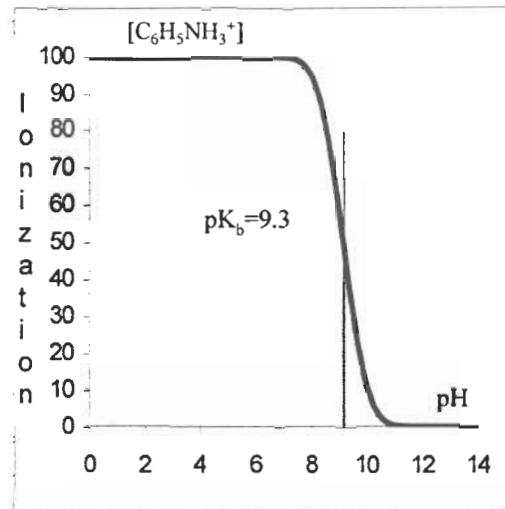
b

Figures 1-7. Effect of the organic eluent component on the solvation of acidic components and their peak shape. Column: Prodigy ODS2 column with void volume of 1.7 ml. UV detection: 254 nm, Inj. Volume: 1 μ L, Temperature: ambient.



Benzoic acid

A



Aniline

B

Figure 1-8. Effect of analyte ionization as a function of pH.

Ionization and HPLC retention in reversed phase HPLC

Let us discuss now the primary retention dependence of the ionizable analyte versus the mobile phase pH. For basic components the retention dependence as a function of pH will show a sigmoidal dependence as seen in Figure 1-9. The retention dependence of basic components on the pH of mobile phase could be subdivided in three regions.

- A. – Fully protonated analyte has a low retention. The analyte is in most hydrophilic form. Its interactions with the hydrophobic stationary phase are suppressed.
- B. Partial protonation region. Coexistence of two analyte forms (protonated and deprotonated) in the mobile phase in equilibrium causing bad peak shape and unstable retention. Since neutral form of the analyte has much stronger retention than protonated form its molecules tend to show greater interaction with the stationary phase. This causes a shift of the ionization equilibrium in the mobile phase towards a formation of deprotonated molecules and further increase of overall retention of the front of chromatographic band. Overall process depends on the superposition of the ionization and adsorption processes and their relative kinetics. Usually, a slight change of the mobile phase pH greatly shifts the retention.
- C. Analyte is in its neutral form (the most hydrophobic) and show the longest retention.

Same type of the retention curve could be obtained for acidic components, but obviously their retention dependence will be the mirror image of that for basic analytes (Figure 1-10)

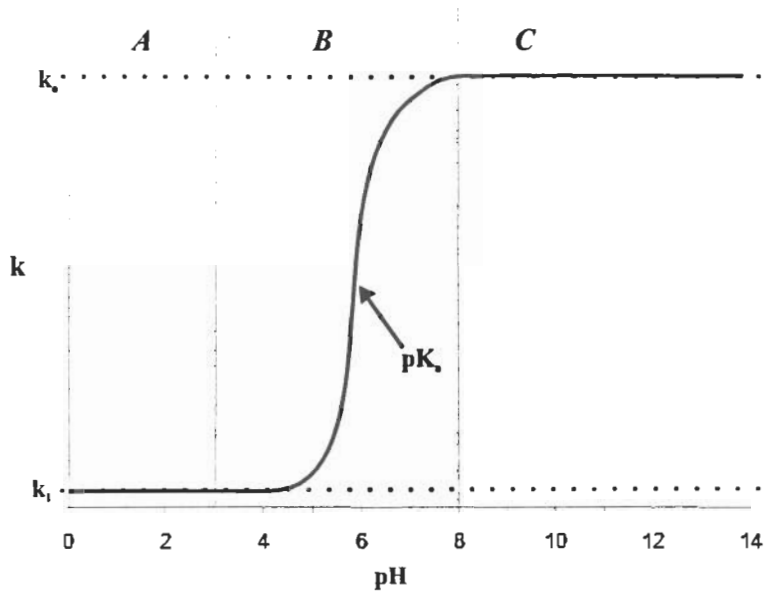


Figure 1-9. General retention dependence of basic analytes on the mobile phase pH. The inflection point of the curve corresponds to the component pK_a .

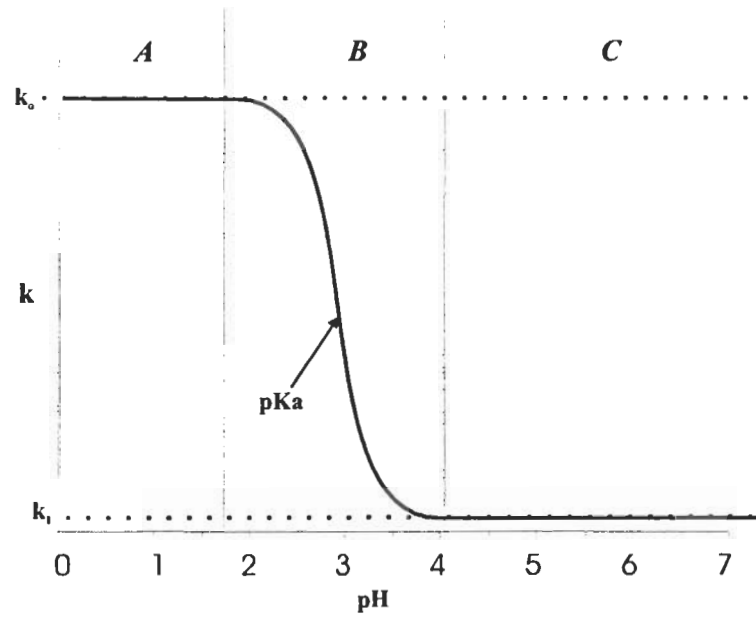


Figure 1-10. General retention dependence of acidic analytes on the mobile phase pH. The inflection point of the curve corresponds to the component pK_a .

These retention profiles could be described by the following equation as a function of eluent pH and analyte pK_a as shown in equation [1-12 and 1-13]^[24].

$$k = \frac{k_0 + k_1 \frac{[H^+]}{K_a(B^+)}}{1 + \frac{[H^+]}{K_a(B^+)}} \quad [1-12]$$

or

$$k = \frac{k_0 + k_1 \exp[2.3(pK_a - pH)]}{1 + \exp[2.3(pK_a - pH)]} \quad [1-13]$$

where k_1 is the retention factor of ionized form; protonated form for base and anionic form for acid (represented by the lower plateaus in Figures 1-9 and 1-10), k_0 is a retention factor of neutral forms for acids and bases (higher plateaus in Figures 1-8 and 1-9); k is current retention factor at given pH; K_a is the analyte ionization constant.

Regions A for basic and C for acidic components show very low if any retention variation with mobile phase pH. Methods employing a mobile phase pH which corresponds to these regions are generally more rugged. On the other hand, each region has its own drawback, and in selecting the initial HPLC conditions and the direction of the separation development one has to account for all possible effects.

Effects in region A (Figure 1-9 and Figure 1-10)

- Basic analytes show relatively low retention (analyte in its ionic form).
- Acidic analytes show extremely long retention times (analyte in its neutral form.)

Effects in region B (Figure 1-9 and Figure 1-10)

- Significant loss of apparent efficiency for both, acidic and basic analytes. Peaks are broad and sometimes show tailing or fronting.
- Very unstable retention. Minor changes in pH or composition of the mobile phase will significantly shift retention.
- Minor changes of the eluent composition can cause significant change in selectivity.

Effects in region C (Figure 1-9 and Figure 1-10)

- Very long retention for basic analytes. Usually requires working with high organic concentration of the mobile phase because pH adjustment may not be efficient.
- Silica is soluble at high pH. If the column has some accessible silanols (which all columns usually do) high pH may cause steady degradation of the packing material. This brings a loss of the efficiency due to the formation of the void volume, or steady change of component retention.
- If the mixture of analytes contains some acidic components, these components will be in anionic form at high pH. Organic analytes in their anionic form usually are strongly solvated and may be completely excluded from the pore space of the packing material. This cause very early elution usually not adjustable by the element composition.

In a summary, HPLC analysis of basic analytes is more beneficial in a low pH region where these components are fully protonated and the problems associated with running at high pH's in the mobile phase may be avoided. The elution of acidic and hydrophobic

neutral components may be obtained by employing a gradient after the separation of basic components is achieved at low pH values.

Modes of reversed phase

Retention is generally based on the hydrophobicity of the solute. At increased organic eluent strength decreases in the retention of the hydrophobic compounds are usually obtained. However, for the analysis of ionizable compounds, the retention mechanism becomes more complicated due to secondary effects such as interaction of the ionizable analytes with components in the mobile phase.

Ion suppression

The pH modification of aqueous phases employed in reversed phase allows the use of chemical equilibria for the separation of polar ionizable compounds. These compounds typically are ionized basic and acidic solutes. Their ionization state could be controlled by the pH of the mobile phase so that secondary equilibria would not influence the separation process. If we analyze a carboxylic acid at a high pH it will be poorly retained. However if we adjust the pH of the mobile phase to more acidic the equilibrium will be driven towards suppressing the ionization. This will increase the retention and the compounds will elute as a more symmetrical peak. The same can be performed for the analysis of basic compounds. For some strongly acidic or basic compounds the adjustment of the pH cannot be used for the ion suppression since the analytes are fully ionized in the pH range of 2 – 8. Therefore, by forming ion pairs with appropriate counterions in the mobile phase, the strong acids and bases could be made electrically neutral and would increase their hydrophobicity. The basic

equations for a reversed phase ion pair chromatography have been covered by several authors [25-26].

Ion –Interaction

Occasionally, highly polar and ionic compounds cannot be analyzed directly using reversed phase technique since they elute near the void volume. Therefore, ion exchange chromatography has been classically used. The drawbacks of using ion exchange chromatography is that the simultaneous analysis of both ionized and unionized solutes is difficult and lower peak efficiencies and shorter column lifetimes than reversed phase packings are obtained. In 1966 Horvath and Lipsky^[27] used a reversed form of the conventional ion-pair chromatography and exploited the dramatic changes in retention of highly polar and ionic compounds with the use of ion-association (ion-pair) reagents that contained hydrophobic moieties. Then in 1975 Wahlund^[6] applied this technique to reversed phase HPLC systems and since that time its applications have grown substantially.

This technique has been known as soap chromatography, ion pair chromatography, paired ion chromatography, solvent-generated (dynamic) ion-exchange chromatography, hataeric chromatography, detergent based cation-exchange, solvophobic-ion chromatography, surfactant chromatography and ion-association chromatography. As can be seen there is a confusion of names for such a well established technique and in a broad sense they all could be classified as ion-interaction chromatography to allow even for mixed modes of retention.

Ion-interaction models for the process of retention

1. Ion pair formation in the mobile phase

Some authors, suggests that ion pairs can be formed in the mobile phase with an counterion and an oppositely charged solute. The retention would then be due to the

interaction of the neutral pair and the nonpolar stationary phase^[6-7,28-31]. However, others such as Westerlund and Theodorsen have suggested that ion-pair formation in the mobile phase (interaction of the neutral pair) and adsorption of the free ion take place^[32].

The chromatographic retention factor, k is related to the equilibrium between liquid mobile and stationary phases by

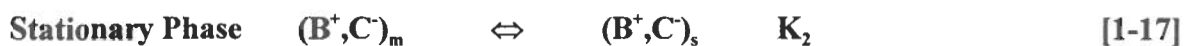
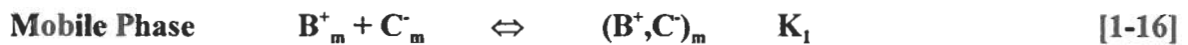
$$k = \phi K \quad [1-14]$$

where K is the analyte distribution constant. And ϕ is the phase ratio (V_s/V_m). It is the volume of the stationary phase (V_s) over the volume of the mobile phase (V_m). This assumes a partitioning model when we have this relationship.

The solute B^+ can bind independently to the stationary phase, according to the following equilibrium when no counterion is present^[28].



Assuming there is counterion present in the mobile phase the ionized solute and the counterion first form a complex, $(B^+C^-)_m$, in the mobile phase, and then the complex binds reversibly to the empty sites on the surface as $(B^+C^-)_s$. K_1 would be the ion-pairing constant and K_2 would be the distribution constant of the ion pair to the stationary phase. The corresponding equilibria is given by:



Horvath stated that the distribution ratio can then be written as follows:

$$D = \frac{[B^+]_s + [B^+, C^-]_s}{[B^+]_m + [B^+, C^-]_m} \quad [1-18]$$

Substitution for the mass action expressions for K_1 , K_2 , and K_o leads to

$$D = \frac{[B^+]_m K_o + K_2 [B^+, C^-]_m}{[B^+]_m + K_1 [B^+]_m [C^-]_m} \quad [1-19]$$

and since

$$[B^+, C^-]_m = K_1 [B^+]_m [C^-]_m \quad [1-20]$$

the following expression for k can be obtained by substitution

$$k = \frac{V_s}{V_m} * \frac{K_o + K_2 K_1 [C^-]_m}{1 + K_1 [C^-]_m} \quad [1-21]$$

This typically shows a rectangular hyperbolic relationship^[28] when the retention factor is plotted versus the concentration of the counterion in the mobile phase $[C^-]_m$.

2. Dynamic ion exchange

In this second limiting case, a complex between the ionized solute is formed directly with the counterion already bound to the surface of the stationary phase. It is postulated that hydrophobic alkyl ions (counter ions of the ion-association reagent) are adsorbed on the reversed phase packing, which then act as a dynamic ion exchanger^[8-9,33-35]. This ion association reagent that is strongly adsorbed on the nonpolar stationary phase forms a charged primary layer. This layer is electrostatically compensated by the eluent counterions. If the ionized solutes have the same charge as the primary layer they will be electrostatically repulsed by the primary layer and hence decrease their retention. However, if the oppositely charged solutes come in contact with the primary layer they will be retained by the primary

layer and increase their retention. Their retention will increase with increasing charge of the primary layer as a result of columbic interactions of the solute ions with the modified charged stationary phase. Increasing the concentration of the counterion may increase the charge of the primary layer.

Knox^[33] proposed that the equilibria may be expressed as follows:



C_m^- is the concentration of the hetaeron in the mobile phase, C_s^- is the concentration of the counterion bound to the surface, B_m^+ is the ionized solute in the mobile phase and $(B^+, C^-)_s$ is the surface concentration of the complex. If the hetaeron binds to the stationary phase surface according to the Langmuir isotherm, then the surface concentration of C_s^- can be represented as follows^[36]

$$[C^-]_s = \frac{K_3 [C^-]_m [C^-]^*}{1 + K_3 [C^-]_m} \quad [1-24]$$

K_3 is the equilibrium constant for binding of the counterion to the stationary phase surface and $[C]^*$ is the maximum surface concentration of bound hetaeron. Using the langmuir approach it is assumed a monolayer will be formed on the surface at high hetaeron concentration in the mobile phase.

By combining equations [1-23] and [1-24] the concentration of the complex $(B^+, C^-)_s$ can be expressed as

$$[B^+, C^-]_s = \frac{K_3 K_4 [B^+]_m [C^-]_m [C^-]^*}{1 + K_3 [C^-]_m} \quad [1-25]$$

Hence, the retention factor may be expressed for this dynamic ion exchange model may be obtained by combining equations [1-14,1-15,1-16], and [1-25]:

$$k = \frac{V_s}{V_m} \cdot \left\{ \frac{K_o [C^-]^* K_3 K_4 [C^-]_m [C^-]^*}{(1 + K_3 [C^-]_m)(1 + K_1 [C^-]_m)} \right\} \quad [1-26]$$

3. Dynamic complex exchange

If a surfactant such as alkyl sulfonate, C^- , are adsorbed onto the reversed phase packing material it may act as a dynamically coated ion exchanger^[37-42]. In contradiction to classical **ligand or ion-exchange chromatography**, the exchanger is not covalently bound but dynamically coated and the surface concentration of the function groups depends on the heteron concentration in the mobile phase. This dynamic ion exchange of ionized compound, B^+ , with another cationic species, Q^+ , (cation of the buffer or added salt, and/or co-ion of C^-) on adsorbed alkyl counterions (C^-) may be represented by the following equilibria:



Where K_3 is the equilibrium constant for the adsorbed counterion C^- and Q^+ on the stationary phase and K_4 is the constant for the exchange of the ionized solute with the adsorbed counterion on the stationary phase. As observed the co-ion of the same charge as the solute competes for the exchange sites of the adsorbed hydrophobic counterion to the stationary phase. The adoption of the Langmuir isotherm is usually **used for the explanation of the retention factor** as a function of concentration of counterion, C^- . If the Langmuir **approach** is used a fixed number of sorption sites have to exist on the stationary phase, W , indicating that when the surface is saturated with the counterion, C^- , no more counterion **will** be adsorbed by the stationary phase. Melin^[41] has showed from the Langmuir isotherm **the**

concentration of counterion, C^- , associated with the other cationic species presence, Q^+ can be written as follows:

$$[(C^-, Q^+)]_s = \frac{WK_3[Q^+]_m[C^-]_m}{1 + K_3[Q^+]_m[C^-]_m} \quad [1-29]$$

The distribution ratio of B^+ can be determined from the equilibria of K_0 , K_3 , and K_4 ,

$$D = \frac{[B^+]_s + [C^-, B^+]_s}{[B^+]_m} \quad [1-30]$$

Then the retention factor may be expressed as follows:

$$k = \frac{V_s}{V_m} * \left\{ K_0 + \frac{WK_3K_4[C^-]_m}{1 + K_3[Q^+][C^-]_m} \right\} \quad [1-31]$$

The retention dependence as a function of concentration will predict again a rectangular hyperbolic relationship, assuming K_0 does not vary with C^-_m .

Horvath^[28-29] has suggested two other dynamic complex exchange mechanisms: 1) Transfer of the ionized solute from the complex formed in the mobile phase to the bound counterion and consequent complex formation at the surface. 2) The ionized solute-counterion complex first binds to the surface that is already covered with bound counterion.

Using solely chromatographic measurements one usually cannot discern which model is describing the retention in the chromatographic system. It is possible depending on the conditions that one or more mechanisms are occurring and that the ion pairing in the mobile phase and dynamic ion exchange are just two limiting equilibria. In order to elucidate which model is prevalent non chromatographic techniques have been employed such as conductance measurements^[43-46]. However, several authors have correlated the retention of solutes with the adsorption isotherms of the hydrophobic counterions, suggesting a dynamic ion exchange model^[9,40,41,43,47].

The ion-exchange model may be prevalent for counterion of a substantial hydrophobicity such as long chain alkyl sulfates as opposed to the ion pair model for hydrophilic counterions ^[48]. Other authors ^[9,33,45] also suggested that with long chain counterion, the ion interaction does not take place in the mobile phase based on the following support ^[49]. A large number of column volumes have to be displaced for the ion-interaction reagent to break through. The retention factors decrease for solutes of the same charge as the ion-association reagents in the mobile phase. Conductance measurements have shown that ion-pair formation does not occur in the mobile phase. The degree of retention of the ionized solutes is directly proportional to the surface charge density generated by adsorption of the counterion.

Regardless of the mechanism of retention, other factors should be considered for ion-pairing applications. These may play an important role in the separation of ionizable analytes. The type, concentration and hydrophobic nature of counter ion and degree of interaction with the analyte may be varied. The pH of the medium, the type and concentration of the organic modifier and the ionic strength may also effect the retention as well as the selectivity. The temperature will also have an effect on the ion association even more so than in regular reversed phase chromatography.

pH and ion interaction

The pH has a significant effect on the ion interaction process and the chromatographic retention. It was shown before that, as bases or acids become ionized they are less hydrophobic and less retained in reversed phase HPLC. However, when an ion-interaction agent is present the ionized form of the analyte is retained longer. For example if no ion interaction agent is present at high pH, the RNH₂ molecule is strongly retained versus the

protonated NH_3^+ , so retention versus pH shows the characteristic sigmoidial curve shown in Figure 1-9 where the maximum retention is seen at high pH and minimum retention at low pH. However, if enough ion interaction reagent such as heptane sulfonic acid is added to cover the stationary phase completely, this would minimize the retention of the neutral molecule RNH_2 . The resulting negative charge on the stationary phase from the adsorbed $\text{C}_6\text{-SO}_3^-$, would cause a strong attraction of the positively charged, NH_3^+ . Now, when the analyte retention is plotted versus pH under the aforementioned ion interaction conditions, the maximum retention occurs at low pH (where the sample is completely ionized) and minimum retention occurs at high pH (sample in neutral form). This can be seen in Figure 1-11.

Ion-interaction reagent concentration

The reversed phase retention process could be converted to an ion-exchange process by changing the amount of ion-pair reagent adsorbed by the stationary phase as described previously. This can be done by varying the concentration of reagent in the mobile phase. The type of reagent also plays a role on the retention of the ionized analyte since the amount adsorbed at a particular concentration is dependent on the hydrophobicity of the alkyl portion. In order to calculate the surface concentration, $(P^*)_s$, the surface area of the packing

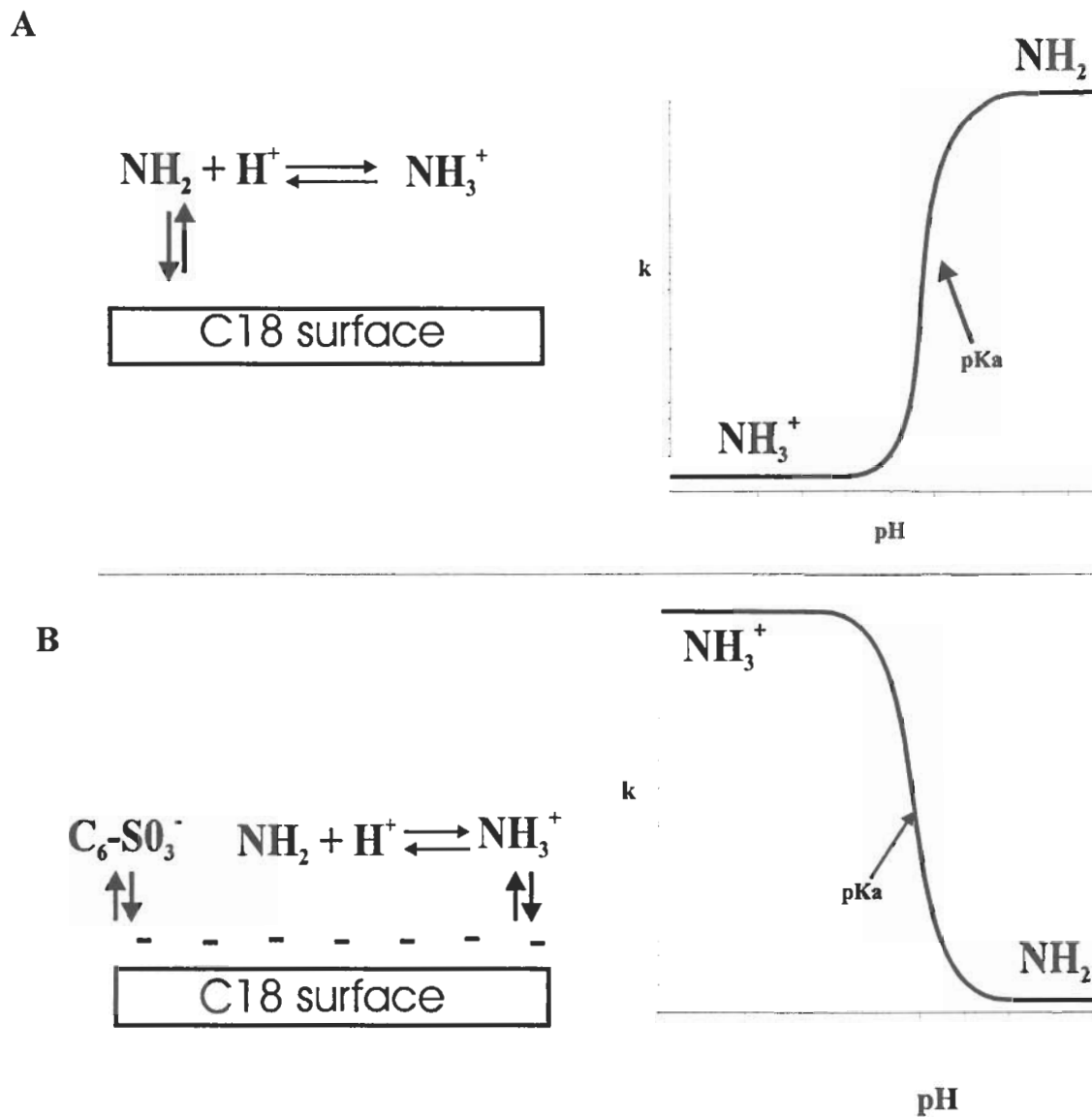


Figure 1-11. Effect of pH and ion-interaction reagent on the basic analyte retention A) top represents retention of a basic compound without the addition of an ion-interaction agent. B) bottom represents the retention of a basic analyte in the presence of an ion-interaction adsorbed on the reversed phase surface.

material must be measured. This can be done by the BET method ^[50] using low temperature nitrogen adsorption giving the corresponding surface area in m²/g. Then a weight of the material in the column is needed. The total surface area within the column can then be calculated by multiplying surface area from BET by the number of grams of silica adsorbent in order to give m². The amount of pairing agent adsorbed by the stationary phase from the standard eluents has been usually done by the break through method described by Knox and Hartwick ^[33]. Once the amount and surface area are determined the surface concentration ($\mu\text{mol}/\text{m}^2$) allows the calculation of the adsorption isotherms. This surface concentration is usually plotted versus the mobile phase concentration for different reagents and is indicative of the column uptake for different reagents.

When the concentration of reagent in the stationary phase (P^s) is plotted versus the concentration of reagent in the mobile phase (P^m) for two different reagents such as C6-sulfonate and C8-sulfonate it is proposed that the column uptake increases for higher reagent concentrations in the mobile phase, but then levels off since the column becomes saturated with the reagent. However, since the C8-sulfonate is more hydrophobic, it is retained more strongly and saturates the column at lower mobile phase reagent concentrations. Therefore, for a given reagent uptake by the column is obtained with a lower concentration of the more hydrophobic C8⁻ reagent as opposed to the less hydrophobic C6⁻ reagent shown in Figure 1-12.

The retention of the ionized compound is predominately determined by the uptake of the reagent and the resulting charge on the surface of the column. However, similar separations may be obtained by reagents of varying hydrophobicity when the reagent

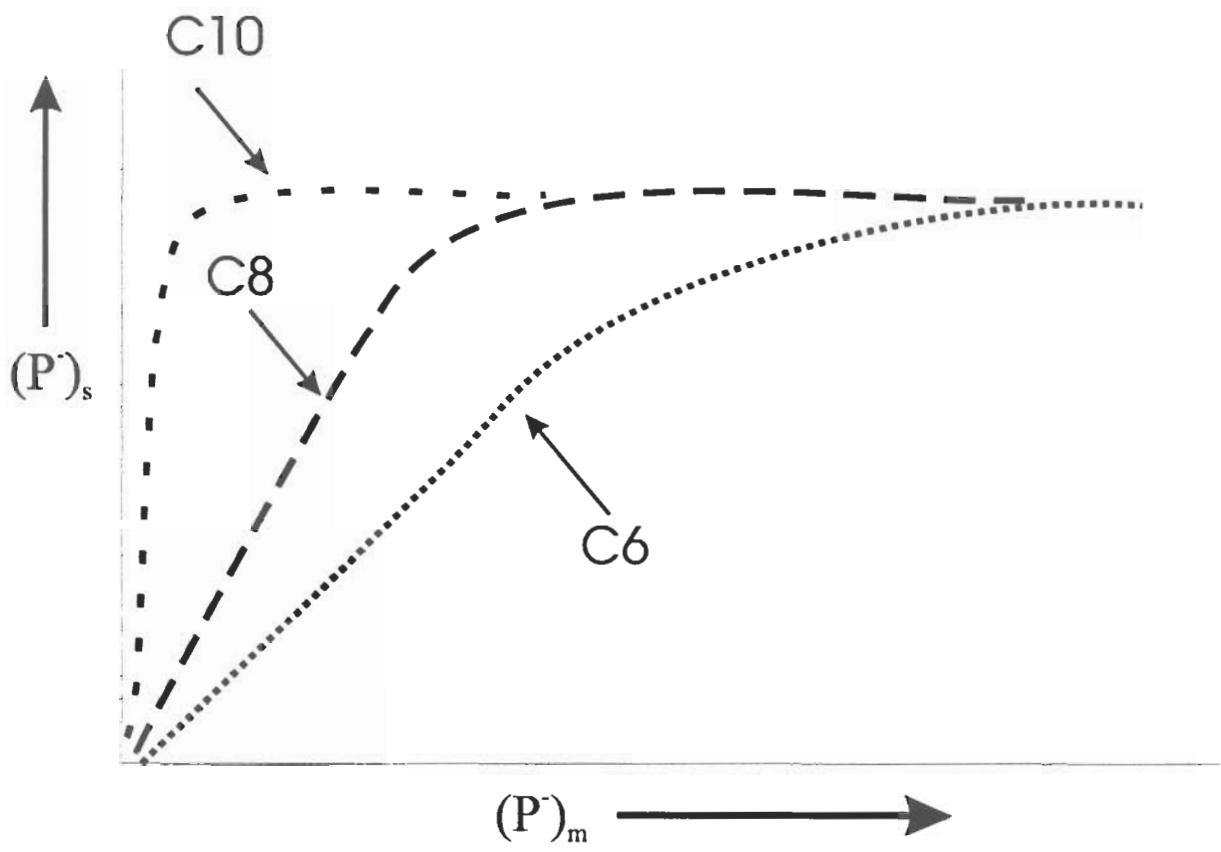


Figure 1-12. The sorption of ion pair reagent as function of concentration of reagents of increasing hydrophobicity (C6, C8, C10⁻ sulfonates)

concentration in the mobile phase is adjusted to give the same molar uptake by the column^[51]. However, this is only true when the counterion concentration is kept constant while the mobile phase concentration of the pairing ion, P_m is increased. Bartha^[52] investigated the effect on retention for adrenaline against the surface concentration, P_s , of different pairing ions with changing the counter ion concentration and a system with counter ion control ($Na^+=175$ mM). It was shown that when salt control was used the pairing ions having different chain lengths result in identical solute retention (solid lines) at a given P_s as opposed to the system with counter ion control (dashed lines) as seen in Figure 1-13.

Similar maxima and little dependence on the pairing ion chain length was also observed by Knox^[33] in a salt controlled methanol-aqueous buffer (20:80) eluents. Knox showed the dependence of retention factor for normetadrenaline as a function of concentration octyl, decyl and lauryl sulphates on ODS-Hypersil from standard eluent (water-methanol, 80:20 made 0.02M in phosphate buffer pH 6.0 and 0.05M in Na^+) at constant sodium ion concentration.

The sample retention increases as the ion-pair reagent concentration in the mobile increases until the column becomes saturated and sample retention levels off. For example, an ionic, hydrophilic sample compound BH^+ , retention may occur due to a result of the ion-exchange process previously shown. As the concentration of the ion pairing reagent in the mobile phase increases so does retention for this protonated basic compound. However, when the column becomes saturated with the reagent and obtains the maximum column charge and the sample retention levels off. Upon further increase in the reagent concentration, the retention may actually start to decrease from this maximum value. This

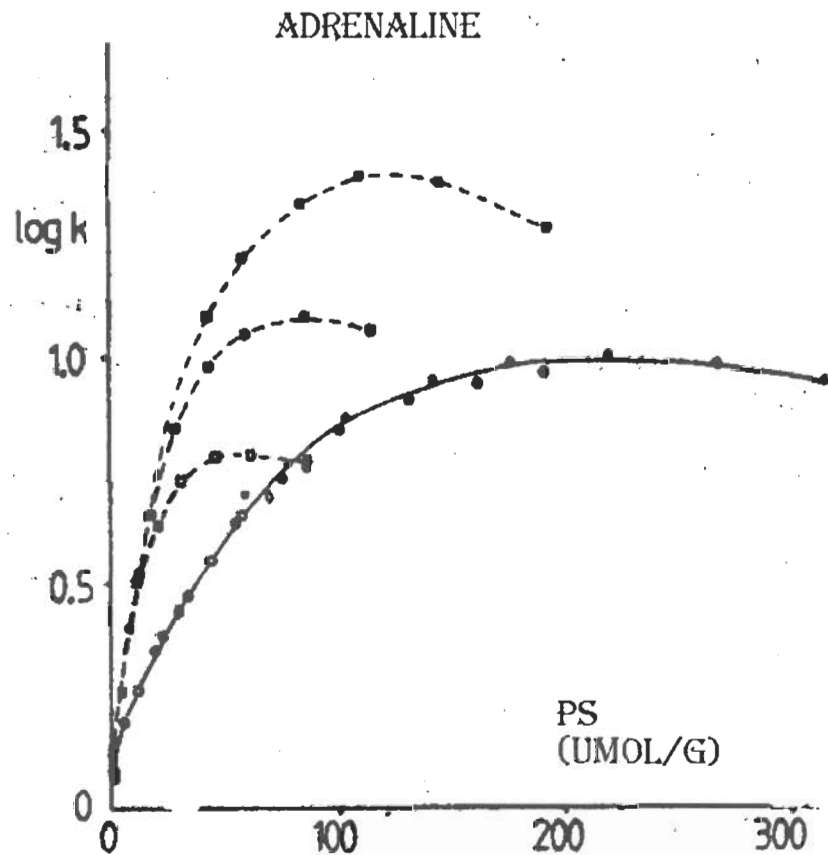


Figure 1-13. Log k data of adrenaline versus the stationary phase concentration, (P_s), of BuSO_3Na , HexSO_3Na and OctSO_3Na in eluents with changing (dotted lines) and constant sodium concentration (solid line). 25 mM H_3PO_4 -25mM NaH_2PO_4 buffer (pH=2.1), on 5 μm ODS-Hypersil at 25°C. The top dotted line is with OctSO_3Na and the bottom dotted line is with BuSO_3Na .^[52]

can be attributed to an increase in the counterion concentration (Na^+) which actually competes with the protonated base on the column.

Effect of salt, buffer concentration and ionic strength

Usually an increase in salt or buffer concentration will result in decreased retention for the compounds that are involved in ion pairing. This is because these compounds can also undergo ion exchange with the ion-pairing reagent. For example, Knox and Hartwick showed the effect of counter ion concentration Na^+ on the retention of protonated basic compounds. This was done by keeping the mobile phase concentration of the ion pairing agent octyl sulphate constant at 5 mmol dm^{-3} and varying the concentration of the sodium ion (10 – 70 mM) by addition of sodium chloride. It was shown for the cationic species, as the concentration of Na^+ increased the retention of the cationic species decreased and a neutral compound benzyl alcohol did not vary its retention.

Applications of ion-interaction chromatography

Therefore, both pH and ion-interaction reagent concentration can be varied to change the selectivity and resolution of desired components. In the next example, the contribution of sample ionization effects and ion-exchange process on sample retention for different bile acids on a reversed phase column is demonstrated. It has been shown that as the ion interaction reagent uptake increases on the column the ion exchange retention becomes more important, whereas reversed phase retention becomes less important ^[53]. In the Figure 1-14a the effect of mobile phase pH on the retention was plotted. In this experiment no ion interaction reagent was added. The same experiments were carried out again in the presence of 1mM tetrabutylammonium, TBA^+ , (corresponding to ~10% saturation of the column) shown in Figure 1-14b. The greatest retention in both experiments showed the highest

retention at low pH and the minimum retention at high pH. However, when the TBA^+ was added the retention at the higher pHs for these ionized acidic solutes showed greater retention compared to a system without ion interaction agent and was attributed to ion pairing. If a higher concentration of the ion interaction reagent was used, the ion interaction effect would have been increased leading to increased retention for the anionic solutes at the high pH. This would cause larger k values for the anionic solutes at high pH versus low pH. Also, with the addition of the ion interaction reagent there was reversal of elution order of several components.

Ion-interaction reagents have also been used not only for the analysis of purely acidic or basic mixtures but also for a composite of bases, acids and neutral compounds. The effect of ion-pair reagent concentration (octyl sulfate) is illustrated in Figure 1-15 for the separation of a positively charged bases Adrenaline (Adr^+), tyrosine amide (Tyr-amd^+), and normetadrenaline (Normet^+), negatively charged acid naphthalene sulfonate (NpS^-) and a neutral compound Benzyl alcohol (BzOH) on a C_{18} column ^[33]. When no ion interaction reagent is present all the protonated basic compound not only coelute but they all elute before the benzyl alcohol and the naphthalene sulfonate. However, upon addition of 14 mM octyl sulfate as the ion pair reagent in the mobile phase ($1.6 \mu\text{mol}/\text{m}^2$) all the basic compound elutes after the alcohol and are resolved from each other. The acidic compound now elutes before the alcohol and the alcohol shows a decreased retention. The increase in retention for the protonated basic solutes is due to ion pairing with the negative charge on the column. The decrease in retention of the NpS^- is due to its repulsion from the negatively charged adsorbed

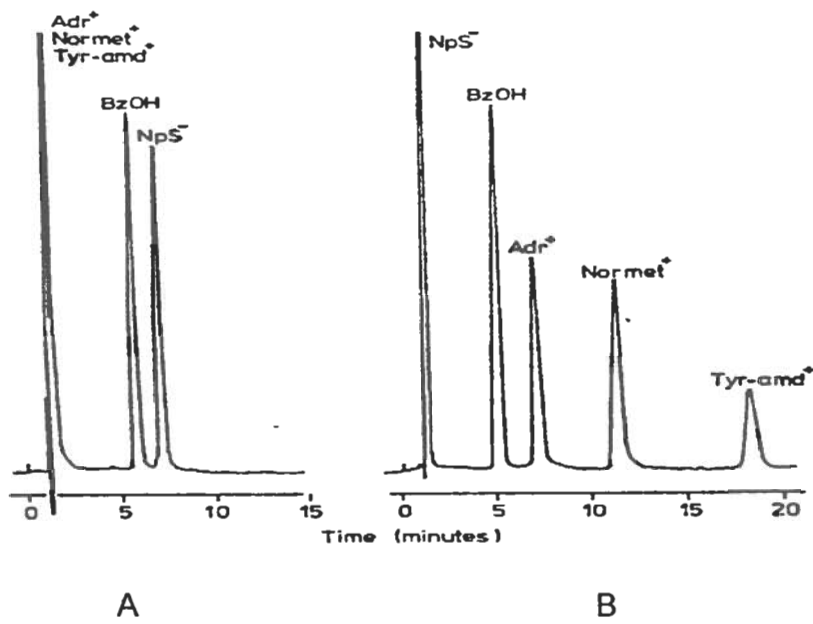


Figure 1-15. Effect of ion-interaction reagent octyl sulfate on the retention of acidic, basic and neutral analytes A) The retention of acidic, basic and neutral analytes when no ion-interaction agent present. B) with ion interaction agent present. ^[33]

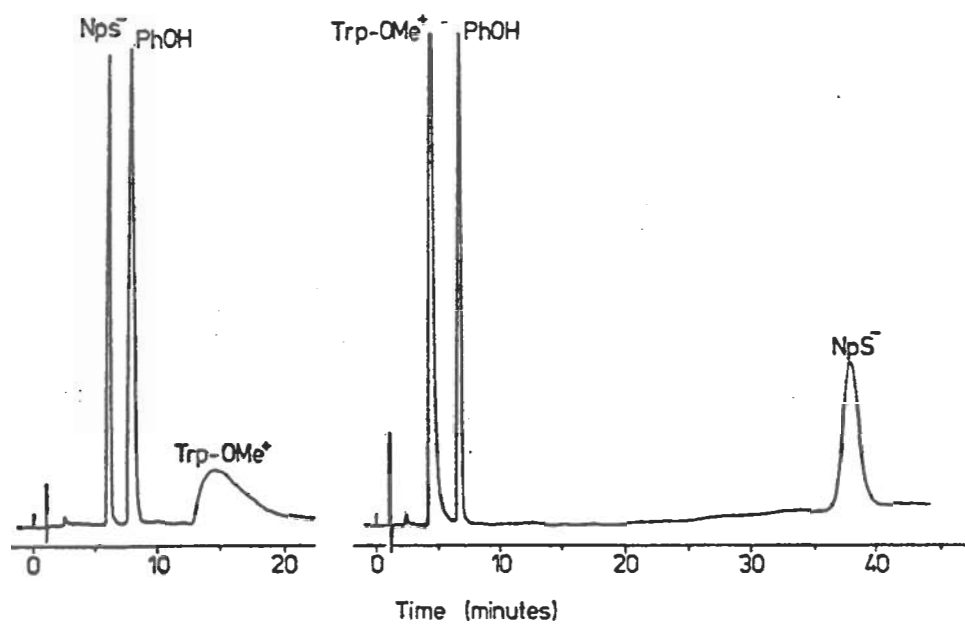
anion on the surface and other authors have seen similar results ^[41,45,48]. The slight decrease in retention for the neutral compound was attributed a lesser interaction with the stationary phase since the bonded phase becomes more polar through adsorption of the counterion ^[41].

These effects are not limited to negatively charged pairing ions. Figure 1-16 shows the effect of the addition of tetrabutyl ammonium iodide (TBAI) on the retention of the naphthalene sulfonic acid, phenol and o-methylester of tryptophan. A reversal of elution order occurs such that Trp-Ome⁺ decreased its retention and NpS⁻ increased its retention eluting after phenol, and the neutral phenol retention decreased slightly.

Effect of organic in reversed phase and ion-interaction chromatography

Generally the reversed phase behavior of nonionized solutes is governed by their hydrophobicity. Therefore the greater the hydrophobic nature of the solute the greater its retention. This is illustrated in Figure 1-17a at various organic compositions with acetonitrile/water and replotted $\ln k$ versus carbon number of alkylbenzenes in Figure 1-17b.

The retention of analytes in reversed phase can be adjusted by changing the mobile phase composition or solvent strength. The stronger the solvent strength of the eluent the less the retention for analytes in the reversed phase mode. Figure 1-18 shows how the retention of a homologous series of alkylbenzenes decreases upon increased concentration of the organic content. The total solvent strength depends on both the organic solvent and its concentration in the mobile phase. The solvent strength for typical organic solvents are MeOH < MeCN < THF. Therefore, an increased concentration of the weaker solvent will be needed to achieve comparable retention factors as with the stronger solvent. For example a greater concentration of methanol is needed to achieve similar retention as with acetonitrile.



A

B

Figure 1-16. Effect of the addition of tetrabutyl ammonium iodide (TBAI) on retention of acidic, basic and neutral analytes. A) The retention of acidic, basic and neutral analytes when no ion-interaction agent present. B) with ion interaction agent present. ^[33]

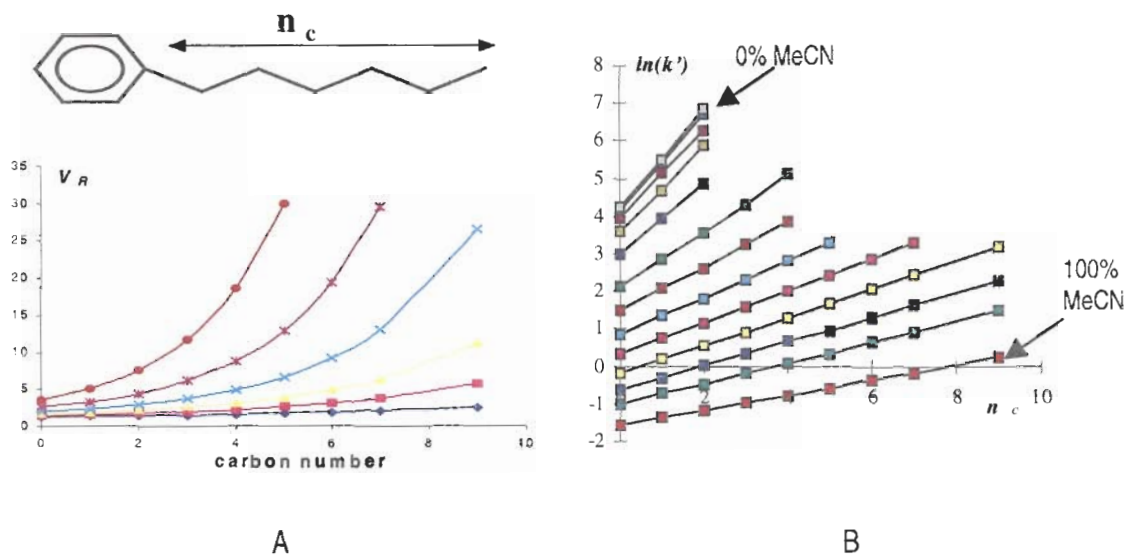
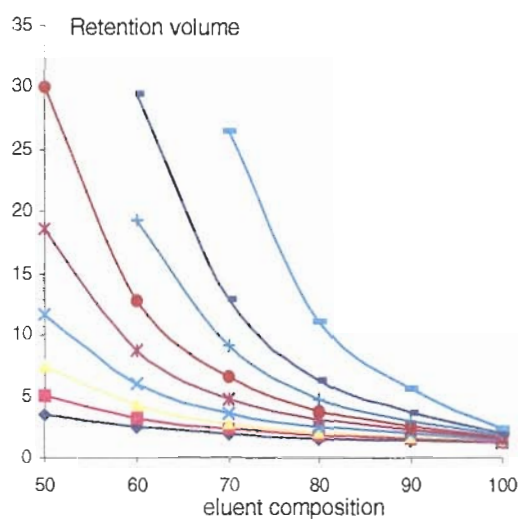
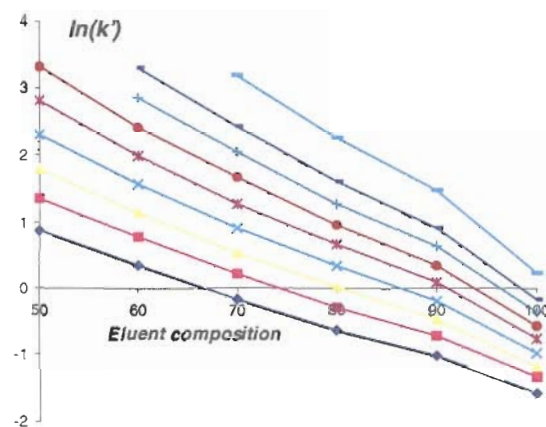


Figure 1-17. Retention volume versus carbon number for a homologous series of alkylbenzenes at various organic composition. A) Retention volume versus carbon number of alkyl chains at various organic compositions. B) \ln retention factor versus carbon number at various acetonitrile compositions: 0,1,5,10,20,30,40,50,60,70,80,90-100% from top to bottom.^[54]



A



B

Figure 1-18. Effect of analyte hydrophobicity and organic eluent composition in reversed phase chromatography. A) Retention volume of benzene – nonylbenzene at various eluent compositions. B) $\ln(k')$ versus the eluent composition of acetonitrile. Conditions: Acetonitrile :water, ambient, Prodigy ODS 2 ,3 μl injection, 25°C Analytes: Benzene – nonylbenzene, no octylbenzene. ^[54]

The dependence of k' on the volume percentage of the modifier is assumed to be linear^[55-56] and others claim a quadratic relationship^[57-58]. The quadratic approach, indicates the deviation from linearity is more pronounced at high concentrations of the modifier. However, there are some authors also have seen curvatures at low concentrations^[59]. Generally, there is no increase in selectivity with an increase of the organic modifier for neutral solutes.

In reversed phase ion pair chromatography, the influence of the solvent may have a greater effect on ionized solutes as opposed to neutral solutes. The influence of type (MeCN and MeOH) and amount of organic solvent on the retention of benzene and anionic solutes (dansyl glycine and dansyl serine) using decyltrimethylammonium as the counterion is shown in Figure 1-19^[60]. The ionized solutes undergoing ion-association chromatography are more effected by changes in the organic solvent composition that that of the nonionic solutes. As observed there is a greater decrease in the slope ($\ln k$ vs. % organic) for the dansyl amino acids in both the acetonitrile and methanol aqueous systems as opposed to benzene. There is a greater decrease of the slope in the acetonitrile system and this has been associated with the greater solvating power of the acetonitrile relative to methanol for quaternary ammonium ions. The slope of decrease for the benzene is comparable in both types of organic systems as opposed to the anionic solutes.

Another possible explanation could be related to amount and type of organic eluent adsorbed on the stationary phase. The mobile phase in reversed phase chromatography is most often a mixture of an aqueous phase and an organic modifier. It has been pointed out by Pyrdé^[61] there will be a region near the surface of the support that has a significantly

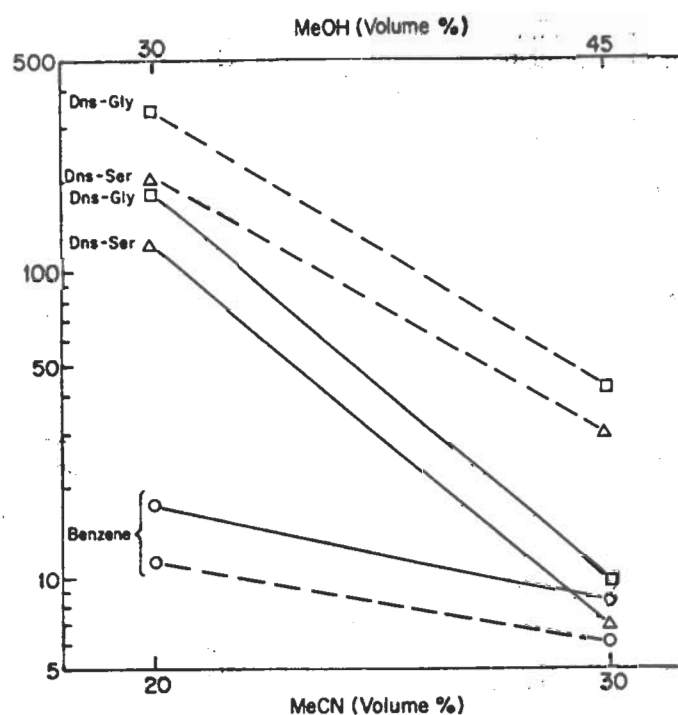


Figure 1-19. Influence of methanol (dotted line) and acetonitrile (solid line) on the retention of benzene and anionic solutes in ion-pair chromatography^[60]. Conditions: 5 mM of decyltrimethylammonium bromide, 0.13 M NH_4Ac , pH 7.1, MeOH and MeCN concentrations as listed. Stationary phase, Hypersil C_8

different composition from that of the bulk mobile phase. This suggests that with a more polar solvent there may be a decreased amount of organic adsorbed such as methanol as opposed to a more non-polar solvent such as acetonitrile. The organic solvent definitely plays a significant role in ion-pair extraction and with this in mind, the determination of the thickness of the adsorbed layer may lead to the elucidation of the different retention mechanism present in eluents containing organic solvents of different polarity. If the thickness of the adsorbed organic layer is sufficient this might suggest a liquid-liquid like extraction of the ion-pairs or individual ions from the pumped eluent composition into the adsorbed organic layer. The amount and thickness of adsorbed organic layers (MeCN, MeOH and THF) on various reversed phase adsorbents C₁- C₁₈ has been determined and is described in Chapter 5.

Summary

The research presented in this dissertation focuses on the retention of ionogenic species with main emphasis placed on basic compounds. For the analysis of basic species the influence of the pH and the type of modifier used to adjust that pH effects the retention to different degrees. The concentration of the counteranion of the acidic modifier also plays a role on determining the retention of the solutes. The concentration of the organic eluent not only plays a role on reducing analyte retention but can also effect its ionization state. This dissertation reviews past studies and applications and outlines the results of experiments performed in our laboratory to increase the selectivity and retention of basic compounds in reversed phase HPLC. It is also important to study the geometric parameters on which these analytes are analyzed in order to further gain insight into the retention mechanism. Also, within this thesis, the characterization of adsorbents, the determination of the void volume

and excess adsorption of organic eluent components is investigated. These detailed studies have been performed in order to develop and support an “adsorption-partitioning” mechanism, which may explain many anomalous effects usually observed in reversed phase chromatography and hopefully will benefit the chromatographic community.

Literature Cited
Chapter 1

1. C. Horvath, B.A. Preiss, and S.R. Lipsky, *Anal.Chem.*, **39**, 1967, 1422
2. C. Horvath and S.R. Lipsky, *J.Chromatogr.Sci.*, **7**, 1969, 109
3. C. Horvath, *High Performance Liquid Chromatography: Advances and Perspectives*, Academic Press, New York, Vol.2, 1980
4. L.R. Snyder, and J.J. Kirkland, *Introduction to Modern Liquid Chromatography*, Wiley-Interscience, New York, Chapter 9, 1974
5. J.T. Eleveld, H.A. Claessens, J.L. Ammerdorffer, A.M. van Herk, and C.A. Cramers, *J.Chromatogr. A*, **677**, 1994, 211
6. K.G. Wahlund, *J.Chromatogr.*, **115**, 1975, 411
7. B. Fransson, K.G. Wahlund, I.M. Johansson, and G. Schill, *J.Chromatogr.*, **125**, 1976, 327
8. J.C. Kraak, K.M. Jonker, and J.F.K. Huber, *J.Chromatogr.*, **142**, 1977, 671
9. J.H. Knox and J. Jurand, *J.Chromatogr.*, **125**, 1976, 89
10. L.R. Snyder, J.J. Kirkland, and J.L. Glach, *Practical HPLC Method Development*, Wiley-Interscience, New York, 1997, 342
11. P.R. Haddad and P.E. Jackson, *Ion Chromatography*, Elsevier, Amsterdam, 1990
12. H.F. Walton and R.D. Rocklin, *Ion Exchange in Analytical Chemistry*, CRC Press, Boca Raton, FL, 1990
13. R. Schwarzenbach, *J.Liq.Chromatogr.*, **2** (2), 1979, 205
14. R. Schwarzenbach, *J.Liq.Chromatogr.*, **334**, 1985, 35
15. S.H. Hansen, P. Helboe, and M. Thomsen. *J.Chromatogr.*, **368**, 1986, 39
16. R.J. Flanagan and I. Jane, *J.Chromatogr.*, **323** 1985 173
17. I. Jane, *J.Chromatogr.*, **111**, 1975, 227
18. K. Sugden, G.B. Cox and C.R. Loscombe, *J.Chromatogr.*, **149**, 1978, 377

19. B. Law, R. Gill, and A.C. Moffat, *J.Chromatogr.*, 301, **1984**, 165
20. J.A. Lewis, D.C. Lommen, W.D. Raddatz, J.W. Dolan, and L.R. Snyder, *J.Chromatogr.*, 592, **1992**, 183
21. Q. Wan, M.C. Davies, P.N. Shaw, and D.A. Barrett, *Anal.Chem.*, 68, **1996**, 437
22. P.J. Shoenmakers and R. Tijssen, *J.Chromatogr. A*, 656, **1993**, 557
23. R. LoBrutto, A. Jones, and Y. Kazakevich, *Proceedings of Eastern Analytical Symposium*, New Brunswick, New Jersey, November, **1999**
24. C. Horvath, W. Melander, I. Molnar, *Anal. Chem.*, 49 (1), **1977**, 142
25. I.M. Johansson, K.G. Wahlund and G. Schill, *J.Chromatogr.* 149, **1978**, 281
26. R. Gloor and E. Johnson, *J.Chromatogr.Sci.* 15, **1977**, 413
27. C.G. Horvath and S.R. Lipsky, *Nature*, 211, **1966**, 748
28. C. Horvath, W. Melander, I. Molnar, and P. Molnar, *Anal.Chem.*, 49, **1977**, 2295
29. W. Melander and C. Horvath, *J.Chromatogr.*, 201, **1980**, 211
30. E. Tomlinson, C.M. Riley, and T.M. Jeffries, *J.Chromatogr.* 174, **1979**, 89
31. C.M. Riley, E. Tomlinson, and T.M. Jeffries, *J.Chromatogr.* 185, **1979**, 197
32. D. Westerlund and A. Theodorsen, *J.Chromatogr.*, 144, **1977**, 27
33. H. Knox and R.A. Hartwick, *J.Chromatogr.*, 204, 3 **1981**
34. J.P.T. Kissinger, *Anal.Chem.*, 49, **1977**, 877
35. A.P. Konijnendijk and J.L.M. van de Venne, *Advances in Chromatography, Proceedings of the 14th International Symposium*, Lausanne, September 22-28, **1979**, 123
36. W.R. Melander and C. Horvath, *High Performance Liquid Chromatography*, Academic Press, New York, Vol 2., **1970**, pp.231-240
37. A.T. Melin, Y. Askemark, K.G. Wahlund, and G.Schill, *Anal.Chem.*, 51, **1979**, 976
38. J.H. Knox and G. Laird, *J.Chromatogr.* 122, **1976**, 17
39. J.P. Crombeen, J.C. Kraak, and H. Poppe, *J.Chromatogr.* **1980**, 243

40. R.P.W. Scott and P. Kucera, *J.Chromatogr.* 175, 1979, 51
41. A.T. Melin, M. Ljungcrantz and G. Schill, *J.Chromatogr.* 185, 1979, 225
42. R.S. Deelder, H.A.J. Linssen, A.P. Konijnondijk, and J.L.M. van de Venne, *J.Chromatogr.*, 185, 1979, 241
43. A. Packer and M. Dowbrow, *Proc. Chem. Soc.*, 1962, 220
44. D.G. Oakenful and D.E. Fenwick, *J.Phys.Chem.*, 78, 1974, 1759
45. B.A. Bidlingmeyer, S.N. Deming, W.P. Price, Jr., B. Sachok, and M. Petrusek, *Advances in Chromatography, Proceedings of the 14th International Symposium*, Lausanne, September 22-28, 1979
46. W. Melander, K. Kalghatgi, C. Horvath, *J.Chromatogr.*, 301, 1980, 201
47. C.P. Terweij-Groen, S. Heemstra, and J.C. Kraak, *J.Chromatogr.* 161, 1978, 69
48. J.H. Knox and J. Jurand, *J.Chromatogr.*, 149, 1978, 297
49. A.M. Krstulovic, and P.R. Brown, *Reversed Phase High Performance Liquid Chromatography*, Wiley, New York, 1982, pp.159-165
50. S. Brunauer, P.H. Emmet, E.J. Teller, *Am.Chem.Soc.*, 60, 1938, 309
51. L.R. Snyder, J.J. Kirkland, and J.L. Glajch, *Practical HPLC Method Development*, Wiley-Interscience, New York, 1997, p.345
52. A. Bartha, H.A.H. Billiet, L. de Galan, and G. Vigh, *J.Chromatogr.*, 291, 1984, 91
53. D.S. Lu, J. Vialle, H. Tralongo, and R. Longera, *J.Chromatogr.*, 268, 1983, 1
54. Y. Kazakevich, *Proceedings of Pittcon Atlanta Conference*, Atlanta, Georgia, March, 1995
55. L.R. Snyder, J.W. Dolan and J.R. Grant, *J.Chromatogr.*, 165, 1979, 3
56. E. Soczewinski, and M. Waksmundzka-Hajnos, *J.Liq.Chromatogr.*, 3, 1980, 1625
57. P.J. Schoenmakers, H.A.H. Billet, R. Tijssen and L. de Galan, *J.Chromatogr.*, 149, 1978, 519
58. P. Jandera, H. Colin, and G. Guiochon, *Anal Chem.*, 54, 1982, 435

59. M.J.M. Wells and C.R. Clark, *J.Chromatogr.*, 235, 1982, 31

60. C. Horvath, High Performance Liquid Chromatography, Advance and Perspectives, Academic Press, New York, Vol.1, 1980, p.186

61. A. Pyrde, *J.Chromatogr.Sci.*, 12, 1974, 486

59. M.J.M. Wells and C.R. Clark, *J.Chromatogr.*, 235, 1982, 31
60. C. Horvath, High Performance Liquid Chromatography, Advance and Perspectives, Academic Press, New York, Vol.1, 1980, p.186
61. A. Pyrde, *J.Chromatogr.Sci.*, 12, 1974, 486

Chapter 2

Effect of organic solvent on the pK_a of ionogenic solutes

Summary

The goal of this chapter is to describe the influence of the organic solvent, on the ionization state of basic and acidic solutes in aqueous/organic medium. The correct determination of the pH in this medium in which the ionogenic solutes (species that have ionizable functionalities) are ionized is needed for the proper determination of the pK_a . The pK_a values determined chromatographically at different organic/aqueous eluent compositions were compared to those determined by potentiometric titrations in water. The chromatographic parameters varied in these studies were the type and amount of pH and organic modifier. The chromatographically determined pK_a of basic compounds in the presence of organic medium showed lower values when plotted versus the pH of solely the aqueous phase than corresponding potentiometric pK_a values. This was attributed to changes in the pH of the aqueous medium upon addition of the organic eluent. For acids, the chromatographic pK_a values were higher than their potentiometric values and the same rationale was assumed. We provide an explanation that allows determination if a pK_a shift occurred or if the shift is solely attributed to a pH shift of the aqueous upon the addition of organic to the eluent. A literature review describing the chromatographic determination of the pK_a and its relation to the pK_a determined by potentiometric titration is also provided.

Historical

The ionization state of solutes in aqueous and organic/aqueous medium has been described extensively in the literature. The basis for determining ionization constants in aqueous/organic medium was that substances, which were poorly soluble in water, could be

highly soluble in a volatile solvent. Therefore the determination of the ionization constant in a mixture of two solvents was needed. The variation in pK_a in aqueous/organic medium will vary from solvent to solvent, due to a change in dielectric constant; specific ion-solvent effects; and suppression of ionization. In solvents of lower dielectric constant, the ionic strength, also plays a larger role in varying the ionization constants.

It was found by Mizutani (1925) ^[1] that alcohols weaken both acids and bases; the pK_a of an acid was raised by about 1.0 pH unit and the pK_a of a base was lowered by about 0.5 unit in 60 % methanol compared to a 100% aqueous medium. The method they used to determine the pH in the aqueous/organic solvent utilized calibration of the pH meter with standards in aqueous/organic mixtures of varying ionic strength. Hall and Sprinkle ^[2] also determined an average decrease 0.54 pK_a units for several aliphatic and aromatic amines from 0 - 50% ethanol. Gutbezahl and Grunwald ^[3] observed a decrease in the basicity of aniline and its N-methylated derivatives from 0 –65% ethanol where the effect of ethanol was the least on the non-methylated substances up to 35%. The decrease in pK_a for these compounds in methanol was also observed by Bacarella et. al. ^[4] up to 80% methanol and upon further increase of the organic content the pK_a 's of the basic species increased, as can be seen in Table 2-I. These results indicate that there is indeed a true pK_a shift. This pK_a shift may be attributed to deviations from classical ion-dipole behavior including specific ion solvation effects associated with basic compounds. The basicity of the compounds changed to different degrees after increasing the organic content and can be seen in Figure 2-1 and Figure 2-2. The change in basicity may play a significant role for the chromatographic analysis of basic compounds and enhancement of the selectivity.

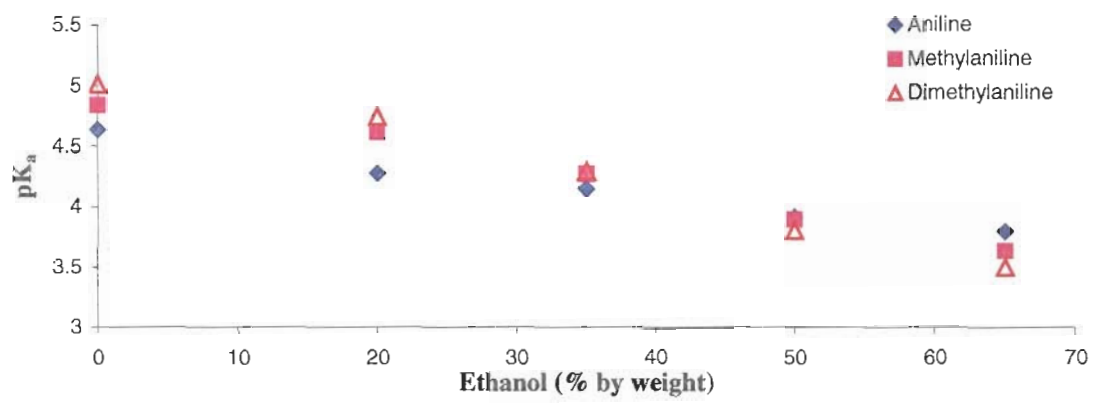


Figure 2-1. Plot of pK_a versus increasing ethanol concentration of three aniline structurally related basic compounds ^[5].

Table 2-I
 pK_a values determined in hydroorganic mixtures for acidic and basic compounds ^[4]

	pK_a values in Methanol/Water at 25.0 °C						
	(Methanol, vol%)						
	0	20	40	60	80	95	100
Aniline	4.62	4.463	4.322	4.168	4.068	4.613	5.804
Methylaniline	4.848	4.698	4.476	4.177	3.9	4.149	5.27
Dimethylaniline	5.15	4.964	4.726	4.306	3.821	3.953	5.02
Acetic acid	4.756	5.011	5.334	5.808	6.5	7.858	9.72
Benzoic acid	4.201	4.514	4.967	5.536	6.286	7.473	9.38
Dielectric constant	78.5	69.2	59.6	50	40.2	33.6	31.5
$1/\epsilon$	0.0127	0.0145	0.0168	0.0200	0.0249	0.0298	0.0317

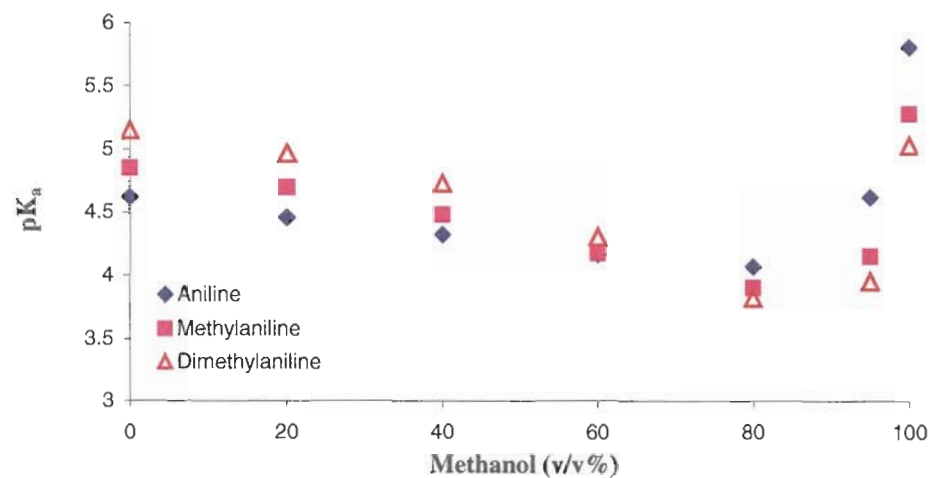


Figure 2-2. Plot of pK_a versus increasing methanol concentration of 3 aniline structurally related basic compounds ^[4].

McCalley observed decreased pK_a values for pyridinal basic solutes in mixtures of MeCN:Water (40:60, v/v), Methanol:Water (55:45, v/v) and THF:water (25:75, v/v%)^[6]. He used a UV spectrophotometric method based on the increased absorptivity of the pyridium cations over that of the unprotonated species to determine the pK_a . Figure 2-3 shows the absorbance spectra of 2,4 dimethylpyridine in methanol-buffer solutions at pH 1.6 and 9.0 (55:45, v/v), and the absorbance was measured at a wavelength of the compounds where the largest difference in absorptivity of the species occurred.

McCalley plotted the absorbance versus the pH of the aqueous phase before the addition of organic and versus the pH^* of the aqueous/organic mixture (pH values obtained with glass electrodes standardized with aqueous buffers in alcohol-water mixtures minus a correction term ^[7]) for his corresponding buffer from the literature. A significant shift in the pK_a was seen when the retention factor was plotted versus the pH of the aqueous phase for both compounds. These pK_a values were estimated to be 3.2 for pyridine and 4.6 for 2,4 dimethylpyridine (Figure 2-4 a and Figure 2-4c). To determine if this was indeed a true pK_a shift or solely a pH shift of the aqueous buffer he plotted the retention factor versus the pH^* of the eluent (Figure 2-4 b and Figure 2-4d). The pK_a determined in this manner was 4.3 for pyridine and 5.8 for 2,4 dimethylpyridine indicating that there is indeed a true pK_a shift. The pK_a values determined by potentiometric titration in water are 5.17 for pyridine and 6.74. This showed a change in pK_a (ΔpK_a) of 0.87 pH units for pyridine and a change in the pK_a (ΔpK_a) of 0.94 pH units for 2,4 dimethylpyridine in methanol/water eluent. The pK_a values determined by plotting retention factor (k) versus the pH^* of the aqueous/organic mixtures in three different eluent systems: MeCN/Water, THF/Water, and MeOH/Water, Table 2-II.

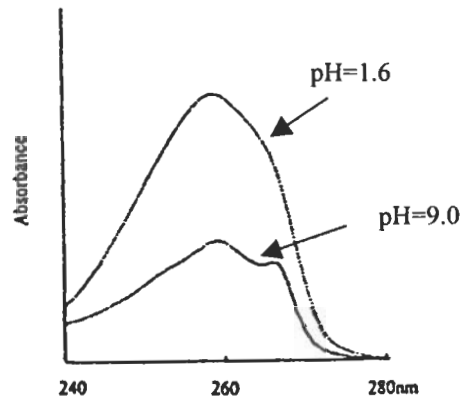


Figure2-3. Absorbance spectra of identical concentration of two basic analytes. Absorbance spectra at identical concentrations 2,4 Dimethylpyridine in methanol-phosphate buffer pH 1.6 (55:45, v/v) upper curve and methanol-phosphate buffer pH 9.0 (55:45,v/v) lower curve. ^[6]

Table 2-IIUV absorbance 255nm for pyridine and UV absorbance 259nm for 2,4-dimethylpyridine ^[6]

Compound	MeCN:	THF	Methanol:
	Phosphate buffer <i>40:60</i>	Phosphate buffer <i>25:75</i>	Phosphate buffer <i>55:45</i>
	pK _a	pK _a	pK _a
Pyridine	3.9	4.1	4.3
2,4-dimethylpyridine	5.0	5.5	5.8

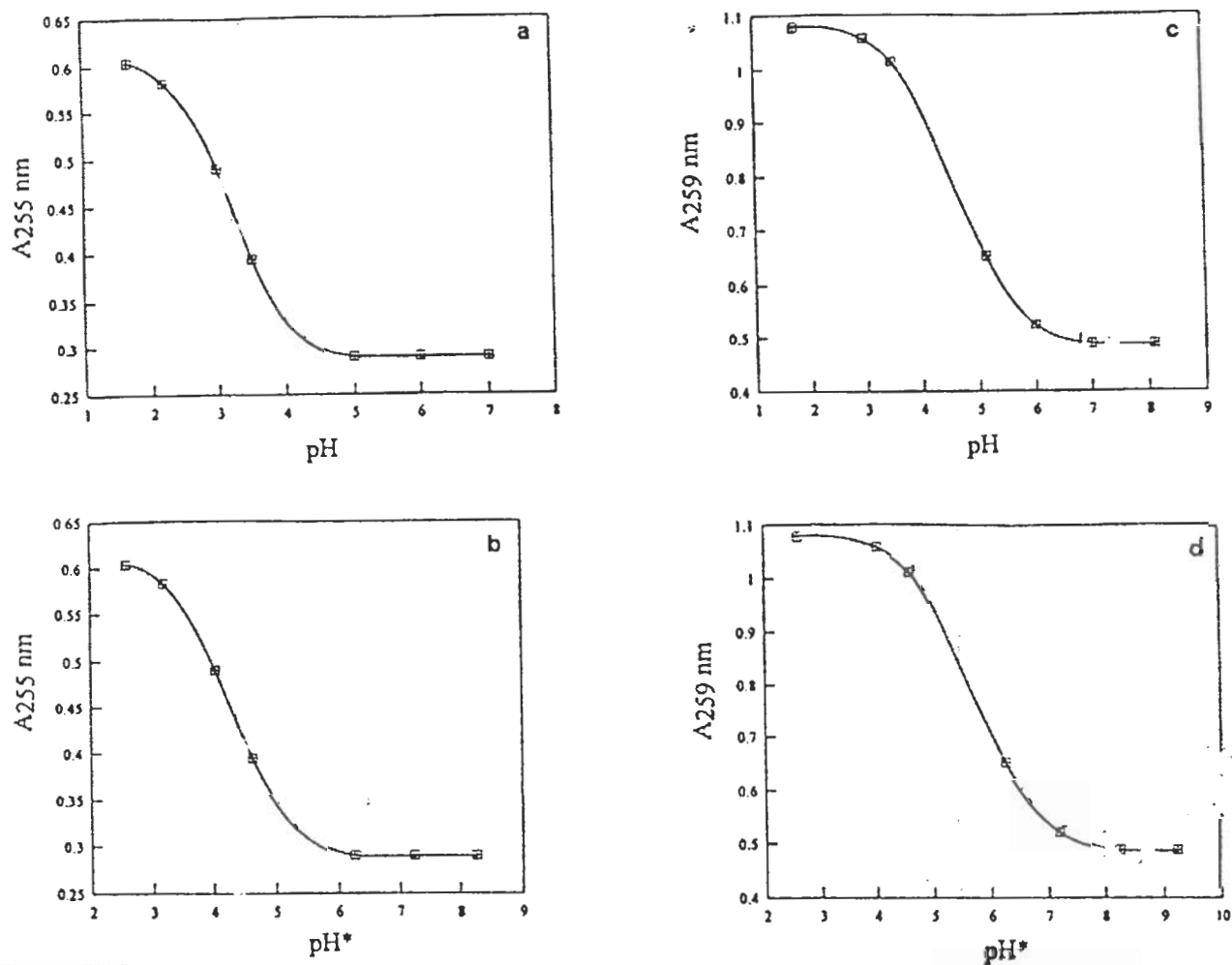


Figure 2-4. Plot of the UV absorbance against the pH. a) pyridine in methanol-phosphate buffer (55:45, v/v); pH measured before organic solvent addition. b) pyridine (same concentration) in methanol-phosphate buffer (55:45, v/v); pH* measured after organic solvent addition. c) 2,4 dimethylpyridine in methanol-phosphate buffer (55:45, v/v); pH measured before organic solvent addition. d) 2,4 dimethylpyridine (same concentration) in methanol phosphate buffer (55:45, v/v); pH* measured after organic solvent addition. ^[6]

At pH 7 it can be seen from Figure 2-4d that the 2,4 dimethylpyridine is predominately in its neutral form in the methanol-phosphate buffer pH 7.0 (55:45, v/v) which is unexpected considering its pK_a in water. These results suggest that the ionization of the basic compound was suppressed. Solutes to be chromatographed by HPLC should be in their completely ionized or neutral forms. However, even if one corrects for a shift in pH of the aqueous solvent, this still may not lead to its corresponding pK_a in the aqueous/organic mixture. This may be attributed to specific solvation effects, including preferential solvation of the organic eluent components on the analyte. The environment in the vicinity of the solute may be different than that of the bulk eluent environment. Also, one has to consider that the ionization of the base at the same pH in aqueous medium as opposed to organic/aqueous medium base may not be equivalent. The ionization of the base may be suppressed in the organic/aqueous medium. In summary there are three effects that may explain why the pK_a in aqueous organic solvents are not the same as determined by titration in water: 1) pH of the aqueous/organic eluent, 2) preferential solvation, and 3) suppression of the ionization of the basic compound or acidic compound in solution.

Change in dielectric constant

The attraction between two charges in a medium may be effected by the dielectric constant of the medium. By definition the dielectric constant can be described as follows: ^[8] In a vacuum there is force along the direction between two charges, q_1 and q_2 , separated by a distance r .

$$F = \frac{q_1 q_2}{4\pi\epsilon_0 r^2} \quad [2-1]$$

where F is the force, C is the unit of charge or coulomb, and ϵ_0 is the vacuum permittivity. There is an attraction between the two charges if they are opposite in sign and F is negative and there is a repulsion if they have the same sign and F is positive. However, to describe the force of attraction in a medium other than vacuum the force is represented by:

$$F = \frac{q_1 q_2}{4\pi\epsilon_0 \epsilon r^2} \quad [2-2]$$

where ϵ is the relative permittivity or dielectric constant of that medium. The work, w_e , is the work needed to bring a charge, q_1 , from infinity to a distance, r , from a charge q_2 in a vacuum can be represented as the integral of $-F dr$ from infinity to r where:

$$w_e = \frac{q_1 q_2}{4\pi\epsilon_0} \cdot \frac{1}{r} \quad [2-3]$$

The dielectric constant is expected to influence the position of the equilibrium in ionic secondary chemical equilibria. This can be seen if one looks at the Gibbs transfer energy using water as the selected reference solvent: ^[9]

$$\Delta G_i^o = \left\{ \frac{NZ_i^2 e^2}{2r_i} \right\} * \left\{ \left[\frac{1}{\epsilon_0} - \frac{1}{\epsilon_w} \right] \right\} \quad [2-4]$$

where N is Avogadro's number, e the electronic charge, Z the charge on the ion, and r_i the spherical radius of i . According to the Born model^[10], a sphere of radius r_i and charge $z_i e_0$ is considered to be equivalent to an ion of radius r_i and charge of $z_i e_0$. It can also be viewed as the sum of the work done to discharge an ion in vacuum and the work done to charge it up in the solvent of a certain dielectric constant. The solvent has an ability to disperse electrostatic charges via ion-dipole interactions, which are inversely proportional to the dielectric constant of the solvent. The dielectric constants of some common eluents are acetonitrile, 37.5, methanol, 32.6, water, 78.5 and THF, 7.6. Therefore, the pK_a of solutes may be affected by

change of the type or amount of organic since the dielectric constant is being varied. The Born treatment ^[10] may be used to estimate the change of pK_a with dielectric constant. The dissociation constant of a substance HA, in a solvent S may be related by means of the Born model to the relative permittivity of the medium, ε, by equations: ^[11]



$$pK_a = pK_a^o - pK_{HS^+}^o - \frac{e^2(z-1)}{2.3r\epsilon kT} \quad [2-6]$$

where K_a^o and $K_{HS^+}^o$ are the intrinsic dissociation constants of the substance and the protonated solvent in the vacuum, respectively, r is taken as standard state and is the average radius of the ions; e is the electronic charge; z is the charge of the species HA; and kT is the energy of thermal agitation. Equation 2-6 shows that if $z \leq 0$, the dielectric constant decreases, and K_a decreases (higher pK_a value). Equation 2-6 also shows that K_a does not change if $z = 1$ and increases when $z > 1$. Typically the case for bases is that the charge does not increase and z can be taken to equal one. Therefore, any changes in the pK_a shift may not be associated with change in the dielectric constant. For neutral or anion acids, on the other hand, the change in the dissociation constant can be attributed to the change in dielectric constant since the value of z is modified depending upon the acid analyte ionization. Equation 2-6 can be rewritten for neutral and anionic acids as:

$$pK_a = a + \frac{b}{\epsilon} \quad [2-7]$$

where a and b are constants for a given substance, and the radius of the ions, r , is assumed to be independent of the solvent composition. Qualitatively this treatment shows that the pK_a of a certain species should increase with decreasing dielectric constant by $(1/\epsilon)$ linearly. Using

Barcella's ^[4] data we did see the pK_a increase linearly for acetic and benzoic acids with increasing methanol content up to about 70%, Figure 2-5. However, for basic compounds this effect was not seen, and there is no relation of the dielectric constant with increasing organic content, Table 2-I.

Bosch ^[12-13] determined pH in methanol-water mixtures based on a proposed equation using the ionic strength; the activity coefficient and the dielectric constant of the mixed organic/aqueous solutions; and the solute's preferential solvation and methanol-water interactions. These pH values obtained were plotted versus the chromatographic retention factors the pK_a of several acidic species (benzoic acid, and isomeric series of nitrobenzoic acids) were obtained. They ^[12-13] state that this procedure is much easier than potentiometric measurement of the pH value determined in the binary solvent used. We compared the data from Barcella ^[4], who determined the pK_a using potentiometric titration of the benzoic acid in methanol/water mixtures using hydro-organic standards of the same composition, with the data from Roses, who used a theoretically based equation for the calculation of the pH values and chromatographically determined pK_a . Surprisingly, the pK_a shift with the increase in organic correlate very well between the two groups' data.

Table 2-III

pK_a values determined by using theoretical approach based on preferential solvation and on methanol-water interaction ^[14]

	pK_a values in Methanol/Water at 25.0 °C (Methanol, vol%)		
	40	60	80
Benzoic acid	4.99	5.48	6.22
2-nitrobenzoic acid	3.02	3.67	4.32
3-nitrobenzoic acid	4.11	4.58	4.97
4-nitrobenzoic acid	4.04	4.47	4.94
Dielectric constant	59.6	50	40.2
$1/\epsilon$	0.0168	0.0200	0.0249

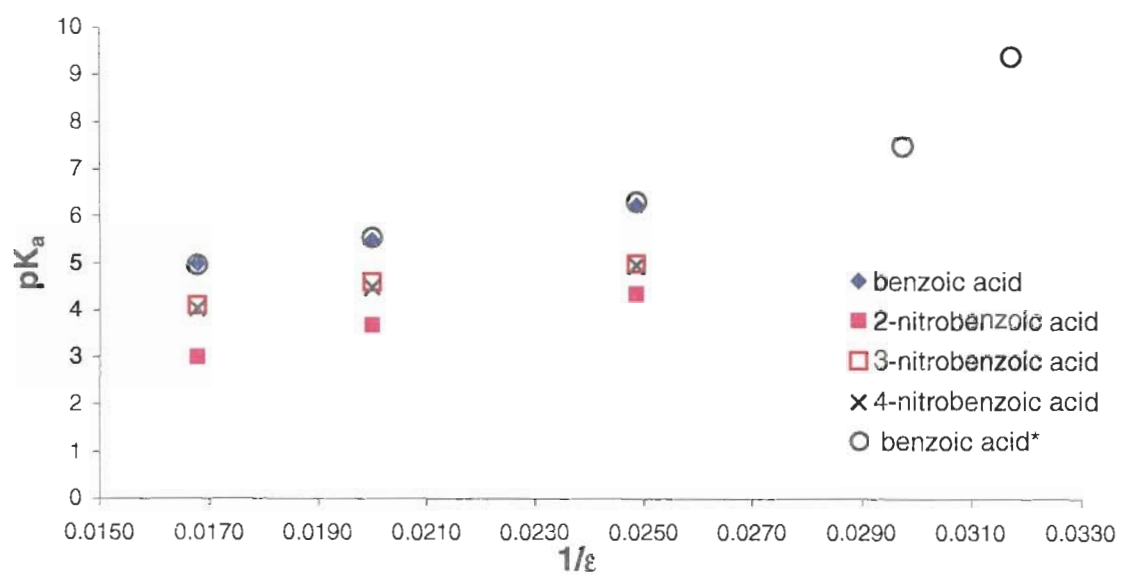


Figure 2-5. Comparison of pK_a determined values using potentiometric methods and theoretical approach. *Barcella^[4] data for benzoic acid using potentiometric titration in methanol/water mixtures and using calibration with hydroorganic standards of the same composition. pK_a for all other compounds is calculated using equation from Roses and Bosch.^[14]

The variation in the pK_a values of acids with solvent composition showed that the pK_a values of acids increase with greater concentrations of methanol, in the solvent according to the model proposed by Roses^[14]. The dissociation of acids in methanol-water and acetonitrile-water is governed by electrostatic interactions and solvation effects^[15]. Therefore, if the organic solvent is present in increasing proportions, there is a decrease in the dielectric constant and this causes a consequent disturbance of the dissociation process leading to the suppression of ionization. The main support for this is that when an acid dissociates, charges are being created [$HA \rightleftharpoons H^+ + A^-$ or $HA^{n-} \rightleftharpoons H^+ + A^{(n+1)-}$] and this could dramatically effect the dissociation process. The dissociation of acids and the electrostatic interaction overwhelms the specific solvation effects. The pK_a value of the acids increases with percent methanol (shown by Roses^[14]) for benzoic acids and with percent acetonitrile (shown by Barbosa^[15] in Figure 2-6) for carboxylic acids.

Bosch and Roses had shown the variation in the pK_a values of polyprotic acids is dependent not only on the solvent composition, but also on the type of acid. They attributed this to the different solute properties of the acids: charge, volume, polarity, and hydrogen acceptor and bonding capabilities. The variation in pK_a , at 50% methanol/water mixture with type of acid, can be observed by comparing the acid's pK_a determined in pure water: phosphoric acid ($\Delta pK_{a1}, 1.10$), and acetic acid ($\Delta pK_{a1}, 0.77$). Contrary to acidic compounds, basic compounds generate no charges upon ionization, and it was speculated that the dielectric constant of the medium does not effect the dissociation process. Actually, we saw previously with the data from Barcella^[4] and Grunwald^[5] that there was no

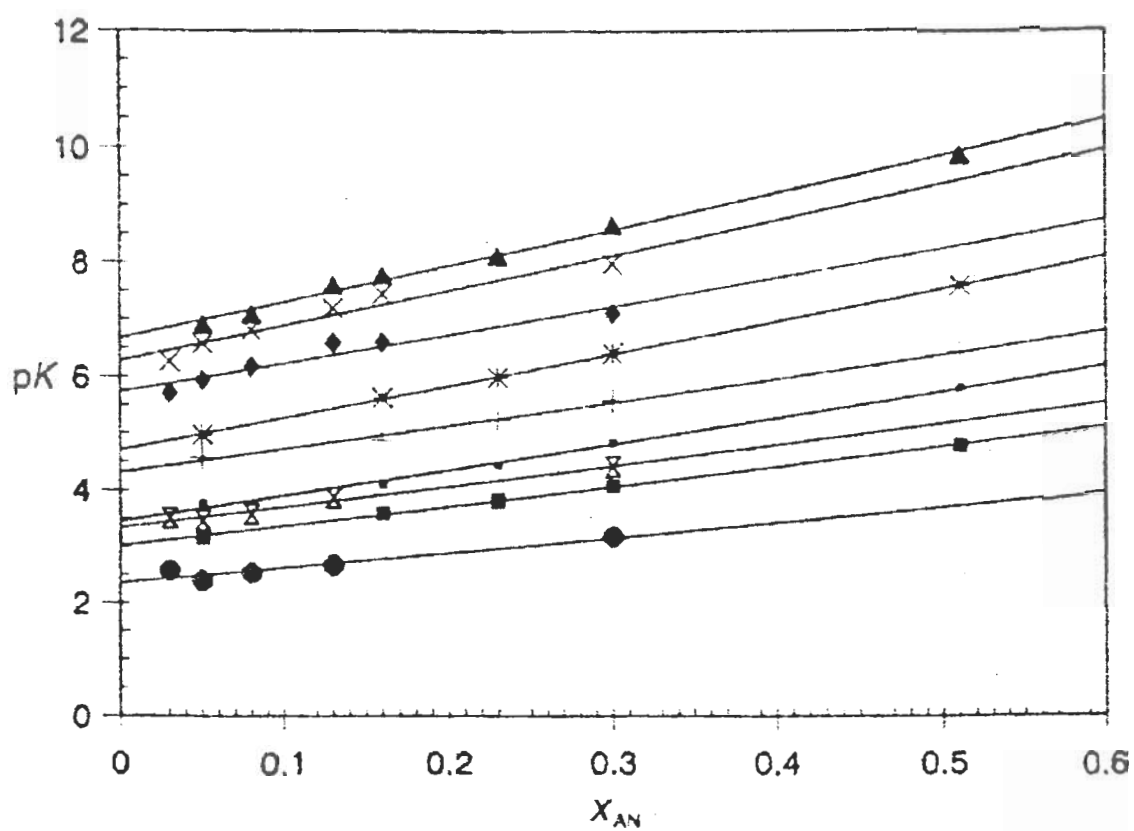


Figure 2-6. Carboxylic acids pK_a values versus mole fraction of acetonitrile^[15], x_{AN} , in acetonitrile-water mixtures. Ethacrynic acid (square), furosemide (+), acetic acid (*), phthalic acid (larger square), norfloxacin (x), fleroxacin (diamond), flumequine (triangle), triglycine (double triangle) and citrulline (circle).

correlation of the shift of the pK_a with the decrease of the dielectric constant (Table 2-I). However, the dissociation of a basic compound such as anilinium may be dependent upon the solvation of the analyte by the eluent components. The difference in basic analyte solvation may explain some of the anomalies obtained for the pK_a s (decrease of the pK_a) of basic compounds at high methanol or ethanol concentrations. The solute in the eluent may interact to varying degrees with solvents in the eluent and may be preferentially solvated by them indicating that the analyte solvation shell is actually different than the eluent composition. This may explain why there is not a consistent change in pK_a per certain percentage of organic modifier between different classes of basic compounds. The steric nature and well as the analyte intrinsic properties in a certain aqueous/organic environment will effect the analyte solvation ^[12]. It has been shown that preferential solvation by water exists in acetonitrile-water mixtures ^[16] and is related to the structural features of these mixtures ^[17-18]. Barbosa ^[15] had shown that when the mole fraction of acetonitrile is less than 15% the water structure remains intact and the acetonitrile molecules gradually occupy the cavities between the water molecules without disrupting the water structure ^[18]. It was shown experimentally ^[19] that no changes in the pK_2 of quinolones were obtained in this water rich region of less than 18% acetonitrile, see Figure 2-7. This correlates well with the data Barbosa obtained for the positive preferential solvation of hydrogen ions by water in acetonitrile-water mixtures. The water molecules favor the immediate vicinity of a hydrogen ion than acetonitrile molecules. Therefore it is assumed that in the highly aqueous medium (0-20% MeCN), the structure of water remains constant; the protonated basic analytes are preferentially solvated

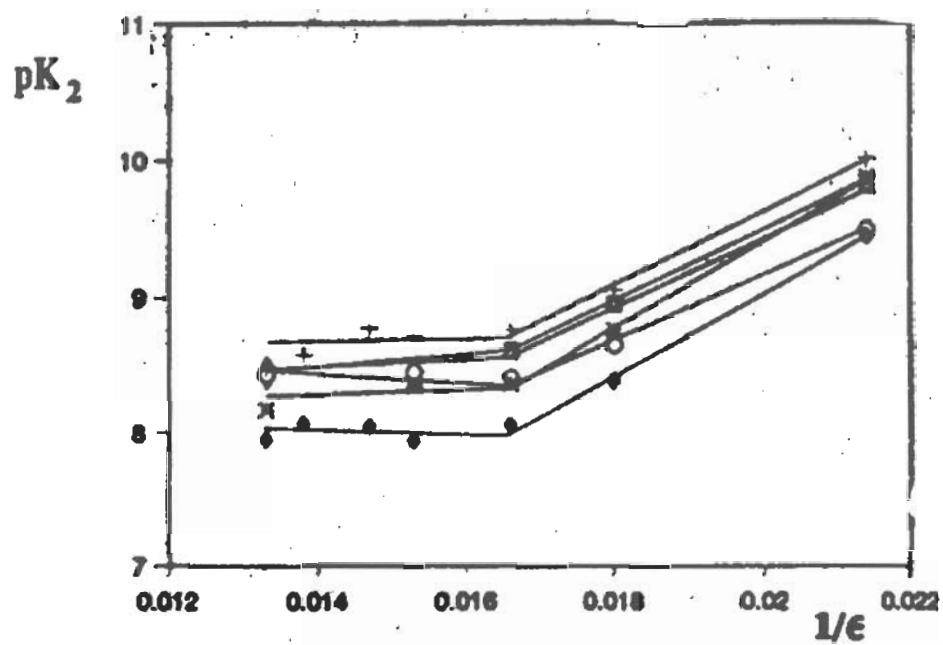


Figure 2-7. Plot of pK_a values (protonated amino group) of selected quinolones versus the reciprocal of the relative permittivity of solvent mixtures, $1/\epsilon$ ^[19]. +, Norfloxacin; closed triangle, Ciprofloxacin; open triangle, Enoxacin; *, Ofloxacin; open circle, Pipemidic acid; closed diamond, Fleroxacin.

by water; and the changes in the pK_a are small. Upon increase of the organic content the number of water molecules in the immediate vicinity of a given hydrogen ion decrease, and the water-acetonitrile mixtures show microheterogeneity^[20], $0.15 < x_{an} < 75$, and the pK_a values change depending on the basic solute or acidic solutes preferential solvation of water.

Effect of analyte structure on pK_a

Prior to the description of pK_a determination it is necessary to understand how the analyte's structure affects its ionization constant. The selectivity obtained in reversed phase chromatography for a variety of iogenic species is dependent on the pK_a of the solute and the pH of the mobile phase. Although, the chromatographer may not have determined the pK_a of a particular compound or compounds if the structure is known, the pK_a may be estimated based on the type and position of substituents attached to the aromatic ring. The effect of position and type of different groups on the aromatic carboxylic acids, aromatic amines and pyridines pK_a values is discussed. These are the types of acidic and basic compounds used in the experimental studies in the following chapters.

The inductive effects of substituents attached to aromatic ionizable species effect their pK_a values^[21]. Generally if a group can produce a positive inductive effect (+I) it is referred to as an acid weakening group and if it can produce a negative inductive effect (-I) it is referred to as an acid strengthening group. Let us look at a group that can produce a positive inductive effect such as the methyl group. This can be illustrated by looking at the pK_a of various acids of increasing alkyl chain length (Table 2-IV). It is noticed that upon addition of the methyl group (formic to acetic) the pK_a increases indicating a weaker acid. However, upon further increase of the chain length this seems to have little effect on the resulting pK_a . This is demonstrated by comparing the pK_a values of acetic and octanoic acid.

Table 2-IV
pK_a values of some common acids

Acid	pK_a
Formic	3.75
Acetic	4.76
Propionic	4.87
Octanoic	4.89

Substituents on the aromatic ring can also decrease the acidity of the compound through a positive mesomeric effect when their double bond has the ability to conjugate with other double bonds [22]. These substituent groups include the halogens, -OMe, -OH, -NR₂ and, to a weaker extent the alkyl groups. Therefore the groups that have these mesomeric properties can transmit the electrons through one or more double bonds to the ionizable group. For example phenyl formic acid (benzoic acid) is a weaker acid than formic acid. The carboxylic anion possesses a positive inductive effect that can be enhanced through the positive mesomeric effect. However, in the absence of a double bond capable of conjugating mesomeric effects are not operational [23].

The substitution on the aromatic ring of aromatic carboxylic acids will have an effect on the resulting pK_a: ortho, meta, and para positions. Since conjugation is not possible in meta substituted species, the meta position is the easiest to explain since the substitution in this position allow a very predictable nature of solely positive and negative inductive effects.. These inductive effects for meta are smaller than when the substituent is in the ortho position due to the greater distance. Using this rationale, it is expected that the inductive effect at the para position to be even smaller than the meta position. However, the para position is capable of allowing mesomerism and therefore many substituents placed in this position show this mesomeric effect. In fact, the inductive effect of the same sign: (+I) and (+M) or (-I) and (-M) enhance the inductive effect with substitution at the para position. When the group has both (-I) and (+M) properties, the electron withdrawing properties are generally stronger at the meta position compared to the para position. The ortho position usually has

the strongest inductive effects for any set of isomers, since the distance is the least and, like the para, it is able to show mesomeric effects due to possible conjugation^[24].

Sometimes a third effect on the pK_a is seen with ortho substitution on aromatic carboxylic acids and is referred to as an “acid strengthening effect”^[23]. This effect can be associated with the steric pressure exerted by the substituent group on the ionizable group so that the group is forced out of the plane of the ring (eg. *t*-butyl benzoic acid, pK_a 3.54). As a result of this distortion, the acid weakening (+M) effect of the benzene ring is decreased and the pK_a may actually decrease substantially.

The weak basicity of aniline is attributed to two factors, the resonance (-M) and the inductive effect (-I) of the benzene ring. This resonance is possible in the neutral molecule and not the ionic state. As expected, the N-R substituents usually increase the basic strength of their (+I) effects and is the greatest with bulky groups, such as *tert* butyl. The bulky group twists the amino group out of the plane of the benzene ring and interferes with the base weakening resonance. Although it is expected that alkyl groups attached in an ortho position to the amino group would induce a positive inductive effect as seen with aromatic carboxylic acids, the effect actually does decrease the base strength because the alkyl groups hinder the approach of the hydrated proton. Meta substituted anilines show the usual inductive effects as seen with the aromatic carboxylic acids. The para substituted anilines may show reinforced inductive effects due to the mesomeric effect of the substituents. The effect of a substituent in pyridine is similar to its effect in aniline, except that there is no “ortho effect” in pyridine because the cation-forming atom does not project beyond the ring.^[23]

Methods used to determine ionization constants

Potentiometric titration is the most convenient method for the determination of ionization constants. This measurement of pH is done by using a cell composed of two half-cells commonly known as electrodes. One of the half-cells is the reference electrode whose potential is known and remains constant throughout the titration. The other half-cell is reversible to hydrogen ions, and the potential changes as the hydrogen ion concentration changes. The measure of the hydrogen ion activity in the solution between the electrodes is the difference in potential between the electrodes. The glass electrode with a saturated calomel electrode is the most commonly used electrode system for potentiometric titration and is usually valid for pH determinations between 2 – 12 . Therefore, it is useful for the determination of pK_a . The main causes for decrease in the accuracy in measurement of pH is that the ionic strength of the analyte solution is low compared to that of the electrolyte buffer solutions. In turn the magnitude of the liquid junction potential is likely to increase. The nature of the test solution is becoming more different than that of the standardizing buffer and can lead to larger errors at increasing differences. Due to high mobilities of the hydrogen and hydroxyl ions the contribution of the liquid junction potential also increases when measuring the pH of solutions below 2 and greater than 11. Therefore the above points must be considered when determining the pK_a of solutes by potentiometric titration and when measuring the pH of the aqueous phase for reversed phase chromatography. The pK_a may be determined chromatographically by plotting the retention of the ionizable solute analyzed with different mobile phases of varying pH. However, pK_a values have also been determined by using ultraviolet spectrophotometry ^[25], where both the ion and the molecule can be isolated in solution and observed independently. The pK_a is obtained from the proportion of

the ion and molecule intensities over a range of pH values. The limitations include that the substance should absorb ultraviolet or visible light and that the absorption of the ionized species should be different from that of the neutral molecule in wavelength and intensity.

Determination of pH values in aqueous/organic mixtures

pH measurements in aqueous/organic mixtures are important when carrying out chromatographic or electrophoretic determinations of retention or mobility as a function of pH. The studies of pH changes aimed at interpreting the ionization effect in non-aqueous mobile phases in RPLC have been restricted by the limited validity of pH measurements made with conventional electrodes calibrated in aqueous solutions [26].

The pH of a solution in pure water is defined as the negative logarithm of the acidity of the hydrogen ion

$$pH \equiv -\log a_{H^+} = -\log \gamma_{H^+} [H^+] \quad [2-8]$$

The pH is typically measured experimentally as an emf (electromotive force) from a glass electrode sensor (pH meter). The operational definition of pH of a solution x is referenced to that of a standard buffer (st)

$$pH_x = pH_{st} = \frac{E_x - E_{st}}{0.06} \quad [2-9]$$

where E_x and E_{st} are the emf values of the solutions respectively. The activity of the hydrogen ion can then be determined using the Nernst law. This equation is only valid for pure aqueous medium. However, in reversed phase HPLC aqueous/organic mobile phases are used, and the apparent pH (pH in the mixed aqueous/organic phase) cannot be determined directly. de Ligny [27] and Bates, [7] presented an excellent explanation for the development of the theory for pH measurement.

An overview of the methods used to determine the pH of the organic/aqueous mixtures will now be given. This will lay a solid foundation for the results and discussion section in which we deal with determining the chromatographic pK_a in aqueous/organic eluents.

The first question one may ask is how can the glass electrode be used for the determination of pH of an aqueous/organic mixture.

Method 1

The use of aqueous standard buffers are used for the determination of pH in aqueous/organic solvents.

$$pH_x^{app} = pH_{st} + \frac{(E_x^* - E_{st})F}{2.3RT} \quad [2-10]$$

where pH_x^{app} is the measured pH value of a tested sample in a mixed aqueous-organic solution referred to an aqueous standard buffer, pH_{st} . pH_{st} is the known value of an aqueous standard buffer and E_{st} is the measured emf of that buffer. In this case the liquid junction potentials $E_{j,x}^*$ and $E_{j,st}$ do not cancel and the operational definition of pH, is pH_x^* :

$$pH_x^* = pH_{st} + \frac{(E_x^* - E_{st})F}{2.3RT} + \frac{(E_{j,x}^* - E_{j,st})F}{2.3RT} \quad [2-11]$$

However the differences between the standard potentials of the glass electrodes between mixed solvents and pure aqueous media have been found to be small and can be ignored [28].

Therefore from equations 2-10 and 2-11 a correction factor δ' , is obtained where

$$\delta' = pH_x^{app} - pH_x^* = \frac{(E_{j,x}^* - E_{j,st})F}{2.3RT} \quad [2-12]$$

It was shown that for methanol-water mixtures over the range 8:92 to 68:32 the liquid junction potential of the electrode was sufficiently constant with pH to establish an

operational scale of pH^* measurements where $pH_x^* = pH_x^{app} - \delta$. The experimental values for δ' have been determined in methanol-water solvents from 0- 68 wt% methanol and 0 – 100 wt% ethanol by Bates and others [7,27-28]. The following equation can be considered for the determination of pH in aqueous/alcohol solvents.

$$pH_x^* = pH_x^{app} - \delta' \quad [2-13]$$

One downside of this method is that it does not consider the effect of the activity coefficients (γ). However, thermodynamic constants and pH depend on the activity coefficients of the ionic species and on their concentrations:

$$pH = -\log a_{H^+} = -\log[H^-]_{H^-} \quad [2-14]$$

When the percentage of the organic modifier in the organic/water solution increases the dielectric constant of the medium and the activity coefficient decrease. The effect of the activity coefficient can be neglected in water, but it may not be ignored at high organic compositions. In fact, the effect may be considerable at high organic composition and may have a great influence on the pH [14].

Method 2

The pH values of a solution may be determined in solvents other than water if the pH meter is standardized by means of a standard solution in the same solvent. The pH of standard solutions can be determined by application of the same method that has been used for the measurement of pH standard solutions in water. The determination of accurate pH values of reference primary standard buffer solutions for standardization of potentiometric sensors is the key pH-metric problem in aqueous-organic solvent mixtures [16]. However this

method is more thermodynamically sound since the activity coefficients and the permittivity of the medium (dielectric constant) are taken into consideration.

The pH^* value (pH in an aqueous-organic system) of a tested mixed solution, designated by pH^*_x , is determined by comparing the measured emf value, E^*_x , with that obtained for a primary standard buffer solution, E^*_{ps} , of known pH^*_{ps} in the identical solvent composition. A set of buffers that can be used between 0 and 100% water/alcohol is given by Bates^[9]. Since, the liquid junction potential is assumed to remain constant in solutions x and ps and cancel in the expression $E^*_x - E^*_{ps}$, pH^*_x can be determined directly:

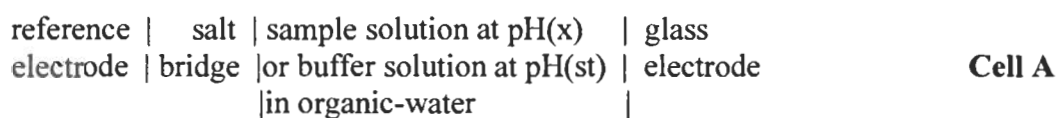
$$pH^*_x = pH^*_{ps} + \frac{(E^*_x - E^*_{ps})F}{2.3RT} \quad [2-15]$$

where F is the Faraday constant, R the universal gas constant, and T is the temperature. The major drawbacks of this method is that the pH meter is to be calibrated with standards of known pH^*_{ps} values.

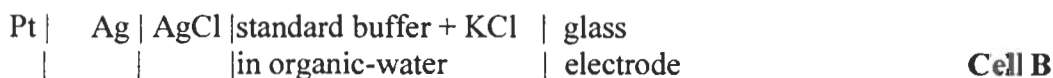
The determination of pH for common HPLC eluent systems using this technique has been limited to alcohol/water mixtures due to lack of pH^*_{ps} values in other binary solvent systems, such as acetonitrile/water mixtures. Recently though Barbosa^[16] determined pH^*_{ps} values for buffer systems in aqueous/acetonitrile mixtures.

The determination of standard buffer solution pH values, pH^*_{ps} , for acetate, succinate, oxalate and phosphate buffers in methanol-water, ethanol-water, and dimethylsulfoxide-water are known and reported in the literature but are subject to no simple interpretation^[7,28-31]. Barbosa also determined accurate pH^*_{ps} measurements of five reference buffer solutions: KH tartrate, KH_2 citrate, KH phthalate, acetate and phosphate buffer in binary acetonitrile-water mixtures at various compositions containing 10,30,40,50,70, and 100 wt% acetonitrile at 298K using IUPAC standardization rules^[16,32]. This was based on emf measurements of

the reversible cell without liquid junction. The equation usually used for the **electrometric pH measurement** ^[33] was equation [2-10] where E_x and E_{st} denote the emf measurements, in cell A, in the sample solutions at unknown pH(x) and in the reference standard buffer solution at known pH(st) respectively,



The reference pH values of the standard buffer solutions are influenced by the nature of the solvent. These pH values may vary with solvent composition more so with acetonitrile-water mixtures than methanol-water mixtures. Determination of the reference pH values involves a complicated procedure ^[16]. The first step is to measure the emf of the Cell B, where the reference standard buffer solution of a fixed molality contains potassium chloride at various known concentrations.



The activities of the hydrogen and chloride ions in solution are directly related to the emf, E of the cell:

$$E = E^\ominus + g \log(a_{H^+} a_{Cl^-}) \quad [2-16]$$

where E^\ominus is the standard emf of the cell. The second step is to determine the pH values for each concentration of potassium chloride, c_{cl^-} , using the Nernst expression of emf, E, for Cell A:

$$p(a_H \cdot a_{Cl^-}) = pH + py_{Cl^-} = \left\{ \frac{E^\ominus - E}{g} \right\} - p_{Cl^-} \quad [2-17]$$

Then the p values in the mixed electrolyte cell B can be obtained by calculation of py_{Cl^-} , the molar activity coefficient. The py_{Cl^-} can be calculated using a form of the Debye Huckel equation.

$$py_{Cl^-} = \frac{AI^{1/2}}{(1 + a_0BI^{1/2})} \quad [2-18]$$

A and B are Debye-Huckel constants and a_0 is the ion size parameter in the solvent mixture, and I is the ionic strength. Using the Bates-Guggenheim convention^[30,33] which is in compliance with IUPAC rules the values of a_0B may be determined at a particular temperature. Also, the ionic strength of the standard buffer-KCl mixed electrolyte needs to be known. Once py_{Cl^-} is determined and plugged back into [2-17] a distinct pH value for each concentration of c_{Cl^-} can be obtained. Then the standard value $pH^*(st)$ for the standard buffer of a certain concentration may be obtained from a plot of pH versus c_{Cl^-} . The $pH^*(st)$ value will be the extrapolated value to the y-intercept where $c_{Cl^-} = 0$. This can be done for each mole fraction, x, or organic component. Plotting $pH^*(st)$ versus the mole fraction of organic, one may obtain the change of pH per certain percentage of organic in an aqueous/organic medium. Figure 2-8 shows the results Barbosa^[16] obtained for 8 different buffers in acetonitrile/aqueous mixtures from 0 – 50% acetonitrile. There was an apparent increase in the pH of the mixed acetonitrile/water phase upon increased addition of organic. We calculated the average change to be 0.28 pH units per 10 percent of acetonitrile, Table 2-V. This data is very useful for chromatographers because it shows that the slopes are similar regardless of the starting pH (3.8 – 10). However, the ionic strength of the buffer should be within the limits of the IUPAC standards if accurate pH values of that buffer are to be

obtained. If high ionic strength buffers are used, deviations may be obtained over the concentration range of acetonitrile since the magnitude of the liquid junction potential is likely to increase. The nature of the test solution is becoming more different than that of the standardizing buffer and can lead to larger errors at increasing differences.

Most recently Bosch ^[12] has investigated several properties (molar volume, molar refractivity, autoprotolysis) of methanol-water mixtures that depend on methanol-water interactions. These may affect the pH of an organic/aqueous mixture and the solvation of the solutes in the mixed solvent, which will both have an influence on the pK_a determination of acid and basic solutes. They determined an interaction constant from the macroscopic properties of the mixture and derived an equation that relates solvent composition with the pK_a values of commonly used acids in methanol-water. They saw a variation in the pK_a values of the acids with the solvent composition. As seen in Figure 2-9, the variation is different for each acid and they found that the pK_a of the acid increases upon increasing the methanol content.

We also calculated the change of the ionization of the specific acids as a function of methanol concentration. The following, Table 2-VI, is the percent change in the pK_a in the acid per 10% methanol.

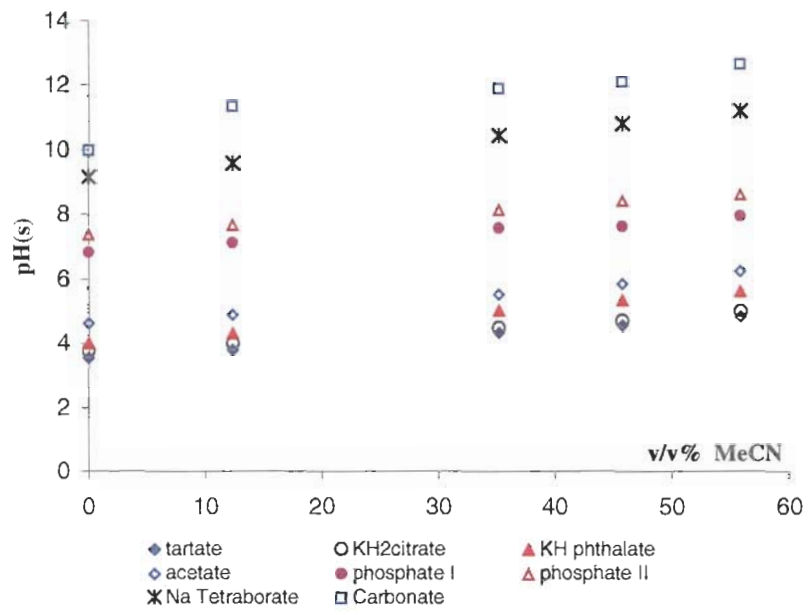


Figure 2-8. pH(s) versus % acetonitrile for 8 different buffer systems ^[16]

Table 2-V

Slope of change of the pH(s) per percent of acetonitrile for eight different buffers. ^[16]

Buffer	Slope
tartate	0.023
KH ₂ citrate	0.022
KH phthalate	0.030
acetate	0.029
phosphate I	0.019
phosphate II	0.022
Na tetraborate	0.036
Carbonate	0.041
Average	0.028

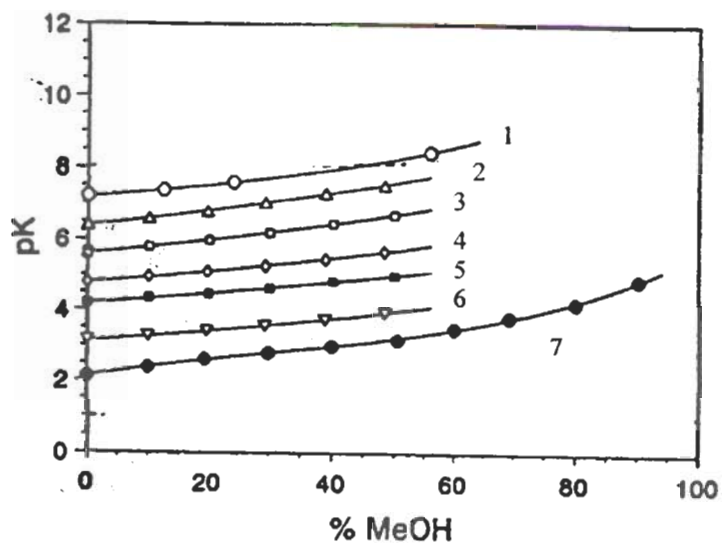


Figure 2-9. Variation of pK_a values of polyprotic acids with the methanol-water composition. 1. pK_{a2} of phosphoric acid, 2. pK_{a3} of citric acid, 3. pK_{a2} of succinic acid, 4. pK_{a2} of citric acid, 5. pK_{a1} of succinic acid, 6. pK_{a1} of citric acid, 6. pK_{a1} of phosphoric acid. Symbols were calculated according to equation 15 in ref^[12].

Table 2-VIChange in the pK_a of common HPLC acidic modifiers per ten percent methanol ^[12]

Acid	ΔpK_a per 10% methanol
Phosphoric (pK_{a1})	0.22
Phosphoric (pK_{a2})	0.21
Citric (pK_{a1})	0.17
Citric (pK_{a2})	0.18
Citric (pK_{a3})	0.24
Succinic (pK_{a1})	0.16
Trichloroacetic	0.19
Formic	0.12
Acetic	0.15
Benzoic	0.21
Anilinum	-0.07

Determination of the pK_a using HPLC

The pH of the aqueous portion of the mobile phase is usually plotted versus the retention factor in chromatographic measurements. The chromatographically determined pK_a values for basic compounds show lower values than those obtained from potentiometric titration in water. The questions that will be answered are: 1) What influences the change in K_a ? 2) Is this due to a true pK_a shift or is it solely attributable to a pH shift of the aqueous portion upon addition of organic? After the organic is added to an aqueous phase of a certain pH the ionization of the acidic modifier is suppressed and behaves as a weaker acid. Therefore a greater amount of acid needs to be added to the aqueous/organic medium in order to obtain the same pH as in the purely aqueous phase. One way to estimate if it is a pH shift or a pK_a shift is to correct for the pH shift of the aqueous phase upon the addition of organic. We can see by the data calculated by Barbosa ^[16] that following a 10% addition of acetonitrile there was a corresponding change of the aqueous pH by 0.28 pH units. If we correct the pK_a value determined by HPLC at a certain organic composition by a specified correction factor, this may lead to the pK_a value of the compound as determined by potentiometric titration in water. For example consider a basic compound such as pyridine whose potentiometric titration value in water is 5.2. Now let us compare this pK_a value with the chromatographically (HPLC) determined pK_a value in an eluent that contains 30% acetonitrile:70% aqueous which is, $pK_a=4.36$. If there was no shift in the pK_a , the $pK_{a(HPLC)}$ should correlate to the potentiometric value minus a correction factor. The correction factor extrapolated from Barbosa data. can be taken to be 0.028 pH units per 10% acetonitrile.

Therefore,

$$4.36 = 5.2 - \{0.028 * 30\} \quad [2-19]$$

The general formula for bases may be written as follows:

$$pK_{a(HPLC)}^{Base} = pK_{a(titrimetric)} - \{0.028 * \%MeCN\} \quad [2-20]$$

A similar expression can be written for acidic compounds

$$pK_{a(HPLC)}^{Acid} = pK_{a(titrimetric)} + \{0.028 * \%MeCN\} \quad [2-21]$$

However, if these values are not equal this might suggest that there is a real shift in the pK_a of the ionizable component. This is presented just as a guideline because it will be shown that there are many other factors affecting the ionization state of ionogenic species in aqueous/organic medium. The properties of the eluent such as the suppression of the ionization of the buffer and the dielectric constant may start to play an increasing role. However if the above holds true that means the chromatographer should be working at ± 2 units of the $pK_{a(HPLC)}$ to ensure that the component will be in the fully ionized or neutral form. For this example, this would correlate to pH values of 2.36 (eg $4.36-2 = 2.36$) or $pH=6.36$ (eg. $4.36+2 = 6.36$.) If one does not correct for the shift of the pH of the aqueous solvent upon addition of organic, the chromatographic interpretation of the retention of ionizable components as a function of pH will be meaningless. This described method will be denoted throughout the thesis as the “pH shift” method.

Another method is to plot the pH of the mixed organic/aqueous eluent versus the retention factor. The pH of the mixed organic/aqueous eluent could be determined by method 1 using aqueous standards but limited to aqueous/alcoholic solvents. Method 2 could also be used to determine the pH of the mixed aqueous/organic eluent. However, this

procedure requires the use of the primary standard buffers at a certain ionic strength and known literature reference values for pH_{st} . The other alternative which is very time consuming is to determine the pH_{st} at a certain ionic strength of the buffer to be used.

Acid error

In strong aqueous solutions of salts and strong acids at pH less than 1 and in certain nonaqueous solutions, the pH response of the glass electrode displays a departure from linearity^[9]. This effect is enhanced if the test solution pH is not bracketed by the calibration standards. This acid error is also known as the negative error because the pH measured in this region will be greater than the true pH. This acid error is not greatly dependent on the temperature. Also, it was found that there is a difference between the behavior of glass electrodes in dilute acid solutions and in concentrated acid solutions. In dilute solutions, the potentials are steady and reproducible but in concentrated solutions there is a lack of reproducibility and a considerable drift toward more negative values^[34]. This effect was observed in our laboratory. We had previously been using a handheld Corning pH meter for our preliminary experiments that was calibrated only with pH 4 and pH 7 aqueous standard solutions. The range of pH's of water adjusted with perchloric acid, however, were from 1 – 8. We noticed that below pH's of 2.0, a large amount of acid had to be added to produce a minor pH change. We further investigated this effect by plotting the concentration of perchlorate anion versus the concentration of H^+ ion. Since, perchloric acid is a strong acid that fully dissociates in water and has a $\text{pK}_a < 0$, there should be a linear relationship between H^+ and ClO_4^- . However, there was a serious deviation from linearity and influence of the acid error on the determined pH was seen. A more in depth study was performed by measuring the pH of four one liter bottles of water modified to different final pH's with

perchloric acid: 1.36, 1.53, 1.83. and 2.14. The two pH meters used for the study were a hand held Corning pH meter calibrated with standards 4 and 7 and a Fischer pH meter with a combination electrode calibrated with standards 1, 2, 4 and 7. The electrode used with the Fisher Scientific, Accumet pH meter¹⁵, was an AccuT standard-size glass combination electrode. These standard size glass body single junction combination electrodes have an Ag/AgCl reference. These electrodes have low electrical resistance, low sodium error, and excellent chemical resistance. The specifications of this electrode are: pH range; 0 to 14 pH, temperature range; 0 to 100°C, Junction; Porous ceramic, accuracy; ± 0.01 pH units at 25°C and the response time of 20 seconds or less. The Corning pH-30 is handheld pH meter. The specifications include: pH range; 0-14 pH, Resolution: 0.01 and accuracy; ± 0.2 pH units at 25°C.

It can be seen with the Corning pH meter that two significantly different dependencies were observed, Figure 2-10. The experimental points for the upper trend correspond to the pH values taken at the beginning of the day. After continued use, it can be assumed that the potential of the pH meter became more steady and corresponded more closely to the pH values obtained with the Fischer pH meter. In all these results, deviation from linearity was seen with both pH meters, but to a much lesser extent with the Fischer pH meter. This indicates that below pH's of 2.0, there is some influence of an acid error, and the need for bracketed standards and possibly the ionic strength of the standards should be matched to the test solutions. These points were considered when determining the pH for further experiments conducted in our laboratory.

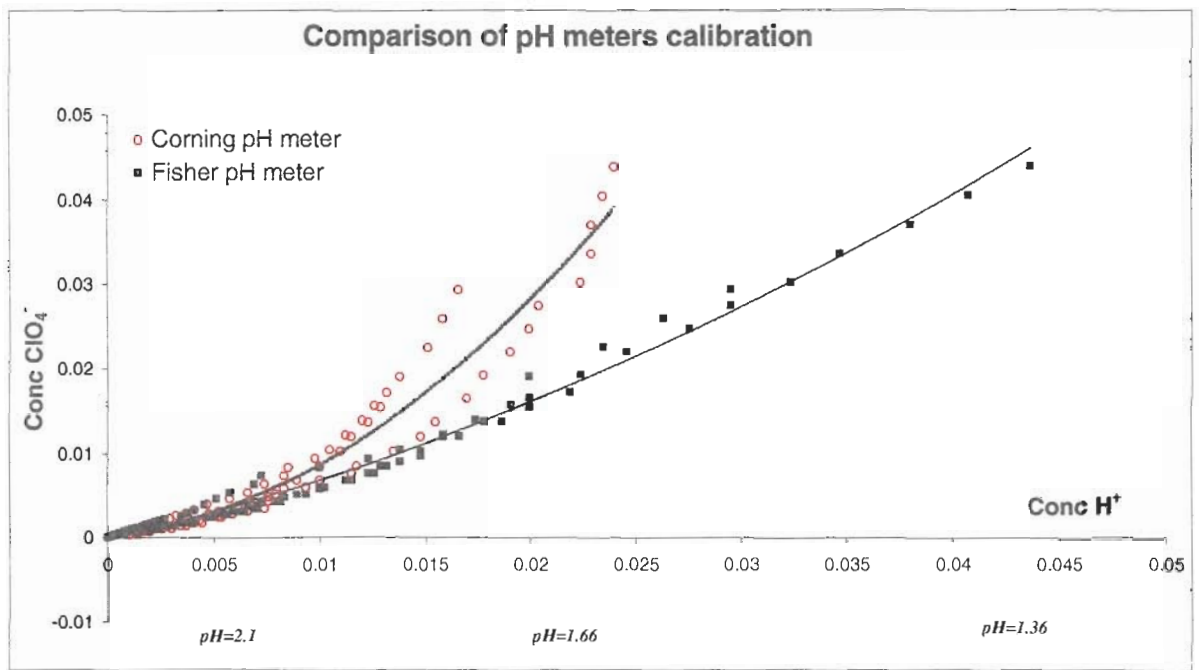


Figure 2-10. Comparison of pH meter efficiency in a low pH region. The type of electrodes and pH meters are described in text.

Experimental

Instrumentation

The chromatographic system used was a model 1100 HPLC from Hewlett Packard (Willington, DE). The chromatograms were processed using HP version software. The column used was a Zorbax Eclipse XDB-C18, (Hewlett Packard, Little Falls, DE), with 150 x 4.6 mm i.d., particle diameter 5 μ m, bonding density 3.4 μ mol/m². The Eclipse XDB-C18 column has a nominal surface area of 180 m²/g, and a pore size of 80Å. This column is a densely bonded dimethyl-silane-substituted stationary phase that is double endcapped with dimethylsilane and trimethylsilane groups and has been demonstrated to be very stable at both low and high pH values [35-36]. A Prodigy ODS-2 column was used (Phenomenex, Torrance, CA), 150 x 4.6 mm i.d., particle size 5 μ m, bonding density 3.4 μ mol/m². The Prodigy ODS-2 column has a nominal surface area of 340m²/g and a pore size of 90Å.

The column temperature was controlled by a circulating water-bath Brinkman Model RC6 Lauda (Lauda-Konigshofen, Germany). pH measurements were performed with a Fisher Accumet pH meter 15 of the aqueous eluent component before the addition of the organic modifier. The electrode was calibrated with standard solutions of pH 1.0, 2.0, 4.0, 7.0, and 10.0.

Chemicals

Orthophosphoric acid (analytical grade), perchloric acid (redistilled) and trifluoroacetic acid (spectrophotometric grade), acetic acid (analytical grade), ammonium acetate (analytical grade) water (HPLC grade), methanol (HPLC grade) and acetonitrile (HPLC grade) were obtained from Sigma Chemical Co. (Milwaukee,WI). Disodium hydrogenphosphate heptahydrate (99.9%) was purchased from Fischer Scientific (Fairlawn,

NJ). All aqueous mobile phases were filtered using a Whatman Nylon 66 membrane filter (Clifton, NJ). The following basic compounds were used: aniline (Baker, Phillipsburg, NJ), N-methyl-aniline (Eastman, Kingsport, TN), pyridine, 2-ethylpyridine, 3-ethylpyridine, 4-ethylpyridine, 2,4-dimethylpyridine, 2,6-dimethylpyridine, 3,4-dimethylpyridine, and 3,5-dimethylpyridine, 2-picoline, 2,3-dimethylaniline, 4-aminobenzoic acid, phenylethylamine, phenylacetic acid and o-,m-,p- toluic acids (Aldrich, Milwaukee, WI).

Chromatographic Conditions

The retention data was recorded at 25°C using isocratic conditions with a flow rate of 1 mL/min for the Zorbax Eclipse XDB-C18. UV detection was at 254 nm for the entire study. The aqueous portion of the mobile phase was a 10mM, 20 mM or 25 mM Disodium hydrogen phosphate buffer, pH=8.96, adjusted with the different acidic modifiers (perchloric, trifluoroacetic acid, or ortho-phosphoric acid) over the pH range of 1.3 to 8.3. The aqueous portion of the mobile phase was a 10 mM Ammonium acetate buffer pH=6.6 adjusted with acetic acid. The organic modifiers used were acetonitrile or methanol and the eluent compositions were 90:10 and 70:30 buffer:organic.

All analyte solutions were prepared by their dissolution in the eluent to give a concentration of 0.1-0.2 mg/mL. Injections of 1-5 μ L of these solutions were made.

The t_0 values corrected for system volume obtained for the Zorbax XDB-C18 and Prodigy ODS-2 columns with the minor disturbance method^[37-38] at 25°C was 1.40 min and 1.69 min., respectively. The t_0 obtained using the first baseline disturbance was 1.45 min and 1.67 min, respectively. The retention factors calculated were the average of triplicate injections. Also, a test mix of aniline and pyridine was used as a system suitability check

before and after each experiment to determine the stability of the column and system performance.

Results and Discussion

Influence of type of acidic modifiers on ionogenic analyte pK_a shift

The pH of a 10mM sodium hydrogen phosphate buffer (8.96) was adjusted with phosphoric, perchloric and trifluoroacetic acid to the desired pH's between 1-8.3 and retention factors were obtained for each pH. Plots of the retention factors for several basic compounds versus pH (modified with phosphoric acid) are shown in Figures 2-11 through 2-14. The pH plotted is the pH of the buffer before the addition of organic eluent. Retention factors level off when $pH \ll pK_a$ and can be seen for a series of alkyl-substituted anilines and pyridines in Figure 2-11 and Figure 2-12 and for an isomeric series of pyridines in Figure 2-13. In figure 2-14, the inflection points are not observed for the benzyl amines, since these compounds have pK_a 's >9 . Experimental pK_a values were determined for all compounds, that had expected pK_a 's within the studied pH range (Table 2-VII).

Eluent composition influence on the pK_a

The chromatographic pK_a , calculated as the inflection point, was calculated for each plot using equation [1-12] and Mathcad software. These pK_a values for the three acidic modifiers and their literature pK_a values are compared in Table [2-VII] and the corresponding figures for two basic compounds are shown in Figure 2-15 and Figure 2-16. The experimental pK_a values were similar regardless of the modifier, but do not correspond that well with the aqueous literature values. The pK_a 's determined in aqueous/organic mixtures are lower than those measured in an aqueous solutions, and this effect has been observed in the literature^[12,23,39,40]. Barbosa et. al^[16] found using potentiometric titrimetry

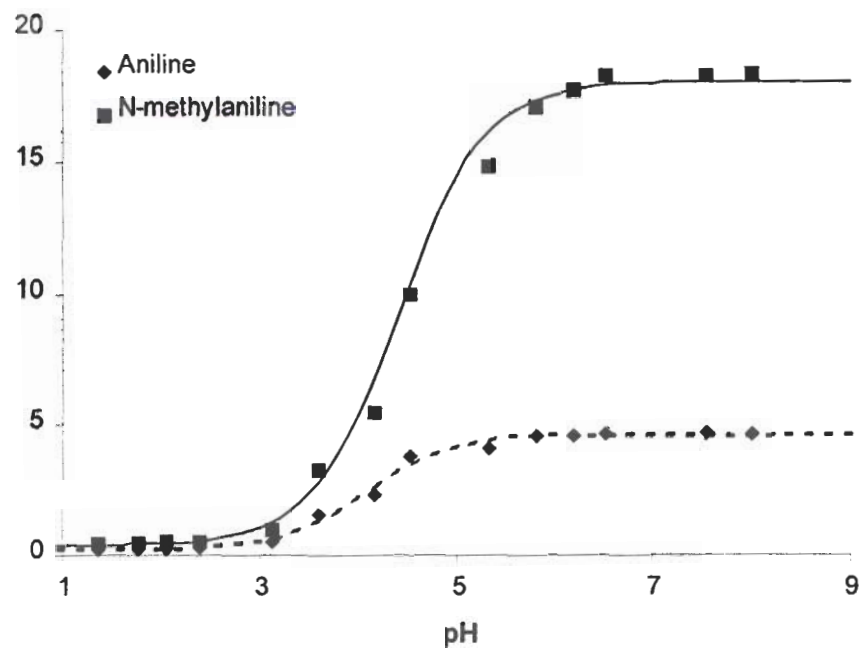


Figure 2-11. Dependence of the retention factor of aniline and N-methylaniline on the mobile phase pH. Column 150x4.6 mm Zorbax XDB-C18; mobile phase: 10/90 Acetonitrile/10mM Disodium Hydrogenphosphate buffer adjusted with phosphoric acid; flow rate, 1.0 ml/min; 25°C, UV, 254 nm; sample:1 μ l injection.

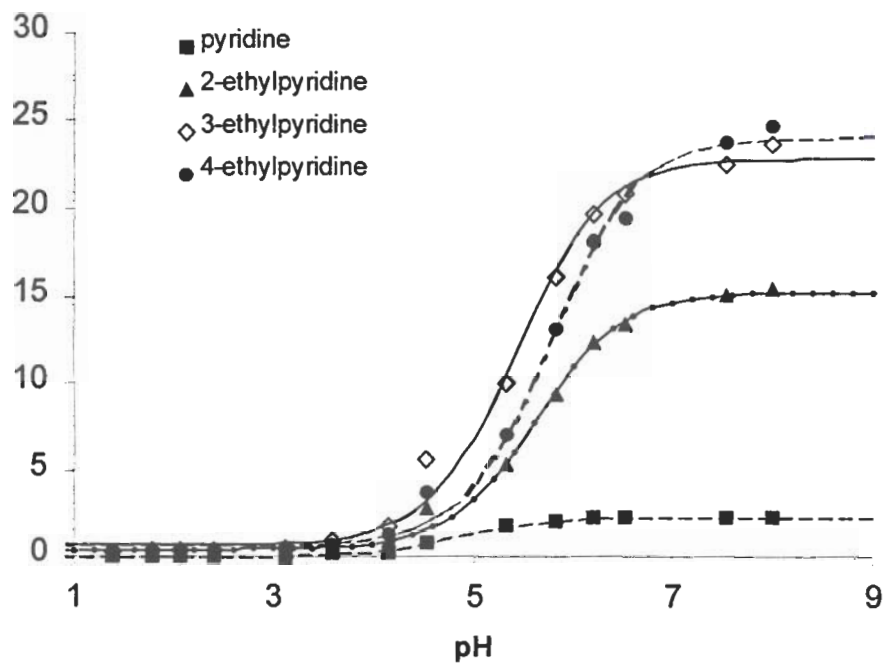


Figure 2-12. Retention factor versus pH for a series of pyridines of increasing hydrophobicity. Chromatographic conditions identical to Figure 2-11.

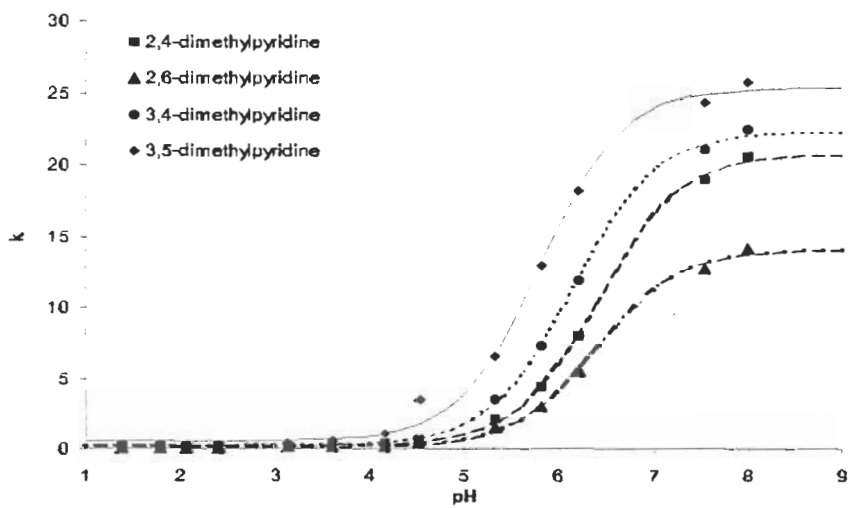


Figure 2-13. Retention factor versus pH for an isomeric series of dimethylpyridines. Chromatographic conditions identical to Figure 2-11.

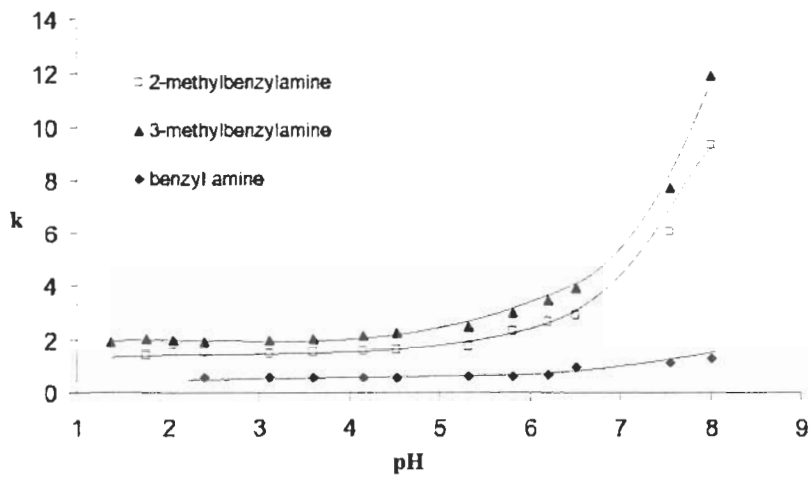


Figure 2-14. Retention factor versus pH for an isomeric series of benzylamines. Chromatographic conditions identical to Figure 2-11

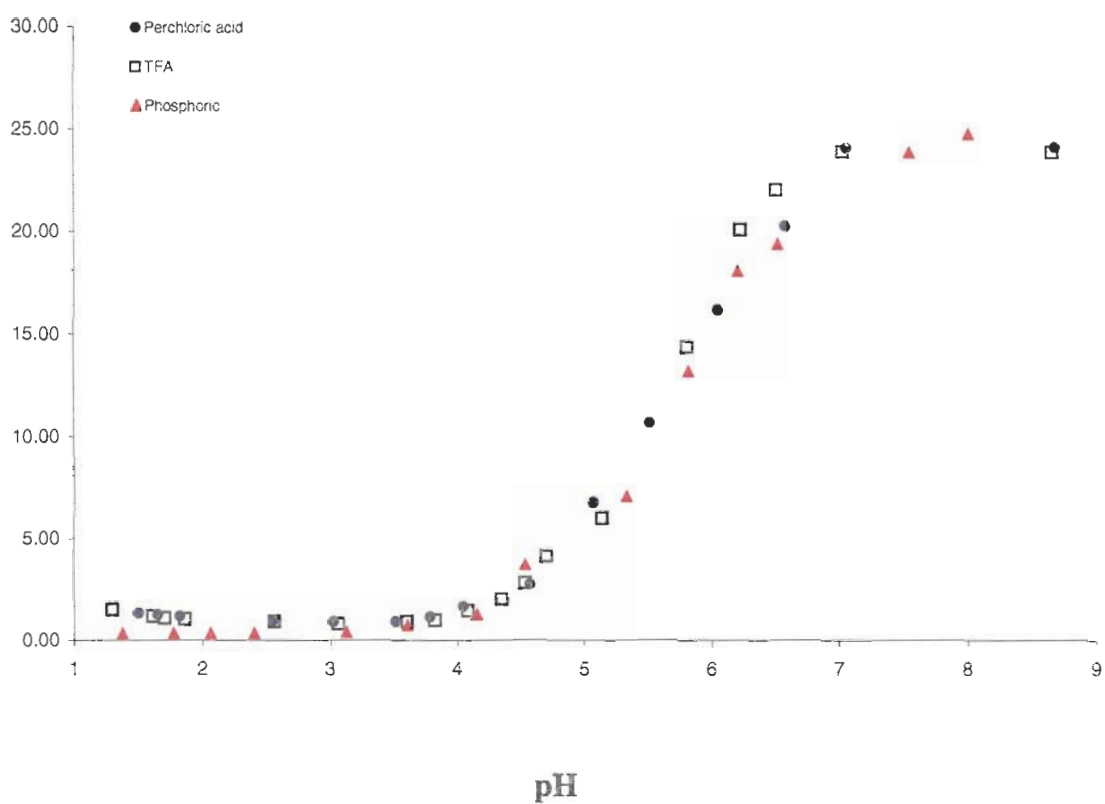


Figure 2-15. Comparison of retention factor for 4-ethylpyridine obtained with three different acidic mobile phase modifiers. Column 150x4.6 mm Zorbax XDB-C18; mobile phase: 10/90 Acetonitrile/10mM Disodium Hydrogenphosphate buffer adjusted with phosphoric acid; perchloric acid or trifluoroacetic acid, flow rate, 1.0 ml/min; 25°C, UV, 254 nm; sample: 1 µl injection.

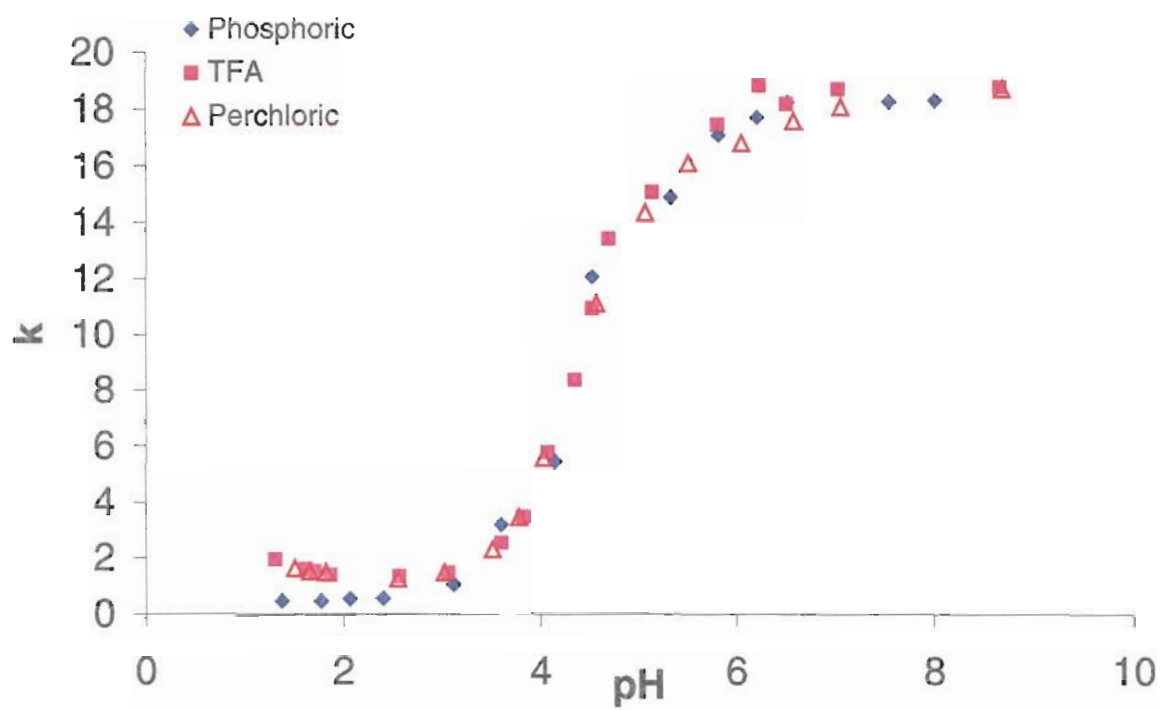


Figure 2-16. Comparison of retention factor for N-methylaniline obtained with three different acidic mobile phase modifiers. Chromatographic conditions as in Figure 2-15.

Table 2-VII
Chromatographic versus titration pK_a values

Compound	Titration pK _a , 25°C in water	Column 2	Column 2	Column 2	%RSD	Average	Δ pK _a
		90% 10mM Na ₂ HPO ₄ : 10%MeCN H ₃ PO ₄ HPLC pK _a , 25°C	90% 10mM Na ₂ HPO ₄ : 10%MeCN TFA HPLC pK _a , 25°C	90% 10mM Na ₂ HPO ₄ : 10%MeCN HClO ₄ HPLC pK _a , 25°C			
pyridine	5.17	4.85	4.75	4.95	1.99	4.85	0.32
2-ethylpyridine	5.89	5.62	5.56	5.55	0.67	5.57	0.32
3-ethylpyridine	5.80 (20°C)	5.41	5.30	5.29	1.31	5.33	0.47
4-ethylpyridine	5.87	5.76	5.65	5.67	1.06	5.70	0.17
2,4-dimethylpyridine	6.74	6.42	6.27	6.28	1.35	6.33	0.41
2,6-dimethylpyridine	6.71	6.40	6.27	6.28	1.16	6.32	0.39
3,4-dimethylpyridine	6.47	6.20	6.02	6.04	1.63	6.09	0.38
3,5-dimethylpyridine	6.09	5.82	5.72	5.69	1.22	5.74	0.35
aniline	4.6	4.08	4.13	4.07	0.82	4.09	0.51
N-methylaniline	4.85	4.40	4.44	4.45	0.56	4.43	0.42

- a. All literature pK_a values were determined at 25°C in water unless otherwise noted ^[41].
- b. All experimental pK_a values were determined in a 90% aqueous buffer containing 10mM Disodium hydrogen phosphate buffer adjusted with perchloric, trifluoroacetic or phosphoric acid and 10% acetonitrile at 25°C. The best fits of the theoretical curves to the experimental data were found by using a nonlinear least squares curve fitting software, Mathcad 8.

that the pK_a of a basic compound shifts by 0.28 pH units per each 10% organic phase added. Similar shifts were seen in our experiments. This decrease in pK_a may actually be due to a shift of the pH of the aqueous phase upon the addition of organic and not a true pK_a shift as we described earlier. In the following theoretical example we propose how to relate the chromatographic pK_a value to that determined by titration. Our goal is to compare, the titration value of $pK_a = 6$ of a basic component to the chromatographic pK_a at 100% aqueous conditions and at 30, 40, 50 and 70% acetonitrile in the mobile phase. The theoretical retention factors versus pH of the aqueous phase in these four compositions are shown in Figure 2-17a. The pK_a value does decrease but all four dependencies may be overlaid if a correction factor is used to normalize the pH to 100% aqueous. There is an apparent decrease in an analyte's pK_a value in the presence of organic when plotted versus the pH of the aqueous; this can be attributed to a change in the pH of the aqueous phase and would be considered a pH shift and not a true pK_a shift. However, not only does the pH of the resulting mobile phase change upon increasing the organic content but also does the elution strength of the mobile phase. As the organic composition increases the retention of the analyte decreases in reversed phase chromatography. The plateau region in Figure 2-17b indicates that the analyte is in its neutral form at the 100% aqueous conditions. It is shown that the retention factor decreases in this region as the organic concentration is increase. The elution strength of the eluent is increased. Hence, if an aqueous phase of $pH = 4$ is prepared, (represented by circles on figure 2-17b), two different factors affect the retention in opposite directions: pH shift increases the retention and the increased organic content decreases the retention. Thus, since the effects influence the retention in opposite directions, it is difficult to predict how much each factor will influence the overall retention. These effects may

Figure 2-17 Retention factor versus pH at different organic compositions (pH shift)

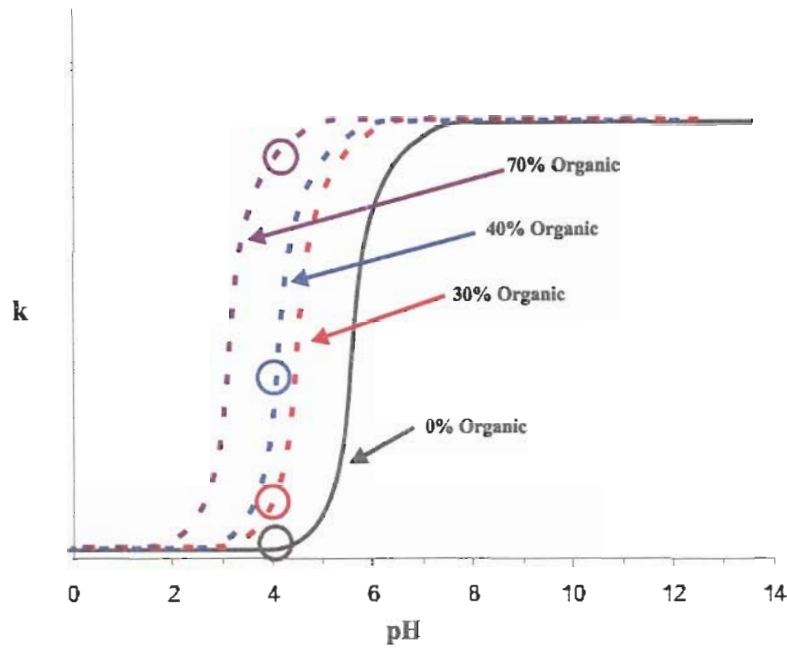


Figure 2-17a. Shows a pH shift upon addition of organic. Note upon the increase of organic the compound becomes less ionized since the starting pH of the mobile phase is shifted to lower values.

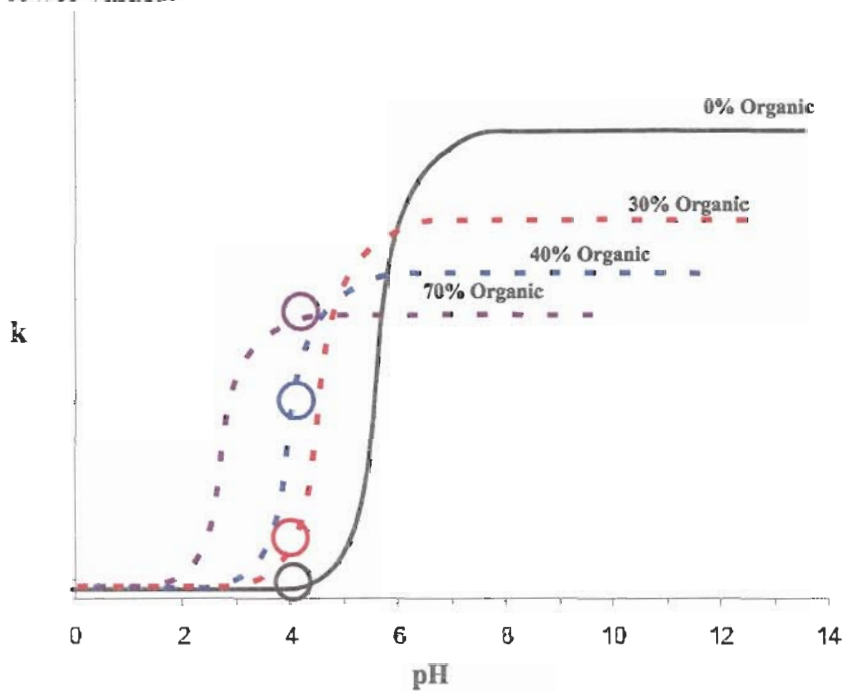


Figure 2-17b. Increase of organic content actually causes a pH shift to lower pH values and increase of the elution strength of the eluent. This is shown by the decrease in retention in the upper plateau region. There are two processes affecting the retention in opposite directions.

explain some of the unexpected retention dependencies seen when analyzing ionizable compounds by reversed phase HPLC.

As shown in Table 2-VII, the pK_a values determined using phosphoric acid led to slightly higher pK_a values than the systems adjusted with the stronger acids such as trifluoroacetic or perchloric acids. As previously stated the electrostatic and solvation effects depend on different solute properties and the variation of the dissociation constant with the solvent composition must be different for each acid. It was shown by Barbosa ^[16] that phosphoric acid exhibits a change in pK_a upon addition of acetonitrile, in acetonitrile-water eluents (10v/v%) to a greater extent ($\Delta pK_a = 0.19$) than acetic acid ($\Delta pK_a = 0.29$). Therefore if the acids have the same pH in the aqueous phase the resulting pH values will be different upon the addition of organic. It would be expected that the pK_a of a base using an aqueous eluent modified with acetic acid would show a larger shift in pK_a than if the aqueous eluent were modified with phosphoric acid. Figure 2-18 shows theoretical shifts in aqueous phases adjusted with different acidic modifiers pH changes upon addition of organic. Acid 1 has a change in pK_a upon addition of organic of $\Delta pK_a=0$, Acid 2 has $\Delta pK_a=1$ and Acid 3 has $\Delta pK_a=2$ in Figure 2-18. Different pHs in the mixed mobile phases (90 aqueous:10 acetonitrile) may be obtained and this can be attributed to the higher pK_a values observed with phosphoric acid as the modifier as opposed to TFA and perchloric acid in our experimental results. This pH shift obtained with a particular acidic modifier is specific to the type of the organic eluent used. It was shown by Bosch that phosphoric acid ($\Delta pK_a = 0.22$) in methanol-water eluents (10v/v%) is more affected than acetic acid ($\Delta pK_a = 0.15$). Hence, if methanol would be used instead of the acetonitrile, a larger pH shift should be observed when phosphoric acid is used as the pH acidic modifier.

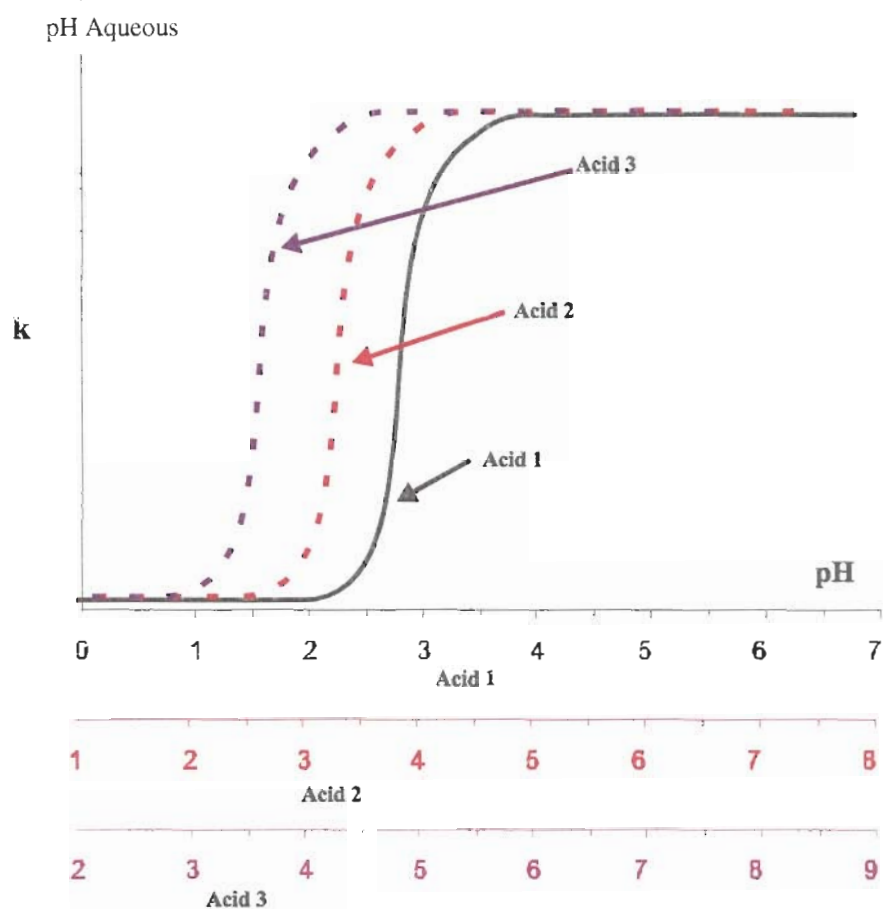


Figure 2-18. Graphical representation of the pH shift for acidic modifiers. Differences in pH shift of the aqueous portion of the mobile phase upon using different acidic modifiers to adjust pH. The pH of the aqueous phase may shift to different degrees upon the same addition (v/v%) of organic when different acidic modifiers are employed.

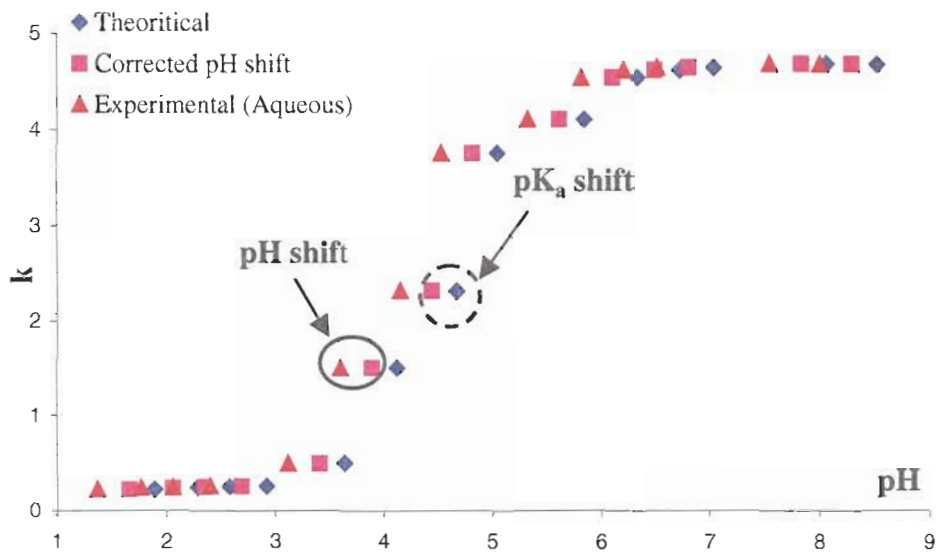


Figure 2-19. Comparison of pH shift and pK_a shift. For each experimentally determined retention factor the pH shift is represented by the horizontal distance from triangle data point to square data point. The pK_a shift is represented by the horizontal distance from the square data point to the diamond data point.

Effect of analyte structure and type of organic solvent

Let us put into perspective the results we obtained for aniline with the phosphoric acid modifier to determine if there was a pK_a shift or solely a pH shift, see Figure 2-19.

This can be done by performing this elementary calculation:

$$pK_a \text{ shift} = pK_{a(\text{tit})} - (pK_{a(\text{HPLC})} + pK_{a \text{ corr.}}) \quad [2-22]$$

The pK_a correction factor for phosphoric acid taken from Barbosa^[16] data is 0.19 pH units per 10% acetonitrile. The pK_a of aniline is 4.6 as determined by titration in water. The pK_a determined by HPLC plotted versus the pH of the aqueous was 4.08. If the sum of equation [2-22] is greater than 0 then there is a corresponding pK_a shift. Therefore for aniline we do actually have a pK_a shift e.g. $[0.33 = 4.6 - (4.08 + 0.19)]$. Table 2-VIII shows all the corrected pK_a values originally listed in Table 2-VII. For all the basic compounds a corresponding pK_a shift is observed. The pK_a shifts vary to different degrees. As discussed previously, this variability may be due to the preferential solvation of the solutes with the mobile phase components. The pK_a values of the pyridine species show a smaller shift in their pK_a values than the aniline species. The rationale for this observation is that the greater the hydrated sphere, the greater the stabilization and the higher the resulting pK_a . We proposed that the protonated pyridine species were stabilized by the greater number of water molecules involved in their hydration spheres in comparison with the corresponding aniline species. The lone pair of electrons on the nitrogen of aromatic amines (aniline and their derivatives) is delocalized over the π system of the ring. This overlap is not possible in the anilinium ion, so the reactant (free amine) is stabilized in comparison with the product. The reaction is shifted to the left since the protonation on the nitrogen is unfavorable. On the

Table 2-VIIIThe effect of pH shift and pK_a shift

Compound	Titration pK _a , 25°C in water	90% 10mM Na ₂ HPO ₄ : 10%MeCN H ₃ PO ₄		pK _a shift Δ pK _a
		HPLC, Aqueous pK _a	Corrected for pH shift	
pyridine	5.17	4.85	5.04	0.13
2-ethylpyridine	5.89	5.62	5.81	0.08
3-ethylpyridine	5.80 (20°C)	5.42	5.61	0.19
2,4-dimethylpyridine	6.74	6.42	6.61	0.13
2,6-dimethylpyridine	6.71	6.40	6.59	0.12
3,4-dimethylpyridine	6.47	6.20	6.39	0.08
3,5-dimethylpyridine	6.09	5.82	6.01	0.08
aniline	4.6	4.08	4.27	0.33
N-methylaniline	4.85	4.40	4.59	0.26

Column 150x4.6 mm Zorbax XDB-C18; mobile phase: 10/90 Acetonitrile/10mM Disodium Hydrogenphosphate buffer adjusted with phosphoric acid; flow rate, 1.0 ml/min; 25°C, UV, 254 nm; sample: 1 μl injection.

other hand the pyridine species upon protonation does not lose its aromaticity since its nonbonding electrons are tightly held and are less available for bonding to a proton. However the protonation of pyridine is still more favorable than the protonation of aniline. The smaller shift in pK_a with the pyridine compounds can be attributed to differential hydration. The protonated pyridine is better hydrated (by hydrogen bonding to the water solvent) than the more favorable aniline (free base) due to the pyridinal nitrogen's ability to hold on to its positive charge ^[22].

The same experiments were conducted with methanol as the organic eluent and perchloric acid as the acidic modifier to adjust the pH of the mobile phase [see Table 2-IX]. If the same procedure is conducted as above to correct for the pH shift and to determine the actual pK_a shift, it is seen that once again the aniline species behaves as a weaker base. Once again, the weaker basicity of the aniline compounds became prevalent. The pK_a shift was much greater with the methanol eluent when compared to the acetonitrile eluent for the aniline compounds. This demonstrates that even the difference in the solvents will cause a significant change in the pK_a that may also be attributed to the preferential solvation of the eluent components.

Reproducibility

The reproducibility of the determination of the chromatographic pK_a was demonstrated by performing the experiment at pH 1.3 to 8.3 three times with two different columns and with two different analysts [see Table 2-X]. The results for the pK_a values do not deviate between the three determinations greater than 1.5%. This correlates to errors of less than 0.04 pH units for the pK_a values of the bases studied. Therefore the results

Table 2-IX
Effect of methanol on shift of pK_a

Compound	Titration pK _a , 25°C in water	Column 2	Δ pK _a
		90 10mM Na ₂ HPO ₄ : 10%MeOH HClO ₄ HPLC pK _a , 25°C	
2-ethylpyridine	5.89	5.799	0.09
3-ethylpyridine	5.80 (20°C)	5.496	0.30
4-ethylpyridine	5.87	5.854	0.02
2,4-dimethylpyridine	6.74	6.52	0.22
2,6-dimethylpyridine	6.71	6.49	0.22
3,4-dimethylpyridine	6.47	6.267	0.20
3,5-dimethylpyridine	6.09	5.951	0.14
aniline	4.6	3.947	0.65
N-methylaniline	4.85	4.232	0.62

Column 150x4.6 mm Zorbax XDB-C18; mobile phase: 10/90 Methanol/10mM Disodium Hydrogenphosphate buffer adjusted with perchloric acid; flow rate, 1.0 ml/min; 25°C, UV, 254 nm; sample: 1 μl injection.

presented before comparing the aniline and pyridine species are within the statistical error and are valid.

Effect of changing concentration of organic and type of buffer system

Basic analytes

We compiled all our experiments in which we changed the organic content from 10% acetonitrile to a higher concentration of acetonitrile to study the effect of changing organic on the chromatographically determined pK_a of basic compounds (see structures, Figure 2-20). The first experiment conducted used a 70% 25 mM Na_2HPO_4 buffer (pH=8.96) with the pH adjusted with perchloric acid: 30% MeCN, Table 2-XI. The second experiment was conducted used a 70% 10 mM Na_2HPO_4 buffer (pH=8.96) with the pH adjusted with perchloric acid : 30 % MeCN, Figure 2-21 and Table 2-XII. The third experiment conducted used a 70% 10mM NH_4OAc buffer (pH=6.76) with pH adjusted with acetic acid: 30% acetonitrile, Figure 2-22, Table 2-XIII.

The pK_a values obtained in the system that contained an acetate buffer showed a large affect on the apparent pK_a shift, Table 2-XIII. The shift observed in the phosphate buffer system, as shown in Table 2-XII was not as great. Actually this can be explained by reviewing Barbosa's data^[16] for acetate buffer which shows a pH shift of 0.3 pH units per 10% acetonitrile. The correction factor used to correct for the pH shift of the aqueous phase in this hydroorganic mixture is 0.9 pH units ($0.3 \times 3 = 0.9 \text{ units}$), when acetate buffer is employed. For phosphate buffer Barbosa shows a pH shift of 0.2 pH units per 10% acetonitrile. Therefore, the correction factor used to correct for the pH shift of the aqueous phase in this hydroorganic mixture is 0.6 pH units ($0.2 \times 3 = 0.6 \text{ units}$), when phosphate buffer is employed.

Table 2-X

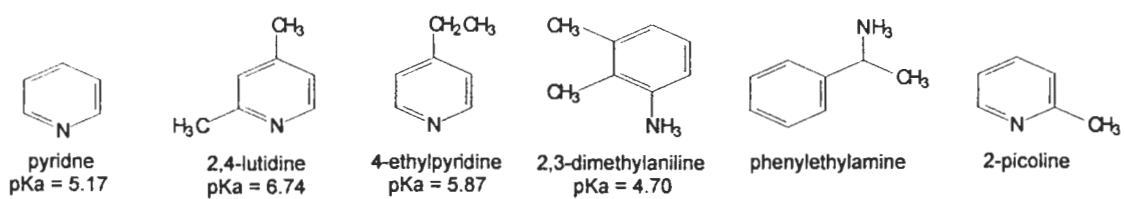
Reproducibility of chromatographically determined pK_a using perchloric acid as acidic modifier.

Compound	Titration pK _a , 25°C in water	Column 2	Run #1 Column 1	Run #2 Column 1	%RSD	Average	Δ pK _a
		90% 10mM Na ₂ HPO ₄ : 10%MeCN HClO ₄ HPLC pK _a , 25°C	90% 10mM Na ₂ HPO ₄ : 10%MeCN HClO ₄ HPLC pK _a , 25°C	90% 10mM Na ₂ HPO ₄ : 10%MeCN HClO ₄ HPLC pK _a , 25°C			
pyridine	5.17	4.947	4.993	4.952	0.51	4.96	0.21
2-ethylpyridine	5.89	5.548	5.623	5.602	0.69	5.59	0.30
3-ethylpyridine	5.80 (20°C)	5.285	5.441	5.32	1.53	5.35	0.45
4-ethylpyridine	5.87	5.672	5.794	5.702	1.11	5.72	0.15
2,4-dimethylpyridine	6.74	6.284	6.31	6.29	0.22	6.29	0.45
2,6-dimethylpyridine	6.71	6.28	6.269	6.26	0.16	6.27	0.44
3,4-dimethylpyridine	6.47	6.035	6.075	6.05	0.33	6.05	0.42
3,5-dimethylpyridine	6.09	5.693	5.755	5.73	0.54	5.73	0.36
aniline	4.6	4.068	4.148	4.15	1.13	4.12	0.48
N-methylaniline	4.85	4.449	4.553	4.54	1.26	4.51	0.34

Table 2-XIEffect of changing organic composition on the analyte pK_a value of basic analytes

Compound	Titration pK_a , 25°C in water	Column 5	ΔpK_a
		70% 25mM Na_2HPO_4 : 30%MeCN HClO ₄ HPLC	
2,6-dimethylpyridine	6.71	5.6	1.11
aniline	4.6	3.7	0.9

Column 150x4.6 mm Zorbax XDB-C18; mobile phase: 30/70 Acetonitrile/25mM Disodium Hydrogenphosphate buffer adjusted with phosphoric acid; flow rate, 1.0 ml/min; 25°C, UV, 254 nm; sample: 1 μ l injection.



The pK_a of phenylethylamine is 9.83 and the pK_a of 2-picoline is 5.96.

Figure 2-20. Structures and pK_a's of some of the basic compounds studied.

Table 2-XII
Effect of changing organic composition on the pK_a value of basic analytes

Compound	Prodigy ODS-2		
	Titration	HPLC	Δ pK _a
	pK _a , 25°C in water	pK _a , 25°C	
pyridine	5.17	4.268	0.90
4-ethylpyridine	5.87	4.785	1.09
2,4-dimethylpyridine	6.74	5.498	1.24
2-picoline	5.96	4.887	1.07
2,3 dimethylaniline	4.70	3.827	0.87
4-aminobenzoic acid	4.85*	5.1**	0.25

Column 150x4.6 mm Prodigy-ODS-2; mobile phase: 30/70 Acetonitrile/10mM Disodium Hydrogenphosphate buffer adjusted with perchloric acid; flow rate, 1.0 ml/min; 25°C, UV, 254 nm; sample: 1 µl injection.

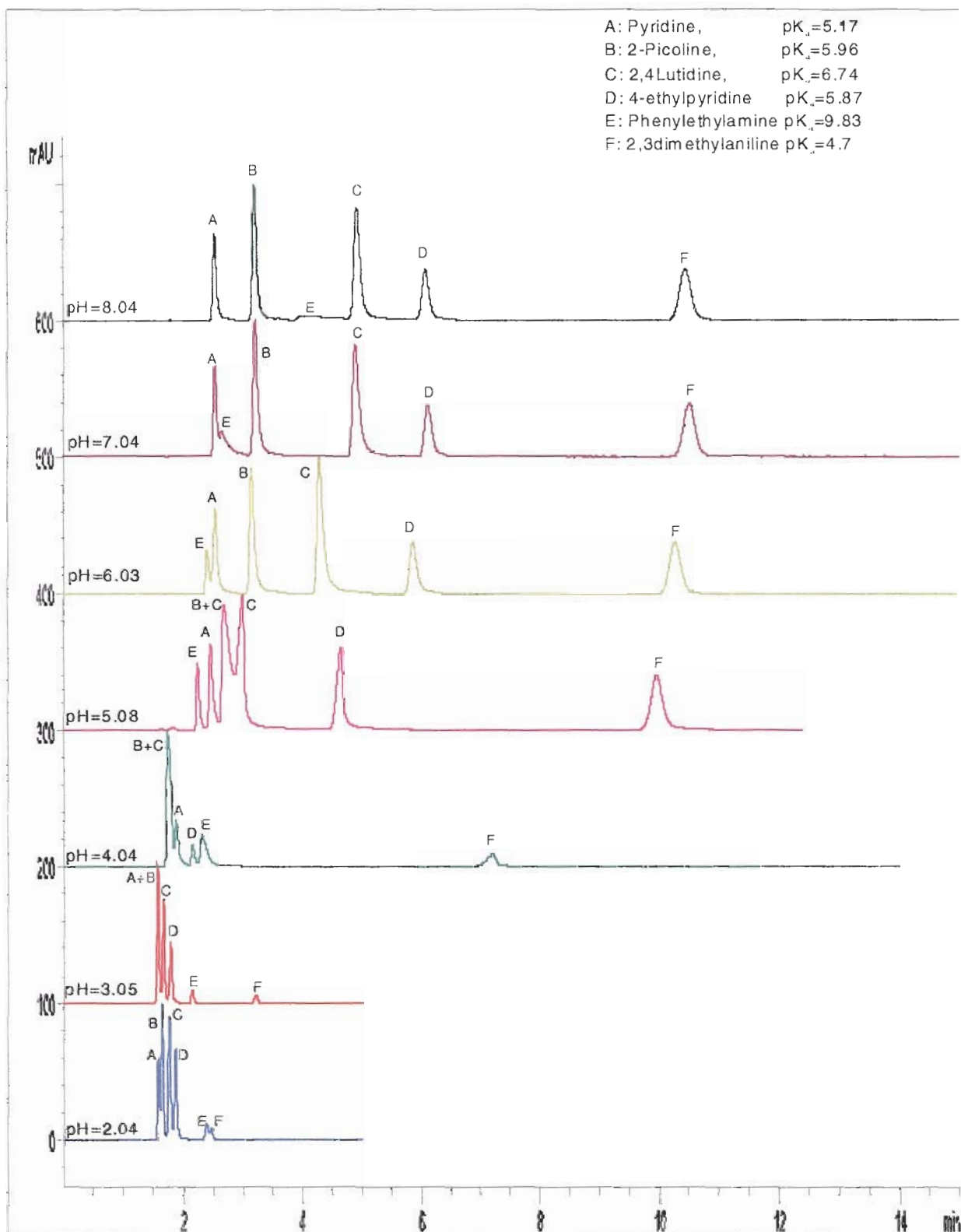


Figure 2-21. Effect of pH on the retention of basic analytes of varied pK_a . Conditions as in Table 2-XII

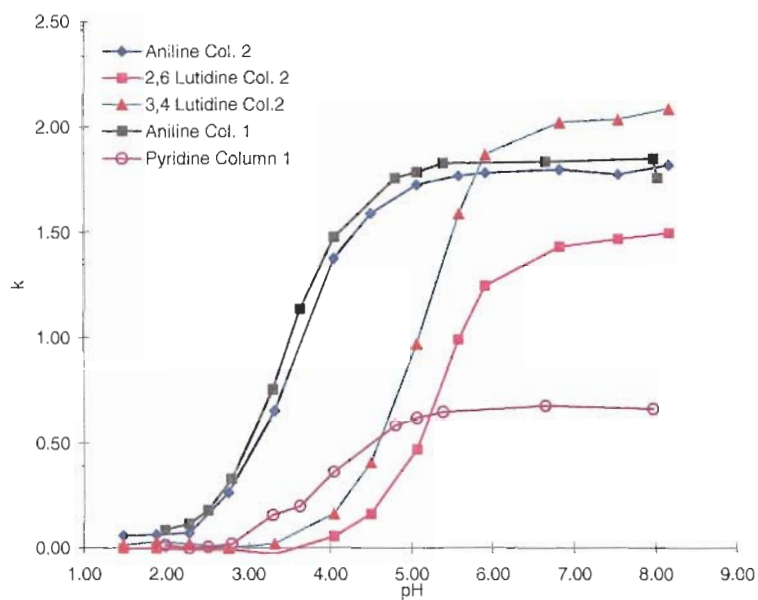


Figure 2-22. Retention factor versus pH of the aqueous phase adjusted with acetic acid. Column 150 X 4.6 mm Zorbax XDB-C18, 70:30, 10 mM NH₄OAc adjusted with x Acetic acid, Flow rate: 1.0 ml/min. Temperature: Ambient

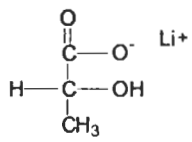
Table 2-XIII
Effect of organic content on the analyte pK_a and reproducibility.

Compound	pK _a , 25°C in water Titration	Column 3	Column 4		
		70% 10mM NH ₄ OAc : 30%MeCN		Column 3	Column 4
		HOAc HPLC	HOAc HPLC	ΔpK_a	ΔpK_a
pyridine	5.17	3.95	-	1.22	
2,4-dimethylpyridine	6.74	-	5.101		1.64
2,6-dimethylpyridine	6.71	-	5.321		1.39
aniline	4.6	3.49	3.553	1.11	1.05

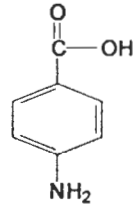
Conditions as in Figure 2-22.

Now let us look at the apparent pK_a shifts determined for pyridine and 2,4 dimethylpyridine in the acetate and phosphate systems. The apparent pK_a shift for pyridine and 2,4 dimethylpyridine in the acetate system were 1.22 and 1.64, respectively [see Table 2-XIII and Figure 2-22]. The apparent pK_a shift for the pyridine and 2,4 dimethylpyridine in the phosphate system [Table 2-XII] were 0.9 and 1.24, respectively. Therefore a greater shift in the apparent pK_a of 0.3 – 0.4 pH units was obtained in the acetate system compared to the phosphate system. However, if the apparent pK_a is corrected for the specific pH shift expected in the particular buffer systems a true pK_a shift in the hydroorganic mixture can be obtained using equation 2-22. For pyridine chromatographed in the acetate system, this shift corresponds to $5.17 - (3.95+0.9) = 0.32$ pH units. For pyridine in the phosphate buffer system this shift corresponds to $5.17 - (4.268+0.6) = 0.30$ pH units. The same procedure can be performed for 2,4 dimethylpyridine. These results show that after correction for the pH shift in a particular buffer system the same pK_a shift is obtained. Therefore for these two basic compounds it is shown that the basic analyte ionization is independent of the acidic modifier employed. This may lead to the development of a universal correction factor for determining the pK_a of basic and acidic compounds on the basis of type of buffer, and type and concentration of organic modifier employed in the mobile phase.

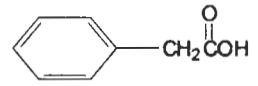
The results shown in Table 2-XI and Table 2-XII show the apparent pK_a shift in the same hydroorganic eluent with different starting concentration of disodium hydrogenphosphate buffer. Although, these results only present a limited set of data, these initial results show that the apparent shift of the pK_a seems to be independent of the buffer concentration. However, a more in depth study must be performed using buffers of



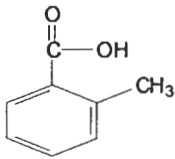
lithium lactate



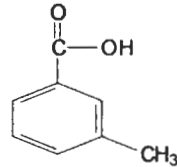
4-aminobenzoic acid



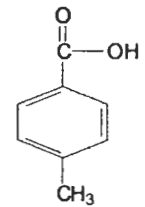
phenylacetic acid



o-toluic acid



m-toluic acid



p-toluic acid

Figure 2-23. Structures of acidic analytes

Table 2-XIV
Chromatographically determined pK_a of acids.

Compound	Titration pK _a , 25°C in water	Column 6	Δ pK _a
		HPLC pK _a , 25°C	
Phenylacetic acid	4.31	4.458	0.15
o-toluic acid	3.9	4.337	0.44
m-toluic acid	4.27	4.467	0.20
p-toluic acid	4.36	4.532	0.17
4-aminobenzoic acid	4.85*	4.982**	0.13

*The pK_a of the amino functionality is 2.5 and of the benzoic group is 4.85

** The pK_a shown is of the benzoic group determined by HPLC

Column 150x4.6 mm Zorbax Eclipse XDB-C₁₈; mobile phase: 30/70 Acetonitrile/20mM Disodium Hydrogenphosphate buffer adjusted with perchloric acid; flow rate, 1.0 ml/min; 25°C, UV, 220 nm; sample:1 μl injection.

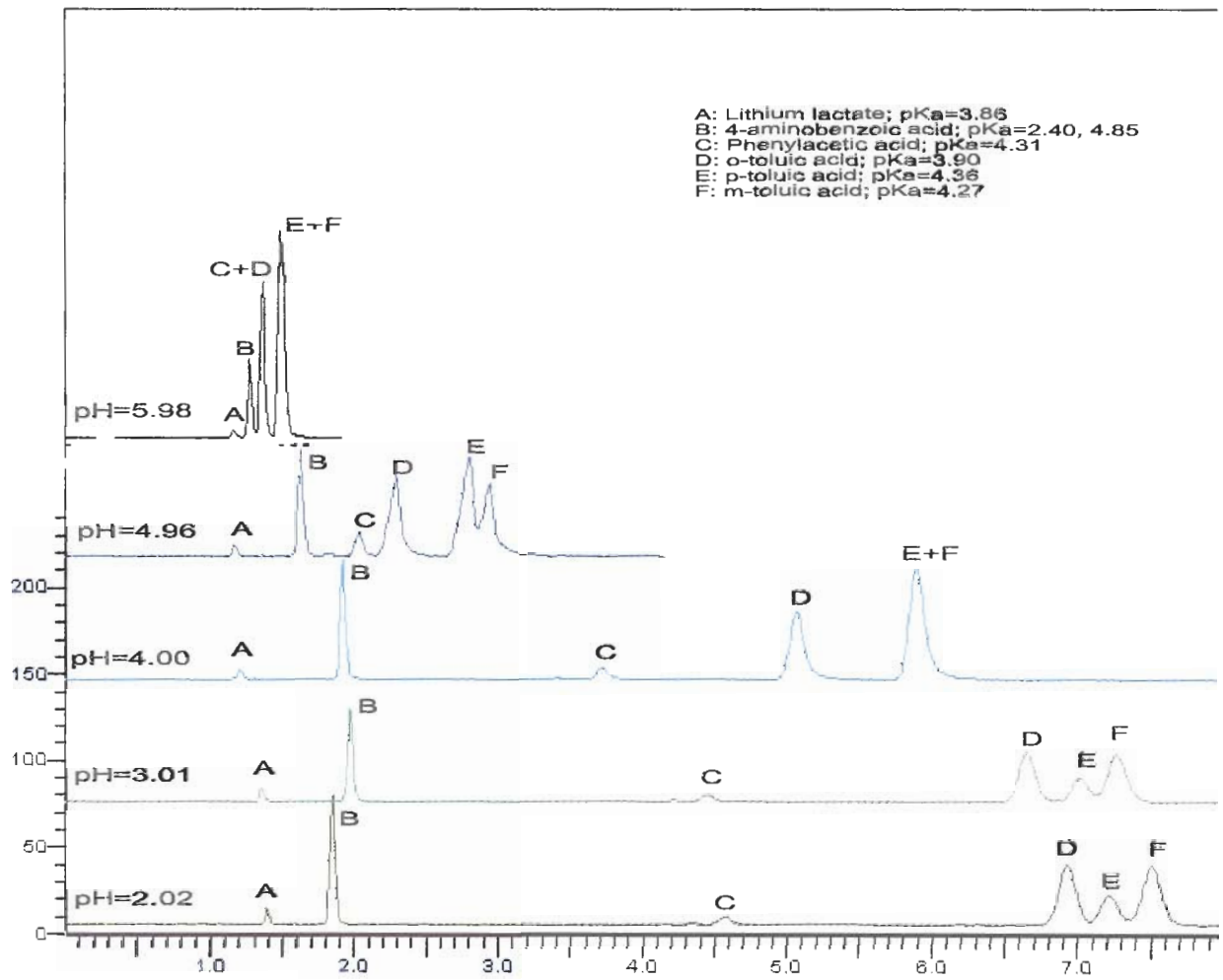


Figure 2-24. Retention of acidic compounds as a function of mobile phase pH. Conditions as in Table 2-XIX.

increasing ionic strength to determine if there is any correlation of the apparent pK_a shift as a function of the ionic strength and of the activity coefficient of the solution.

Acidic analytes

The apparent pK_a shift was also studied for acidic analytes as well. For acidic analytes, we expect a shift to higher pH values since we are suppressing the ionization of the acidic analyte in the aqueous phase. The structures of the acid analytes used for this study are shown in Figure 2-23. The chromatograms of a mixture of six acids at the various pH's are also given in Figure 2-24. It was shown that in an eluent, 70% aqueous (20mM Disodium Hydrogenphosphate buffer adjusted with perchloric acid):30% MeCN there is an apparent pK_a shift to greater values. The average pK_a shift for this set of various aromatic benzoic acids is 0.07 pH units per 10% acetonitrile in this phosphate buffer system, (see Table 2-XIV). This apparent shift in pK_a is much lower than with basic compounds. These results that show a lower pK_a shift for acidic compounds provide more supporting evidence that the ionization of acids and bases are affected to different degrees in hydroorganic mixtures. For acidic compounds the effect of the dielectric constant plays a larger role than for basic compounds, but other factors such as the analyte solvation, type of buffer and organic and acidic modifier employed may also have an effect as well.

Conclusion

Small changes in the pK_a of ionogenic species may correlate to large changes in retention in HPLC when the pH of the aqueous/organic phase is in the vicinity of the pK_a of the solute. This may lead to changes in the selectivity and may affect the resolution of ionizable components within a mixture. However, modification of the pH and the organic

may serve as a valuable tool for the method optimization in reversed phase HPLC for ionogenic solutes.

Literature Cited
Chapter 2

1. M. Mizutani, *Zeits. Physik. Chem.*, **118**, **1925**, 318
2. N.F. Hall, and M.R. Sprinkle, *J.Amer.Chem.*, **54**, **1932**, 3469
3. E. Grunwald and B.J. Berkowitz, *J.Amer.Chem.Soc.*, **75**, **1953**, 559
4. A.L. Bacarella, E. Grunwald, H.P. Marshall and E.L. Purlee, *J.Org.Chem.*, **20**, **1955** 747
5. E. Grunwald and B.J. Berkowitz, *J.Amer.Chem.Soc.*, **75**, **1953**, 559
6. D.V. McCalley, *J.Chromatogr.A.*, **664**, **1994**, 139
7. R.G. Bates, M. Paabo and R.A. Robinson, *J.Phys.Chem.*, **67**, **1963**, 1833
8. P.W. Atkins, *Physical Chemistry*, Oxford University Press, **1978** , 338
9. R.G. Bates, *Determination of pH. Theory and Practice*, Wiley-Interscience, New York, Chapter 8, **1973**
10. M. Born, *Z.Physik*, **1**, **1920**, 45
11. O. Budewsky, *Foundation of Chemical Analysis*, Ellis Horwood, Chichester, **1979**
12. E. Bosch, P. Bou, H. Allemann, and M. Roses, *Anal.Chem.*, **68**, **1996**, 3651
13. E. Bosch, C. Rafols, and M. Roses, *Anal. Chim.Acta*, **302**, **1995**, 109
14. M. Roses, I. Canals, H. Allemann, K. Siigur, and E. Bosch, *Anal.Chem.*, **68**, **1996**, 4094.
15. J. Barbosa, D. Barron, R. Berges, V. Sanz-Nebot and I. Toro , *J.Chem.Soc. Faraday Trans.*, **93**, **1997**, 1915
16. J. Barbosa, and V. Sanz.-Nebot, *J.Chem.Soc.Faraday Trans.*, **90**, **1994**, 3287
17. Y. Marcus, *J.Chem.Soc., Faraday Trans.* **85**, **1989**, 381
18. A.J. Easteal, and L.A. Woolf, *J.Chem. Thermodyn.*, **20**, **1988**, 693
19. J. Barbosa, R. Berges, I. Toro, V. Sanz-Nebot, *Talanta*, **44**, **1997**, 1271
20. J. Barbosa, V. Sanz-Nebot, I. Toro, *J.Chrom.A.*, **725**, **1996**, 249

21. S.Ege, Organic Chemistry, D.C.Heath and Company, Toronto, Canada, 1994
22. J. March, Advanced Organic Chemistry, Wiley , New York, 1992
23. A. Albert, E.P. Serjeant, The Determination of Ionization Constants, 3rd ed., Chapman and Hall, 1984, 140
24. L.G.Wade, Organic Chemistry, Prentice Hall, New Jersey, 1991
25. J. Clark, and A.E. Cunliffe, Chemistry and Industry, March 17, 1973, 281
26. T. Mussini, F. Mazza, *Electrochim Acta*, 32, 1987, 855
27. C.L. de Ligny, P.F.M., Luykx, M. Rehbach, and A.A. Weinecke, *Recl.Trav.Chim.*, 79, 1960, 699 and 79, 1960, 713
28. W.J. Gelsema, C.L. de Ligny, and H.A. Blijleven, *Rec. Trav.Chim.* 86, 1967, 852 and 85, 1966, 647
29. M. Paabo, R.A. Robinson and R.G. Bates, *J.Amer.Chem.Society*, 87 (3), 1965, 415
30. S. Rondinini, P.R. Mussini, T. Mussini, *Pure Appl Chem*, 59, 1987, 1549
31. T. Mussini, P. Longui, I. Marcolungo, P.R. Mussini, S. Rondinini, R. Fresenius, *J.Anal.Chem.*, 339, 1991, 608
32. J. Barbosa and V. Sanz-Nebot, R. Fresenius, *J.Anal Chem*, 353, 1995, 148
33. A.K. Covington, R.G. Bates and R.A. Durst, *Pure Appl.Chem*, 57, 1985, 531
34. W.H. Beck, J. Caudle, A.K. Covington, and W.F.K. Wynne-Jones, *Proc. Chem.Soc.*, 110, 1963, 123
35. J.J. Kirkland, J.W. Henderson, J.J. DeStefano, M.A. van Straten, H.A. Claessens, *J.Chromatogr.A*, 762, 1997, 97
36. J.J. Kirkland, M.A. van Straten, H.A. Claessens, *J.Chromatography A*, 797, 1998, 111
37. Y.V.Kazakevich, H.M. McNair, *J.Chromatogr. Sci.*, 31, 1993, 317
38. E.H. Slaats, W. Markovski, J. Fekete, H. Poppe, *J.Chromatogr.*, 207, 1981, 299
39. D.S. Kora. E. Tesarova, M. Popl, *J.Chromatogr. A*, 758, 1997, 37
40. J. Nawrocki, *J.Chromatogr. A.*, 779, 1997, 55

41. J.A. Dean, Langes Handbook of Chemsitry, McGraw-Hill, Inc., New York, 14th ed, 1992

Chapter 3

Effect of the Eluent pH, type and concentration of Acidic Modifiers on the HPLC Retention of Basic Analytes.

Summary

The retention of ionogenic organic bases in liquid chromatography is strongly dependent upon the pH of the mobile phase. Chromatographic behavior of a series of substituted aniline and pyridine basic compounds of different stereochemistry and pK_a values has been studied on C_{18} bonded silicas using various aqueous/organic eluents with different pHs.

The effect of different acidic modifiers on solute retention over a pH range from 1.3 to 8.6 was studied. The acidic modifiers used were: perchloric, trifluoroacetic, and phosphoric acid. In a low pH region of pH 1–4 significant increase in basic analyte retention was observed. The retention of the basic compounds at low pH showed major deviations from expected chromatographic behavior. When a basic analyte is protonated, any further decrease of the mobile phase pH should not alter its retention. The lower plateau region of the sigmoidal curve described in Chapter 1 usually represents this dependence.

The increases in retention were attributed to the interaction with counteranions of the acidic modifiers. The acidic counteranions were believed to disrupt the analyte solvation after ion-interaction with the protonated basic analytes. Counteranions that have been shown to increase the disorder of water are called chaotropic counteranions ^[1]. The increase in retention is related to the chaotropic nature of the counteranion and its concentration in the mobile phase. It was also shown that by increasing the concentration of counteranion of the acidic modifier the resolution and selectivity could be optimized.

In this chapter we will distinguish the difference between distinct ion pair formation and ion-association. The influence of the dielectric constant and the concentration of organic modifier of the eluent were also studied.

Introduction

When developing HPLC methods for pharmaceutical compounds, it is often necessary to control the retention of particular analytes by changing and optimizing certain experimental variables: pH of mobile phase, types and concentration of mobile phase additives, buffers, eluent composition, and columns with different geometric parameters. Generally, the retention of basic compounds as a function of pH shows sigmoidal dependence (Figure 1-9, chapter 1). A lower pH led to ionization of the basic analyte and resulted in decreased retention. However, if oppositely charged ions are present in the liquid phase, they will have a tendency to attract one another. This attraction may depend on the dielectric constant of the mobile phase and the solvation of individual ions. The retention factors of protonated nitrogen containing species had been altered when different acidic modifiers were employed in the eluent ^[2-29]. The concentration and hydrophobic nature of the counteranions of the modifier had shown to play an integral part of this effect. Analyte structure and the degree of solvation, including any secondary interaction, had also shown to affect its retention. This effect is attributed to the ionic interaction of protonated analyte with oppositely charged species, that may result in either the formation of stable ion pairs, or the disruption of the analyte solvation. Ion interaction will be used as a general term to denote all different effects related to the analyte ionic interactions.

Historical

Hydrophobicity of the counteranion

The effect of phosphoric acid at low pH on the retention of several zwitterionic solutes, (peptides and proteins) on a C₁₈ column were investigated [2-4]. In the literature authors have suggested that the addition of phosphoric acid led to a decrease in retention due to the formation of hydrophilic ion-paired complexes. However, others have shown ion-pair formation with the phosphate counterion caused an increase in peptide retention due to the reduction in hydrophilicity of the positively charged residues through ion-pair formation [5]. The effects of phosphoric and trifluoroacetic acids on peptide retention on a C₁₈ column were compared and greater retention factors were obtained with trifluoroacetic acid (TFA) [6]. The virtual polarity of the peptide was reduced due to its interaction with TFA, since TFA is less polar than phosphoric acid. However, other authors found the addition of trifluoroacetic acid actually decreased the retention of opiates drugs (protonated at pH's less than 7)[7]. They attributed the decreased retention to ion pair formation. The effects of TFA and perfluoroalkonic (perfluoropropionic and perfluorobutyric) acids on the retention of polar peptides on a C₁₈ column were compared [8]. A significant increase in retention of the peptides with the perfluoroalkonic acids was obtained. This can be explained by the increased lipophilicity of the counteranions and ion-pair complex formation. Similar effects were also obtained for peptides and proteins as the n-alkyl chain length of the perfluorinated carboxylic acid homologues [9-10] increased. The authors suggested these hydrophobic ion-pairing reagents had altered the RP-HPLC column into a dynamic ion exchanger [10]. First, the ion-pairing agent was adsorbed onto the stationary phase. Then, the protonated basic analytes interact with the counterion of the ion-pair reagent through ion exchange. A hydrophobic ion pairing agent (decyl sulfate, at pH=2.1) increased the retention of six

hydrophilic amino acids ^[11]. The formation of ion-pairs with the surfactant counterions in the mobile phase led to the increased retention of the ion-pair complex.

In general, the retention of basic nitrogen containing compounds increased as pH decreased. This phenomenon is attributed to the formation of an ion-pair with the hydrophobic counteranions.

Concentration of the counteranion of the acidic modifier

On a C₁₈ column, the retention of positively charged analytes (adrenaline, normetadrenaline and tyrosine amide) increased as concentration of octyl sulfate increased ^[12]. The authors suggested ion-pair interaction occurs between the negative charge of the octyl sulfate adsorbed on the surface and the positive charge of the solute ions. The retention of three positively charged basic compounds aniline, benzylamine, and phenylethylamine increased as the concentration of the negatively charged sodium octanesulfonate increased. This trend was observed on a C₁₈ column when methanol-water (pH 3) was used as the eluent ^[13]. This behavior was attributed to an ion-interaction mechanism, where the unpaired lipophilic alkyl ions were first adsorbed on the bonded phase.

Analyte Structure

A study on a C₈ reversed phase column at low pH showed the retention of four non-helical peptides increased in the presence of perchlorate ions compared to a system without perchlorate ^[14]. It was shown that the retention of peptides increased as number of the charged lysine residues increased. The authors suggested the ion-pair formation of the protonated lysine residues with the perchlorate anion led to the decrease of the hydrophilicity of the residues (increased retention). Other studies showed that peptide retention was not only dependent on the hydrophobicity and the concentration of the counteranion, but also on

the number of positively charged groups in the peptides ^[6]. As concentration of counteranions increased, the retention of nitrogen containing basic compounds increased.

Analyte solvation and secondary interactions

It has been shown, as the pH was decreased from pH 3 to pH 1, the retention for aminoindanol, a basic pharmaceutical compound, increased when perchloric, trifluoroacetic, nitric and phosphoric acid were used as acidic modifiers on a silica based crown ether column ^[15]. The authors attributed this effect to the type and concentration of the acid counteranion, which affected the solvation of the analyte. Another study showed when mobile phase additives such as perchlorate, nitrate, were employed the retention of propranolol (basic racemate) increased on a Chiracel OD-R column ^[16]. This increase in retention was attributed to the properties of the counteranions such as degree of hydration, polarizability and any secondary interactions among the cations and anions that may effect the ion interaction equilibrium. It was also mentioned that other primary, secondary and tertiary amines showed a similar dependence^[16]. The increase in retention in a low pH region of basic ophthalmic compounds on a C₁₈ column was observed when phosphate, trifluoroacetate and perchlorate were employed as counteranions ^[17]. This effect was attributed to the different degree of solvation of the ophthalmic compounds influenced by the different counteranions.

Comparison of retention models

The retention of protonated basic compounds is dependent upon the pH, type and concentration of mobile phase additives. Most of the experimental work has shown an increased retention of the protonated analyte with decreasing pH or increasing acidic

modifier concentration. Several models proposed for the effect of these anionic reagents upon retention of the protonated species were discussed in detail in Chapter 1.

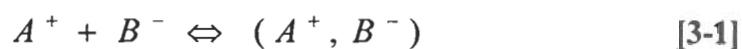
One model suggests the formation of an ion-pair with the solute in the mobile phase with consequent retention of the neutral complex on the reversed phase column [18-22]. Another model suggests ion-pair formation in the mobile phase and adsorption of the noncomplexed free ionic analyte, such as a protonated basic analyte [23]. Yet another model suggests the modification of the hydrophobic character of the stationary phase where the counteranion of the acidic modifier is first sorbed onto the column, followed by a dynamic ion-exchange process occurs where the solute molecules interact with the sorbed counteranion. [12,24-27]. This model can be employed when a surfactant-like acidic modifier is used and this modifier contains a hydrophobic moiety of significant size (such as octylsulfonic acid) [12,26,28]. On the other hand, for modifiers of lower hydrophobicity, such as inorganic acids, the model of ion pair formation in the mobile phase is commonly used [29].

Regardless of where the ion interaction occurs, generally an increase in retention was observed with more hydrophobic counteranions. Also, an increase in concentration of the ion-interaction reagent was observed to increase the analyte retention. The influence of the type and concentration of acidic modifier is usually associated with the formation of ionic pairs with protonated analyte [17-29]. In case of inorganic acids, such as H_3PO_4 , $HClO_4$, or TFA, the formation of ionic pairs in the mobile phase is suggested. This effect is dependent on the ion charge and the solvent's dielectric constant. The formation of stable ionic pairs is most favorable for smaller ions with high charges in solvents of low dielectric constant. Therefore, the formation of stable ionic pairs in water will usually occur only to a small extent [30-31].

The coulombic attraction between opposite ions is somehow suppressed by the solvation of the analyte with increasing polarity of the solvents. This suggests another possible mechanism, the ion-association of the protonated basic analyte with the counteranion of the acid that affects the solvation of the analyte. The higher the disruption of the analyte solvation shell, the greater the analyte retention. The increased retention is due to a decrease of the virtual polarity (hydrophilicity of the solvated cluster) of the analyte. The increase in retention is also related to the chaotropic nature of the counteranion. Counteranions that have been shown to increase the disorder of water are called chaotropic counteranions ^[1]. The greater the concentration of a chaotropic counteranion in the eluent, the greater the increase in retention of the protonated basic analyte.

Ion-Pair formation versus Ion Association

Oppositely charged species can be bound to one another which form a partially or fully neutralized species. (A⁺,B⁻) is denoted as the neutral ion-paired species.



Bjerrum ^[32] first suggested that a pair of oppositely charged ions may get trapped in each others coulombic field followed by the formation of an ion pair. The paired ions form an ionic dipole with a net charge of zero. The ion pair is formed on the basis of coulombic interactions of spherical ions. If the ions are separated by a distance *a* greater than a certain minimum value, the free ions exist in solution (Debye Huckel theory will hold true). When the **distance** is less than *q* then nonconducting ion-pairs are formed [Figure 3-1b].

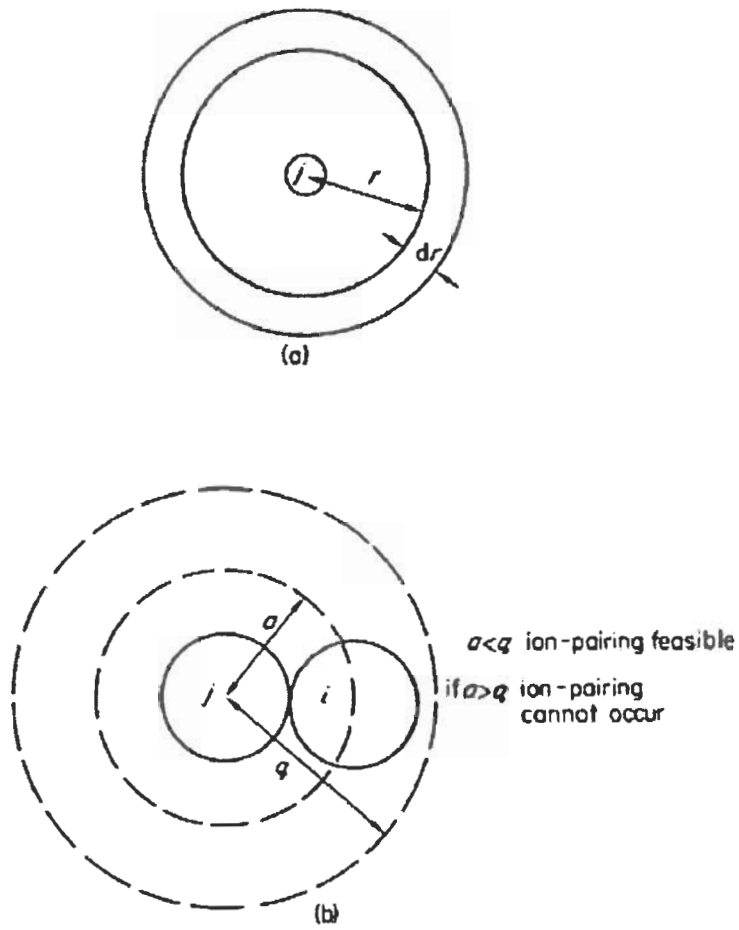


Figure 3-1. Schematic Diagram of Ion-pairing. a) Model for determination of distribution of i-ions within shells of specified dimensions about j-ions. b) Relation of a to q for ion-pairing.^[30]

The certain minimum value for this is given by:

$$q = \frac{z_i z_j e^2}{2 DkT} \quad [3-2]$$

Equation 3-2 may be derived from a consideration of the Boltzmann distribution of i-type ions in a thin shell of thickness dr at a distance r from a central j-type ion. [Figure 3-1a] Let us now consider the probability P_r , of finding an i ion with a shell thickness dr , at radius r from a reference ion j of opposite charge. The probability, P_r , that an ion i is in this spherical shell is proportional, to the ratio of the volume $4\pi r^2 dr$ of the shell to the total volume V of the solution; to the total number N_i of ions present and to the Boltzmann factor $\exp^{(-U/kT)}$, where U is the potential energy of an ion, i , at a distance r from an ion j of opposite charge [33].

$$P_r = 4\pi r^2 dr \frac{N_i}{V} e^{-\frac{U}{kT}} \quad [3-3]$$

N_i/V is the concentration n_i^0 of i ions in the solution and

$$U = \frac{-z_i z_j e_o^2}{\epsilon r} \quad [3-4]$$

and upon substitution

$$P_r = (4\pi n_i^0) r^2 e^{\frac{z_i z_j e_o^2}{\epsilon kT}} dr \quad [3-5]$$

Therefore the probability of finding a negative ion near an ion of positive charge is dependent mainly on the radius from a reference ion j and the dielectric constant of the medium. For small values of r at a constant temperature, the probability functions are dominated by (U/kT) and P_r increases with decreasing r and with decreasing dielectric

constant of the medium. However, for larger values of r the exponent approaches 1 and P_r increases with increasing r since the volume $4\pi r^2 dr$ of the spherical shell increases as r^2 .

Therefore, it is assumed that lowering of the dielectric constant will encourage association. If the sum of the ion radii is known, then a maximum value of the dielectric constant could be calculated denoting where ion-pairing would cease. Conductance measurements have been used as in the literature^[30] to determine if the maximum values of D obtained are in good correlation with theory. In essence, at values less than this critical D , the conductance should level off. This is shown in Figure 3-2.

Denison and Ramsey expanded on the Bjerrum approach to account for van der Waals interactions between oppositely charged ions as well as the fact that the translational entropy of the free ions is greater than that of the ion pair^[34]. Their resulting expression for the ion pair association constant, K_A can be written as follows:

$$\ln K_A = \ln K_A^* + \frac{|Z_A Z_B| e^2}{akT\epsilon} \quad [3-6]$$

where K_A^* is the noncolumbic contributions to K_A , and Z_A , and Z_B are the charges on ions A and B, e is the electron charge, k is the Boltzmann constant, and T is the absolute temperature. Assuming K_A^* remains constant with change in solvent, equation 3-6 predicts that $\ln K_A$ will decrease with $1/\epsilon$. This however is only qualitatively correct since the specific solvation of ions and ion-pairs may play a significant role on the position of the equilibrium.

Therefore, in solvents possessing different functionalities large differences in ion-pair formation may be possible. Due to the solvation of ions two type of ion-interaction species

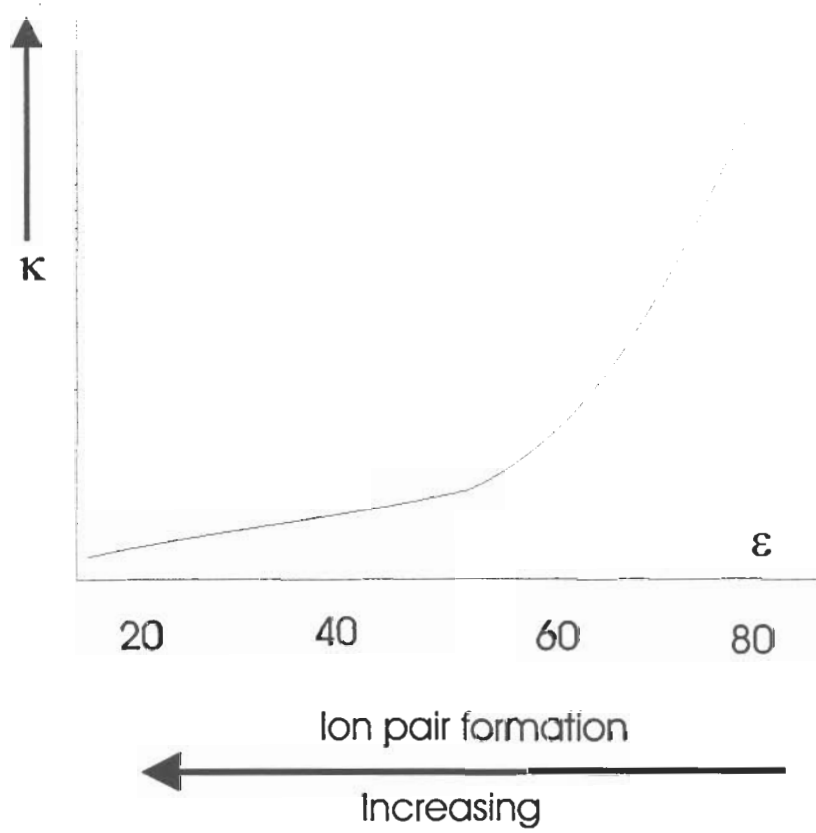
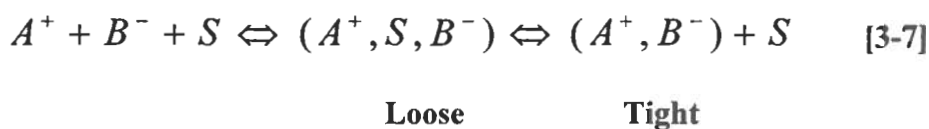


Figure 3-2. Schematic of conductance versus dielectric constant.

can be formed: a) tight or contact ion-pairs and b) loose or solvent separated ion pairs^[35-36]. In the first case the ions of opposite charge are in the proximity of the nearest neighbor shells of each other and form stable ionic pairs with a net charge of zero. In the second case, the solvation shell of at least one of the ions is maintained in the ion-associated species. Szwarc^[37] and Fuoss^[38] have envisioned this as a two step process.



S are the solvent molecules, A^+ is the protonated analyte and B^- is a negatively charged species. The tight contact ion pair is formed from the removal of solvent around the ions. Other authors have also discussed the treatment of ion pair formation on the basis of the distinction between loose or solvent separated ion pairs and intimate or touching ion pairs^[39-41].

Szwarc stated “It is sometimes difficult to distinguish between the two types of ion-pairs but we must realize that we may often (but not exclusively) be dealing with solvent separated ion-pairs in the typical chromatographic systems, particularly if the ions are well solvated.” Hence we will consider tight contact ion-pairs as ion-paired ions and loose solvent separated species as ion-associated ions. The basic analyte (cationic form) solvation may be disturbed as a consequence of changing the organic concentration and/or type and concentration of anion. The main focus of this chapter is to discuss the disruption of the analyte solvation and how this consequently leads to an increase in the basic analytes retention.

In the literature, the majority of the studies in the low pH region have been performed with analytes of zwitterionic nature, such as peptides and proteins. The effects of the type and concentration of inorganic mobile phase additives on the retention of small basic analytes at a low pH region have only been studied to a small extent in the literature. In this chapter the effect of the type and concentration of several counteranions of the acidic modifiers on the retention of primary, secondary, and tertiary nitrogen containing compounds on typical reversed phase C18 columns will be investigated in detail. The compounds used in this study were a series of substituted aniline and pyridine compounds.

Experimental

Apparatus: The chromatographic system used was a HP model 1100 HPLC from Hewlett Packard (Little Falls, DE). The chromatograms were processed using HP software. The column used was Zorbax Eclipse XDB-C18, (Hewlett Packard, Little Falls, DE), 150 x 4.6 mm i.d. and 250 x 4.6 mm i.d. , particle diameter 5 μ m, bonding density 3.4 μ mol/m². The Eclipse XDB-C18 column has a nominal surface area of 180 m²/g, and a pore size of 80Å. This column is a densely bonded dimethyl-silane-substituted stationary phase that is double endcapped with dimethyl and trimethylsilane groups and has been demonstrated to be very stable at both low and high pH values ^[42-43]. Another column used was Luna-C18 column, (Phenomenex, Torrance, CA), 150 x 4.6 mm i.d., particle diameter 5 μ m, bonding density 3.0 μ mol/m². The Luna C18 column has a nominal surface area of 300 m²/g, and 90 Å pore size.

The column temperature was controlled by a circulating water bath Brinkman Model RC6 (Lauda-Konigshofen, Germany). pH measurements were performed with a Fisher Accumet pH meter 15 on the aqueous eluent component before addition of the organic

modifier. The electrode was calibrated with pH 1.0, 2.0, 4.0, 7.0, and 10.0 standard solutions.

Chemicals

Orthophosphoric acid (analytical grade), perchloric acid (redistilled) and trifluoroacetic acid (spectrophotometric grade), water (HPLC grade), and acetonitrile (HPLC grade) were obtained from Sigma Chemical Co. (Milwaukee, WI). Sodium hydrogenphosphate heptahydrate and sodium perchlorate was purchased from Fischer Scientific (Fairlawn, NJ). All aqueous mobile phases were filtered with Whatman Nylon 66 membrane filter (Clifton, NJ). The following basic compounds were used: aniline (Baker, Phillipsburg, NJ), N-methyl-aniline (Eastman, Kingsport, TN), pyridine, 2-ethylpyridine, 3-ethylpyridine, 4-ethylpyridine, 2,4-dimethylpyridine, 2,6-dimethylpyridine, 3,4-dimethylpyridine, 3,5-dimethylpyridine, *o*-chloroaniline and 4-tertbutylpyridine, 2-n-propylpyridine, 4-n-propylpyridine, benzylamine, 2-methylbenzylamine, 3-methylbenzylamine, and 4-methylbenzylamine (Sigma, Milwaukee, WI). The following beta blockers were used: Nadolol, (S)-(-)-propranolol hydrochloride, Atenolol, Pindolol, Metolol, Sigma (Milwaukee, WI). The following neutral compounds were used: caffeine, phenol and theophylline, Sigma (Milwaukee, WI). The following acids were used 4-aminobenzoic acid, phenylacetic acid, and ortho, meta and para toluic acids, Sigma (Milwaukee, WI).

Chromatographic Conditions

The retention data was recorded at 25°C using isocratic conditions with a flow rate of 1 mL/min for the Zorbax Eclipse XDB-C18. UV detection was at 254 nm for the entire study except for the beta blockers which was 225 nm. The aqueous portion of the mobile phase was a 5 mM, 10mM, 17.5mM, 25 mM, or 50mM Disodium hydrogen phosphate buffer

(pH=8.96) adjusted with the different acidic modifiers (perchloric, trifluoroacetic acid, or ortho-phosphoric acid) over the pH range of 1.3 to 8.3. The organic modifier used was acetonitrile and the eluent composition was 90:10 buffer:organic. For the studies without the phosphate buffer, water was mixed with perchloric, phosphoric and trifluoroacetic acids, in the pH range 1.3 to 2.1. All analyte solutions except for the benzylamines were prepared by their dissolution in the eluent to give a concentration of 0.1-0.2 mg/mL. Benzylamines were dissolved in 70/30 water/acetonitrile to give a concentration of 0.2 mg/mL. Injections of 1-5 μ l of these solutions were made.

The t_0 value obtained for the Zorbax XDB-C₁₈ column with the minor disturbance method [44-45] at 25°C was 1.46 min and the t_0 obtained using the first baseline disturbance was 1.45 min. The retention factors calculated were the average of triplicate injections. Also, a test mix of aniline and pyridine was used as a system suitability check before and after each experiment to determine the stability of the column and system performance.

Results and discussion

Comparison of the effect of acidic modifiers on retention using 10mM sodium hydrogen phosphate buffer

Phosphoric acid

The pH of a 10mM sodium phosphate buffer was adjusted with phosphoric acid and the retention factors were obtained for each pH. The pH plotted is the pH of the buffer before the addition of organic eluent. A plot of the retention factors for several basic compounds versus pH is shown in Figures 3-3. Retention factors level off at $\text{pH} \ll \text{pK}_a$ as is seen for an isomeric series of pyridines (Figure 3-3).

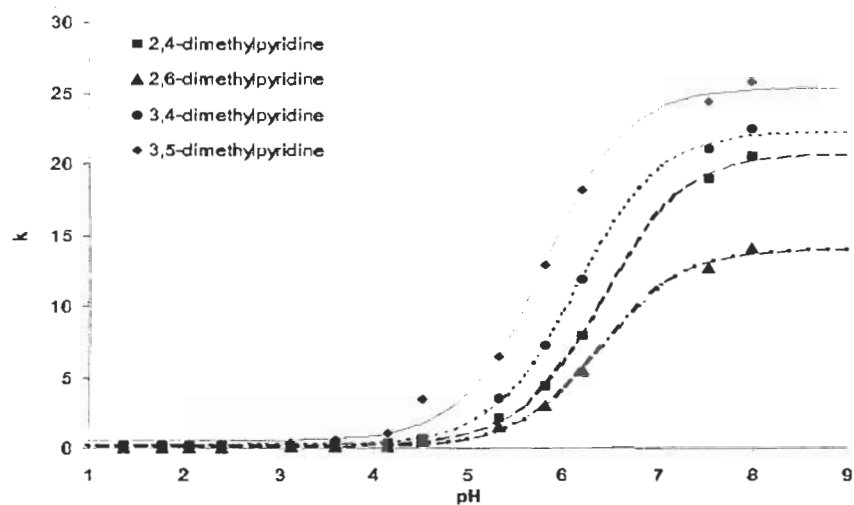


Figure 3-3. Retention factor versus pH for an isomeric series of dimethylpyridines. Chromatographic conditions. Column 150x4.6 mm Zorbax XDB-C18; mobile phase: 10/90 Acetonitrile/10mM Sodium Phosphate buffer adjusted with phosphoric acid; flow rate, 1.0 ml/min; 25°C, UV, 254 nm; sample: 1 μ l injection.

Trifluoroacetic acid and Perchloric acid

The pH of a 10mM disodium hydrogen phosphate buffer adjusted with perchloric or trifluoroacetic acid instead of phosphoric acid led to the same dependence of analyte retention on pH, until a pH=3. As seen in Figure 3-4 the decrease of mobile phase pH below 3 leads to a slight increase of the analyte retention. At pHs' above 4 the curve shows the typical sigmoidal behavior of Figure 3-3. In the low retention region even a small change of the retention will have a significant effect on the resolution since chromatographic peaks are narrow (Figure 3-5). Also, the symmetry factor for 4-ethylpyridine increased with the decrease of pH from 4.1 to 1.3 (see Table 3-1). The symmetry factor was obtained from the HP1100 software ^[46]. Similar trends in the increase of symmetry factor with decrease of pH from 4.1 to 1.3 were observed for the other basic analytes studied. All basic analytes studied have shown an increase of retention volume (see Table 3-II) with a decrease of pH using both perchloric and trifluoroacetic acid (Table 3-III).

Similar effects have been observed ^[47-48] in the literature and were described as resulting from interaction with residual silanols on the stationary phase. Increased retention factors at pH's < 4 for 4-aminopyridine and 2-phenylethylamine on a SGX C18 column were observed ^[47]. An increase in retention factor for some substituted anilines on a Hypersil ODS column at pH's less than four was also claimed to be caused by strong ion-exchange interactions with accessible silanols ^[48]. The pK_a values of normal silanols on a silica surface are estimated to have a value of 7. The pK_a depends on the environment and amount metal impurities in the silica matrix ^[49-51]. The effect of pH on silanol retention activity should resemble their titration curve. At low pH, accessible residual silanols **will be protonated** and **should show minimal activity**, any further decrease of the pH should not have any effect.

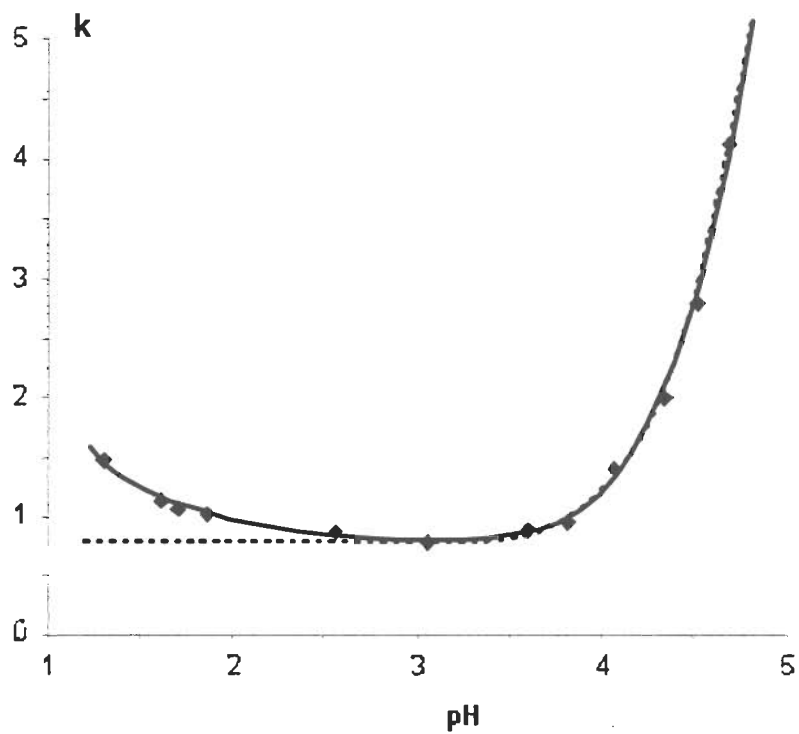


Figure 3-4. pH dependence of the retention of 4-ethylpyridine. Column 150x4.6 mm Zorbax XDB-C18. Mobile phase: Acetonitrile:10mM Disodium hydrogenphosphate buffer adjusted with trifluoroacetic acid, (10:90); flow rate, 1.0 ml/min; 25°C, UV, 254 nm; sample: 1 μ l injection.

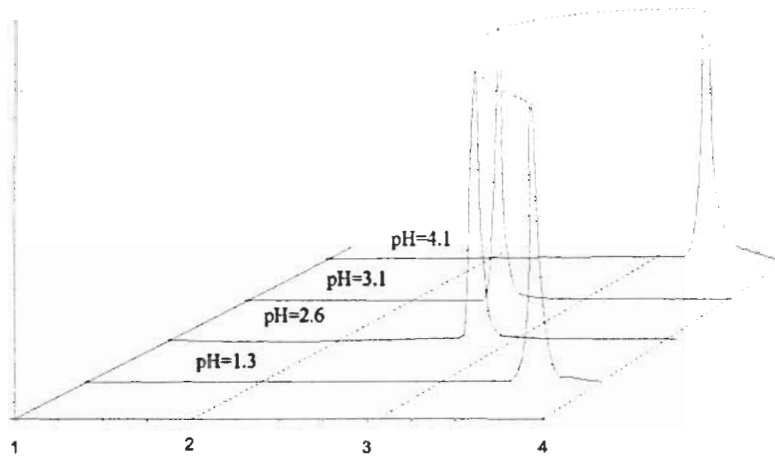


Figure 3-5. The effect of TFA (pH adjustment) on retention of 4-ethylpyridine. Column and chromatographic conditions same as in Figure 6. Retention time at pH=4.1 is 3.5, at pH=3.1 is 2.6 at pH=2.6 is 2.7 and at pH=1.3 is 3.6.

Table 3-I
Increase in symmetry factor for 4-ethylpyridine with decrease in pH

pH	Symmetry factor
4.08	0.63
3.06	0.69
2.56	0.72
1.3	0.83

Table 3-II
Retention factor at each pH adjustment with trifluoroacetic acid

pH	aniline	N-methylaniline		
4.08	2.50	5.79		
3.82	1.64	3.49		
3.6	1.26	2.54		
3.06	0.78	1.47		
2.56	0.74	1.34		
1.86	0.82	1.38		
1.7	0.88	1.49		
1.61	0.91	1.60		
1.3	1.04	1.93		
pH	pyridine	2-ethylpyridine	3-ethylpyridine	4-ethylpyridine
4.08	0.46	0.98	1.88	1.40
3.82	0.30	0.67	1.18	0.95
3.6	0.22	0.58	0.99	0.89
3.06	0.14	0.50	0.78	0.79
2.56	0.15	0.55	0.83	0.87
1.86	0.17	0.64	0.94	1.02
1.7	0.19	0.67	0.99	1.06
1.61	0.20	0.72	1.06	1.14
1.3	0.23	0.92	1.38	1.48
pH	2,4-dimethylpyridine	2,6-dimethylpyridine	3,4-dimethylpyridine	3,5-dimethylpyridine
4.08	0.68	0.47	0.91	1.24
3.82	0.57	0.41	0.73	0.89
3.6	0.54	0.39	0.68	0.77
3.06	0.53	0.39	0.68	0.70
2.56	0.61	0.43	0.75	0.76
1.86	0.72	0.52	0.90	0.91
1.7	0.75	0.54	0.92	0.94
1.61	0.81	0.57	1.00	1.00
1.3	1.05	0.73	1.28	1.31

Column: 150x4.6 mm Zorbax XDB-C18; mobile phase: Acetonitrile-10mM Disodium hydrogenphosphate buffer adjusted with trifluoroacetic acid, pH=1.3-8.6 (10:90); flow rate, 1.0 ml/min; Temperature: 25°C, UV detection: 254 nm; sample: 1 µl injection.

Table 3-III
Retention factor at each pH adjustment with perchloric acid

pH	aniline	N-methylaniline		
4.04	2.53	5.60		
3.78	1.69	3.47		
3.51	1.18	2.29		
3.02	0.79	1.47		
2.55	0.70	1.26		
1.82	0.83	1.47		
1.65	0.85	1.50		
pH	pyridine	2-ethylpyridine	3-ethylpyridine	4-ethylpyridine
4.04	0.34	1.10	2.05	1.63
3.78		0.77	1.31	1.11
3.51	0.26	0.58	0.95	0.89
3.02	0.17	0.56	0.86	0.88
2.55	0.17	0.56	0.84	0.90
1.82	0.22	0.71	1.05	1.14
1.65	0.22	0.74	1.09	1.20
pH	2,4-dimethylpyridine	2,6-dimethylpyridine	3,4-dimethylpyridine	3,5-dimethylpyridine
4.04	0.70	0.50		1.44
3.78	0.64	0.47	0.82	0.98
3.51	0.56	0.41	0.71	0.78
3.02	0.62	0.45	0.77	0.78
2.55	0.64	0.47	0.79	0.80
1.82	0.82	0.59	1.01	1.02
1.65	0.84	0.61	1.03	1.03
pH	2-methylbenzylamine	3-methylbenzylamine	4-methylbenzylamine	
4.04	3.06	3.99	3.97	
3.78	2.99	3.87	3.86	
3.51	2.83	3.71	3.67	
3.02	3.24	4.20	4.16	
2.55	3.39	4.43	4.40	
1.82	4.38			
1.65		5.64	5.58	

Column:150x4.6 mm Zorbax XDB-C18; mobile phase: Acetonitrile-10mM Disodium hydrogenphosphate buffer adjusted with perchloric acid,pH=1.65 - 8.6 (10:90); flow rate, 1.0 ml/min; Temperature: 25°C, UV detection: 254 nm; sample: 1 µl injection.

Our experiments have shown differences in analyte retention when different types and concentrations of acidic modifier were employed. These effects were observed on the same column. The increased retention was obtained with both trifluoroacetic and perchloric acid modifiers, but not with the phosphoric acid modifier. This suggests that the observed effect could be attributed to the influence of the acidic mobile phase modifier and not to any specific pH or pH influence on the stationary phase properties.

As can be seen from Figure 3-6 as pH decreases so does the retention of aniline, until pH=2.6. Upon further decrease of the pH the retention factor starts to increase. The advantage of using a higher perchlorate concentration is that at these low pH's interactions with silanols or secondary equilibria effects will be nonexistent. Hence, better peak shapes are obtained with a simultaneous increase in retention. It is also shown that as the pH approaches the experimental pK_a the peak shape becomes broad and severe fronting is observed. This is attributed to secondary equilibria effects.

Comparison of modifiers

Figure 3-7 shows an overlay of the retention factors for 4-ethylpyridine as a function of pH using three different acid modifiers. At high pH's the retention factors of 4-ethylpyridine (neutral at these pHs), with all three acidic modifiers show a plateau effect. The experimental pK_a values obtained for 4-ethylpyridine was similar with the three different modifiers (see Table 2-VII, Chapter 2). The sigmoidal curves obtained are very similar with all three acidic modifiers in the pK_a region. Upon further decrease of the pH, the retention factors obtained are similar until pH's = 4. Below pH 4, 4-ethylpyridine shows different retention factors and this change is specific to the type of acidic modifier used. The decrease of pH with addition of trifluoroacetate and perchlorate caused an increase in retention

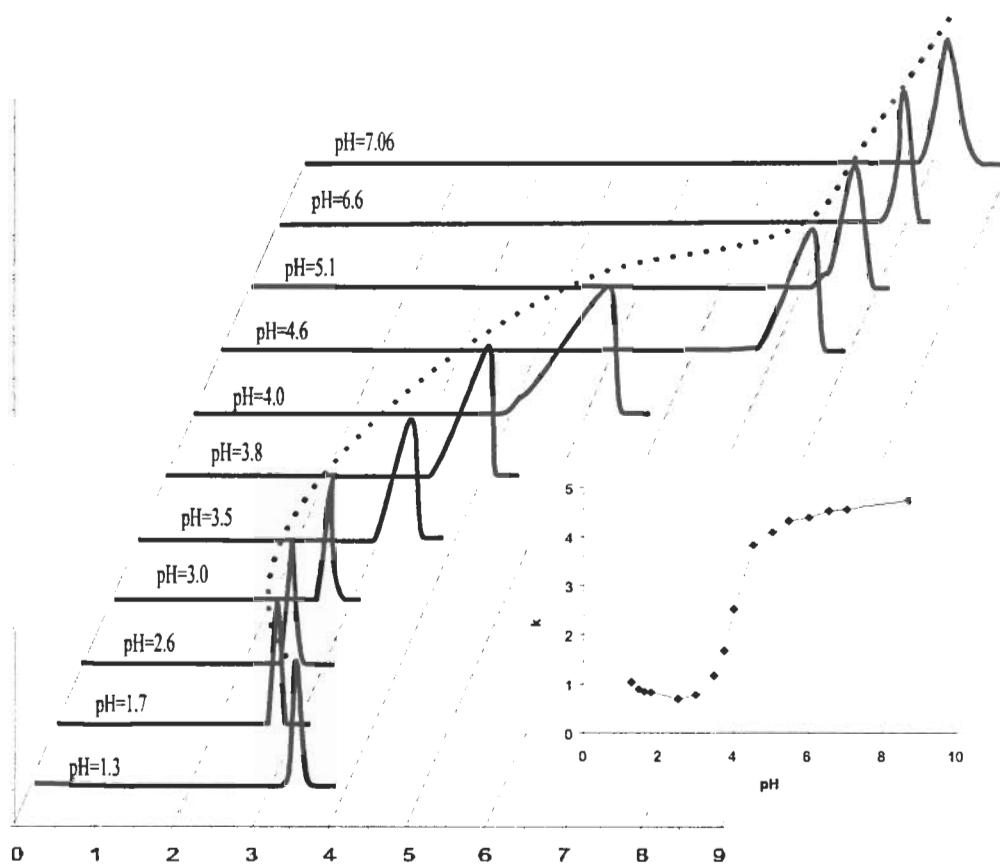


Figure 3-6. Effect on retention of aniline when perchloric acid was used as the acidic modifier throughout pH region 1.3 – 7.1. Column 150x4.6 mm Zorbax XDB-C18; mobile phase: Acetonitrile-10mM Disodium hydrogenphosphate buffer adjusted with perchloric acid, pH=1.3-8.6 (10:90); flow rate, 1.0 ml/min; 25°C, UV, 254 nm; sample: 1 μ l injection.

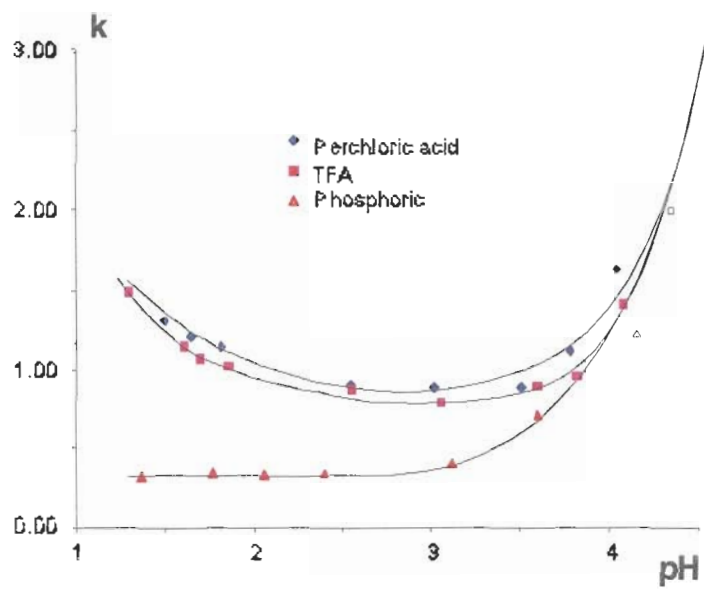


Figure 3-7. Comparison of retention factors of 4-ethylpyridine as a function of pH with three different acidic modifiers. Same chromatographic conditions as Figure 3-6 except for mobile phase modifiers.

whereas with the phosphate counteranion a “plateau-like” effect was observed.

Perchlorate and trifluoroacetate counteranions must have different effects upon the solvated protonated analyte in the mobile phase as opposed to the phosphate counteranion. The decrease of mobile phase pHs was achieved by an increase in concentration of perchloric and trifluoroacetic acid. This increase in concentration led to an increase in retention for all the basic analytes. An ion-association mechanism is suggested. In the proposed explanation, both type and concentration of the counteranion play an important role on the increased retention of the basic analytes.

Chaotropic Effect

In a low pH region, different acids affect the retention of the basic analytes to different degrees (Figure 3-7). In this region the basic analyte is generally in the protonated form and the acid is either partially or fully ionized. The counteranion of the acid, which is negatively charged, may and probably does associate with the positively charged basic analyte. The counteranions can alter the retention of the basic analytes due to differences in charge density, polarizability, and solvation. Ions that have a less localized charge, high polarizability and lower degree of hydration usually show a significant effect on the retention of basic analytes and are known as chaotropic ions^[16]. These chaotropic ions are known to change the structure (hydrogen bonding) of water in the direction of greater disorder^[1]. Therefore, the hydrogen bonding of the solvation shell of the basic analytes may be disrupted in the presence of chaotropic anions. The counteranions of the acids employed in our studies (perchlorate, trifluoroacetate and dihydrogenphosphate) fall into this class of chaotropic anions.

Water molecules having a strong dipolar nature tend to arrange themselves in a structural network. Within this network there are regions where unassociated water molecules can enter causing only a minor disruption to the network structure. The network of water molecules is in dynamic equilibrium since at one moment a water molecule could be part of the network and at next it could be free within the interstitial region of the network structure. This describes the bulk structure of water when no ions are present ^[33].

If cations are present in the water, ion-dipole forces attract water molecules to cations and these water molecules are oriented in the ionic field of the cation. These water molecules are no longer associated with the network of the bulk water. These water molecules are somewhat immobilized and can be considered as a shell of oriented immobilized water molecules around the cation^[33]. At longer distances from the cation, the influence of the ionic field is weaker and the orientation of the water molecules is unaffected. Water molecules in the region between the solvent shell and the bulk water are neither completely oriented nor disoriented. Depending upon the distance from the cation their orientation will be different. Within this region the structure of water is also broken down to different degrees. The same three layers maybe found around the anion. However, with anions of increasing delocalized charge there will be a smaller solvation of the ion.

There is an attraction between the oppositely charged ionic species. This attraction may not only disrupt the bulk structure of water as the ions approach each other, but may also disrupt the primary sheath of water molecules oriented around the ions. Once this primary sheath is disrupted the hydrophobicity of the cation is increased as well as its retention.

For example, if the cation is a protonated basic analyte, and the counteranion is a perchlorate anion the increase in concentration of the perchlorate anion would cause a

disruption of the solvent sheath around the basic analyte. At increasing concentrations of perchlorate the basic analyte's hydrophobicity would be increased, resulting in increase of retention. Not only would this effect depend on the concentration of the counteranion but also on the type. Some counteranions could effect the disruption of this primary sheath to increasing degrees. This would be dependent on the ionic field it can induce, its own solvation and its ability to hydrogen bond with water.

The ionization of the acidic modifier is also effected by the mobile phase pH. The chaotropic effect, discussed above is dependent on the concentration of the free counteranion. Figure 3-8 illustrates the pH dependence of the dissociation of acids used as the pH modifiers in our study.

The dihydrogenphosphate counteranion exhibits strong hydrogen bonding properties and at pH's less than 4.1 has a single negative charge. It may act as a hydrogen donor through its hydrogen atoms and as a proton acceptor through the phosphone group. Even though dihydrogenphosphate is not fully ionized in the low pH region it may still affect the solvation shell of the protonated basic analyte since it carries a negative charge. For example phosphoric acid at pH=1.3, is only partially ionized (14%). The majority of the ionized form of phosphoric acid consists of dihydrogenphosphate anions. For the basic compounds analyzed in the low pH region no significant increases in retention were obtained with the phosphate buffer salt.

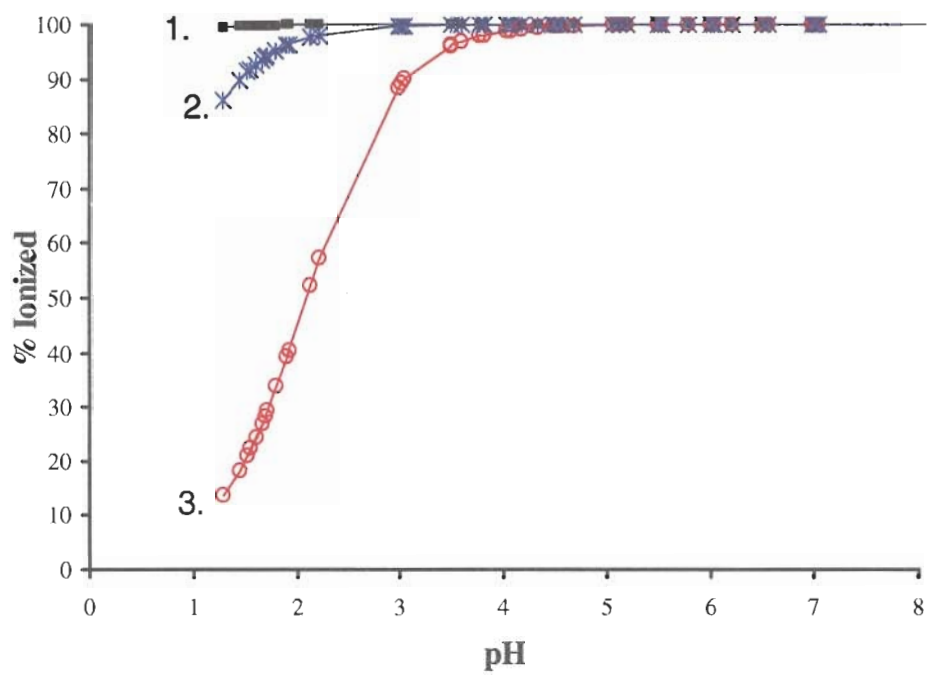


Figure 3-8. pH dependence of ionization of acidic modifiers.

1. Perchlorate, $pK_a \leq 0$, **2.** Trifluoroacetate, $pK_a=0.5$, **3.** Dihydrogenphosphate, $pK_a=2.1$

The trifluoroacetate anion has a negative charge that is delocalized; furthermore, the dispersal of charge is even greater due to the strong electron withdrawing effect of fluorine atoms. The pK_a of TFA is 0.5 indicating that it is mostly ionized within the pH region studied. However, ionization of trifluoroacetate decreases when the pH is below 2.0. For example, for the lowest pH (1.3) the trifluoroacetate is only 85% ionized. Also, the TFA counteranion exhibits weak hydrogen bonding with water molecules, as a proton acceptor through its carboxylate group. Compared to dihydrogen phosphate it has a lower degree of hydration and a lower electron density and in theory should behave as a stronger chaotropic agent. Hence, the higher increase in retention of the basic analytes at increasing concentrations of trifluoroacetate was seen in Figure 3-4.

The perchlorate counteranion has a single negative charge delocalized over all four of its oxygen atoms and can hydrogen bond only weakly. It is the most polarizable of all three counteranions studied and is completely ionized throughout the whole studied pH region. At increasing concentrations of perchlorate anion there was an increase in basic analyte retention (Figure 3-6).

The increase in analyte retention was similar for both perchloric and trifluoroacetic acids systems that contained 10mM of phosphate buffer salt [Table 3-II and 3-III]. The concentration of the perchloric acid and the trifluoroacetic though were not the same at similar pH values so the chaotropic effect may actually be hidden within the plot of k versus pH.

Many factors influence the role of the chaotropic anion including the pH of the mobile phase, and the molar concentration of the ionized counteranion. pH effects the ionization of both the acid and the base. The molar concentration of the ionized counteranion

of the acidic modifier must also be taken into consideration since different amounts must be added to obtain the same pH. In the case of perchloric acid, since it is a strong acid, it readily dissociates in water and the molar concentration can be calculated directly from the volume added. On the other hand, the trifluoroacetic and phosphoric are not strong acids and do not fully dissociate at the pHs studied. In order to calculate the concentration of their ionized form, the equilibrium constant, and the initial concentration before dissociation and the subsequent equilibrium concentrations need to be known. Once these are known, the equilibrium concentrations are substituted into the equilibrium expression for weak acids and the resultant concentration may be calculated from the amount of acid added. As the amount of acid increases there will be a consequent increase in concentration of the counteranion.

As the concentration of the counteranion increases the solvation of the protonated basic analyte decreases. The primary sheath of water molecules around the basic analytes is disrupted and this decreases the solvation of the basic analyte. The decrease in solvation causes an increase in the area of the hydrophobic part of the solute exposed to the polar portion of the mobile phase. This effectively makes the basic analyte more hydrophobic and leads to increased interaction with the hydrophobic stationary phase. At increasing concentration of the counteranion (decrease in pH) there are more counteranions to disrupt the hydrogen bonding of the water molecules and this leads to an increase in retention for the basic analytes.

The specific solvation of the anions is of importance as well. One way this has been studied is by looking at the single-ion free energies of transfer, ΔG°_t , from water to methanol and water to acetonitrile two commonly used reversed phase solvents for some common cations and anions. The more negative ΔG°_t , the greater the ion solvation in the organic

solvent relative to water^[52]. Water and methanol are proton-donating and accepting solvents and acetonitrile are dipolar bases. Water and methanol can be considered as hard acid and bases and acetonitrile as a soft base. It is known that hard acids attract hard bases and soft acids attract soft bases. Hard-hard interactions are mainly electrostatic whereas soft-soft interactions are mainly covalent in nature. Let us take a look at two anionic species for which the single ion free energies of transfer from water are available^[53] in Table 3-IV. As can be seen acetate is a hard base is best solvated with water and with MeCN the least. We would expect that trifluoroacetate to have similar solvation. Dihydrogenphosphate however should be expected to even lower single ion free energies since it can behave as a hydrogen bond acceptor and donor. On the other hand the solvation of perchlorate is independent of the solvent since it is not a hydrogen bond acceptor and it is only weakly solvated by water. From this perspective the counteranions of the acid modifiers should be solvated in aqueous/methanol and aqueous/acetonitrile from greatest to least as follows: $\text{H}_2\text{PO}_4^- > \text{CF}_3\text{OAc}^- > \text{ClO}_4^-$.

Another possible mechanism used in the literature for similar effects is ion pairing. An ion-pair as explained previously may be formed when a pair of oppositely charged ions become entrapped in each other's coulombic field. This is dependent on factors such as the temperature, the number of ions, size and the charge of the ions, and the dielectric constant of the medium^[30]. In the case of HPLC the medium is the mobile phase. The lower the dielectric constant of the medium the greater the probability of stable ion-pair formation.

Table 3-IVSingle-ion free energies of transfer, ΔG_t^0 , from water to methanol and water to acetonitrile^[53]

Ion	ΔG_t^0 (kcal mol ⁻¹) at 25°C		
	H ₂ O	MeOH	MeCN
ClO ₄ ⁻	0	1.4	1.1
OAc ⁻	0	3.8	13.3

the dielectric constant of water is approximately 80 and the dielectric constant of acetonitrile is 35. The mobile phase that was employed in these studies was 90% aqueous and 10% acetonitrile. The estimated dielectric constant of this mobile phase is 75 ^[54]. It has been described ^[30] ion-pairing in aqueous media rarely occurs since the coulombic attractive forces are small when the dielectric constant is large but in non-aqueous solvents of low dielectric constant (such as acetonitrile) ion-pairs are favored.

In our experiments that had a predominately aqueous mobile phase, we suggest a disruption of the analyte solvation shell, rather than an ion-pairing effect that caused the increase in retention. We had shown that with an increase in organic content the disruption of the analyte solvation increases since there is a greater attraction between the charged species and causes an increased expulsion of water from the solvation shell of the protonated basic analyte. This is demonstrated in Chapter 4 where we proposed a model to describe the analyte desolvation process and consequently obtained a solvation parameter.

If indeed ion-pairing was occurring the retention of the neutral ion-pair complex should exhibit a greater retention than is observed. For example, the retention of a neutral basic analyte exhibits a greater interaction with the stationary phase and increased retention versus the ionized form of the basic analyte. However, the observed increase in retention is greater than the retention of an ionized species but much less than the retention of a neutral species. Therefore the increase in retention we believe can be attributed to the disruption of the analyte solvation via ion-association and not due to retention of the neutral ion-paired complex. This rationale can be used as additional supporting information that an analyte solvation-desolvation process is indeed occurring.

Comparison of trifluoroacetic acid, phosphoric and perchloric acid without addition of buffer

The comparison of the chaotropic strength of the dihydrogenphosphate, trifluoroacetate and perchlorate anions was performed in the pH range of pH 1.3 – 2.2, pH 1.4 - 1.9 and 1.3 -2.0 respectively. These experiments were performed on the Eclipse XDB-C18 column without the addition of buffering salts in the mobile phase. The dependencies of retention factors on pH for two different counteranions are seen in Figures 3-9a and 3-10a. The concentrations of these counteranions at the same pH's are different within this pH region. The concentrations for the TFA in this pH region were 13 - 45 mM. The concentrations for the perchlorate anion were 14 - 68 mM and for the dihydrogenphosphate anion from 5 – 41 mM. Therefore, a more accurate representation of the strength of the anionic chaotrope is evident when the k versus concentration of perchlorate anion, dihydrogenphosphate and trifluoroacetate anion are plotted (Figure3-9b and 3-10b).

A greater chaotropic effect was observed with the perchlorate anion. At every concentration studied, perchloric acid showed a greater effect on basic analyte retention than trifluoroacetic acid. This can be attributed to the greater chaotropic nature of the perchlorate ion. Similar results were obtained with all other basic analytes studied. A slight increase in retention was observed with the dihydrogenphosphate anion.

When the retention factor is plotted versus the pH (Figures 3-9a and 3-10a) the increase in retention with the perchlorate modifier is more significant. The representation of retention factor versus concentration (Figures 3-9b and 3-10b) actually defines the strength of the chaotropic anion. The chaotropic anion disrupts the solvation of the basic analytes and the degree of the analyte desolvation is dependent on the nature and the concentration of the counteranion.

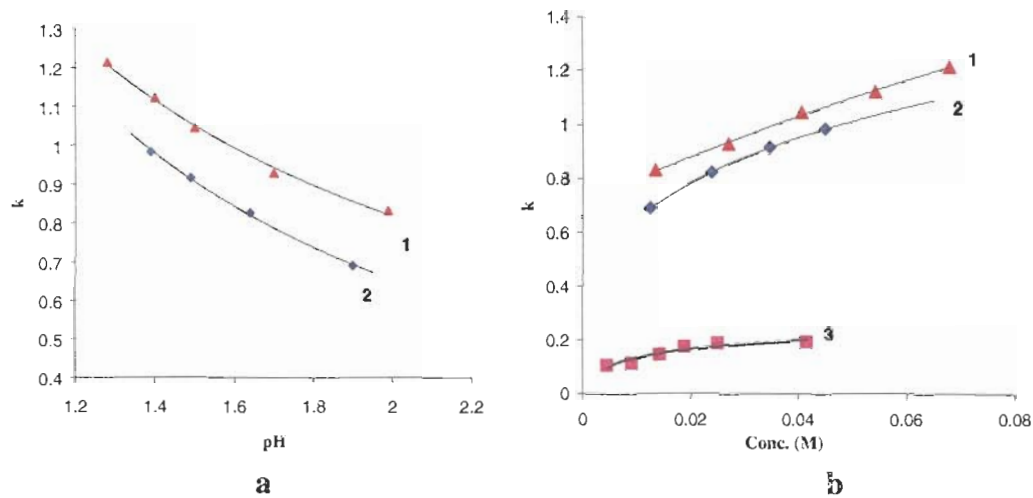


Figure 3-9. Comparison of the chaotropic effect on 3,4 dimethylpyridine caused by trifluoroacetate, dihydrogenphosphate and perchlorate counteranions plotted against mobile phase pH (a) and counteranion concentration (b) Line 1 is for perchloric acid and Line 2 is for trifluoroacetic acid and Line 3 is for phosphoric acid. Conditions: Luna C18 column, 90 Aqueous:10 acetonitrile adjusted with corresponding acid, 254nm, 1 μ L injection, Ambient temperature.

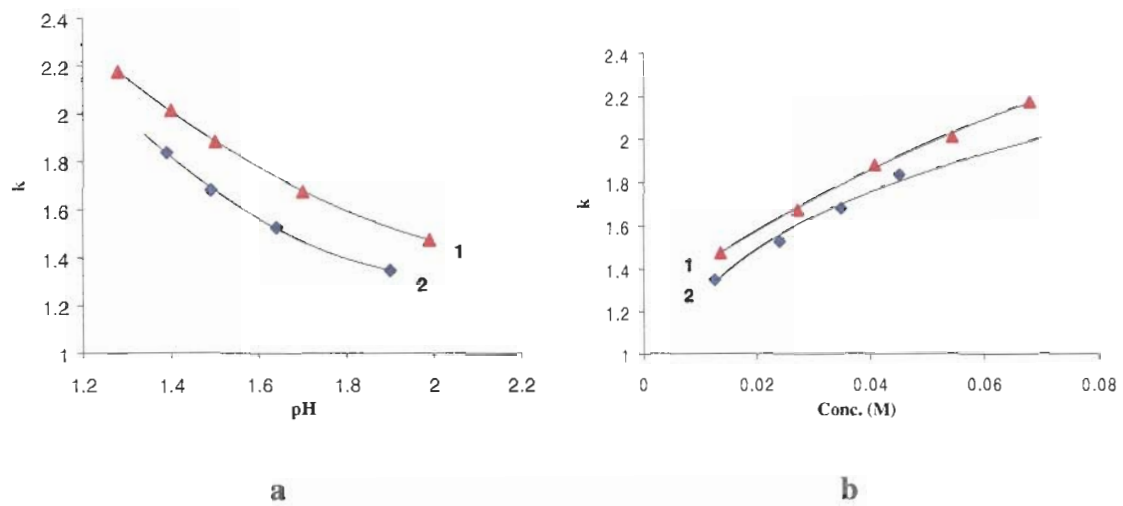


Figure 3-10. Comparison of the chaotropic effect on 2-propylpyridine caused by perchlorate and trifluoroacetate counteranions plotted against mobile phase pH (a) and counteranion concentration (b). Line 1 is for perchloric acid and Line 2 is for trifluoroacetic acid. Identical chromatographic conditions as in Figure 3-9.

The perchlorate anion showed a more significant effect upon the retention than the trifluoroacetate modifier in this unbuffered system. The dihydrogenphosphate anion also showed an increased retention in the unbuffered system while in the phosphate buffered system no increases in retention were observed. However, in the phosphate buffer system the effect of TFA and perchlorate anions upon the analytes retention were similar. The difference in strength of the chaotropic anions may be hidden when the results were plotted versus the pH and not the anion concentration. Also, due to the buffering capacity of the phosphate buffer a greater amount of all three acids were needed to reach the desired low pH's. Therefore, the concentrations of counteranions not only were present in larger concentrations but they were also different in the same pH range with the buffered system and a fair comparison could not be made. It is suggested that at lower concentrations of the counteranions the slope of the increase in retention may be greater than at higher concentrations. The retention seems to asymptotically level off at higher concentrations of anions. Also, due to the presence of the dihydrogen phosphate anions from the buffer the effects of the trifluoroacetate and perchlorate anions on the solvation of the basic analytes may have been suppressed to different degrees. The ionic strength in mixed mobile phases with buffers and added salts may start to play a role on the retention since the activity coefficient of the eluent is changing and in essence may change the analyte solvation properties.

The same effects were observed on a Phenomenex Luna-C18 column when phosphoric acid and perchloric acid was used to adjust the pH of the mobile phase in an unbuffered system. The concentrations for the dihydrogenphosphate anion were 5 - 80 mM. Figure 3-11 shows the retention factor plotted against the concentration of

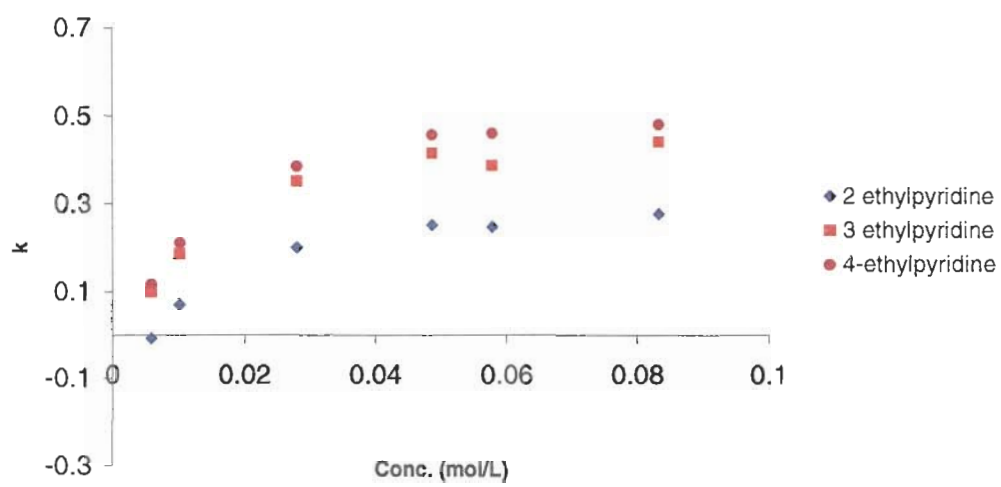


Figure 3-11. Effect of concentration of H_2PO_4^- against retention factor. Conditions: Luna C18 column, 90 Aqueous:10 acetonitrile, 254nm, 1 uL injection, Ambient temperature

dihydrogenphosphate. It can be seen that at higher concentrations of dihydrogenphosphate, increased resolution is obtained between the three isomeric species.

pH versus concentration effects

Is it actually a pH effect or concentration effect of the acidic modifier that alters the basic analyte retention?

It is a concentration effect. This effect is caused primarily by the concentration and type of counteranion employed in the mobile phase. As a result of addition of acid there is a consequent increase in the concentration of the counteranion of the acid and a simultaneous decrease in pH. pH affects the protonation of the analyte. Only, the protonated analyte species could undergo ionic association with the counteranion of the acid that was employed. Hence, when the protonated base interacts with the counteranion this leads to changes in its solvation and the increase of its hydrophobicity. At higher concentrations of counteranion of the acidic modifier, the protonated basic analyte is desolvated to a greater extent. This causes an increase in analyte retention.

There are two ways in which the concentration of the counteranion may be increased:

- 1) Increase the amount of acid added
- 2) The addition of a salt that contains the same counteranion as the acid.

In the first approach not only does the concentration change but so does the pH. Therefore, with an increase in concentration of acid there is a decrease in pH. A plot of the concentration of perchlorate anion from all different experiments (perchloric acid adjustment and perchloric acid + NaClO₄) versus retention factor are shown Figure 3-12. In one experiment the concentration was changed solely by adjusting the concentration of perchloric acid and obviously the pH changed. In several other experiments increasing

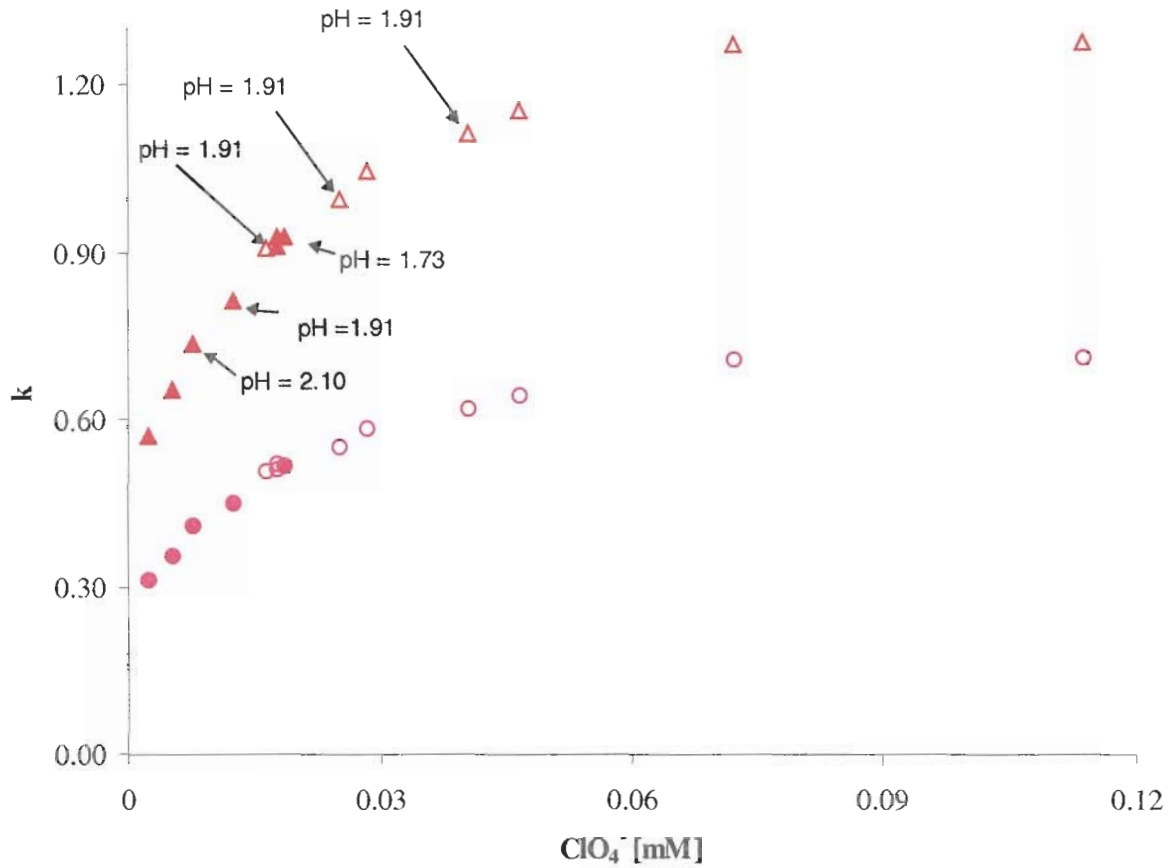


Figure 3-12. Retention factor of 2 ethylpyridine and 4 ethylpyridine versus concentration of perchlorate anion. Upper dependence (closed and open triangles) are for 4-ethylpyridine and the bottom dependence (open and closed circles) are for 2-ethylpyridine. Closed triangles and circles represent the retention factors obtained with a buffer whose concentration was modified solely with the addition of perchloric acid (variable pH). Open triangles and circles represent the retention factors obtained with a buffer whose concentration was modified with the addition of perchloric acid and sodium perchlorate at a constant pH. Conditions: Zorbax Eclipse XDB-C18, 90% Aqueous adjusted with Sodium perchlorate and/or perchloric acid.10% Acetonitrile, Temperature: 25°C, Wavelength: 254 nm

concentrations of sodium perchlorate were added to mobile phases of a certain pH. For example, a pH=1.91 mobile phase was subdivided into 3 portions and sodium perchlorate at different concentrations were added. A pH 2.0 mobile phase was treated in the same fashion. The mobile phases in which sodium perchlorate were added are represented by Run # 5,9,11 (pH=1.91) and Run # 10,12,13,14 (pH=2.0) shown in Table 3-5. In Figure 3-13 is the retention factor versus concentration for a series of pyridinal and aniline compounds from the aforementioned experiments. It is shown that the increase in retention is independent of other ionic species in the mobile phase in this perchlorate system and the increase can be solely attributed to interaction with the perchlorate anion.

A similar experiment was carried out on Zorbax Eclipse XDB-C18, 25 cm x 0.46 id, 99:aqueous:1 MeCN eluent to investigate the effects of concentration of perchlorate anion on the retention of a pyridinal compound and lactic acid ^[55]. Similar effects can be seen in Figures 3-14 and 3-15. In Figure 3-14, the concentration of the perchlorate anion was increased by addition of perchloric acid. In Figure 3-15, a 50 mM potassium phosphate buffer was employed. Therefore due to the buffering capacity higher concentrations of perchloric acid were needed to obtain the same pH's as in Figure 3-14. As a result greater retention times were obtained. On the other hand if the 2nd approach is used the addition of the salt will increase the concentration of the counteranion at a constant pH (Figure 3-16). As shown in Figure 3-16 the concentration of the perchlorate anion was increased by the addition of NaClO₄, which led to the most significant increase of the analyte retention without a change in pH. The following Figure 3-17 is a graph showing the

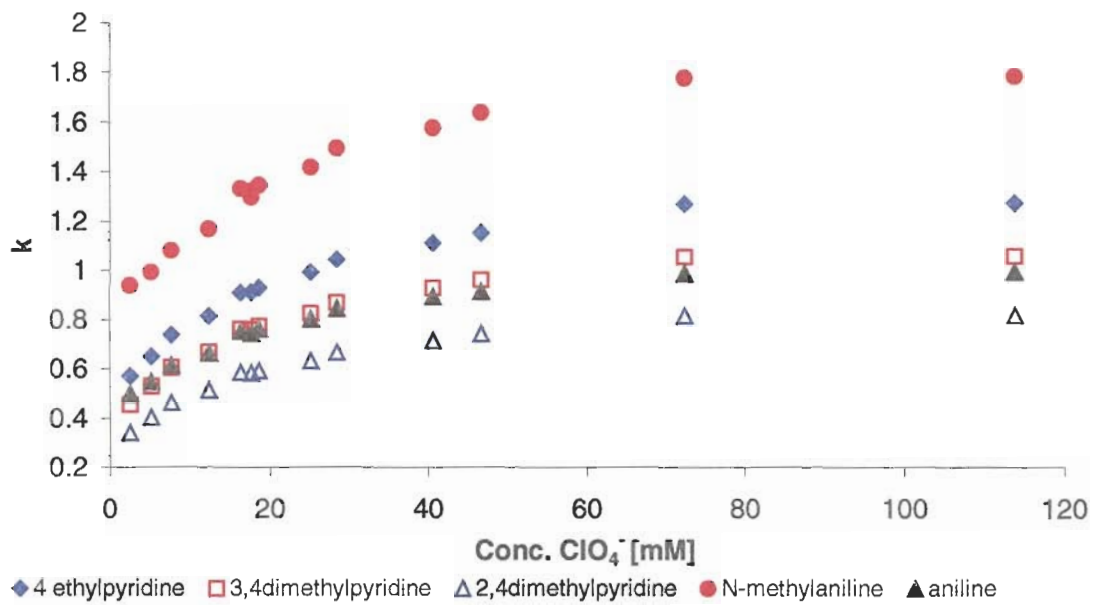


Figure 3-13. Retention factor of basic analytes versus concentration of perchlorate anion.

Table 3-V

Retention factors of basic compounds obtained at increasing perchlorate concentrations.

Run #	1	2	3	4	5	6	7
	acid	acid	acid	acid	buffer salt	acid	acid
pH	2.59	2.25	2.1	1.91	1.91	1.78	1.78
conc (mM) ClO ₄ ⁻	2.5	5.2	7.7	12.4	16.4	17.71	17.71
conc (M) ClO ₄ ⁻	0.0025	0.0052	0.0077	0.0124	0.0164	0.01771	0.01771
aniline	0.50	0.55	0.61	0.66	0.75	0.76	0.74
pyridine	0.03	0.04	0.06	0.07	0.09	0.10	0.09
N-methylaniline	0.94	0.99	1.08	1.17	1.33	1.32	1.30
N,Ndimethylaniline	1.17	1.22	1.31	1.40	1.61	1.58	1.54
2,4dimethylpyridine	0.34	0.41	0.47	0.52	0.59	0.60	0.58
3,4dimethylpyridine	0.46	0.53	0.61	0.67	0.76	0.77	0.76
2ethylpyridine	0.31	0.36	0.41	0.45	0.51	0.52	0.51
4 ethylpyridine	0.57	0.65	0.74	0.81	0.91	0.93	0.91
2 n proylpyridne	0.98	1.08	1.21	1.31	1.46		1.46
4 n propylpyridine	1.92	2.16	2.41	2.65	2.97		2.97
Run #	8	9	10	11	12	13	14
	acid	buffer salt					
pH	2	1.91	2	1.91	2	2	2.01
conc (mM) ClO ₄ ⁻	18.7	25.2	28.5	40.6	46.7	72.4	113.9
conc (M) ClO ₄ ⁻	0.0187	0.0252	0.0285	0.0406	0.0467	0.0724	0.1139
aniline	0.76	0.80	0.84	0.89	0.91	0.99	0.99
pyridine	0.09	0.10	0.11	0.12	0.12	0.14	0.14
N-methylaniline	1.34	1.42	1.50	1.58	1.64	1.78	1.78
N,Ndimethylaniline	1.62	1.72	1.81	1.91	1.98	2.18	2.19
2,4dimethylpyridine	0.59	0.63	0.67	0.71	0.74	0.81	0.82
3,4dimethylpyridine	0.77	0.82	0.87	0.93	0.96	1.05	1.06
2ethylpyridine	0.52	0.55	0.58	0.62	0.64	0.71	0.71
4 ethylpyridine	0.93	0.99	1.05	1.11	1.15	1.27	1.27
2 n proylpyridne	1.50	1.59	1.67	1.78	1.85	2.02	2.04
4 n propylpyridine	3.06	3.25	3.42	3.63	3.76	4.12	4.14

*The makeup of the aqueous portion of the mobile phase is indicated. Buffer salt indicates that sodium perchlorate was added to the solution to increase the concentration of perchlorate anion without changing the pH.

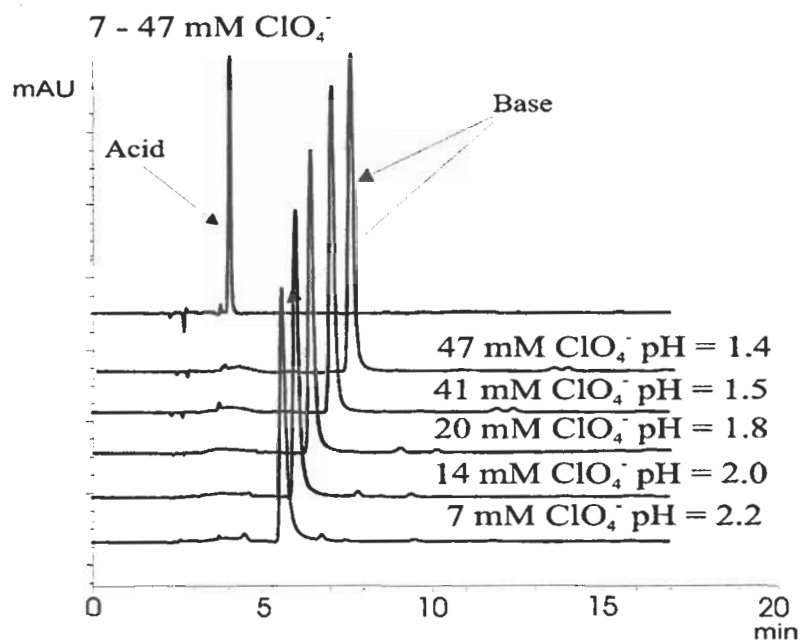


Figure 3-14. Increase in retention of basic compound at increasing perchlorate concentrations at a variable pH. Conditions: 99:1, Aqueous :MeCN, Column: 25 x 0.46 cm Zorbax Eclipse XDB-C18 column, Temperature: ambient, 25 μ L injection volume.

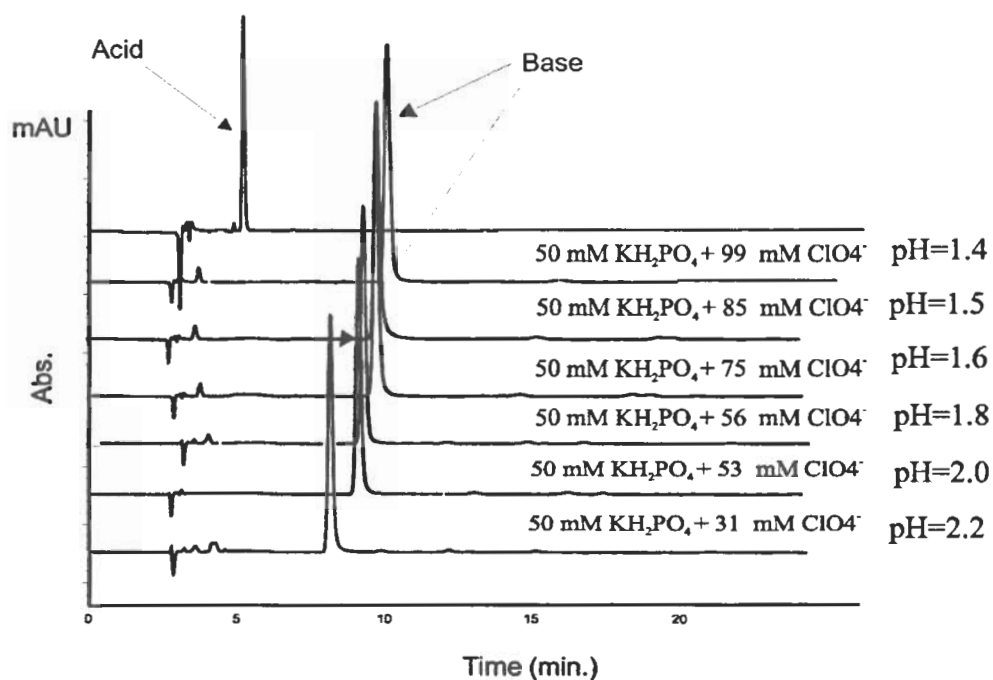


Figure 3-15. Increase in retention of basic compound at increasing perchlorate concentrations at a variable pH of potassium phosphate buffer. Increased amounts of perchloric acid were needed to obtain same pH values as in Figure 3-14 due to buffering capacity of phosphate buffer.

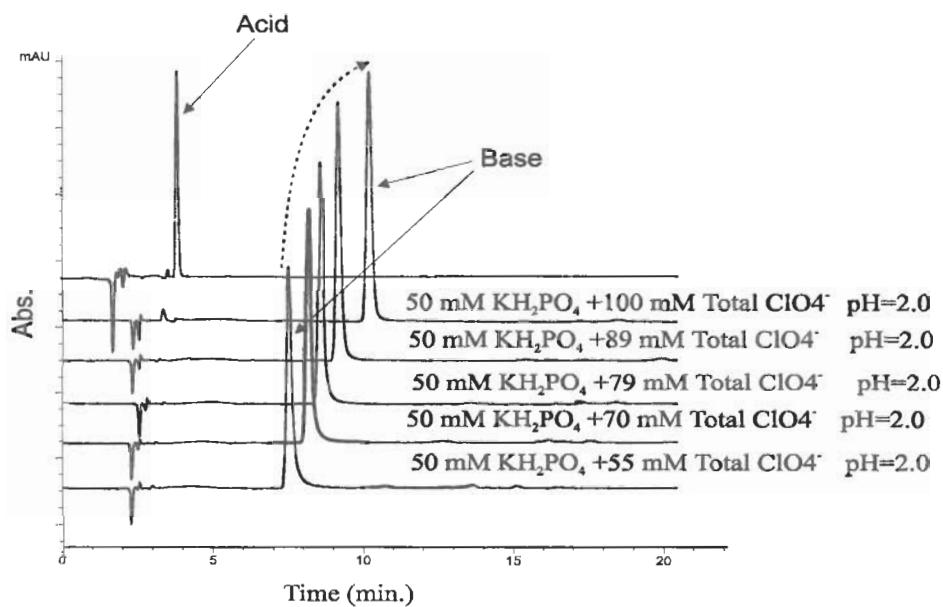


Figure 3-16. Increase in retention of basic compound observed with increased concentration of perchlorate at constant pH. Starting concentration of perchlorate anion from perchloric acid is 15mM in order to reach pH=2.0 Further addition of sodium perchlorate salt led to increased retention of the basic analyte.

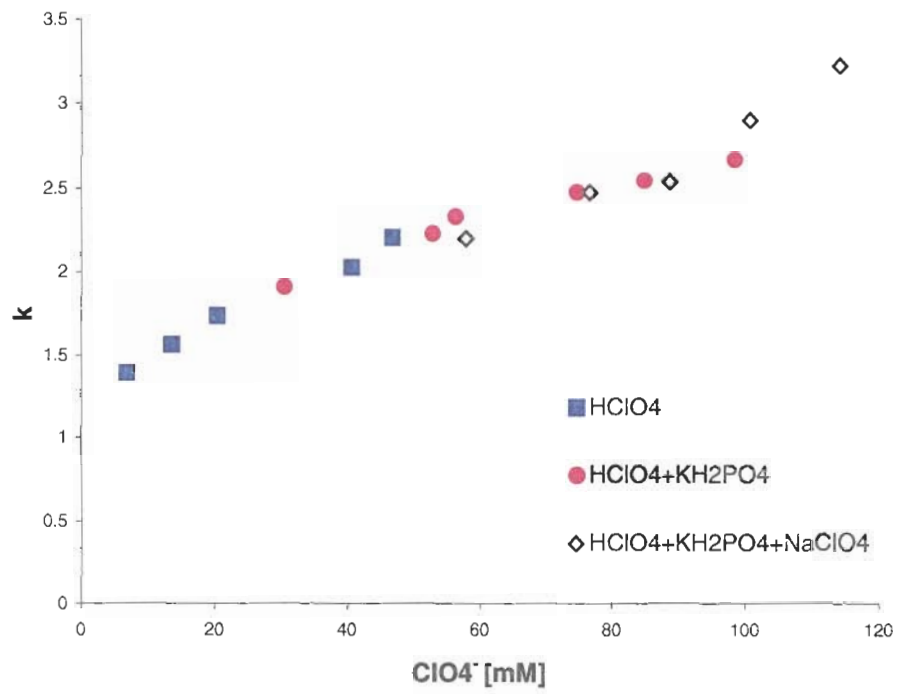


Figure 3-17. Effect of retention factor versus concentration of perchlorate anion on basic analyte. A: Mobile phase pH adjusted with perchloric acid, B: 50mM potassium phosphate buffer with pH adjustment using perchloric acid C: Mobile phase pH adjusted with perchloric acid and then addition of NaClO₄ salt.

retention factors versus concentration of perchlorate anion obtained in Figures 3-14, 3-15, 3-16 at the three different experimental conditions. It was shown regardless of pH the counteranion concentration is the determining factor that effects the analyte's solvation and ultimately its retention.

However, in the system that contained perchloric acid, potassium dihydrogenphosphate buffer and sodium perchlorate some deviations from the expected asymptotic behavior were seen. This maybe due to the influence of the ionic strength of the mobile phase. Altering the ionic strength may effect the electrostatic interactions between the ionic species with a resultant change in the activity coefficient. The value of the chemical potential may be altered and this can lead to a variation in the ionic equilibria. The non ideality of those electrostatic interactions between ionic species is related to the ionic strength:

$$I = \frac{1}{2} \sum z_i^2 c_i \quad [3-8]$$

At low concentrations of electrolyte ($I \leq 0.1$ M) the effect of the nonideality on the activity coefficient of an ionic species, γ_i , can be explained by the Debye-Huckel equation:

$$-\ln \gamma_i = \frac{Az_i^2 \sqrt{I}}{1 + Ba^o \sqrt{I}} \quad [3-9]$$

where z_i is the charge of an ion i , a^o is the ion size parameter, and A and B are constants. Equation 3-9 shows that with an increase of the ionic strength γ_i decreases. However, in this experiment the total ionic strength of the buffer is greater than 0.1 M. Upon increasing the concentration of the electrolyte the activity coefficient of the solvent may decrease due to strong ion-solvent bonding ^[56] and as a consequence γ_i of the solute may increase at high

salt concentrations. In order to calculate the activity coefficient for these higher concentrations one may use the Davies equation ^[57]. This equation is valid up to ionic strengths of 0.3 M. At higher salt concentrations a semiempirical expression suggested by Lietzke may be used ^[58].

Figure 3-18 illustrates the retention factor versus the total ionic strength in each of the three eluent systems. The first two systems seem to vary linearly with the ionic strength. However in the 3rd data system a deviation from the linearity of retention factor versus ionic strength was observed for the last two data points. The same deviation was seen in the plot of *k* versus concentration of perchlorate anion.

The effect of the perchlorate concentration on the retention of an acidic compound, lactic acid is shown in Figures 3-14, 3-15, 3-16. The lactic acid ($pK_a = 4.2$) is in its unionized form at the working pHs of all 3 systems. The retention of lactic acid is unaffected by the addition of perchlorate concentration. This is expected since ionic interactions with the negatively charged perchlorate anion should not occur. Figure 3-19 illustrates a plot of the retention factor for lactic acid versus perchlorate ion concentration.

Comparison of using different starting phosphate buffer concentrations

We investigated the effect of the ionic strength further. The effect of the sodium phosphate buffer at different starting concentrations modified with phosphoric acid versus sole adjustment with phosphoric acid was studied. It can be seen in Figure 3-20 that when a sodium phosphate buffer was employed (25 mM and 50 mM) that differences in the retention dependencies versus concentration of dihydrogenphosphate counteranion were observed.

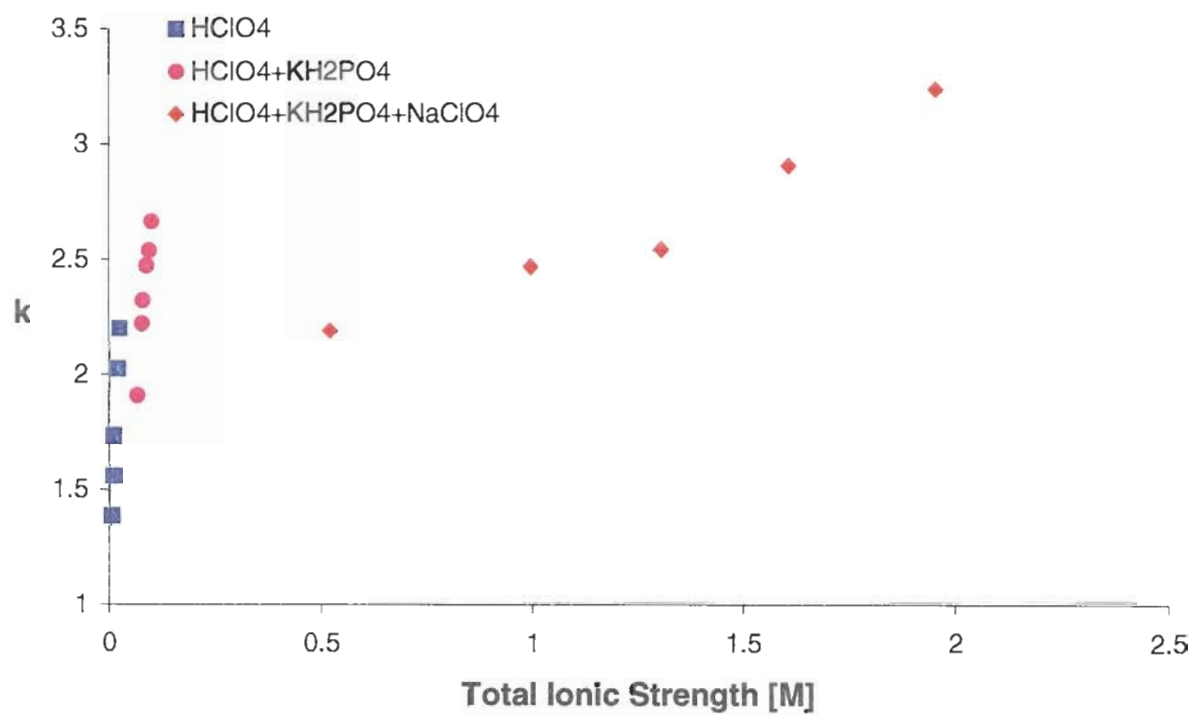


Figure 3-18. Effect of total ionic strength on the retention of pyridinal compound

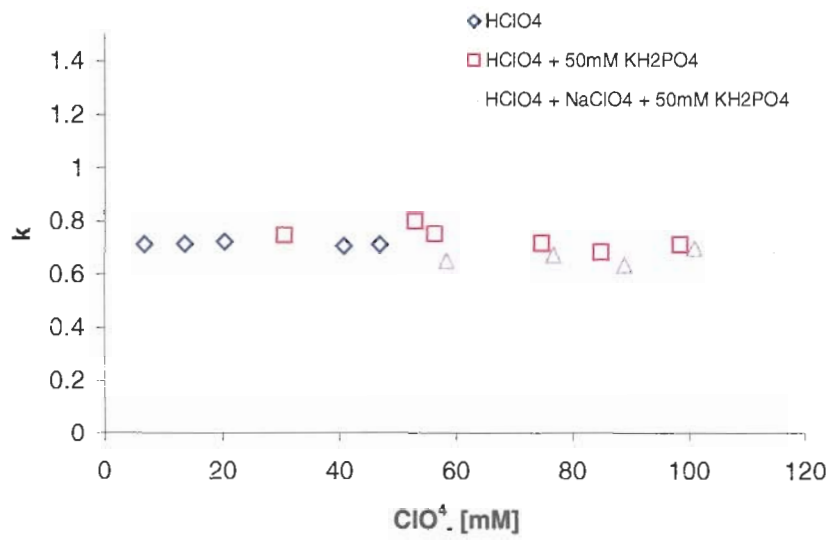


Figure 3-19. Effect of perchlorate anion concentration on the retention factor of Lactic acid

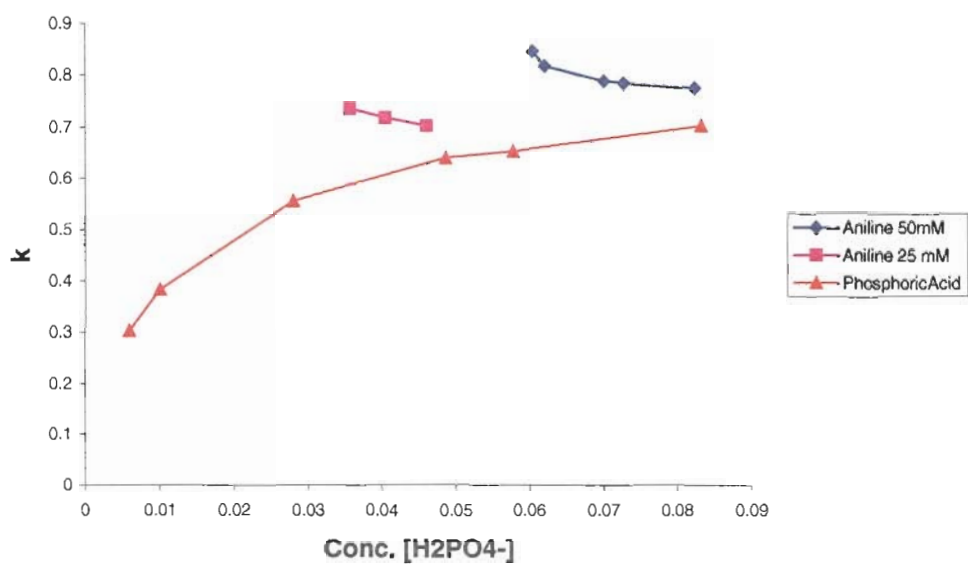


Figure 3-20. Retention factor versus concentration phosphate not corrected for ionic strength. Column:150 x 4.6 mm Luna C18; mobile phase: (10:90) Acetonitrile-0, 25, and 50mM Disodium hydrogenphosphate buffer adjusted with phosphoric acid, all pH values below pH 2.2; flow rate, 1.0 ml/min; Temperature: 25°C, UV detection: 254 nm; sample: 1 µl injection.

The retention factor did not plateau at the higher concentrations of anions. However, in Figure 3-21 when we plot the k versus the ionic strength the retention factors seem to follow a similar retention dependency versus concentration as seen in Figure 3-11. The concentration used in Figure 3-11 was made by using solely phosphoric acid and no buffer. The decrease in retention factor with the 25 mM and 50 mM phosphate buffer are real dependencies. The same experiment with these two buffer systems were repeated on a different Luna column and the same trend was observed. Conclusion is that there definitely is an effect from the changing ionic strength. The influence of the Na^+ ions are somehow interfering with the analyte desolvation process. Future experiments must be carried out at constant ionic strength to elucidate the role of the Na^+ ion, and the activity coefficient on the retention factors for basic analytes.

This phenomenon was further investigated in which 5 different starting concentrations of dihydrogenphosphate buffers were prepared and their pH was modified with phosphoric acid. No direct dependency between k versus conc. H_2PO_4^- could be drawn. However, upon plotting the k versus the total ionic strength of the aqueous portion of the mobile phase the retention factor showed a distinct knee in this dependence and asymptotic behavior at greater concentrations, Figure 3-22 and 3-23. These experiments were performed with 5 different initial buffer concentrations, 5, 10, 25, 75 and 90 mM of Na_2HPO_4 . These experiments were all done on a Zorbax Eclipse XDB-C18 column at 90% aqueous:10% acetonitrile.

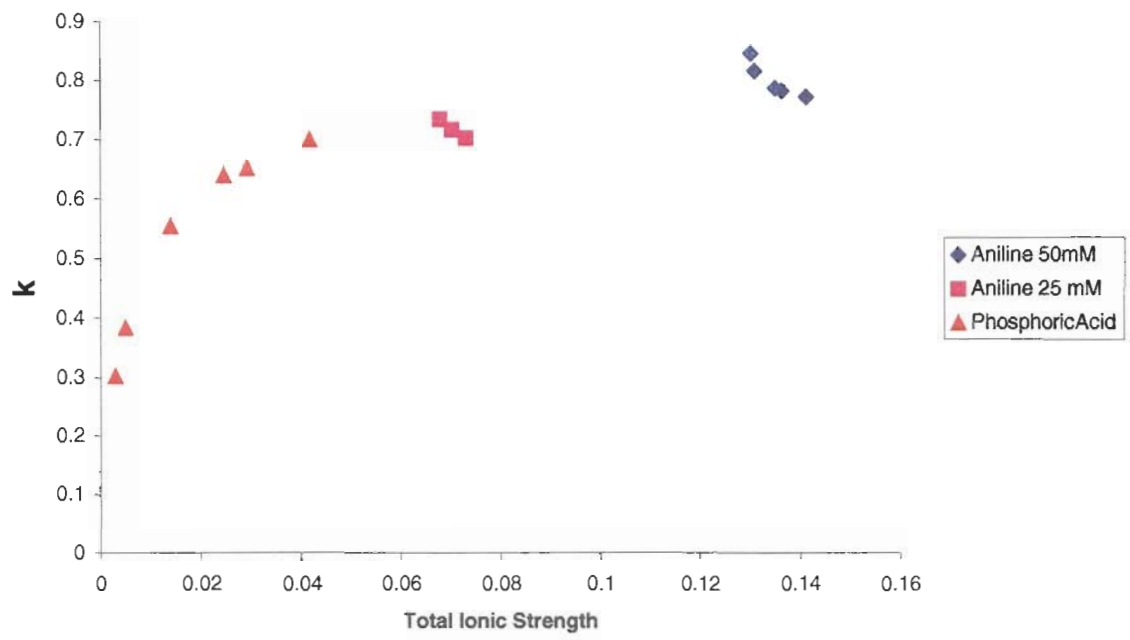


Figure 3-21. Retention factor versus Total ionic strength. Experimental conditions same as in Figure 3-20.

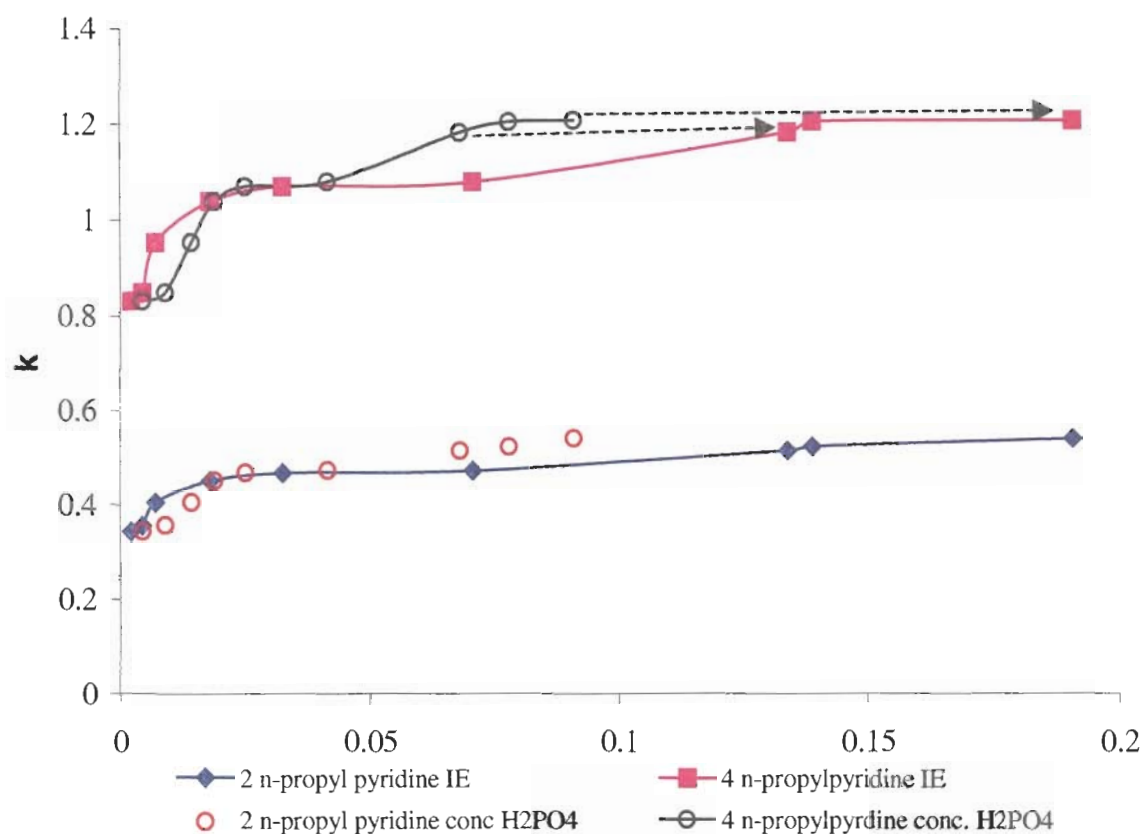


Figure 3-22. Retention factor versus concentration of dihydrogen phosphate and total ionic strength. 2 n-propylpyridine (bottom) and 4 n-propylpyridine (top). Dotted lines represent the corresponding ionic strength of the aqueous phase at the particular buffer concentration of H₂PO₄⁻. IE denotes versus ionic strength and H₂PO₄⁻ denotes versus concentration H₂PO₄⁻.

Column: 150 x 4.6 mm Zorbax Eclipse XDB-C18; mobile phase: (10:90) Acetonitrile: 5, 10, 25, 75 and 90 mM Disodium hydrogenphosphate buffer adjusted with phosphoric acid, all pH values below pH 2.2; flow rate, 1.0 ml/min; Temperature: 25°C, UV detection: 254 nm; sample: 1 µl injection.

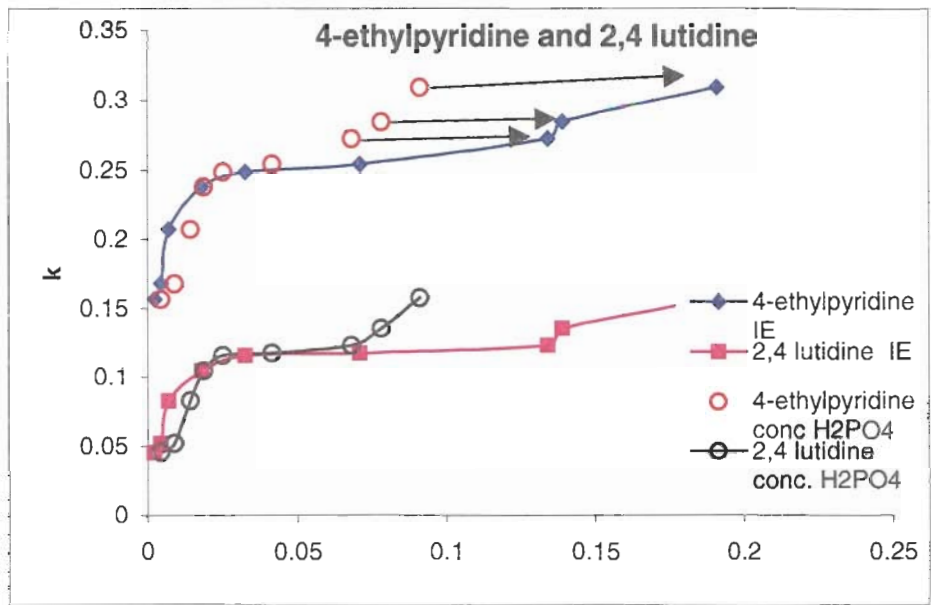


Figure 3-23 Retention factor versus concentration of dihydrogenphosphate and total ionic strength. IE denotes versus ionic strength and H_2PO_4 is versus conc. $H_2PO_4^-$. Experimental conditions same as Figure 3-22.

The effect of starting sodium dihydrogenphosphate buffer concentration (5 mM, 10 mM, 17.5 mM, 25 mM and 50 mM) using perchloric acid as the acidic modifier on the retention of basic compounds was studied. It can be seen in Figure 3-24 that regardless of the initial buffer concentration at low concentrations of perchlorate anion the retention factor is independent of the other ionic species except the perchlorate anion. However, at increasing concentration of perchlorate anion there is some deviation from the normal expected asymptotic behavior. This can be attributed to the difference in the ionic strength and also competing effects between the dihydrogenphosphate anions and perchlorate anions. There may be opposing effects occurring. Further investigation of this matter is needed. The basic analyte retention depend on the type and concentration of the acidic counteranion used in the eluent. Moreover, the initial buffer concentration of the buffer used in the eluent may also play a crucial role in the retention of the basic analyte.

Effect on acidic, neutral, and zwitterionic components

Figure 3-25 show the chromatograms for five acids and zwitterionic component at varying concentration of perchlorate anion at pH=2.0. There was no change in retention for five acids o,m,p toluic acid, phenyl acetic acid, and lactic acid and a zwitter ionic component, 4-aminobenzoic acid using a 20 mM dihydrogen phosphate buffer adjusted with perchloric acid to pH=2.0 (30.6 mM perchlorate) and then increased the concentration to 70.6 mM with NaClO₄. This is expected since the acids are all in their neutral form and the 4-aminobenzoic acid is only partially prtonated at pH=2. For the concentration of an small inorganic anion such as perchlorate to have an effect on the retention of basic compounds these compounds

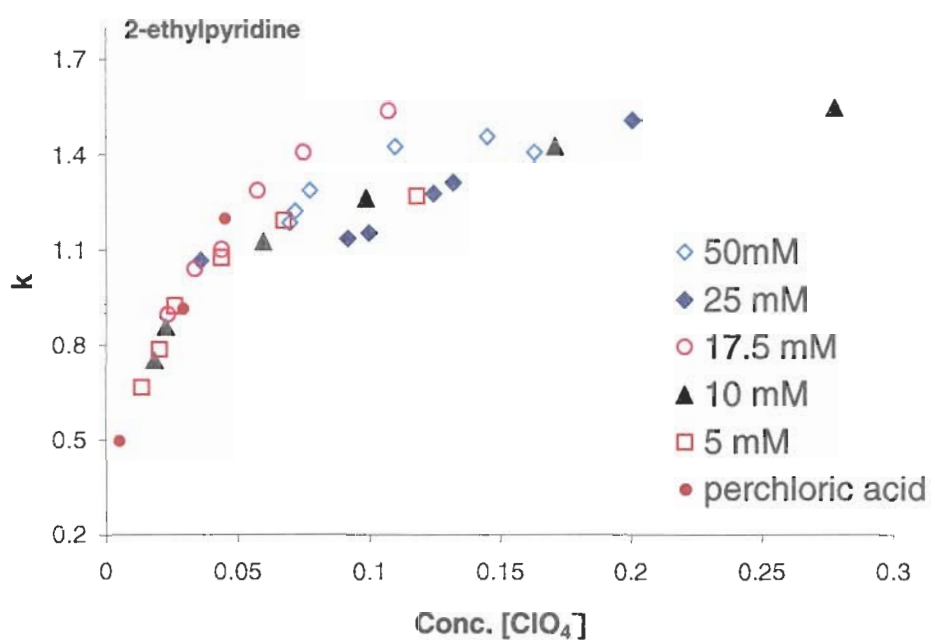


Figure 3-24 Effect of initial phosphate buffer concentration followed by adjustment with perchloric acid. Column:150 x 4.6 mm Zorbax Eclipse XDB-C18; mobile phase: (10:90) Acetonitrile-5, 10, 17.5, 25, and 50 mM Disodium hydrogenphosphate buffer adjusted with perchloric acid, all pH values below pH 2.2; flow rate, 1.0 ml/min; Temperature: ambient, UV detection: 254 nm; sample: 1 μ l injection.

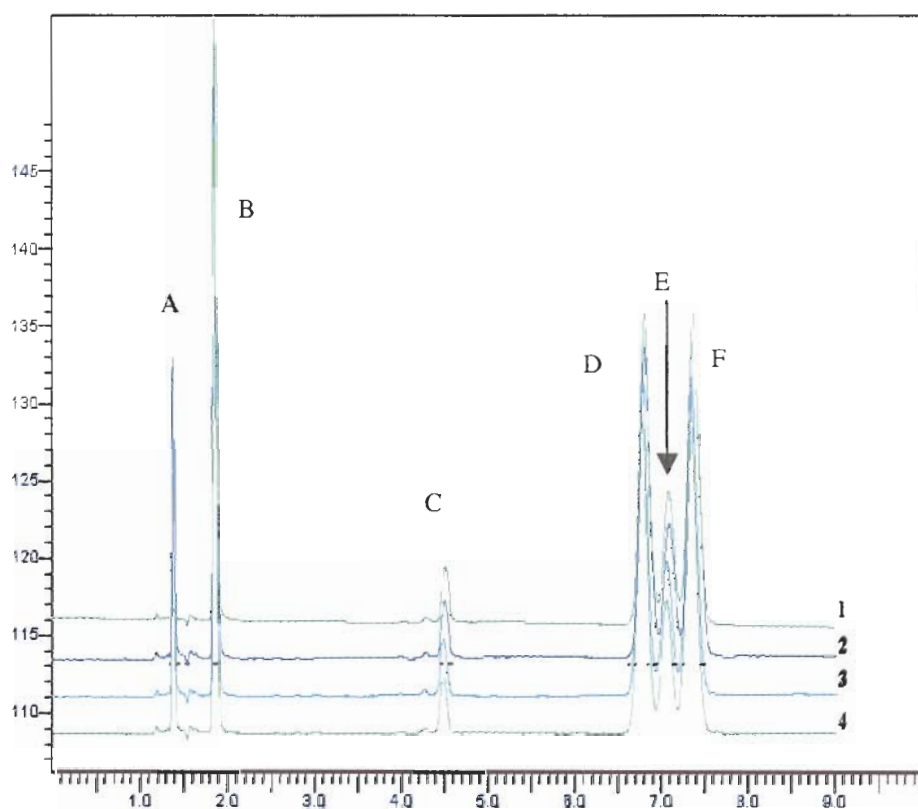


Figure 3-25 Plot of acids and zwitterionic components at different perchlorate concentrations at pH=2.0. 1. 30.6 mM ClO_4^- , 2. 45 mM ClO_4^- , 3. 60 mM ClO_4^- , 4. 70.6 mM ClO_4^- . Compounds: A. Lactic acid, B. 4-aminobenzoic acid, C. Phenylacetic acid, D. o-toulic acid, E. m-toulic acid, F. p-toluic acid. Column: 150 x 4.6 mm Zorbax Eclipse XDB-C18; mobile phase: (10:90) Acetonitrile-20 mM Disodium hydrogenphosphate buffer adjusted with perchloric acid, pH 2.0; Concentration of perchlorate increased with addition of sodium perchlorate. flow rate, 1.0 ml/min; Temperature: ambient, UV detection: 254 nm; sample: 1 μl injection.

should be predominately in their protonated form. The same results were observed for phenol, a neutral compound, analyzed at 10, 20, 30, 40 and 50% MeCN at 25°C with the addition of 1 – 70 mM concentration of perchlorate anions in the mobile phase. The retention for this neutral compound did not change as a function of increasing perchlorate concentration. The chaotropic agent does not effect the retention of these acidic and neutral compounds it offers the chromatographer the ability to vary only the retention of the ionized basic compounds in a mixture that would also contain acidic and neutral species.

Advantages of using Chaotropic agents

Peak Shape

The employment of chaotropic agents in the mobile phase at low pH has shown to increase retention and peak symmetry of protonated basic analytes. This offers the possibility to work in a pH region that would minimize secondary equilibria effects and silanol interactions. Problems that are often associated with HPLC analysis of basic compounds are severe peak asymmetry and poor efficiency. These are usually associated with interaction with residual silanols. In other literature the peak shapes of these basic analytes have also been improved by using tertiary and quaternary amines as silanol blockers [59]. Other approaches include electrostatically shielded stationary phases, which have also shown to improve peak shapes for basic analytes [60]. Our suggested chaotropic approach offers the chromatographer an alternative to obtain acceptable peak shapes and enhanced retention without additional additives in the mobile phase.

Resolution

In the absence of buffer the effect of the perchlorate modifier on basic analyte retention was also investigated. The study was performed with pyridine and various alkyl

mono and disubstituted compounds. These compounds include derivatives with substitution of alkyl groups at the ortho, meta and para positions with respect to the basic nitrogen group. It was shown that for basic compounds with similar structure and pK_a 's, interaction with the anionic chaotrope will increase the retention. The dependence of retention factor on mobile phase pH is shown in Figure 3-26 and Figure 3-27. As the pH is decreased, the retention of the components is increased with a simultaneous increase in resolution between the most basic species. This illustrates the possibility of obtaining increased resolution at a low pH region. This can be attributed to the differences in the analytes solvation. The basic analyte may be solvated to different degrees due to the steric nature of substituents in the vicinity of the protonated nitrogen group and the overall stereochemistry of the basic analyte. The greater the disruption of the analyte's solvation by ionic interaction with the perchlorate anion, the greater the increase in retention.

Selectivity

Elution order for basic compounds with different pK_a 's in the low pH region can be reversed, while the retention of one compound may be governed by ionization and the other by chaotropic effects. The elution sequence for the studied basic analytes may be changed solely by adjusting the buffer with different acidic modifiers, changing the concentration of the counteranion and/or by adjusting the pH. Depending upon the pK_a of the basic compound, the retention may not be affected by the anionic chaotrope. Thus, if a basic analyte is not predominately protonated in the pH region studied, the chaotropic effects may not be observed. On the other hand if a basic analyte is fully protonated, the effect of the

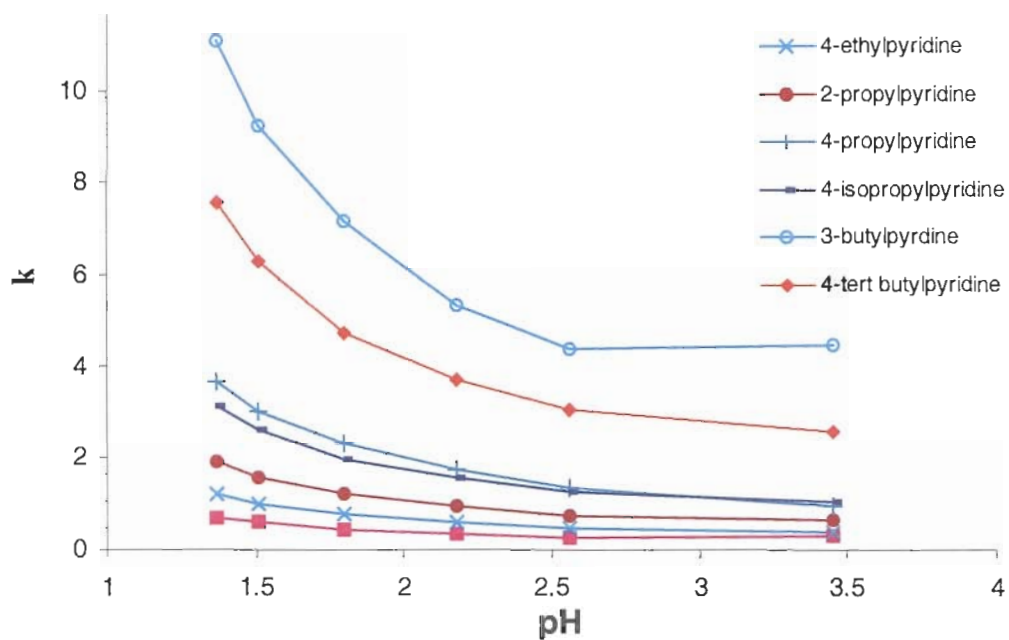


Figure 3-26. Effect of eluent pH adjusted with perchloric modifier for a series of substituted pyridines. Column 150x4.6 mm Zorbax XDB-C18; mobile phase: (10:90) Acetonitrile-HPLC grade water adjusted with perchloric acid, pH=1.3-2.6; flow rate, 1.0 ml/min; 25°C, UV, 254 nm; sample: 1 μ l injection.

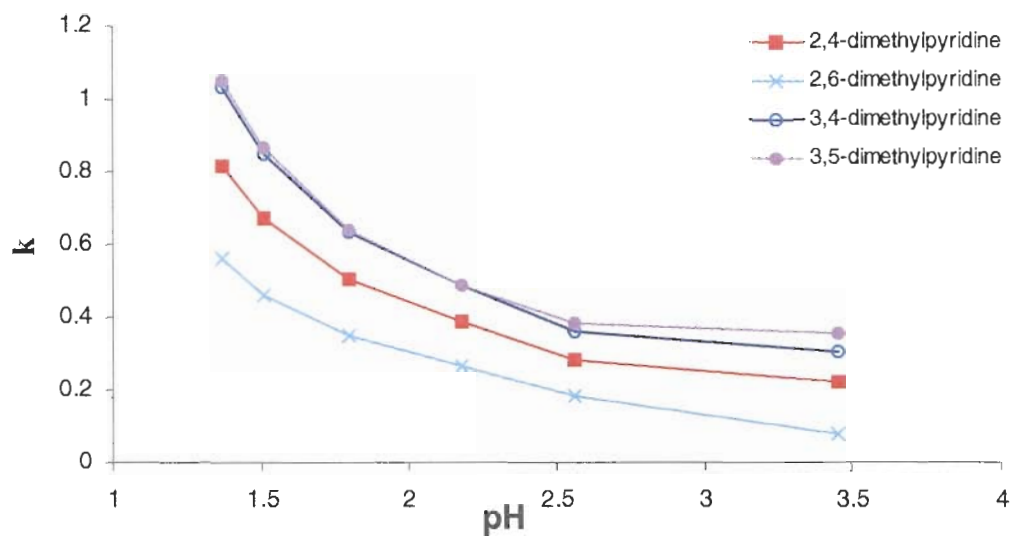


Figure 3-27. Effect of eluent pH adjusted with perchloric acid for an isomeric series of disubstituted pyridines. Identical chromatographic conditions as in Figure 3-26.

chaotropic agent upon its solvation will be significant on the retention factor. This effect is illustrated in Figure 3-28.

The pK_a of *o*-chloroaniline and phenylethylamine is 2.64 and 9.83 respectively. The pH of the mobile phase was adjusted between pH 1.6 –1.8. The concentration of perchlorate anion in this pH range was 25 and 10 mM respectively. In this pH region, the *o*-chloroaniline is not fully ionized while phenylethylamine is. A decrease in retention was observed for *o*-chloroaniline. This was attributed to an increase of its ionization. An increase in concentration of the perchlorate anion from 10mM to 25mM led to an increase in retention for phenylethylamine due to the chaotropic effect. A dramatic reversal of elution order was obtained.

The chaotropic effect was applied as an effective approach for the separation of a mixture of various basic compounds with different pK_a 's and stereochemistries. These effects were observed upon further lowering the pH of the mobile phase, which led to increased concentration of counteranion. The retentions of some basic compounds were dominated by their ionization and others were dominated by the chaotropic effect. The decreased eluent pH led to a decrease in retention of partially ionized basic compounds and the increase of concentration of counteranion led to the enhanced retention for the fully ionized basic compounds. The increase in selectivity and reversal in elution order of several basic compounds were observed.

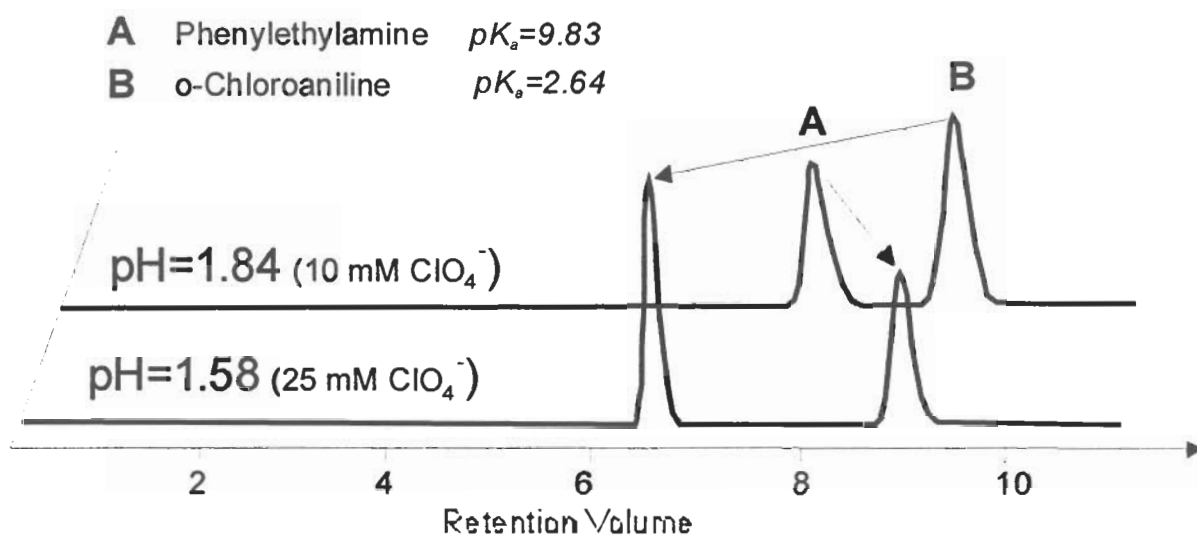


Figure 3-28. Decrease in retention of o-chloroaniline is governed by ionization while increase in retention of phenylethylamine is governed by chaotropicity. Column 15x0.46cm Zorbax XDB-C18; mobile phase: (10:90) Acetonitrile-HPLC grade water adjusted with perchloric acid, pH=1.58 and pH 1.84; flow rate, 1.0 ml/min; 25°C, UV, 254 nm; sample: 1 μ l injection.

Specific Applications (Beta Blockers)

Pharmaceutical industries are currently involved in the purification and production of β -adrenergic blockers for their use in cardiovascular treatment and medication. The following experiments were performed to mimic the optimization of the experimental HPLC conditions for the separation of β -adrenergic blockers using the “chaotropic approach”. The retention of β -adrenergic blockers is studied on an HPLC system as a function of the mobile phase chaotropic counteranion concentration. The optimal resolution among the beta blockers at different perchlorate concentrations were determined. Beta blockers are compounds that contain basic functional groups. The pK_a of all beta-blockers is greater than pK_a of 9. Their retention at a pH range of (7-9) is high since the basic analytes are in their neutral state and are more hydrophobic. The need to optimize the conditions at a low pH region is needed to obtain shorter run times and faster sample throughput.

Figure 3-29 showed retention of the basic compounds increases from 0.59 mM to 50 mM for all analytes except for theophylline. The mobile phase pH was adjusted to pH 3.0 with perchloric acid. The concentration of perchlorate was increased with the addition of sodium perchlorate. Theophylline is a neutral analyte at pH's less than 8, an increase in its retention is not expected. At a ClO_4^- concentration of 0.59 mM, atenolol, theophylline and 4-ethylpyridine coelute and nadolol has the highest retention. Increasing the perchlorate concentration to 5.6 mM shows an increase in retention for atenolol, 4-ethylpyridine and nadolol. Furthermore, increasing the concentration of perchlorate anion to 10.6mM leads to greater retention of the basic analytes. Theophylline shows no significant increase in retention.

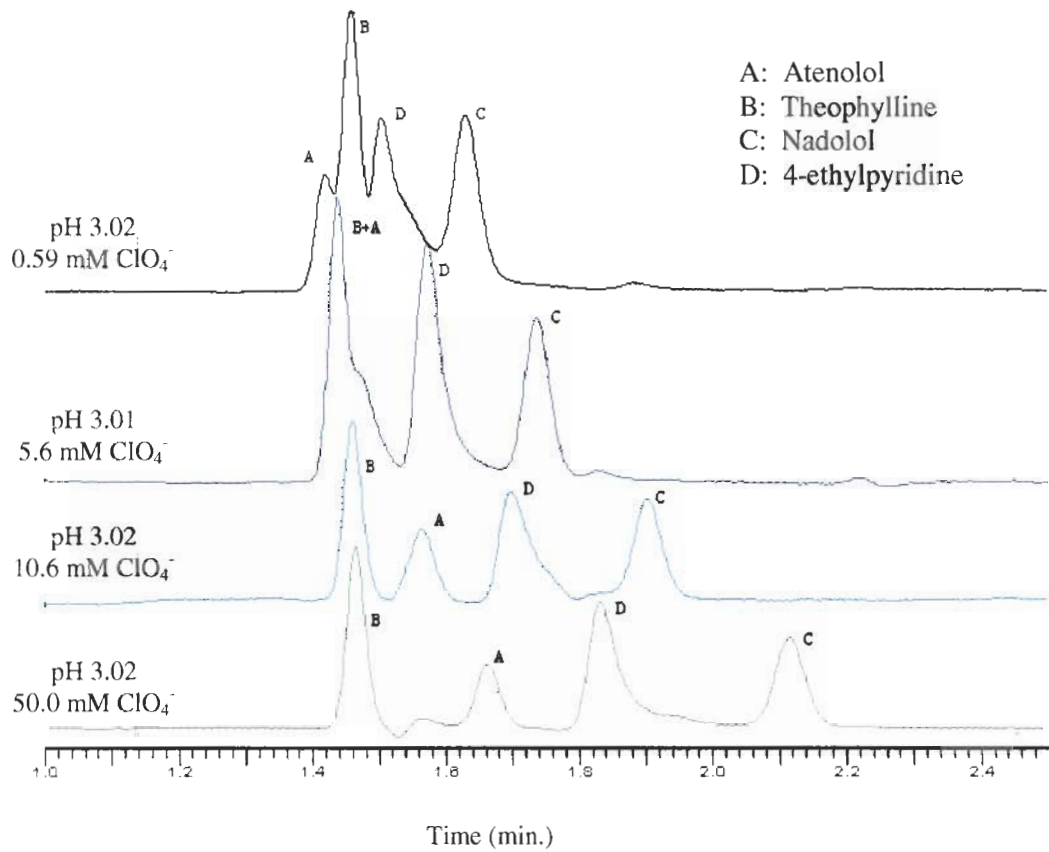


Figure 3-29. Effect of perchlorate concentration on retention of beta blockers, Theophylline and 4-ethylpyridine. Column: Zorbax Eclipse XDB-C18, 15 x 0.46 cm, Eluent: 30% Acetonitrile:70% Aqueous adjusted with perchloric acid and sodium perchlorate, pH=3.0, Injection volume: 1 μ L, Wavelength: 225 nm, Flow rate: 1 mL/min.

At 10.6 mM perchlorate concentration, all the compounds are resolved and a reversal of elution order is obtained between atenolol and theophylline. Further increase in perchlorate concentration to 50 mM yielded a greater resolution among all the compounds studied. The retention of theophylline is unchanged since it is neutral at pH 3.0. Therefore, the optimal resolution for this mixture was obtained at a concentration 50 mM ClO_4^- .

The second mixture analyzed was comprised of atenolol, caffeine, nadolol and phenylethylamine. The overlaid chromatograms are shown in Figure 3-30. At a perchlorate concentration of 0.59 mM, atenolol and phenylethylamine were resolved while caffeine and nadolol coeluted. Caffeine is a neutral compound at pH 3.0. Increasing the perchlorate concentration to 5.6 mM increases the retention for atenolol, nadolol and phenylethylamine. Upon further increase of the perchlorate concentration to 10.6 mM, all the analytes were resolved. The retention increased of all compounds except caffeine.

The last mixture consisted of six β -blockers and *o*-chloroaniline, at several perchlorate concentrations. The overlaid chromatograms are shown in Figure 3-31. All beta blockers had shown increased retention at greater perchlorate concentrations. At a perchlorate concentration, of 0.59 mM all compounds were resolved. However atenolol, nadolol, pindolol, and metoprolol were eluting near the void volume (1.4 ml). Increasing the perchlorate concentration to 10 mM had shown an increase in retention for all compounds except *o*-chloroaniline. The pK_a of *o*-chloroaniline is 2.64. The mobile phase pH is 3.0, indicating that the *o*-chloroaniline is not fully protonated. Ion association between

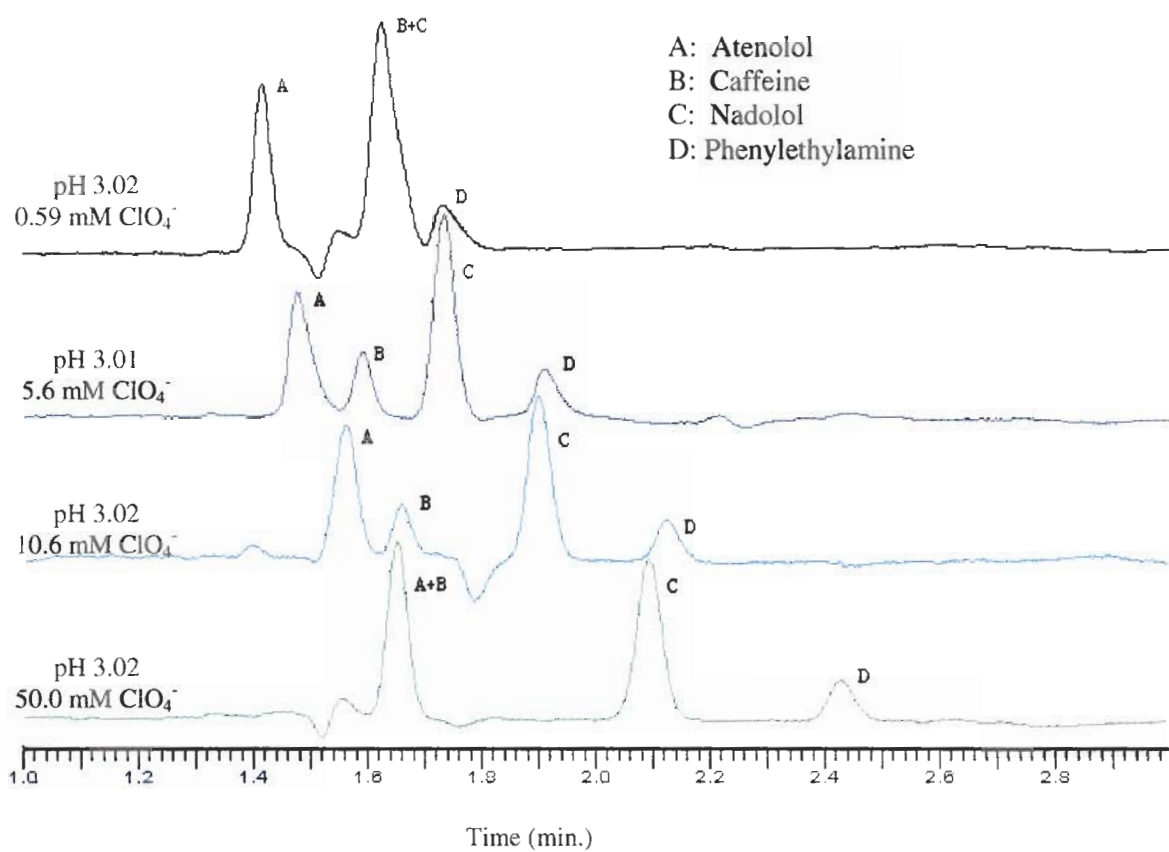


Figure 3-30. Effect of perchlorate concentration on retention of beta blockers, Caffeine and phenylethylamine. Conditions as in Figure 3-29.

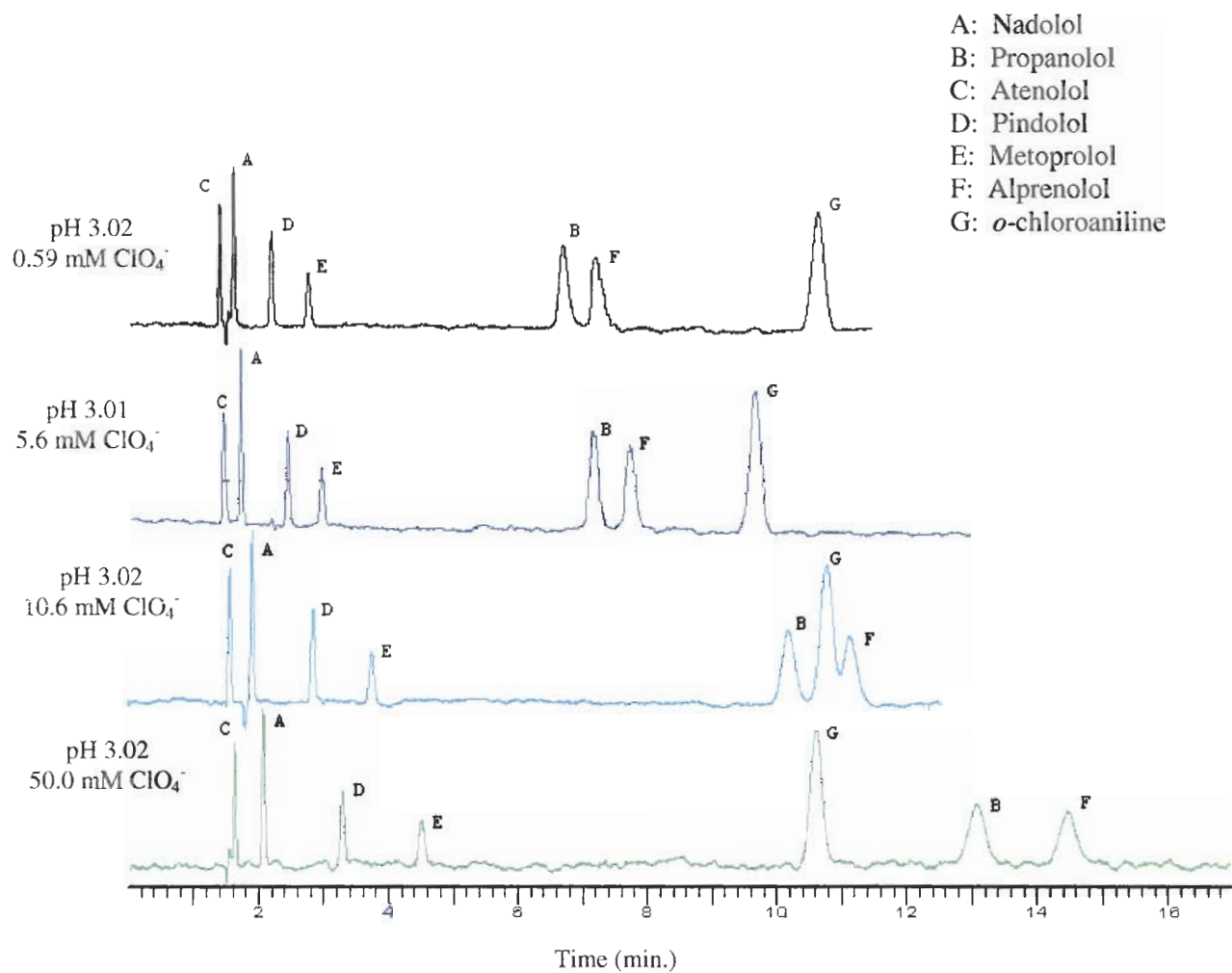


Figure 3-31. Effect of perchlorate concentration on retention of beta blockers and *o*-chloroaniline. Conditions as in Figure 3-29.

o-chloroaniline and perchlorate does not occur to a great extent, and thus no increase in retention was observed. When the perchlorate concentration was increased to 10.6 mM the resolution among the first four compounds (Compounds C, A, D, and E) was enhanced. The retention of the beta blockers was increased to different degrees. This was attributed to the differences in the analyte solvation. Propranolol and alprenolol retention also increased and were less resolved from the *o*-chloroaniline. Alprenolol actually eluted after *o*-chloroaniline at this concentration of perchlorate in the eluent. At a perchlorate concentration of 50 mM atenolol, nadolol, pindolol and metoprolol were resolved to a greater extent. In addition, a reversal of elution order was obtained between *o*-chloroaniline and propranolol. The optimal resolution among the components for this mixture was obtained at 50 mM perchlorate concentration.

Conclusions

The advantages of working with chaotropic agents in a low pH region have been demonstrated for the elution of pyridine, aniline, benzylamine and their alkylsubstituted derivatives. The differences in type of counteranion of the acidic modifier or salt had a significant effect on the retention of the basic compounds. The basic compound needs to be ionized for its solvation to be affected by the anionic chaotrope. Once the compound was ionized, a further decrease in pH led to an increase in the concentration of the counteranion, which consequently led to an increase in retention. The increased retention is independent of the pH, since it is the concentration of the anionic chaotrope in the mobile phase that dominates the retention. Therefore, after a desired mobile phase pH is obtained (two units lower than the pK_a of the basic compound) the concentration of the anionic chaotrope may be increased by the addition of inorganic salt without affecting the pH. This chaotropic

approach allows chromatographers a greater ability to separate basic compounds of similar pK_a 's and stereochemistries due to the difference in the analyte solvation. Additionally, increase in selectivity may be observed when analyzing ionizable compounds with different pK_a 's. The retention of one analyte may be governed by the analyte ionization state while the retention of another analyte may be affected by its interaction with the anionic chaotrope. This work proposes additional possibilities for resolution improvement of both acids and bases at low pH values.

Literature Cited

Chapter 3

1. Y. Hatefi, W.G. Hanstein, *Proc. Natil. Acad. Sci. U.S.A*, 62, 1969, 1129
2. W.S. Hancock, C.A. Bishop, R.L. Prestidge, D.R.K. Harding, and M.T.W. Hearn, *Science*, 200, 1978, 1168
3. W.S. Hancock, C.A. Bishop, R.L. Prestidge, D.R.K. Harding, and M.T.W. Hearn, *J.Chromatogr.*, 153, 1978, 391
4. M.T.W. Hearn, C.A. Bishop, W.S. Hancock, D.R.K. Harding, G.D. Reynolds, *J.Chromatogr.*, 2, 1979, 1
5. D. Guo, C.T. Mant, and R.S. Hodges, *J.Chromatogr.*, 386, 1987, 205
6. D. Corradini, K. Kalghatgi, and C. Horvath, *J.Chromatogr.A.*, 728, 1996, 225
7. C.E. Dunlap III, S. Gentlemen, L.I. Lowney, *J.Chromatogr.*, 160, 1978, 191
8. D.R.K. Harding, C.A. Bishop, M.F. Tarttelin, and W.S. Hancock, *Int. J. Peptide Protein Res.* 18, 1981, 214
9. J.D. Pearson, M.C. McCroskey, *J.Chromatogr. A.*, 746, 1996, 277
10. H.P.J. Bennett, C.A. Browne and S. Solomn, *J. Liq. Chromatogr.*, 3, 1980, 1353
11. I. Molnar and C. Horvath, *J.Chromatogr.*, 142, 1977, 623
12. J.H. Knox and R.A. Hartwick, *J. Chromatogr*, 204, 1981, 3
13. B.A. Bidlingmeyer, S.N. Deming, W.P. Price, B. Sachok and M. Petrussek, *J.Chromatogr.*, 186, 1979, 419
14. T.J. Sereda, C.T. Mant, and R.S. Hodges, *J.Chromatogr.A*, 776, 1997, 153
15. R.A. Thompson, Z. Ge, N. Grinberg, D. Ellison, and P. Tway, *Anal. Chem.*, 34, 1995, 1580
16. A. Ishikawa, T. Shibata, *J. Liq. Chromatogr.*, 16, 1993, 859
17. R. LoBrutto and Y.V. Kazakevich, *Proceedings of Intl. Symposia HPLC 98*, St. Louis, MI, 1998
18. Cs. Horvath, W. Melander, I. Molnar and P. Molnar, *Anal. Chem.*, 49, 1977, 2295

19. Cs. Horvath, W. Melander, and I. Molnar, *J.Chromatogr.*, 125, 1976, 129
20. K.G. Wahlund, *J.Chromatogr.*, 115, 1975, 411
21. B. Fransson, K.G. Wahlund, I.M. Johansson, and G. Schill, *J. Chromatogr.*, 125, 1976, 327
22. W.R. Melander and C. Horvath, *J.Chromatogr.*, 201, 1980, 211
23. D. Westerlund, and A. Theodorsen, *J.Chromatogr.*, 144, 1977, 27
24. A.P. Konijnedijk and J.L.M. van de Venne, *Advances in Chromatography, Proceedings of the 14th International Symposium*, Lausanne, September 22-28, 1979
25. J.C. Kraak, K.M. Jonker, and J.F.K. Huber, *J.Chromatogr.*, 142, 1977, 671
26. P.T. Kissinger, *Anal. Chem.*, 49, 1977, 883
27. J.H. Knox and J. Jurand, *J.Chromatogr.*, 125, 1976, 89
28. B.A. Bidlingmeyer, S.N. Deming, W.P. Price, Jr., B. Sachok, and M. Petrussek, in *Advances in Chromatography, Proceedings of the 14th International Symposium*, Lausanne, September 22-28, 1979
29. E. Tomilson, T.M. Jefferies, and C.M. Riley, *J.Chromatogr.*, 159, 1978, 315
30. D.R. Crow, *Principles and Applications of Electrochemistry*, Chapman and Hall, London, 1st ed., 1974
31. M. Szwarc, *Ions and Ion Pairs in Organic Reactions*, Vol. I, Chapter.I, Wiley (Interscience), New York, 1972
32. N. Bjerrum, *Kgt. Danske Vidensk. Selsk.* 9, 1926, 7
33. J.O'M. Bockris and A.K.N. Reddy, *Modern Electrochemistry*, Vol. 1, Plenum Press, New York, 1970, 251
34. J.T. Denison and J.B. Ramsey, *J.Am.Chem.Soc.* 77, 1955, 2615
35. H. Sadek, and R.M. Fuoss, *J.Am.Chem.Soc.* 76, 1954, 5897
36. S. Winstein, E. Clippinger, A.H. Fainberg, and G.C. Robinson, *J.Am.Chem.Soc.* 76, 1954, 2597

37. M. Szwarc, *Ions and Ion Pairs in Organic Reactions*, Vol. I, Chapter I, Wiley (Interscience), New York, 1972
38. R.M. Fuoss, *J.Phys.Chem.* 82, 1978, 2427
39. A.Winstein, W.R.Clippinger, F.A.Fainberg, and L.B.Robinson, *J.Am.Soc.*, 76, 1954, 2597
40. R.Grunwald, *Anal.Chem.*, 26, 1954, 1696
41. B.Eigen and R.K.Wicke, *J.Phys.Chem.*, 55, 1954, 702
42. J.J. Kirkland, J.W. Henderson, J.J. DeStefano, M.A. van Straten, H.A. Claessens, *J.Chromatogr.A*, 762, 1997, 97
43. J.J. Kirkland, M.A. van Straten, H.A. Claessens, *J.Chromatogr.A*, 797, 1998, 111
44. Y.V. Kazakevich and H.M. McNair.. *J. Chromatogr. Sci.*, 31, 1993, 317
45. E.H. Slaats, W. Markovski, J. Fekete, H. Poppe, *J. Chromatogr.*, 207, 1981, 299
46. HP software, manual
47. D. Sykora, E. Tesarova, M. Popl, *J.Chromatogr.A*, 758, 1997, 37
48. Q. Wan, M.C. Davies, P.N. Shaw, and D.A. Barrett, *Anal. Chem.*, 68, 1996, 437
49. D.N. Strazhesko, V.B. Strelko, V. Belyakov and S.C. Rubanik, *J.Chromatogr.*, 102, 1974, 191
50. M.L. Hair and W. Hertl, *J.Phys.Chem.*, 74, 1970, 91
51. P. Schindler and H.R. Kamber, *Helv.Chim.Acta*, 51, 1968, 1781
52. C. Horvath, *Advances and Perspectives*, Academic Press, New York, Vol. 1, 1980, 127.
53. A.J. Parker, *Pure Appl. Chem.*, 25, 1971, 345
54. C. Schwer, and E. Kenndler, *Anal.Chem.*, 63, 1991, 1801
55. F. Chan, R. LoBrutto, Y.V. Kazakevich, *Proceedings of Pharmaceutical Technology Symposium*, New Brunswick, NJ, October, 1999
56. W.J. Moore, *Physical Chemistry*, Prentice Hall, New York, 1962, 350
57. C.W. Davies, *J.Chem.Soc.*, 1938, 2093

58. M.H.Lietze, R.W.Stoughton and R.M.Fuoss, *Proc. Nat.Acad.Sci., US*, **50**, **1968**, 39
59. R.J.M. Vervoort, M.W.J. Derksen, A.J.J. Debets, *J.Chromatogr.A.*, **765**, **1997**, 157
60. R.J.M. Vervoort, F.A. Maris and H. Hindriks, *J.Chromatogr.*, **623**, **1992**, 207

Chapter 4

Development of model for Analyte desolvation/solvation process

Summary

This goal of this chapter is to develop a model to describe the effects of counteranion concentration on the basic analyte desolvation process. Basic analytes that are in their protonated form are solvated in aqueous and organic media. In chapter 3, we found that different acidic modifiers employed in the eluent disrupt the analyte's solvation to different degrees, each of which has a significant effect on their HPLC retention. The desolvation of a protonated basic analyte was determined to be a function of the counteranion concentration and was denoted as the chaotropic effect. The increase in concentration of a particular counteranion enhanced the retention of the basic analytes at a low pH region. The theoretical model based on solvation-desolvation equilibrium was applied to explain the dependencies of the retention factor versus counteranion concentration. The following equation was derived.

$$k = \frac{k_s - k_{us}}{K \cdot [A^-] + 1} + k_{us} \quad [4-1]$$

Where k is the retention factor, k_s and k_{us} denote the limiting retention factor of the corresponding solvated and unsolvated forms of the basic analytes, K is the analyte solvation parameter, and $[A^-]$ is the concentration of the counteranion. The solvation parameters for different classes of basic compounds including pyridines, anilines and benzylamines were compared. The influence of the type of counteranion and its effect on the limiting retention factors of the solvated and desolvated forms were also compared and contrasted. The intrinsic properties of the counteranion employed, such as delocalization of charge,

polarizability, hydrogen bonding ability and ionization at a certain pH, were also considered in their relation to the basic analyte desolvation.

It was observed that the dissociation of the buffer salts, acidic modifiers and basic analytes were greatly influenced by the organic solvent and organic composition. In addition, the type and concentration of the organic modifier was also shown to effect the analyte solvation. This can be attributed to solvation of the analyte with the eluent components. Acetonitrile is not able to solvate the analyte as readily as methanol does. Acetonitrile may not form hydrogen bonds with water molecules while methanol can. Upon solvation of the analyte, methanol may form a partially hydrophilic shell that could be retained on the reversed phase adsorbent. Furthermore, the effect of temperature on the analyte solvation was also studied.

Introduction

Basic analytes in solution are solvated by water as well as organic eluent components. The composition of the immediate surroundings of a solute may differ from the composition of the bulk mixture and this may be explained in terms of preferential solvation. Preferential solvation is attributable to the presence of excess molecules of either of the eluent components in these surroundings^[1]. The variation of the preferential solvation is mostly related to the structural features of these mixtures^[2]. However, if the solute show no preference for the solvent molecules, the solvent composition in the immediate neighborhood of the solute, is the same as in the bulk liquid. It has been shown that there is preferential solvation of hydrogen ion in acetonitrile-water mixtures^[3,4], acetate ions^[5], fluoroquinolones^[6], other buffer species^[7] including tartrate, citrate, phthalate and phosphate ions.

In order to understand the preferential solvation of the solutes in binary eluent systems, the preferential solvation has to be studied for the binary solvent mixtures themselves. Two eluent systems commonly used in reversed phase HPLC are: 1) Acetonitrile: Water and 2) Methanol: Water will be discussed. These two solvents are different in chemical nature. Acetonitrile can be considered as a polar aprotic solvent and methanol a protic solvent. Protic solvents have acidic protons, usually in the form of O-H or N-H groups. These groups form hydrogen bonds with negatively charged groups. Smaller anions are solvated more strongly than larger anions in a protic solvent. The solvent approaches a small anion more closely and forms stronger hydrogen bonds. A higher energy is required to strip off solvent from a small strongly solvated ion such as fluoride comparing to a large diffuse less strongly solvated ion like iodide. In contrast with protic solvents, aprotic solvents cannot solvate an anion as readily. However, polar aprotic solvents such as acetonitrile have strong dipole moments to enhance solubility even though they have no O-H or N-H groups to form hydrogen bonds with the anions.

The molecules in these mixtures are thought to be surrounded by molecules of the same species as well as both species depending on the eluent composition. This may explain why the composition of the immediate surroundings of a solvent particle may be different compared to the bulk media. Preferential solvation occurs when an excess or a deficiency of molecules of one of the solvent species are present in the aforementioned surroundings. If there is a mutual attraction of two solvents, then there is a negative enthalpy of mixing and a positive enthalpy of mixing is obtained when self-interactions are dominant over the mutual ones. Binary solvent mixtures are stable as a single liquid phase assuming that the second derivative of the Gibbs free energy of mixing at a given temperature and pressure is positive

over the entire composition range ^[1]. However, when this preference is dominant at a certain composition region the second derivative of the Gibbs free energy of mixing is negative within this region, and the mixture may split into two or more phases.

The Gibbs free energy of mixing is

$$\Delta G_{12}^E = (ZRT) \{x_1 \ln[(N_{11}/S)^{1/2} / x_1] + x_2 \ln[(N_{22}/S)^{1/2} / x_2]\} \quad [4-2]$$

where N_1 and N_2 are the molecules of solvents 1 and 2 in the mixture, having the bulk mole fractions $x_1 = N_1/(N_1+N_2)$ and $x_2 = 1-x$, respectively. In pure liquid 1 each molecule has Z_1 neighbors, and in pure liquid 2 each molecule has Z_2 neighbors, but in the mixture the number of neighbors each molecule has is a weighted average, Z . S are the total number of pairs of neighbors in the system and N_{11} and N_{22} are the number of like neighbors of molecules.^[1]

The preferential solvation of water by acetonitrile is dominant only when the mole fraction of acetonitrile is greater than 0.7 ^[5]. In these systems the self interactions of each component are favored over the mutual interactions from mole fraction 0.1 to 0.7. However, in methanol water mixtures, these systems show large positive values of the preferential solvation over the whole concentration range. This indicates that strong mutual interaction of the components rather than self interactions are preferred. Bosch describes the process describing preferential solvation in alcohol-water systems in great detail ^[8].

The composition of water-acetonitrile mixtures may be thought as of consisting of at least three regions ^[9-10]. When water is predominate in the mixture there is a region where the water structure remains more or less intact as acetonitrile molecules are added intrinsically into the cavities of this structure. On the acetonitrile rich side, there exists a

region where individual water molecules interact with the individual acetonitrile molecules. However, at intermediate compositions, there are clusters of molecules of the same kind, which consist of mutually hydrogen-bonded water molecules, surrounded by regions where molecules of the two kinds are near each other (at the surface of the clusters). The presumed water-cluster has a lower ability to donate a hydrogen atom toward the formation of a hydrogen bond than water in its ordinary structure. However, the water cluster still has a considerably higher ability than water bonded to acetonitrile in the high acetonitrile region^[4]. Other aqueous aprotic-solvents systems show the same behavior. Marcus has described the overall picture of the preferential solvation of water and acetonitrile mixtures from various studies^[4]. As acetonitrile is added to water, it first enters the cavities of the water structure^[11]. Monte Carlo simulation^[12], ultrasonic velocity^[13], and negative enthalpies of mixture at high dilutions have been used to describe the solvation by water and the water structure in the vicinity of the hydrogen atoms. The limit of the mole fraction of acetonitrile beyond which the acetonitrile can no longer be accommodated within the cavities of the structure or ordinary water is about 0.15, but various methods place this limit at various locations in the range $0.1 \leq x_{\text{CH}_3\text{CN}} \leq 0.33$. Beyond this limit there is a great influence of acetonitrile and there is a disruption of the water structure^[6]. However, in this middle range of compositions microheterogeneity sets in; microheterogeneity is where the water clusters of the hydrogen bonded structure are enhanced relative to that of pure water. This self association in terms of microheterogeneity was discussed by many authors^[14-23]. At acetonitrile mole fractions greater than 0.7 however the water clusters are present in lesser amounts and further from each other and new types of interactions set in. These interactions which are disregarded in the middle range now play an important role. This region may be

envisioned as discrete water-MeCN complexes surrounded by the MeCN solvent. These complexes are suggested to be $\text{CH}_3\text{CN} \cdots \text{HOH}$ and $\text{CH}_3\text{CN} \cdots \text{HOH} \cdots \text{NCCH}_3$ [4,24].

A model is developed to describe the effect of the analyte desolvation process upon addition of counteranions in the mobile phase similar to Langmuir^[25] performed for adsorption processes. The effects of preferential solvation will be considered in the description of the dependence of the solvation parameter as a function of type and amount of organic in the mobile phase and temperature.

Experimental

Apparatus: The chromatographic system used was a HP model 1100 HPLC from Hewlett Packard (Little Falls, DE). The chromatograms were processed using HP software. The column used was Zorbax Eclipse XDB-C18, (Hewlett Packard, Little Falls, DE), 150 x 4.6 mm i.d., particle diameter 5 μm , bonding density 3.4 $\mu\text{mol}/\text{m}^2$. The Eclipse XDB-C18 column has a nominal surface area of 180 m^2/g , and a pore size of 80 \AA . This column is a densely bonded dimethyl-silane-substituted stationary phase that is double endcapped with dimethyl and trimethylsilane groups. This column has been demonstrated to be very stable at both low and high pH values^[26-27]. The other column used was a Luna-C18 column (Phenomenex, Torrance, CA), 150 x 4.6 mm i.d., particle diameter 5 μm , bonding density 3.0 $\mu\text{mol}/\text{m}^2$. The Luna C18 column has a nominal surface area of 300 m^2/g and a pore size of 90 \AA .

The column temperature was controlled by a circulating water-bath Brinkman Model RC6 Lauda (Lauda-Konigshofen, Germany). The pH was measured using a Fisher Accumet

pH meter 15 on the aqueous eluent component before the addition of the organic modifier. The electrode was calibrated with pH 1.0, 2.0, 4.0, 7.0, and 10.0 standard solutions.

Chemicals

Orthophosphoric acid (analytical grade), perchloric acid, (redistilled) water (HPLC grade), acetonitrile (HPLC grade) and methanol (HPLC grade) were obtained from Sigma Chemical Co. (Milwaukee, WI). Sodium hydrogenphosphate heptahydrate and sodium perchlorate were purchased from Fisher Scientific (Fairlawn, NJ). All aqueous mobile phases were filtered using Whatman Nylon 66 membrane filter (Fisherlane). The following basic compounds were used: aniline (Baker), N-methyl-aniline (Eastman, TN), pyridine, 2-ethylpyridine, 3-ethylpyridine, 4-ethylpyridine, 2,4-dimethylpyridine, 2,6-dimethylpyridine, 3,4-dimethylpyridine, 3,5-dimethylpyridine (Aldrich), 4-tertbutylpyridine, 2-n-propylpyridine, 4-n-propylpyridine, benzylamine, 2-methylbenzylamine, 3-methylbenzylamine, and 4-methylbenzylamine (Lancaster Laboratories, Lancaster, PA).

Chromatographic Conditions

The retention data was recorded at ambient temperature and temperature controlled between 5-45°C using isocratic conditions with a flow rate of 1 mL/min using the Zorbax Eclipse XDB-C18 column. The retention data was recorded at 25°C using isocratic conditions with a flow rate of 1 ml/min using the Luna C18 column. UV detection was at 254 nm for the entire study. The aqueous portion of the mobile phase was a 5-90 mM disodium hydrogenphosphate buffer (pH=8.96) adjusted with ortho-phosphoric acid over the pH range of 1 – 3 or an aqueous phase adjusted solely with phosphoric acid. Another study used a mobile phase of water adjusted with perchloric acid over the pH range of 1-3 with the addition of NaClO₄ or an aqueous phase adjusted solely with perchloric acid. Acetonitrile

and methanol were used as the organic modifiers. The eluent composition was varied from 90:10 (aqueous : organic) to 50:50 (aqueous :organic).

All analyte solutions with the exception of the benzylamines were prepared by their dissolution in the eluent to give a concentration of 0.1-0.2 mg/ml. Benzylamines were dissolved in 70/30 water/acetonitrile to give a concentration of 0.2 mg/ml. Injections of 1-5 μ l of these solutions were made.

The t_o values obtained for the Zorbax XDB-C18 column was determined using the minor disturbance method ^[28-29] within the temperature range of 5 – 45°C. The t_o for the Luna C18 column was 1.63 min. The retention factors calculated was the average of triplicate injections showing %RSD less than 1.5%. Also, a test mixture of aniline and pyridine was used as system suitability check before and after each experiment to monitor the performance and the stability of the column.

Results and Discussion

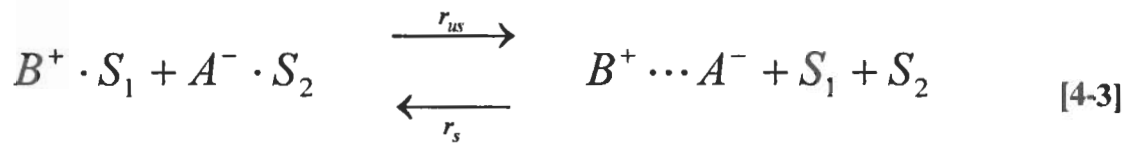
Analyte Desolvation/Solvation Model

The retention factor, k , may be related to the counteranion concentration as was shown in equation 4-1.

The assumptions on which this model are based on:

1. Analyte concentration in the system is low enough that analyte-analyte interactions could be considered nonexistent.
2. Chromatographic system is in thermodynamic equilibrium.

The analyte solvation-desolvation equilibrium inside the column could be written in the following form:



Where B^+ is a protonated basic analyte with its own specific solvation S_1 ; A^- is a counteranion with its own specific solvation S_2 ; $B^+ \cdots A^-$ is the desolvated ion-associated complex; r_s is the rate of solvation and r_{us} is the rate of desolvation. A certain amount of analyte injected $[B]$ will be in its protonated form $[B^+]$, and a certain amount will interact with an oppositely charged species $[B^+A^-]$ shown in equation 4-4. The protonated form will be considered as the solvated form. The amount of analyte in its solvated and unsolvated forms can be considered as a fraction of the certain amount injected: θ , solvated fraction and $1-\theta$, as the unsolvated fraction shown in equation 4-5.

$$[B^+] + [B^+A^-] = [B] \quad [4-4]$$

Hence,

$$\frac{[B^+]}{[B]} + \frac{[B^+A^-]}{[B]} = 1, \text{ where } \frac{[B^+]}{[B]} = \theta, \frac{[B^+A^-]}{[B]} = 1 - \theta \quad [4-5]$$

The solvated form at equilibrium consists of the protonated analyte with solvation shell intact and the solvated counteranion. The unsolvated form is described when the protonated analyte and the counteranion are electrostatically attracted to each other. As a consequence, water is expelled due to their interaction. A solvation parameter K can be obtained from this equilibrium. At equilibrium the rates of desolvation and solvation are assumed to be equal:

$$\frac{r_{us}}{r_s} = \frac{[1-\Theta]}{[\Theta] \cdot [A^-]} = K \quad [4-6]$$

where $K = r_{us}/r_s$ is the analyte equilibrium solvation parameter. Equation [4-6] can be rearranged to solve for θ :

$$\Theta = \frac{1}{K[A^-] + 1} \quad [4-7]$$

The completely solvated and unsolvated forms of the molecule will each have a limiting retention factor. The total retention factor is the sum of the retention factor of the solvated form multiplied by the solvated fraction (θ) and the retention factor of the unsolvated form multiplied by the unsolvated fraction ($1-\theta$). Substitution of the solvated and unsolvated fractions into equation 4-8 will give the final form for the total retention factor, [4-10] with three parameters which include K , k_s , and k_{us} .

$$k = k_s \cdot \Theta + k_{us} \cdot (1 - \Theta) \quad [4-8]$$

Substituting θ

$$k = k_s \cdot \left\{ \frac{1}{K[A^-] + 1} \right\} + k_{us} \cdot \left\{ 1 - \frac{1}{K[A^-] + 1} \right\} \quad [4-9]$$

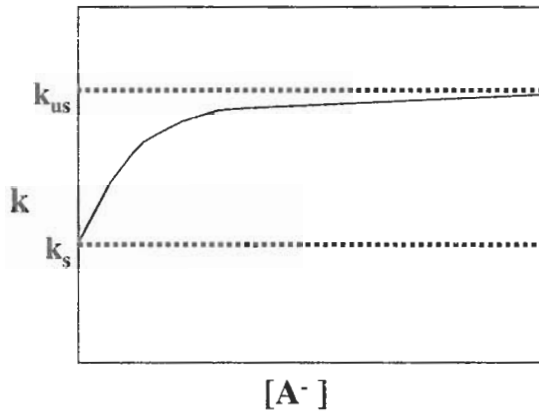
and the final form can be rewritten as:

$$k_{(A^-)} = \frac{k_s - k_{us}}{K \cdot [A^-] + 1} + k_{us} \quad [4-10]$$

This expression represents Langmuir type retention dependence on the counteranion concentration. Increase of the counteranion concentration leads to the asymptotic approach

to the retention of its unsolvated form, k_{us} shown in Figure 4-1. Where $[A^-] \rightarrow \infty$, $k = k_{us}$. In absence of counteranion concentration, i.e. $[A^-] = 0$, the protonated analyte is completely solvated and has the lowest possible retention, k_s . Equation [4-10] is the general form that may describe the analyte desolvation process. The specific solvation of the analyte and the counteranion may be dependent upon the temperature and type of organic modifier and the modifier concentration.

Theoretical Dependence of k vs. conc.



2-ethylpyridine

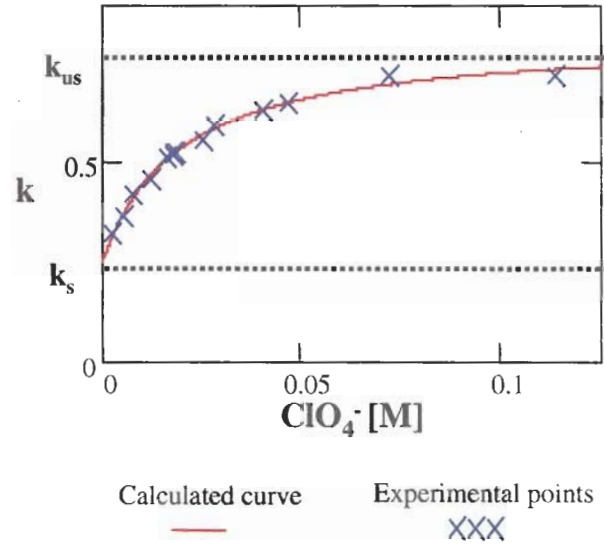


Figure 4-1. Theoretical dependence of retention factor versus concentration of acidic modifier counteranion. a) Theoretical dependence of k versus concentration and b) Excellent correlation of the experimental points fit using equation [4-11] for 2-ethylpyridine. The excellent correlation was obtained for all the other basic analytes studied in the various eluent compositions at various temperatures.

Influence of type of counteranion on solvation parameter

Retention factors of the basic analytes versus concentration of dihydrogen phosphate (Figure 4-2) and versus perchlorate (Figure 4-3) were determined on a Zorbax XDB-C18 in 90% aqueous buffers 10% acetonitrile. Also, the retention factor of the basic analytes versus concentration of dihydrogen phosphate was determined on a Phenomenex Luna C18 column. The basic analytes were assumed to be in their protonated forms at the working pHs, 1.1 – 2.6 accounted for pH and pK_a shift in the organic medium. Figure 4-2 showed the retention dependence as a function of concentration of three isomeric pyridinal compounds using phosphoric acid as the pH modifier. Figure 4-3 shows the retention dependence on the same column using perchloric acid and NaClO_4 as the mobile phase modifiers. The superimposed curves for each compound showed excellent correlation with the experimental points as shown in Figure [4-1b] for all basic compounds studied. The best fits of the theoretical curves to the experimental data were obtained using equation 4-10 with a nonlinear regression program, MathCad 8. This fitting procedure allowed the estimation of the K , solvation parameter, k_s and k_{us} , of the solute in the HPLC mobile phase. This estimation takes into the assumption that the experimental data are consistent with the proposed theoretical model. These values are shown in Tables 4-I, 4-II, and 4-III. Theoretically, the retention factor should approach the same retention factor for the completely unsolvated form when both acids (perchloric and phosphoric acids) are employed (Table 4-I and Table 4-III). However, the limiting retention factor obtained for the unsolvated analyte when phosphate counteranion is employed is smaller. This may be attributed to a superposition of other ion-association processes that actually may interfere

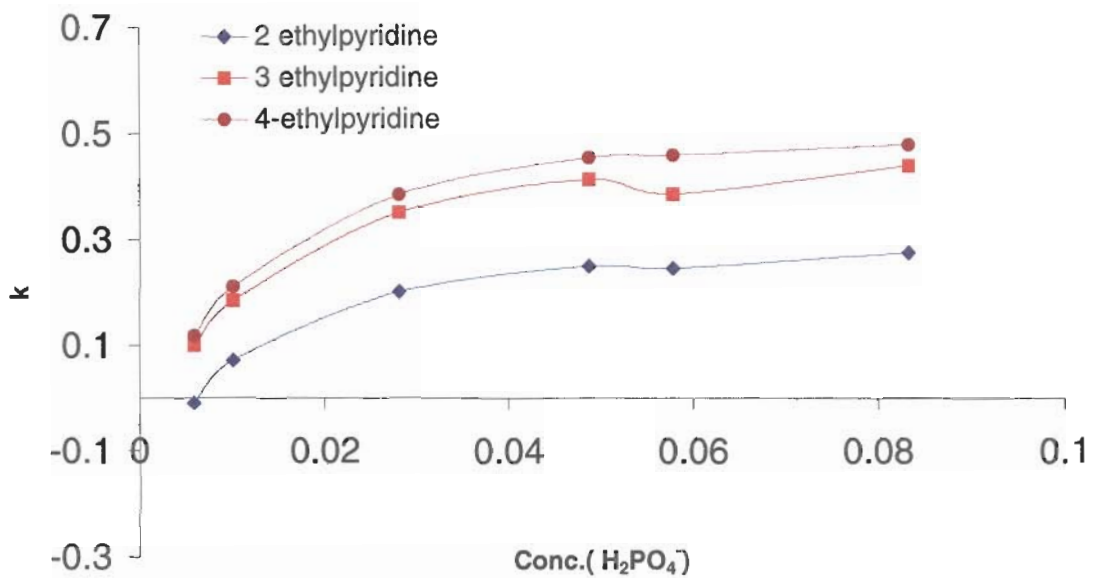


Figure 4-2. Change of the retention of basic analytes at low pH with the increase of the concentration of dihydrogenphosphate counteranion. Concentration region 4.3 – 72.7 mM of dihydrogenphosphate anion. Column: 15x0.46cm Zorbax XDB-C18; mobile phase: (10:90) Acetonitrile- Aqueous Disodium hydrogenphosphate buffer adjusted with phosphoric acid and/or solely phosphoric acid, pH=1.83 –2.26 flow rate, 1.0 ml/min; Temp.: ambient, UV, 254 nm; sample:1 μ l injection.

Table 4-I

Retention factors and Solvation parameters obtained using dihydrogen phosphate as the counteranion and acetonitrile/water eluent on Zorbax Eclipse XDB-C18 column.

	aniline	N-methylaniline	N,N-dimethylaniline	2,4-dimethylpyridine	3,4-dimethylpyridine
k_s	0.089	0.111	0.327	-0.095	0.039
k_{us}	0.283	0.54	0.679	0.148	0.238
K	0.061	0.132	0.076	0.14	0.089
	2-ethylpyridine	4-ethylpyridine	2-n-propylpyridine	4-n-propylpyridine	Pyridine
k_s	-0.019	0.102	0.273	0.697	-0.137
k_{us}	0.131	0.327	0.58	1.318	-0.065
K	0.075	0.064	0.056	0.051	0.097

Conditions as in Figure 4-2.

Table 4-II

Retention factors and Solvation parameters obtained using dihydrogen phosphate as the counteranion and acetonitrile/water eluent on Luna-C18 column.

	aniline	2-ethylpyridine	3-ethylpyridine	4-ethylpyridine	2,4-lutidine
k_s	-0.037	-0.31	-0.222	-0.205	-0.357
k_{us}	0.555	0.318	0.49	0.554	0.366
K	0.06	0.157	0.139	0.125	0.177
	2,6-lutidine	3,4-lutidine	3,5-lutidine	pyridine	
k_s	-0.277	-0.235	-0.234	-0.261	
k_{us}	0.26	0.466	0.472	0.083	
	0.131	0.133	0.133	0.104	

Concentration region 6 – 83 mM of dihydrogenphosphate anion. Column: 15x0.46cm Phenomenex Luna-C18; mobile phase: (10:90); Acetonitrile- Aqueous adjusted solely phosphoric acid, pH=1.1 – 2.23 flow rate, 1.0 ml/min; Temp.: ambient, UV, 254 nm; sample: 1µl injection.

Table 4-III

Retention factors and Solvation parameters obtained using perchlorate as the counteranion and acetonitrile/water eluent on Zorbax Eclipse XDB-C18 column.

	aniline	pyridine	N-methylaniline	N,N-dimethylaniline	2,4-dimethylpyridine
k_s	0.4	1.71E-03	0.787	1.006	0.261
k_u	1.107	0.154	2.048	2.581	0.923
K_s	0.056	0.079	0.042	0.033	0.055
	2-ethylpyridine	4-ethylpyridine	2 n proylpyridne	4 n-propylpyridine	3,4-dimethylpyridine
k_s	0.247	0.459	0.797	1.514	0.353
k_u	0.809	1.45	2.571	5.172	1.199
K_s	0.051	0.049	0.038	0.042	0.053

Concentration region 2.5 – 114 mM of perchlorate anion. Column: 15x0.46cm Zorbax XDB-C18; mobile phase: (10:90); Acetonitrile- Aqueous perchloric acid and NaClO₄ and/or solely phosphoric acid, pH=1.78 –2.6 flow rate, 1.0 ml/min; Temp: 25°C, UV, 254 nm; sample:1µl injection.

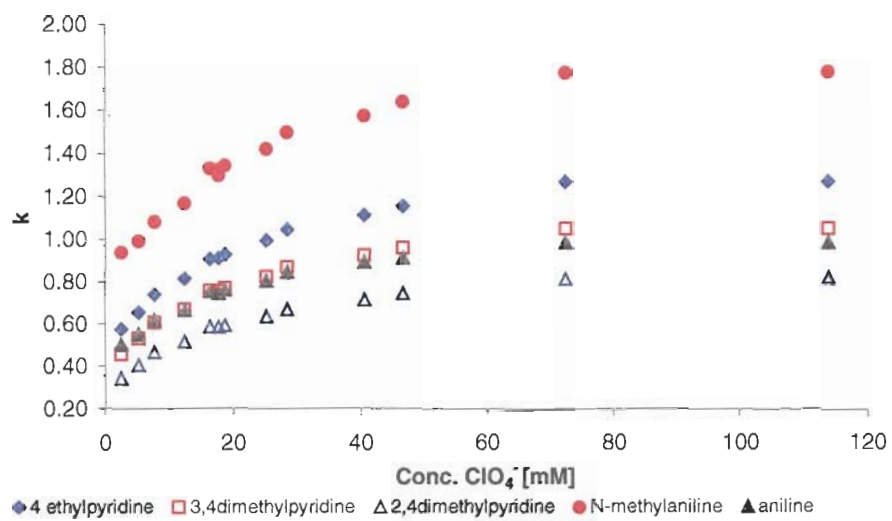


Figure 4-3. Change of the retention of basic analytes at low pH with the increase of the concentration of perchlorate counteranion. Conditions same as in Table 4-III.

with the pure “desolvation-solvation” process. Another explanation is the solvation of the ion-associated species. Since, the phosphate counteranions are able to participate in hydrogen bonding, they may be solvated as well. Upon ion-association with the protonated basic analyte, the retention is decreased due to interaction of this hydrophilic ion-associated complex with the stationary phase. The solvation parameter values obtained for the basic analytes in Table 4-I and Table 4-III were greater when phosphoric acid was used compared to the system when perchloric acid was used. The difference in the solvation parameters obtained with both systems for the basic analytes studied are shown in Table 4-IV. The sharper the knee of the analyte retention dependence on the counteranion concentration, the greater the solvation parameter. This would indicate that the dihydrogen phosphate anion has a greater effect on the analyte solvation. If there is solvation of the ion-associated complex, this may actually be suppressing the limit of the unsolvated retention factor and in essence leading to a lower plateau region. Further study of anions that are not easily solvated such as perchlorate will have to be studied. These may include hexafluorophosphate and heptafluoroborate which both have a high charge delocalization and low degree of hydration.

Another study investigated the influence of the dihydrogenphosphate counteranion on the retention of basic analytes using two different types of C₁₈ columns. For the Luna C₁₈ and Zorbax XDB C₁₈ packing materials, the retention of the basic solutes increased as the concentration of dihydrogen phosphate in the mobile phase increased. The solvation parameters are larger for all cases when the Luna C₁₈ column was used illustrated in Table 4-II and the solvation parameters determined on the Zorbax column are shown in Table 4-I.

Table 4-IV

Comparison of solvation parameters obtained when using dihydrogenphosphate and perchlorate anions and acetonitrile/water eluent on Zorbax Eclipse XDB-C18 column.

Counteranion		pyridine	2-ethylpyridine	2-n-propylpyridine	2,4-lutidine
H ₂ PO ₄ ⁻	K	0.097	0.075	0.056	0.14
ClO ₄ ⁻	K	0.079	0.051	0.038	0.055
	Δ K	0.018	0.024	0.018	0.085
		4-ethylpyridine	4-n-propylpyridine	3,4-dimethylpyridine	
H ₂ PO ₄ ⁻	K	0.064	0.051	0.089	
ClO ₄ ⁻	K	0.049	0.042	0.053	
	Δ K	0.015	0.009	0.036	
		aniline	N-methylaniline	N,N-dimethylaniline	
H ₂ PO ₄ ⁻	K	0.061	0.132	0.076	
ClO ₄ ⁻	K	0.056	0.042	0.033	
	Δ K	0.005	0.09	0.043	

(Conditions as in Figure 4-2 and 4-3)

The limiting retention factor for the unsolvated form was greater on the Luna C₁₈ column and this can be attributed to the greater surface area of the packing material making it more retentive for the solute component. However, on the Luna C₁₈ column, the solvation parameters for the same solute were generally greater than on the Zorbax Eclipse XDB-C₁₈ column. The solvation parameter describes the analyte desolvation process above the surface of the packing material and it should not be influenced by the type of packing material used. However, we have shown that there is an existence of an adsorbed organic layer on top of the bonded phase [Chapter 5]. Therefore the retention of the solutes would be dependent on their distribution coefficient into this layer and their consequent adsorption onto the bonded layer. The analyte components may partition from the mobile phase composition into this layer. Depending on the distribution coefficient of the solute species, this might lead to differences in its retention. If the layer is of different thickness this may effect the partitioning process in the adsorbed layer as well. The difference in the thickness of the layer may effect the flow distribution of the ions and consequently, the fewer perchlorate anions present, the lesser the analyte may be desolvated.

Effect of type of eluent on the solvation parameter

The plots of chromatographically determined retention factor of a representative set of basic analytes versus concentration of perchlorate anion were determined on a Zorbax XDB-C₁₈ column in 90%Aqueous : 10%Acetonitrile, Figure 4-4, and 90%Aqueous : 10% Methanol, Figure 4-5. There are differences in the limiting retention factors, k_s and k_{us} , obtained for the components at a certain concentration when methanol and acetonitrile were used. This may be attributed to the solvation of the methanol as well as the water on the basic analytes. The solvation parameter, K , for the basic analytes at the same chromatographic conditions are different when acetonitrile and methanol are used. The

solvation parameter values in Tables 4-III (acetonitrile) and Table 4-V (methanol) indicate that methanol may actually participate in the analyte solvation due to its ability to form hydrogen bonds as opposed to acetonitrile. Therefore a sharper knee of the analyte retention dependence on the perchlorate concentration is obtained. This was supported by literature that large positive values of the preferential solvation in the methanol-water binary system suggested strong mutual interactions of the components are preferred over the self interactions between methanol molecules. Marcus^[24] determined a negative enthalpy of mixing indicating the mutual interaction of the two solvents. Therefore, methanol may also solvate the analyte and aid in the analyte desolvation process. In this observed system the perchlorate anion and the methanol solvent molecules produced a synergistic effect on the analyte solvation. The different combinations of the same counteranion and different solvents may not only lead to differences in the analyte solvation but differences in the resolution between components as shown in Figures 4-4 and 4-5. The resolution between 2-ethylpyridine and 4-ethylpyridine is enhanced in the perchlorate-acetonitrile system when compared to that of the “perchlorate-methanol” system.

Effect of concentration of organic solvent on the solvation parameter

The influence of the concentration of perchlorate anion on the retention of basic analytes were determined on a Zorbax XDB-C18 column in Aqueous (adjusted with perchloric acid and/or NaClO₄): acetonitrile or methanol mobile phases containing organic ranging from 10 – 50%. Figure 4-6 shows a representative set of basic compounds analyzed at 90% aqueous:10% acetonitrile at 35°C. Figure 4-7 shows the plot of retention factor versus concentration of 2-ethylpyridine performed at different organic compositions of 10 – 50% acetonitrile. The plot indicates that the limiting retention factor, k_{us} , for the unsolvated

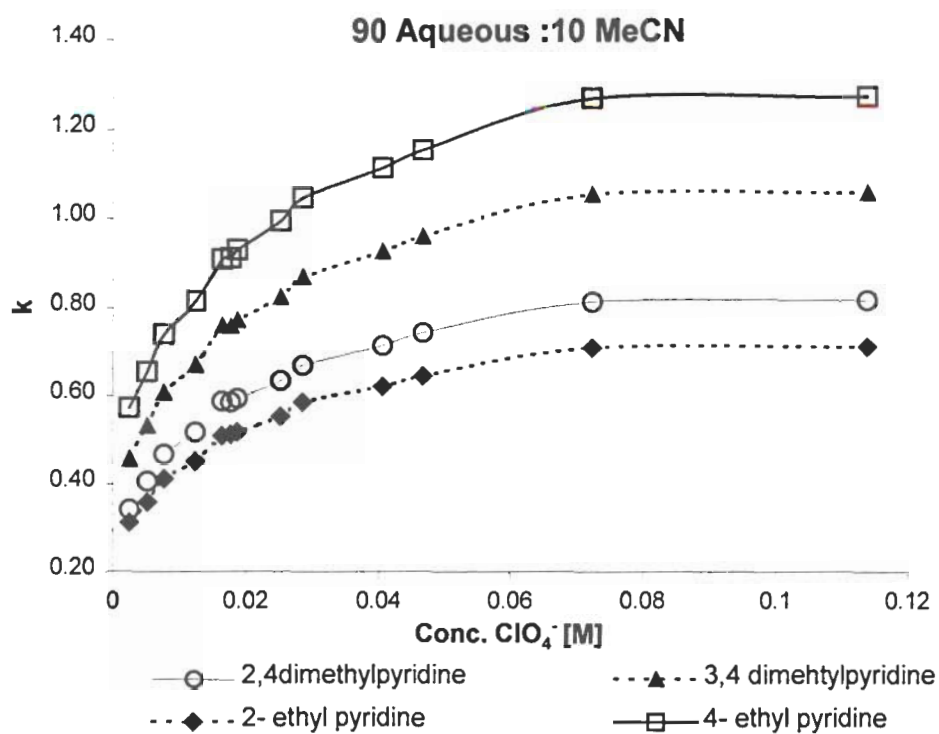


Figure 4-4. Retention factor versus perchlorate concentration at 90% Aqueous: 10% Acetonitrile. Same conditions as in Figure 4-3.

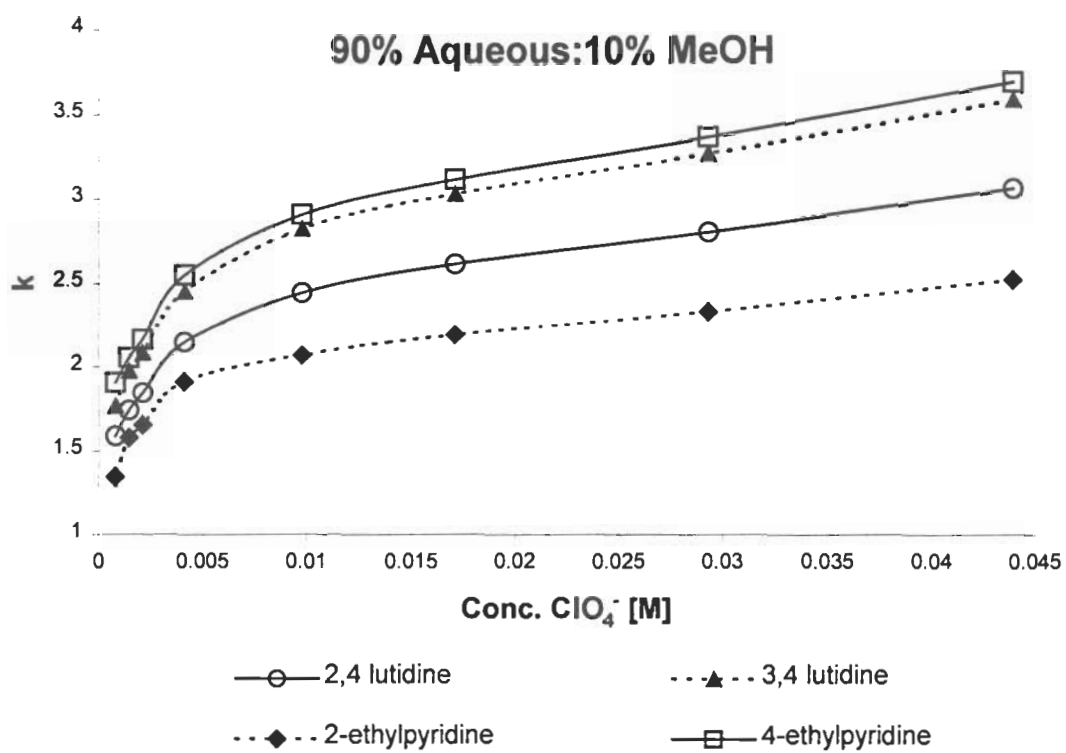


Figure 4-5. Retention factor versus perchlorate concentration at 90% Aqueous:10% Methanol. Concentration region 0.08mM - 44mM of perchlorate anion. Column: 15x0.46cm Zorbax Eclipse XDB-C18; mobile phase: (90:10); Methanol- Aqueous adjusted with perchloric acid, pH=1.4-2.9 flow rate, 1.0 ml/min; Temp.: 25°C, UV, 254 nm; sample:1µl injection.

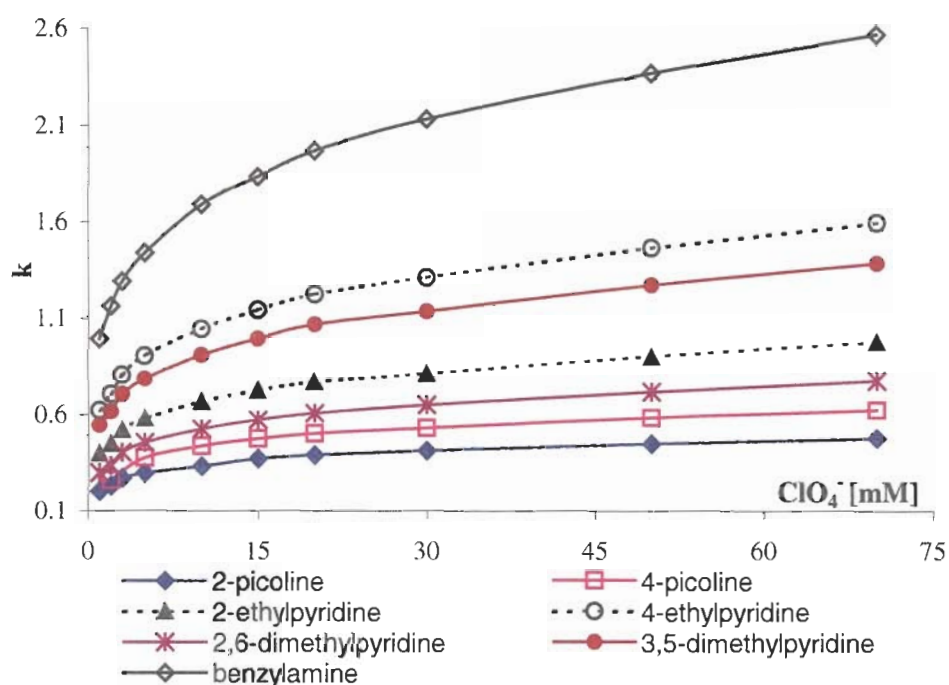


Figure 4-6. Retention factor versus concentration, 35°C for pyridinal and benzylamine compounds. Conditions: Concentration region 1 – 70 mM of perchlorate anion. Column: 15x0.46cm Zorbax XDB-C18; mobile phase: (90:10); Acetonitrile- Aqueous adjusted with perchloric acid and NaClO₄ and/or solely perchloric acid, pH=2.6-2.9 flow rate, 1.0 ml/min; Temp.: 35°C, UV, 254 nm; sample: 1µl injection.

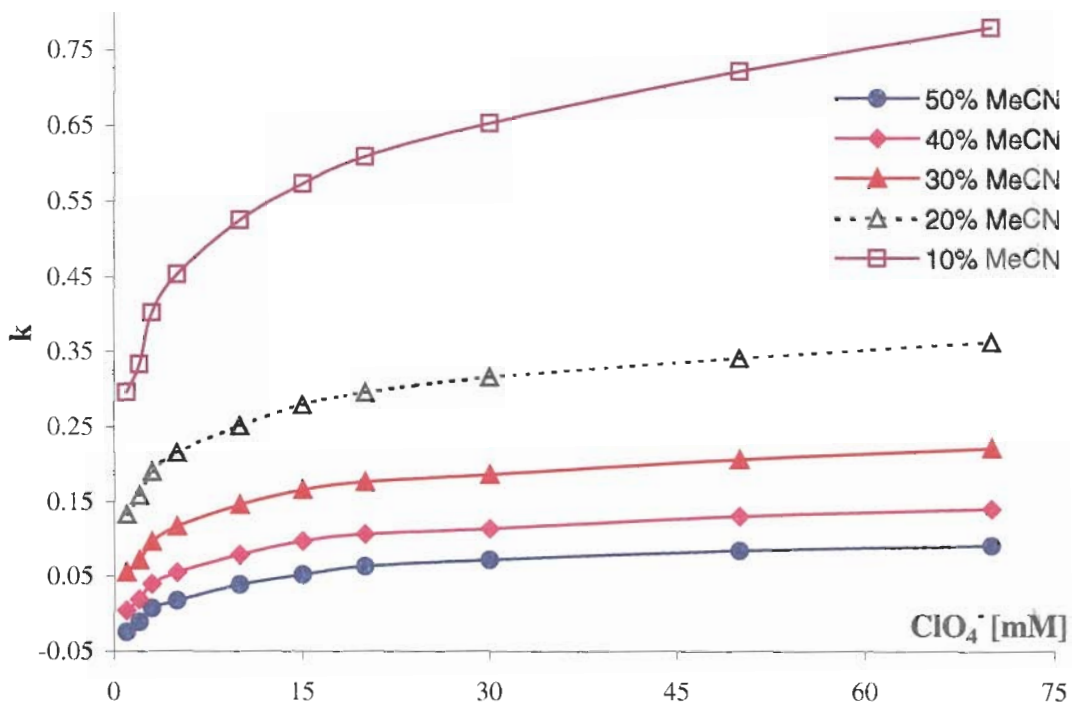


Figure 4-7. Retention factor of 2-6 dimethylpyridine versus concentration at different mobile phase compositions, 35°C. Conditions: Concentration region 1 – 70 mM of perchlorate anion. Column: 15x0.46cm Zorbax XDB-C18; mobile phase: Acetonitrile-Aqueous adjusted with perchloric acid and NaClO_4 and/or solely perchloric acid, pH=2.6-2.9, Aqueous content varied from 50 –90%; flow rate, 1.0 ml/min; Temp.: 35°C, UV, 254 nm; sample: 1 μ l injection.

Table 4-V

Retention factors and Solvation parameters obtained using perchlorate as the counteranion and methanol/water eluent on Zorbax Eclipse XDB-C18 column.

	aniline	N-methylaniline	2,4-dimethylpyridine
k_s	1.747	2.547	1.456
k_u	3.446	5.492	3.237
K	0.05	0.089	0.13
	3,4-dimethylpyridine	2-ethylpyridine	4-ethylpyridine
k_s	1.621	1.195	1.759
k_u	3.812	2.545	3.961
K	0.126	0.233	0.111

Same conditions as in Figure 4-5.

form approaches the asymptotic limit at a faster rate as the acetonitrile content increases.

When applying equation 4-11, we obtained K , k_s , k_{us} and these values are shown in Tables 4-VI to Table 4-XI. The solvation parameter also increases indicating that the asymptotic limit for the unsolvated retention factor is achieved at much lower concentrations of the perchlorate anion. This may be attributed to the disruption of the analyte solvation by the acetonitrile molecules at increasing concentrations. As shown in the studies performed with the preferential solvation of hydrogen ions in water/acetonitrile mixtures, increasing the acetonitrile content breaks apart the original water structure that are preferentially hydrating the hydrogen ions. It was shown that at mole fraction >0.15 acetonitrile, acetonitrile can no longer be accommodated within the cavities of the structure of ordinary water. The same phenomenon may be occurring at the analyte solvation shell. Hence, the increase of acetonitrile is actually aiding in the desolvation process. Plots of the solvation parameter versus % acetonitrile obtained at 35°C and 45°C are shown in Figures 4-8 and 4-9. The desolvation parameter increases predominately in the region of 10 –40% Acetonitrile. The observed effects show that the increase in acetonitrile content aids in the desolvation process, causes a greater disruption in the analyte solvation, and ultimately allows the limiting retention factor for the unsolvated form to be obtained at lower concentrations of counteranion.

Another rationale is that as the concentration of acetonitrile increases the dielectric parameter decreases. This permits the two oppositely charged species to be attracted to each other with a greater force, since force is inversely proportional to the dielectric parameter. Upon doing so, this permits greater analyte desolvation as the perchlorate anion approaches the protonated basic analyte by expulsion of water from the analyte solvation shell.

Table 4-VI

Retention factor and solvation parameters obtained using perchlorate as the counteranion and MeCN/Water (50:50) eluent on Zorbax Eclipse XDB-C18 column at 35°C.

	2-picoline	4-picoline	2-ethylpyridine	4-ethylpyridine
k_s	-0.054	-0.045	-0.035	-0.032
k_{us}	0.065	0.076	0.116	0.137
K	0.168	0.143	0.152	0.156
	2,6-dimethylpyridine	3,5-dimethylpyridine	benzylamine	R-methylbenzylamine
k_s	-0.037	-0.032	-0.023	-0.014
k_{us}	0.104	0.128	0.154	0.198
K	0.124	0.157	0.103	0.119

Conditions: Concentration region 1 – 70 mM of perchlorate anion. Column: 15x0.46cm Zorbax XDB-C18; mobile phase: (50:50); Acetonitrile - Aqueous adjusted with perchloric acid and NaClO₄ and/or solely perchloric acid, pH=2.6-2.9, flow rate, 1.0 ml/min; Temp.: 35°C, UV, 254 nm; sample: 1µl injection.

Table 4-VII

Retention factor and solvation parameters obtained using perchlorate as the counteranion and MeCN/Water (40:60) eluent on Zorbax Eclipse XDB-C18 column at 35°C.

	2-picoline	4-picoline	2-ethylpyridine	4-ethylpyridine
k_s	-0.041	-0.022	-6.01E-03	5.82E-03
k_{us}	0.10	0.115	0.168	0.205
K	0.21	0.166	0.166	0.151
	2,6-dimethylpyridine	3,5-dimethylpyridine	benzylamine	R-methylbenzylamine
k_s	-0.013	1.09E-03	0.014	0.043
k_{us}	0.152	0.188	0.238	0.322
K	0.132	0.156	0.12	0.104

Conditions: Concentration region 1 – 70 mM of perchlorate anion. Column: 15x0.46cm Zorbax XDB-C18; mobile phase: (40:60); Acetonitrile- Aqueous adjusted with perchloric acid and NaClO₄ and/or solely perchloric acid, pH=2.6-2.9, flow rate, 1.0 ml/min; Temp.: 35°C, UV, 254 nm; sample: 1µl injection.

Table 4-VIII

Retention factor and solvation parameters obtained using perchlorate as the counteranion and MeCN/Water (30:70) eluent on Zorbax Eclipse XDB-C18 column at 35°C.

	2-picoline	4-picoline	2-ethylpyridine	4-ethylpyridine
k_s	7.90E-03	0.023	4.50E-02	7.50E-02
k_{us}	0.165	0.19	0.265	0.339
K	0.174	0.155	0.153	0.127
	2,6-dimethylpyridine	3,5-dimethylpyridine	benzylamine	R-methylbenzylamine
k_s	0.034	6.00E-02	0.101	0.16
k_{us}	0.235	0.305	0.43	0.606
K	0.129	0.137	0.107	0.089

Conditions: Concentration region 1 – 70 mM of perchlorate anion. Column: 15x0.46cm Zorbax XDB-C18; mobile phase: (30:70); Acetonitrile- Aqueous adjusted with perchloric acid and NaClO₄ and/or solely perchloric acid, pH=2.6-2.9, flow rate, 1.0 ml/min; Temp.: 35°C, UV, 254 nm; sample: 1µl injection.

Table 4-IX

Retention factor and solvation parameters obtained using perchlorate as the counteranion and MeCN/Water (20:80) eluent on Zorbax Eclipse XDB-C18 column at 35°C.

	2-picoline	4-picoline	2-ethylpyridine	4-ethylpyridine
k_s	7.50E-02	0.099	1.39E-01	2.05E-01
k_{us}	0.267	0.323	0.452	0.642
K	0.149	0.121	0.117	0.098
	2,6-dimethylpyridine	3,5-dimethylpyridine	benzylamine	R-methylbenzylamine
k_s	0.113	1.73E-01	0.306	0.482
k_{us}	0.386	0.558	0.94	1.486
K	0.108	0.106	0.074	0.064

Conditions: Concentration region 1 – 70 mM of perchlorate anion. Column: 15x0.46cm Zorbax XDB-C18; mobile phase: (20:80); Acetonitrile- Aqueous adjusted with perchloric acid and NaClO₄ and/or solely perchloric acid, pH=2.6-2.9, flow rate, 1.0 ml/min; Temp.: 35°C, UV, 254 nm; sample: 1µl injection.

Table 4-X

Retention factor and solvation parameters obtained using perchlorate as the counteranion and MeCN/Water (10:90) eluent on Zorbax Eclipse XDB-C18 column at 35°C.

	2-picoline	4-picoline	2-ethylpyridine	4-ethylpyridine
k_s	1.85E-01	0.195	3.71E-01	5.97E-01
k_{us}	0.51	0.668	1.062	1.784
K	0.089	0.100	0.073	0.059
	2,6-dimethylpyridine	3,5-dimethylpyridine	benzylamine	
k_s	0.271	5.21E-01	0.962	
k_{us}	0.846	1.542	2.892	
K	0.078	0.06	0.057	

Conditions: Concentration region 1 – 70 mM of perchlorate anion. Column: 15x0.46cm Zorbax XDB-C18; mobile phase: (10:90); Acetonitrile- Aqueous adjusted with perchloric acid and NaClO₄ and/or solely perchloric acid, pH=2.6-2.9, flow rate, 1.0 ml/min; Temp.: 35°C, UV, 254 nm; sample: 1µl injection.

Table 4-XI

Retention factor and solvation parameters obtained using perchlorate as the counteranion and MeCN/Water (10:90) eluent on Zorbax Eclipse XDB-C18 column at 25°C.

	2-picoline	4-picoline	2-ethylpyridine	4-ethylpyridine
k_s	6.17E-01	0.688	8.46E-01	1.12E+00
k_{us}	1.17	1.44	2.04	3.205
K	0.1	0.086	0.078	0.068
	2,6-dimethylpyridine	3,5-dimethylpyridine	benzylamine	
k_s	0.731	1.02E+00	1.643	
k_{us}	1.699	2.802	5.236	
K	0.082	0.069	0.066	

Conditions: Concentration region 1 – 70 mM of perchlorate anion. Column: 15x0.46cm Zorbax XDB-C18; mobile phase: (10:90); Acetonitrile- Aqueous adjusted with perchloric acid and NaClO₄ and/or solely perchloric acid, pH=2.6-2.9, flow rate, 1.0 ml/min; Temp.: 25°C, UV, 254 nm; sample: 1µl injection.

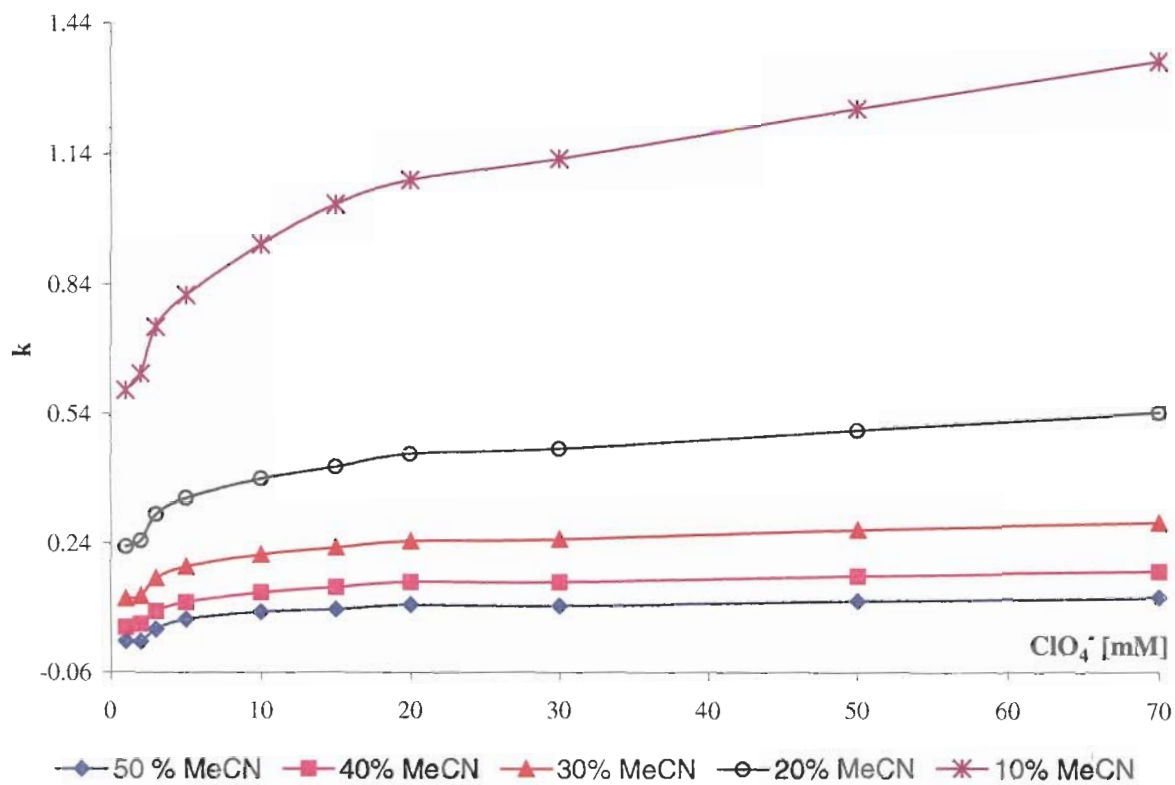


Figure 4-8. Retention factor of 4-ethylpyridine versus concentration at different mobile phase compositions, 45°C. Conditions: Conditions: Concentration region 1 – 70 mM of perchlorate anion. Column: 15x0.46cm Zorbax XDB-C18; mobile phase: Acetonitrile-Aqueous adjusted with perchloric acid and NaClO_4 and/or solely perchloric acid, pH=2.6-2.9, Aqueous content varied from 50 –90%; flow rate, 1.0 ml/min; Temp.: 45°C, UV, 254 nm; sample: 1 μ l injection.

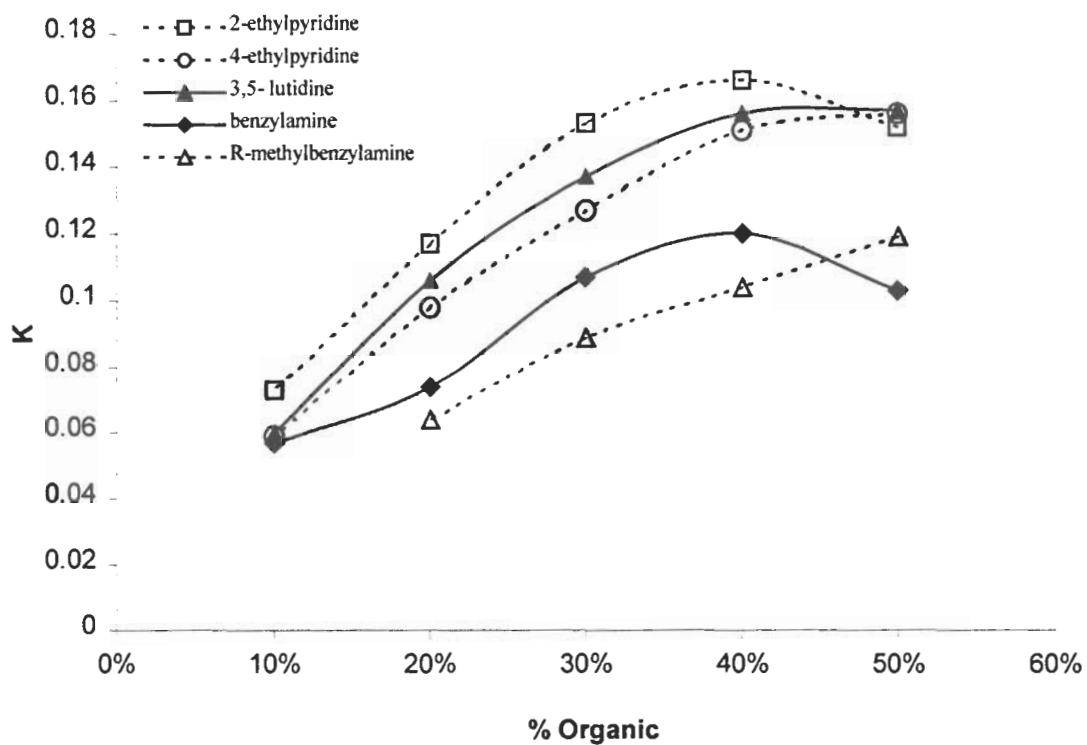


Figure 4-9. Solvation parameter, K , dependence as a function of organic concentration, 35°C. Conditions: Conditions: Concentration region 1 – 70 mM of perchlorate anion. Column: 15x0.46cm Zorbax XDB-C18; mobile phase: Acetonitrile- Aqueous adjusted with perchloric acid and NaClO_4 and/or solely perchloric acid, pH=2.6-2.9, Aqueous content varied from 50 –90%; flow rate, 1.0 ml/min; Temp.: 35°C, UV, 254 nm; sample:1 μ l injection.

Solvation Parameters vs Organic at 45 C

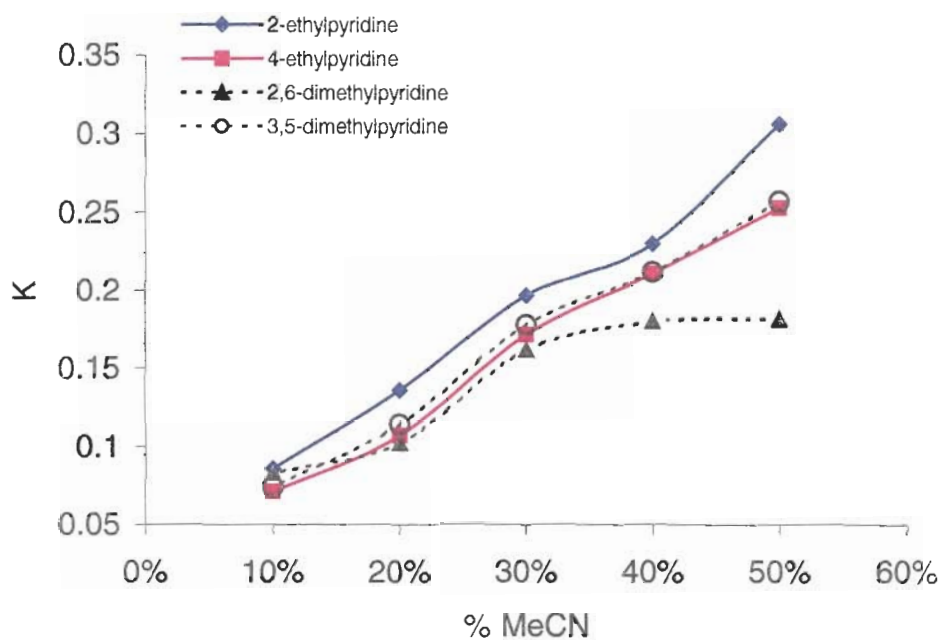


Figure 4-10. Retention factor versus concentration at different mobile phase compositions, 45°C. Conditions: Conditions: Concentration region 1 – 70 mM of perchlorate anion. Column: 15x0.46cm Zorbax XDB-C18; mobile phase: Acetonitrile- Aqueous adjusted with perchloric acid and NaClO₄and/or solely perchloric acid, pH=2.6-2.9, Aqueous content varied from 50 –90%; flow rate, 1.0 ml/min; Temp.: 45°C, UV, 254 nm; sample:1µl injection.

Effect of temperature on the solvation parameter

The structure of water is broken down, as the analyte is desolvated at increasing chaotropic counteranion concentration. As there are progressively greater amount of chaotropic anions in the eluent the disruption of the hydrogen bonding between the water molecules is increased. These counteranions undergo relatively small changes in enthalpic energy during transfer from an aqueous phase to an organic phase^[30]. The energetics of this process may be determined by plotting the $\ln K$ (solvation parameter) versus $1/T$. There should not be any significant dependence of the solvation parameter, $\ln K$, as a function of reciprocal temperature within the concentration range if indeed this is a purely entropic process. The slope of this dependence is $\Delta H/RT$ and the intercept is denoted by $\Delta S/R$. If the slope is zero that concludes that ΔH is zero. $\ln K$ would not be dependent on the enthalpy but solely on the entropic term indicating that the chaotropic process is purely entropically driven.

$$\ln K = \frac{\Delta G^\circ}{RT} = \Delta H - T\Delta S \quad [4-11]$$

$$\ln K = \frac{\Delta H}{RT} - \frac{\Delta S}{R} \quad [4-12]$$

If slope is unchanged $\Delta H = 0$ then $\ln K$ would be dependent solely on the entropy:

$$\ln K = \frac{\Delta S}{R} \quad [4-13]$$

However, at increasing temperatures the dielectric parameter is decreased and this may permit the two oppositely charged species to approach each other at a closer distance and hence lead to a greater disruption of the solvation. It was proposed before that the lower the dielectric parameter the greater the probability that the desolvation process may occur.

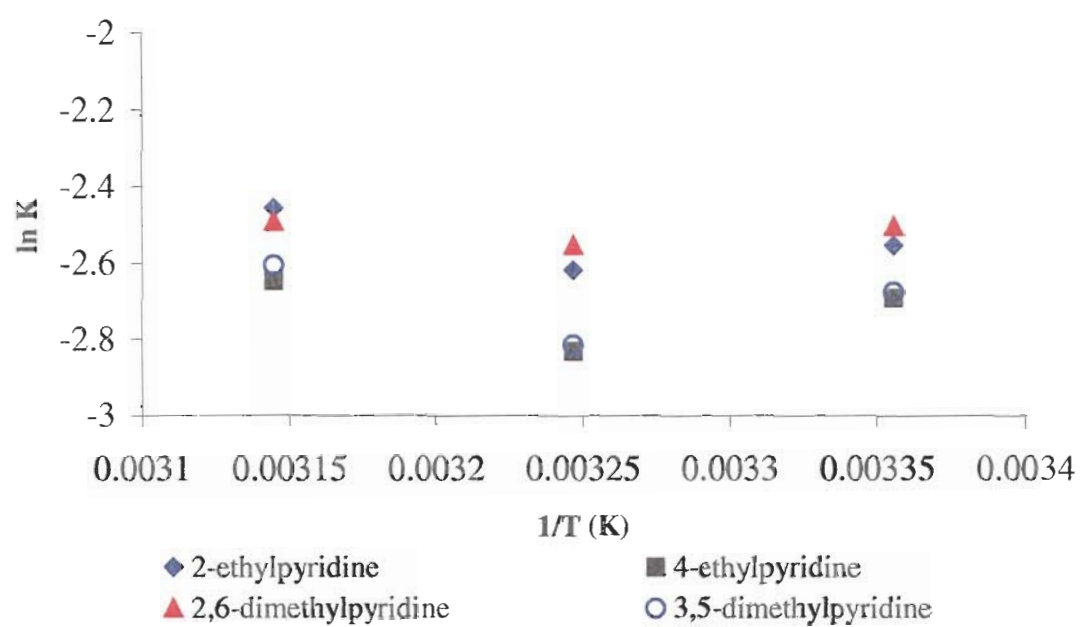


Figure 4-11. Influence of the solvation parameter as a function of inverse temperature.

The preliminary experiments have currently been done only at 25°C, 35°C and 45°C and from the preliminary results we do not see a significant change in the solvation parameter upon decreasing the temperature. These results were obtained at 90% Aqueous :10% MeCN. Similar results were obtained at all other mobile phase composition of MeCN:Water (10-50% MeCN). The solvation parameter at solvent compositions from 10 –50% MeCN is independent of the temperature within the temperature range of 25 – 45°C. In Figure 4-11 $\ln K$ versus inverse temperature are plotted for basic analytes analyzed at 90% aqueous: 10% acetonitrile from 25°C – 45°C. Further studies will be carried out at 5, 10 and 15°C to investigate this phenomenon in depth. We can speculate that indeed the chaotropic process is entropically driven and the influence of the dielectric constant on the solvation parameter is not visible in the studied temperature region.

Effect of pH on the retention of basic analytes using this model

The increase of the retention of the basic analyte should follow the dependence on the concentration described in equation 4-11. This dependence can be attributed to disruption of the protonated analyte solvation. However, if the analyte is not fully protonated, the limiting retention factors for the solvated and unsolvated forms will be higher when compared to the limiting retention factors for a fully protonated analyte. The analyte is not only in equilibrium with the solvation-desolvation process, but also with the ionization process.

This effect was observed when aniline, $pK_a = 4.6$, and N-methylaniline, $pK_a = 4.2$ were analyzed within a pH region (pH 2.6 – pH 2.9) where the analytes were not fully protonated. The pK_a of aniline accounting for the pH shift in 10% MeCN is about 4.3 and that of N-methylaniline is about 3.9. If these analyte were in a 50%aqueous:50% acetonitrile mixture, their estimated apparent pK_a could be taken to be 3.6 for aniline and 3.4 for N-

methylaniline. They would be fully protonated at pH values less than 1.6 and 1.4 respectively. If these analyte were in 90% aqueous:10% acetonitrile mixture their estimated apparent pK_a could be taken to be 4.3 for aniline and 3.9 for N-methylaniline. In the 90%Aqueous:10%MeCN eluent these analytes would be fully protonated at pH values less than 2.3 and 1.9 respectively. Hence, at all studied acetonitrile/water compositions these analytes were not fully protonated.

Figures 4-12 and 4-13 show the retention factor versus concentration of perchlorate anion using different starting mobile phase pH values 2.6 and 2.9 for the analysis of aniline, N-methylaniline and other basic compounds (apparent pK_a values are 4.9 or greater) in both the 10% and 50% hydroorganic mobile phases. It is observed with the 10% MeCN system that the aniline and N-methylaniline do not follow the dependence shown in equation 4-11. However it is observed that lower retention factors were obtained when the pH of the mobile phase was 2.6 versus 2.9. Therefore the analyte decreased its retention due to its protonation and consequent analyte solvation. Theoretically, K , the solvation parameter is the same when different amounts of protonated species are available. Due to lack of data, a good fit could not be obtained using 4-11 for the retention factors versus concentration at pH 2.6 and the corresponding data at pH 2.9. If these points were obtained a plot such as Figure 4-14 may be proposed. Evidently, this was observed solely these two aniline species with (low pK_a) while the retention factors measured for the other basic compounds with higher pK_a 's were independent of the starting pH and solely depend on the concentration of perchlorate as equation 4-11 suggests. This effect was observed at all 5 acetonitrile/water compositions (10-50% acetonitrile).

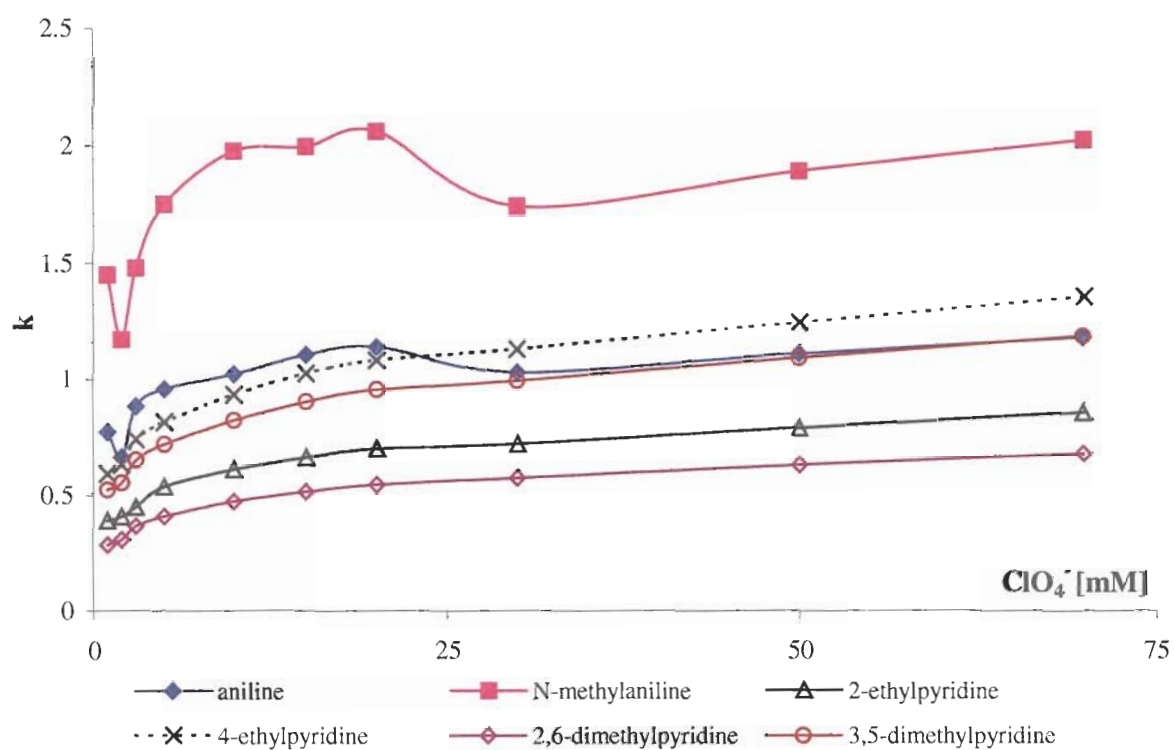


Figure 4-12. Retention factor versus concentration of perchlorate. Conditions: Zorbax Eclipse XDB-C₁₈, Temp.; 45 °C, Eluent: 90% Aqueous adjusted with HClO₄ and NaClO₄, conc. 1 – 70 mM, pH=2.6 –2.9, 10% acetonitrile . Note that concentrations 2mM, 30 mM, 50 mM, 70 mM were adjusted to pH 2.6 with perchloric acid and all the rest of the concentrations were adjusted to pH 2.9 with perchloric acid.

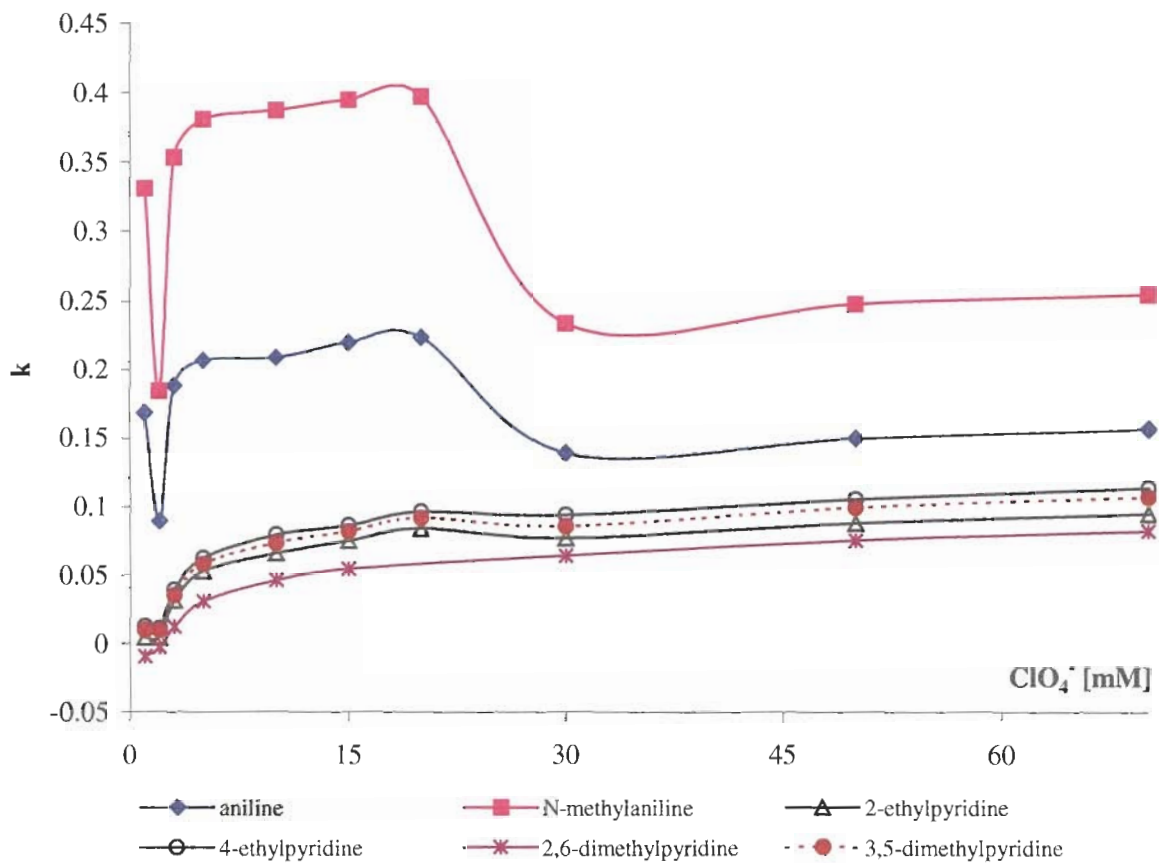


Figure 4-13. Retention factor of basic compounds versus concentration of perchlorate. Conditions: Zorbax Eclipse XDB-C₁₈, Temp.; 45 °C, Eluent: 50% Aqueous adjusted with HClO₄ and NaClO₄, conc. 1 – 70 mM, pH=2.6 –2.9, 50% acetonitrile. Note that concentrations 2mM, 30 mM, 50 mM, 70 mM were adjusted to pH 2.6 with perchloric acid and all the rest of the concentrations were adjusted to pH 2.9 with perchloric acid.

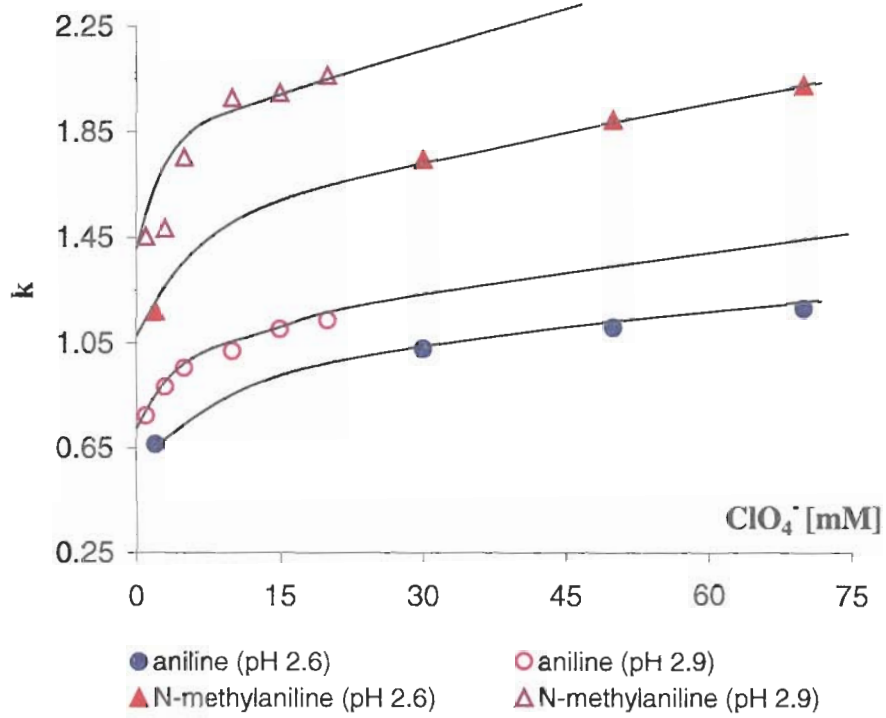


Figure 4-14. Retention factor of aniline and N-methylaniline versus concentration at two pHs: 2.6 and 2.9. Conditions are identical to those in Figure 4-12.

The elution order of the basic components changed upon increase of acetonitrile content in the eluent, Figures 4-12 and 4-13. The difference in the retention dependencies for the aniline and N-methylaniline species at the two pHs is observed in Figures 4-12 and 4-13.

This can be attributed to the greater shift in the pH of the mobile phase upon increased addition of organic modifier. Hence at 50% acetonitrile with mobile phase pHs of the aqueous phase of 2.6 and 2.9, i.e. aniline (apparent pK_a , 2.3) is less protonated than at lower acetonitrile content 10%. Typically in reversed phase HPLC (describing retention using the partitioning model) as the organic modifier concentration is increased we do not expect to observe a change in the selectivity of the components and expect a consequent decrease in retention having the same elution order at 10% versus 50%. However, as the concentration of the organic modifier was increased, the reversal of elution order between aniline and 4-ethylpyridine becomes apparent. Note this effect is due to the pH shift of the aqueous phase in the hydroorganic mixture.

Effect of type and organic composition at different concentrations of perchlorate anion

Generally, as the elution strength of the mobile phase is becoming stronger the decrease in retention should decrease linearly when $\ln K$ is plotted versus organic concentration if one assumes partitioning or adsorption as the dominant retention mechanism^[31-32]. However, if this is not occurring deviations from the linearity can be attributed to some other retention determining process. Figures 4-15 – 4-17 show the retention dependence as a function of acetonitrile composition at the different concentrations of perchlorate ion employed. As the acetonitrile content is increased, there is a deviation from this linearity at around 30% acetonitrile for the lower concentrations of perchlorate anion. It has been shown that there is an adsorbed acetonitrile layer on top of the bonded

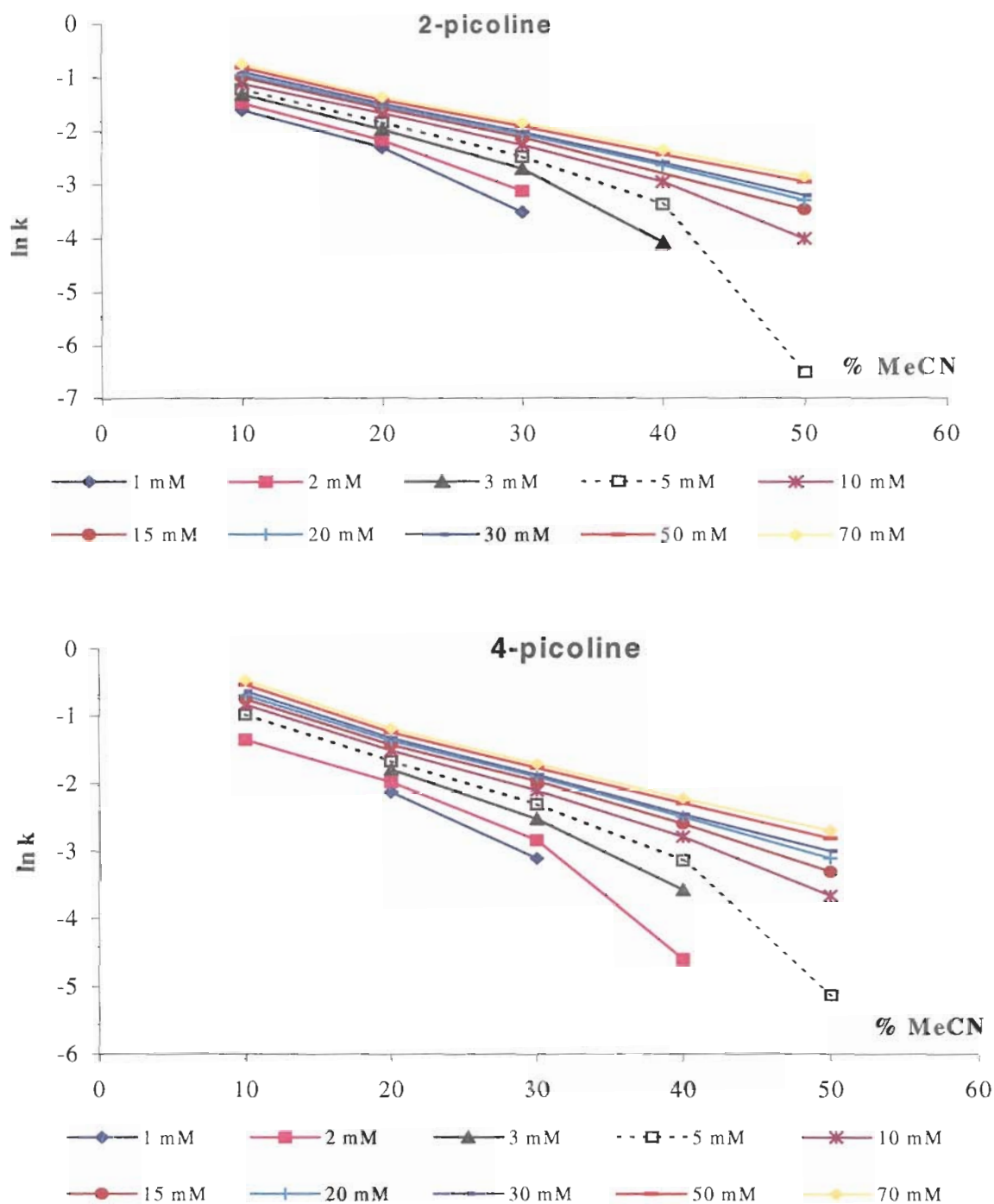


Figure 4-15. Effect of acetonitrile content on the retention of 2-picoline and 4-picoline at varying perchlorate concentrations. Conditions: Concentration region 1 – 70 mM of perchlorate anion. Column: 15x0.46cm Zorbax XDB-C18; mobile phase: Acetonitrile-Aqueous adjusted with perchloric acid and NaClO₄ and/or solely perchloric acid, pH=2.6-2.9, Aqueous content varied from 50 –90%; flow rate, 1.0 ml/min; Temp.: 35°C, UV, 254 nm; sample: 1µl injection.

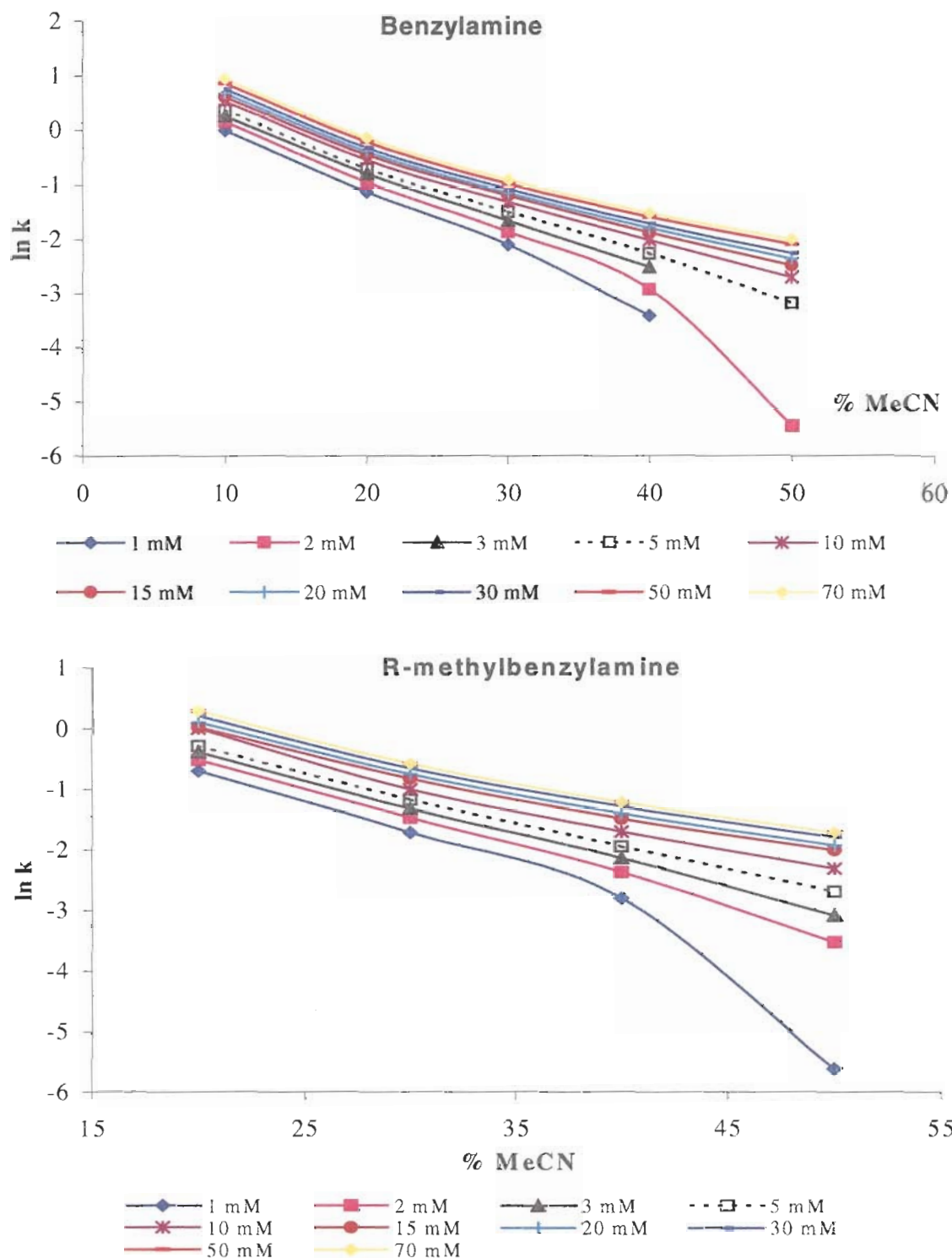


Figure 4-16. Effect of acetonitrile content on the retention of benzylamine and R-methylbenzylamine at varying perchlorate concentrations. Conditions as in Figure 4-15.

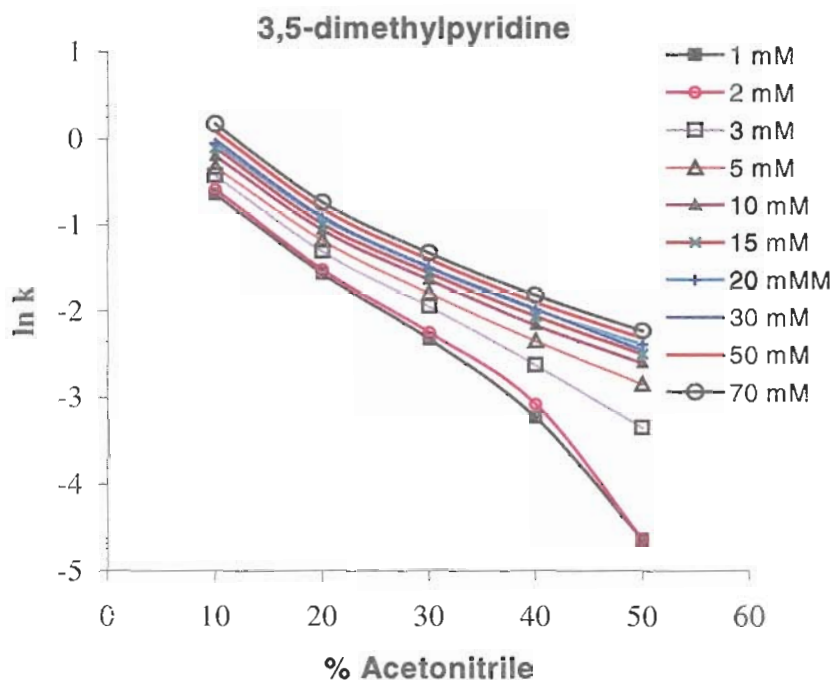
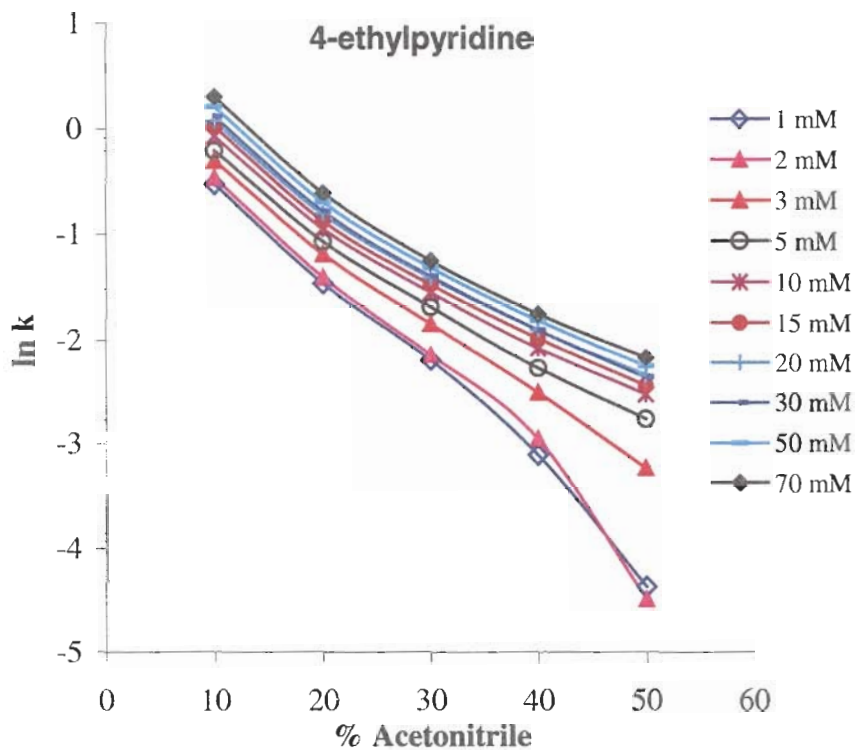


Figure 4-17. Effect of acetonitrile content on the retention of 4-ethylpyridine, and 3,5-dimethylpyridine at varying perchlorate concentrations. Conditions as in Figure 4-15 except temperature is 45°C.

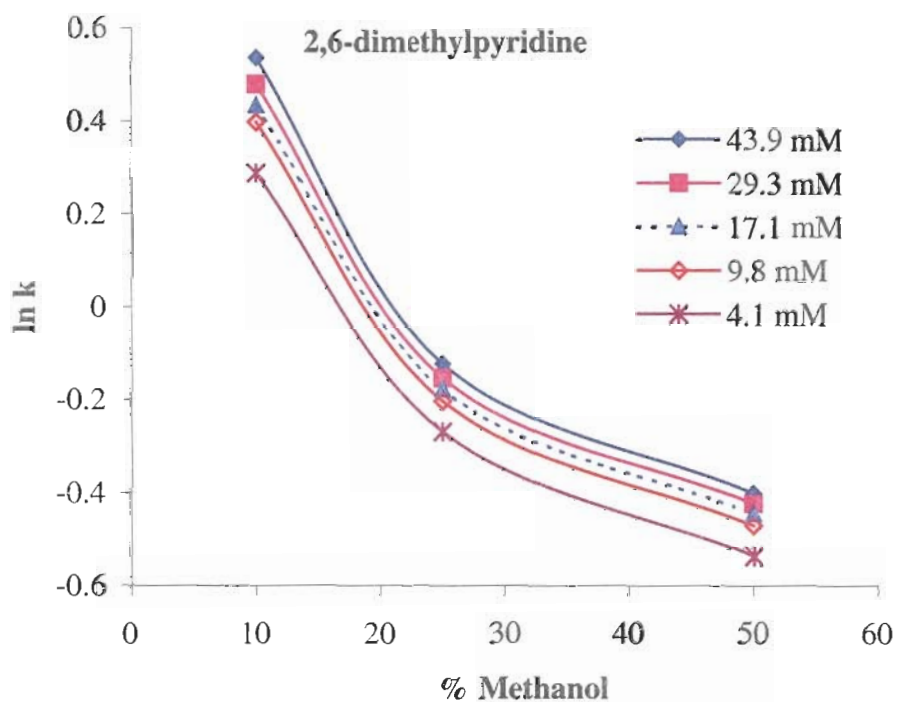
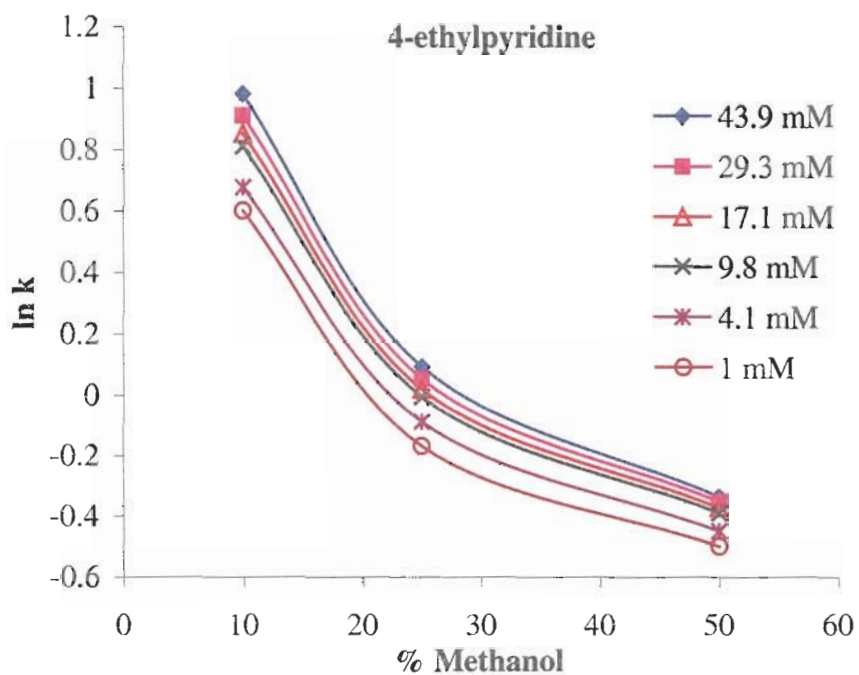


Figure 4-18. Effect of methanol content on the retention of basic analytes at varying perchlorate concentrations. Conditions: Concentration region 4 – 44 mM of perchlorate anion. Column: 15x0.46cm Zorbax XDB-C18; mobile phase: Methanol- Aqueous adjusted with perchloric acid and NaClO₄ and/or solely perchloric acid, pH=2.6-2.9, Aqueous content varied from 50 –90%; flow rate, 1.0 ml/min; Temp.: 45°C, UV, 254 nm; sample: 1µl injection.

phase and this might suggest a complex retention process. This layer has been shown to increase upon increasing the acetonitrile content from 10% acetonitrile to 50% acetonitrile. (Further discussion in Chapter 5). This layer is at its maximum at 50% acetonitrile and has a thickness approximately of 12 Å. If this is occurring then the partition of the ion-associated complex and/or ions will be effected. It can be proposed that at the lower perchlorate concentrations where the analyte is more solvated, it has a lower partition coefficient and hence its retention will be decreased. Figures 4-18 show the retention dependence as a function of methanol composition at the different concentrations of perchlorate employed. In these plots, it is evident that at all the concentrations employed and at the various organic compositions the retention factor was effected to the same degree. Methanol does also show some adsorption on the bonded phase but it is only monomolecular adsorption. The layer does not have a sufficient thickness to support partitioning of the solutes. Therefore, it is evident, that the determination of this adsorbed organic layer is required for the accurate description of reversed phase processes.

Conclusion

Chromatographic experiments performed at different counteranion concentrations allowed the description of the protonated basic analyte desolvation process. Performing the experiments at different MeCN/water compositions indicated that upon increasing the acetonitrile composition that the organic solvent aided in the desolvation process. Temperature studies also indicated that the chaotropic process is entropically driven. Other studies showed that even if the basic analyte is not fully protonated that the desolvation process occurs and that the limiting retention factors for the unsolvated and solvated analytes are greater than the basic analytes in their fully protonated form. We also showed that at

different organic/water compositions for correct comparison of the retention dependencies and determination of the basic analyte ionization state that the effect of the organic eluent on the resulting eluent pH must be accounted for.

Literature Cited

Chapter 4

1. Y. Marcus, *J.Chem.Soc., Faraday Trans.*, **85**, **1989**, 381
2. A.J. Easteal, and L.A. Woolk, *J.Chem.Thermodyn.*, **20**, **1988**, 693
3. Y. Marcus, *Pure Appl. Chem.*, **58**, **1986**, 1721
4. Y. Marcus, and Y. Migron, *J.Phys.Chem.*, **95**, **1991**, 400
5. J. Barbosa, D. Barron, R. Berges, V. Sanz-Nebot, and I. Toro, *J.Chem.Soc., Faraday Trans.*, **93** (10), **1997**, 1915
6. J. Barbosa, R. Berges, I. Toro, V. Sanz-Nebot, *International Journal of Pharmaceutics*, **149**, **1997**, 213
7. J. Barbosa, and V. Sanz-Nebot, *J.Chem.Soc., Faraday Trans.*, **90** (21), **1994**, 3287
8. E. Bosch, C. Rafols, M. Roses, *Anal. Chim. Acta*, **1995**, 302, 109
9. M.I. Davies, *Thermochim. Acta*, **63**, **1983**, 67
10. A.J. Easteal, *Aust. J. Chem.*, **32**, **1979**, 1379
11. T. Krygowsky, P.K. Wrona, U. Zielkowska, C.Reichardt, *Tetrahedron*, **41** **1985**, 4519
12. W.J. Dunn, III, P.I. Nagy, *J.Phys.Chem.* **94**, **1990**, 2099
13. K. Subbaragaiah, N.M. Murthy, S.V. Subrahmanyam, *J. Chem. Soc., Faraday Trans.* **78**, **1982**, 165
14. D.A. Armitage, M.J. Blandamer, M.J. Foster, N.J. Hidden, K.W. Morcom, M.C.R. Symons, M. Wooten, *J. Trans. Faraday Soc.*, **64**, **1968**, 1193
15. M.J. Blandamer, N.J. Blundell, J. Burgess, H.J. Cowless, I.M. Horn, *J.Chem.Soc., Faraday Trans.* **86**, **1990**, 277
16. S. Balakrishnan, A.J. Easteal, *Aust. J. Chem.* **34**, **1981**, 943
17. M.J. Blandamer, J. Burgess, B.C. Clark, P.P. Duce, J.M. Scott, *J.Chem.Soc., Faraday Trans. I*, **80**, **1984**, 739
18. C. Moreau, G. Douheret, *Thermochim. Acta* **13**, **1975**, 385
19. A.J. Easteal, *Aust. J. Chem.* **33**, **1980**, 1667

20. H.G. Hertz, H.Z. Leiter, *Phys. Chem.*, Wiesbaden, 133, 1982, 45
21. H. Leiter, C. Albayrak, H.G. Hertz, *J. Mol. Liq.* 27, 1984, 211
22. M.I. Davis, G. Douheret, *Thermochim. Acta* 104, 1986, 203
23. C. Moreau, G. Douheret, *J. Chim. Phys.* 71, 1974, 1313
24. Y. Migron, Y. Marcus *J. Chem. Soc. Faraday Trans.*, 87, 1991, 1339
25. I. Langmuir, *J.Chem.Soc.* 40, 1918, 1361
26. J.J. Kirkland, J.W. Henderson, J.J. DeStefano, M.A. van Straten, H.A. Claessens, *J.Chromatogr.A*, 762, 1997, 97
27. J.J. Kirkland, M.A. van Straten, H.A. Claessens, *J.Chromatogr.A*, 797, 1998, 111
28. Y.V. Kazakevich , H.M. McNair.. *J. Chromatogr. Sci.*, 31, 1993, 317
29. E.H. Slaats, W. Markovski, J. Fekete, H. Poppe, *J.Chromatogr.*, 207, 1981, 299
30. Y. Hatefi, W.G. Hanstein, *Proc. Natil. Acad. Sci. U.S.A*, 62, 1969, 1129
31. M.Jaroniec, *J.Chromatogr. A*, 656, 1993, 37-50
32. A.Vailaya, Cs. Horvath *J.Chromatogr. A*, 829, 1998, 1-27

Chapter 5

Geometry of Chemically Modified Silica and its relation to retention mechanism in reversed phase HPLC

Summary

The goal of this chapter is to study the effect of alkylsiloxylation on the surface area and pore size distribution as well as the interparticle, pore, and void volumes of silica based HPLC packing materials. Correlation of the decrease of the pore volume with the increase of the modifier chain length was found. The determination of the conformation of the bonded layer is discussed. The organic components of commonly used eluent systems including THF, acetonitrile, and methanol of reversed phase HPLC have been shown to exhibit excessive specific interactions with hydrophobic stationary phases. These interactions cause the accumulation (excess adsorption) of the organic solvent on the adsorbent surface. We determined these excess adsorption isotherms and void volumes for over 20 columns packed with adsorbents modified with different chain lengths and bonding densities.

Existence of the liquid adsorbed phase of different composition than the eluent suggests a complex retention mechanism for analytes in RP HPLC columns. suggests that the classical adsorption and partitioning models may not hold true for the retention of analytes in the reversed phase mode. On the basis of our results, it is suggested that analytes partition from the binary eluent into the adsorbed organic liquid phase, followed by adsorption on the hydrophobic surface of bonded alkyl chains.

Introduction

The analysis of basic compounds by HPLC especially under reversed phase conditions; over the years have been characterized by long and variable retention times, poor efficiency of separation and excessive peak tailing. Many of the strategies that have been used to control these effects, are ion-pair and ion-suppression chromatography. The peak shapes generally have been improved by using tertiary and quaternary amines as silanol blockers, by using electrostatically shielded stationary phases, or by decreasing ionization of the basic samples. Those so-called silanol blockers were thought to act as competitors for the active sites that caused chromatographic problems. The underlying problem still to this day is attributed to some form of interaction with unbounded silanol groups that remain on the silica surface after bonding ^[1]. It is assumed that at least part of this interaction is ionic in nature. The silica surface of an alkyl modified adsorbent could act as a weak cation exchanger for aromatic bases over a very wide range of organic solvent concentrations ^[2-3]. In order to study the phenomena of the interaction of basic compounds on a reversed phase support it is clearly necessary to first study the silica surface and the geometric parameters of the modified silicas.

Silica

Silica is the most widely used normal phase packing that is commercially available. It is available in various forms having standard particle sizes ranging from 3 to 10 μm and surface areas from 200 to 500 m^2/g ^[4]. It is classified as an acidic adsorbent since its surface consists of acidic hydroxyl groups that are covalently bound to the Si atoms. Silica contains weak Brønsted acidic sites and does not contain any Lewis acid sites.

The silica gel surface is heterogeneous and consists of siloxane and silanol groups [5]. The active silanol groups on the surface are electron acceptors and can form hydrogen bonds with polar or unsaturated molecules. Silanols exist in several forms: single (isolated or free), geminal, bound and reactive surface hydroxyls (vicinal). Free silanols contain a Si atom that has three bonds in the bulk structure and a fourth bond attached to a single OH group. Geminal silanols contain two hydroxyl groups that are attached to one silicon atom. A bound hydroxyl is denoted as hydrogen bound surface hydroxyl. The bound hydroxyl is bound to two silica atoms and does not have any free hydrogens. The reactive surface hydroxyls have two hydroxyl groups attached to two different silicon atoms. One hydroxyl group contains a bound hydrogen and the other hydroxyl group contains a free hydrogen.

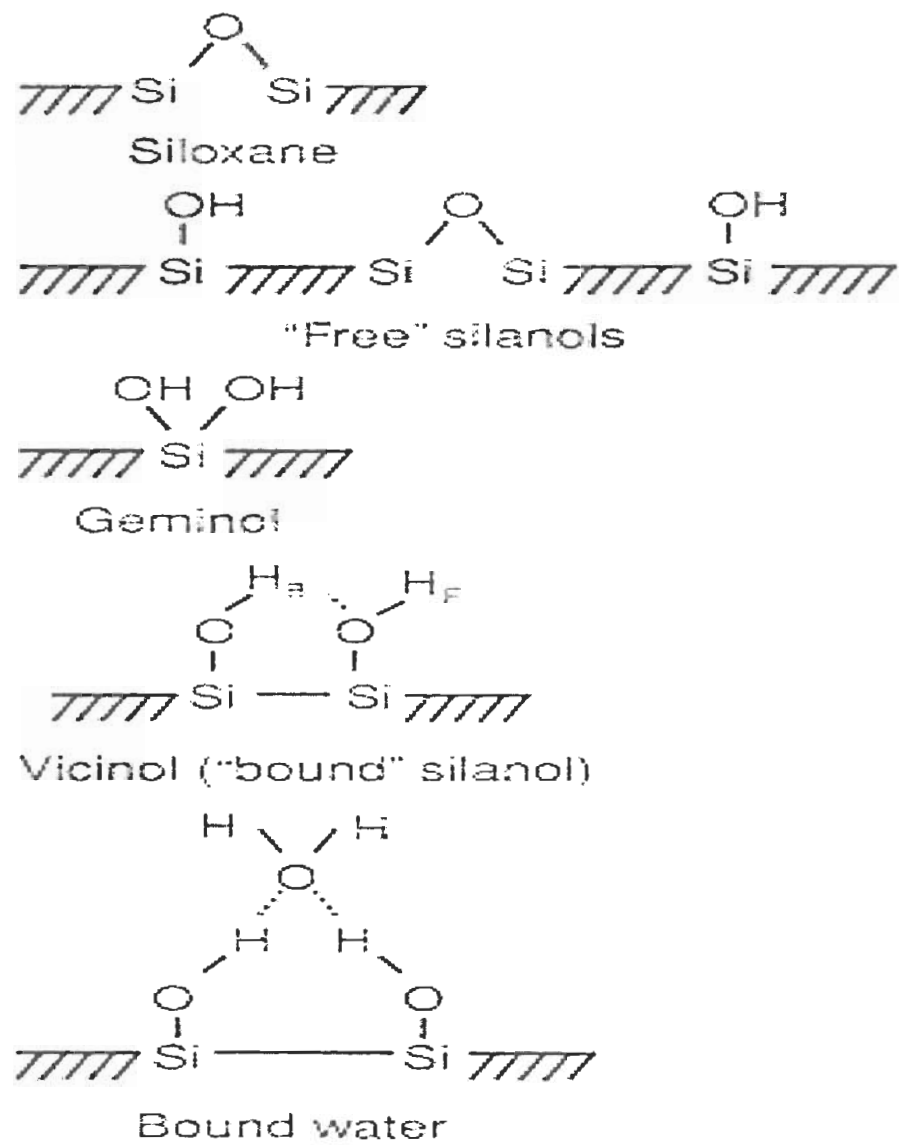


Figure 5-1. Active surface groups on silica gel. ^[6]
 H_B indicates bound hydrogen; H_F indicates free hydrogen.

Among all hydroxyls formed, the reactive surface hydroxyls are believed to have the greatest relative strength as adsorption sites ^[4]. At higher temperatures (200- 400°C), surface siloxane groups are formed from the condensation of reactive and geminal silanols and decomposition of free silanols.

The geometric properties of silica also play a role on the retention of analytes, since they vary the surface activity. Since the silica surface is heterogeneous, different silica gels have varied surface hydroxyls, and therefore their concentrations can be different in pores of different dimensions. Generally, the smaller the pore diameter the higher the surface area of the corresponding silica. It also has been shown that higher concentrations of reactive and bound hydroxyls are present in smaller pore silicas, typically with a pore diameter less than 100 Å, whereas free hydroxyls predominate on large pore silicas having pore diameters greater than 150Å ^[7].

Silica may have different amounts of adsorbed water on the surface, which decreases the activity of the silica since the water blocks the underlying surface. If the silica is heated to between 150°C and 250°C the water may then be removed without the loss of surface hydroxyls and therefore the silica retains maximum activity ^[8]. Water is selectively adsorbed onto reactive hydroxyls and since the concentration of the reactive hydroxyls is greater in small pore silicas there is a large deactivation effect, consequently leaving a surface of bound hydroxyls. Deactivation of the large pore silicas generally leaves mostly free hydroxyls. Therefore, heavily deactivated large pore silicas when compared to small pore silicas have a higher surface activity due to the presence of free hydroxyls versus bound hydroxyls ^[4].

The silica may also be contaminated by metal impurities such as aluminum, nickel and iron depending upon the synthesis of the silica or the manufacturing process. These metals may be present in silica backbone either in the form of oxides, hydrous oxides or through oxygen bonds attached to the Si metal atom ^[9]. The metal impurities may also have an effect upon the chromatography causing peak tailing due to complexation with the trace metal impurities. The acidity of the surface silanols is increased with the presence of these metal impurities. Depending upon the pH of the silica, metal ions can exist in either non-hydrated or hydrated forms.

Chemically Modified Phases

The introduction of chemically modified phases has made a tremendous impact in liquid chromatography. Developments and improvements in the technology to form reproducible bonded layers have revolutionized these techniques. Stationary phases based on porous silicas have been chemically modified with ligands of various chemical nature and size. The bonded layer can be considered as a hydrocarbon entity of a certain thickness, and the total content of the bonded organic material can be varied by changing the alkyl group length, the specific surface area of the silica, and the bonding density.

Since the introduction of chemically bonded reversed phase packings, the separation mechanism has been a subject of great controversy. The solute interaction in reversed phase chromatography has been considered to proceed by two different limiting mechanisms: partitioning ^[10-13] and adsorption ^[10,14]. Partitioning was ascribed as the solute distribution between the mobile phase and the bonded phase. Adsorption mechanism was assumed as adsorption of solutes on the hydrocarbon surface layer.

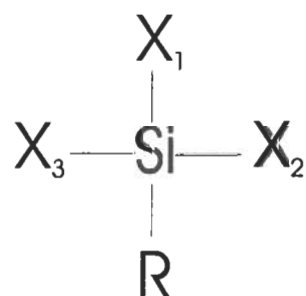
Some authors consider the mechanism to be a mixture of adsorption and partition ^[14]. To complicate matters further, it is possible that when the eluent is a mixed solvent, the less polar component could accumulate near the apolar surface of the stationary phase and form an essentially stagnant layer of that more non-polar liquid. As a result, solutes could partition between this adsorbed layer on top of the stationary phase and the bulk mobile phase ^[15].

Therefore, this suggests a complex retention mechanism involving liquid-liquid partitioning followed by adsorption. The biggest problem in distinguishing between these mechanisms is that the surface topology is not clearly defined. In order to elucidate the distinction between both mechanisms, the bonded layer structure will be discussed. In this chapter we also will give a description of both mechanisms as well as a “partition-adsorption” mechanism.

Stationary Phases and Properties

Bonded Phases

The chemical structure of silanizing agents employed in the preparation of alkyl bonded phases for RPLC can be represented by the general formula (1).



Where R is the alkyl chain of interest. One of the substituents X₁, X₂, X₃ must be a reactive group such as chloro or methoxy in order to react with an active hydroxyl on the

silica surface. However, all three may be reactive, as is the case with a trichlorosilane. The area of organosilicon chemistry over the last 40 years has received much attention with the development of a variety of bonded phases using various mono, di and tri alkylchlorosilanes ^[16].

Silane derivatives that have only one reactive group react with the surface silanol groups where X_1 and X_2 are methyl groups, X_3 is a chloro group, and the R group may be $C_1 - C_{18}$. This is called monofunctional or monomeric bonding. The most popular are the C_8 and C_{18} bonded phases. The reaction is represented as follows in Figure 5-2.

However, when X_1 and X_2 is a chloro group it may also react with adjacent silanols on the surface. On the other hand due to steric limitations not all Si-Cl bonds of di or trisilane will react with the silica surface. If so, these unreacted Si-Cl will be converted to Si-OH when the packing is exposed to the atmosphere, additional silanols may be created, and even more silanols may remain on the surface unreacted. These silanols may give rise to a chemical reaction with sample or mobile phase components, especially with ionizable basic solutes. Therefore, the goal is to achieve the maximum surface coverage with the alkyl ligands. The rationale is that by increasing the phase surface coverage, a greater percentage of the silica silanols are either chemically modified or made inaccessible to interaction with the solutes, and the peak tailing that is generally seen with the basic compounds, may be reduced.

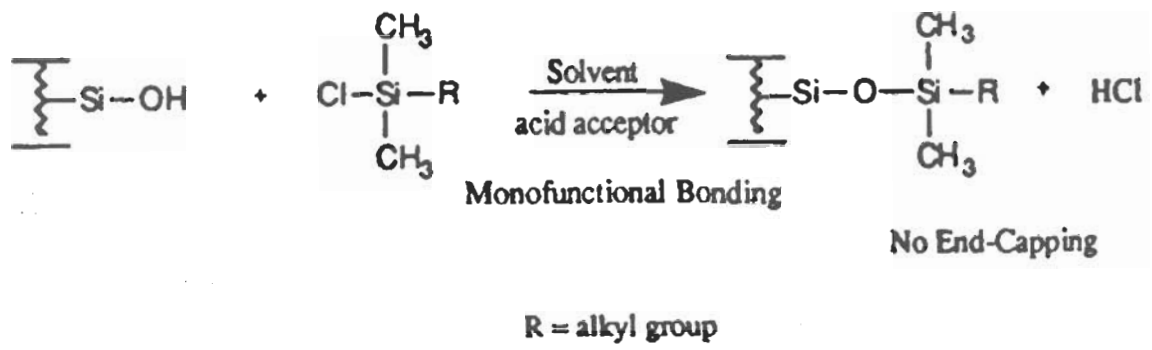


Figure 5-2. Reaction scheme of monofunctional bonding of ligands to the silica surface^[17]

The surface coverage is usually reported in units of $\mu\text{mol}/\text{m}^2$ or ligands/ nm^2 . Berendsen and de Galan ^[18] derived expressions for the calculation of surface coverage values accounting for the weight increase of silica due to the attachment of the ligands and the loss of hydrogen in the silanzation reaction.

$$N = \frac{10^6 P_c}{1200 n_c - P_c (M - 1)} \cdot \frac{1}{S} \quad [5-1]$$

where P_c is the percent carbon loading of the bonded phase, n_c is the number of carbon atoms in the silane reagent, S is the surface area of the native silica, and M is the molecular weight of the bonded silane ligand. The extent to which the surface is modified is dependent upon the reaction conditions as well as the physical and chemical properties of the substrate and silane reagent. The surface silanol concentration is typically taken to be $8 \mu\text{mol}/\text{m}^2$ (4.8 silanols per square nanometer). However, due to steric constraints, about only one half of these groups can be chemically modified because the attached ligands may shield the neighboring unbounded silanols from reaction. The limit is also affected by silane functionality, reactivity, and size. For example small reactive silanes such as trimethylchlorosilane provide higher surface coverages compared to dimethyloctadecylchlorosilanes. Most of the coverages reported in the literature are typically less than $4 \mu\text{mol}/\text{m}^2$ and are generally prepared from dimethyl-monochlorosilanes ^[19].

This may be associated with the different mechanisms of coverage of the surface with the modifier ^[20]: statistical (random) coverage, where modifiers bond independently of each other, island like coverage, where a bonded ligand favors the attachment of

another ligand within close vicinity, and uniform (homogenous) coverage. The properties of the adsorbent will differ depending on the type of distribution, both at low and high degrees of surface coverage. There has been no direct explanation for these effects. Possible explanation for the different coverages of a surface with a modifier may be associated with the energetic non-uniformity of the surface or the variations of the concentrations of silanol groups at different regions of the surface. The bonding density also depends on the alkyl chain length if small pore size silicas are used. The decrease of the bonding density with decreasing average pore diameter of the silica support is attributed to the steric hindrance, which prevents a free arrangement of long alkyl chains within the pores of small diameter. The bonding density depends on the ratio of the pore size and the length of the modifier alkyl chain^[18,21-22]. The explanation for this phenomenon is illustrated in Figure 5-3. The surface coverage of the short alkyl chains such as RP-3 is limited by the steric hindrance of the methyl groups attached to the silane silicon atom. However, as the alkyl chain length increases, the curvature of the silica surface becomes more important and the surface coverage is limited by the steric hindrance of the terminal ends of the alkyl chains. Berendsen^[18] stated “the decrease in coverage is not determined by the available BET-surface area of the bare silica support, but by the area at the point where the bonded chains end.” This leads to smaller surface coverage values on smaller pore size silicas as opposed to wider pore silicas.

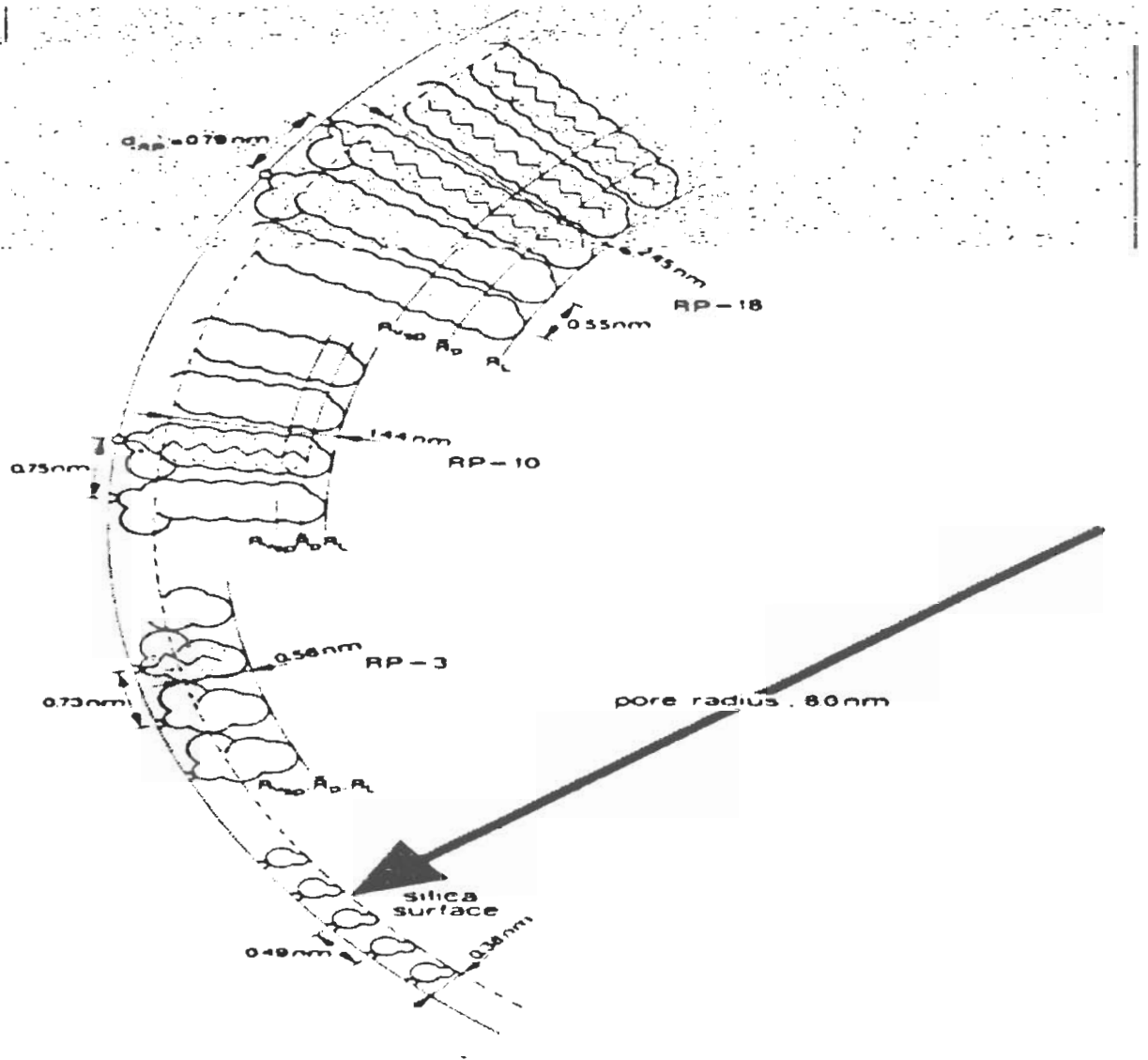


Figure 5-3. Pore model for bonded phases illustrating the steric hindrance effect originating from pore curvature and phase length [18]

The elucidation of the structure of the bonded phase is an area of great controversy. Chromatographic characterization of chemically bonded phases is valuable in predicting the bulk properties of the LC columns but minimal information may be obtained about the immobilized ligands. The investigation of the bonded layer structure has been done by a variety of spectral techniques including infrared and fluorescence spectroscopy, small angle neutron scattering and NMR, but have led to different conformation of the bonded phases. Another area of debate is the effect on the conformation of the bonded layer upon exposure to organic solvents. It has been suggested that permeation of the eluent components into the bonded layer and additional structuring of the layer in comparison to dry samples does occur and has been observed by IR ^[23] and NMR ^[24-28] spectroscopy. Small angle neutron scattering measurements have shown that the C₈ monomeric phases have a thickness of 7Å - 13Å and C₁₈ monomeric phases have a thickness of 14Å - 20Å ^[29]. Since, it is assumed there is possible penetration of the eluent components many models of the bulk structure of the bonded layer have been envisioned. We will phenomenologically describe some of the more popular bulk conformational structures that have been adapted.

The bonded phase covalently attached to the underlying silica surface has been envisioned as a picket fence, molecular fur (brush type), “stacked”, and completely collapsed. The molecular conformation of the phase has been attributed to many factors such as the pore size, alkyl chain length, and the type of solvent the bonded phase is exposed to.

Picket fence

In the “picket fence” or brush type the bonded layer is composed of a very dense layer of the alkyl chains. The adsorption of the analytes would occur only at the top of the alkyl bonded layer. In this view of a very dense arrangement of alkyl chains, the elute molecules would not be able to penetrate into the bonded layer, and hence the effect of silanol groups on the chromatographic retention of analytes would be minimal. Also this would suggest the stationary phase accessible to the solute would be very similar for alkyl ligands of different chain lengths. Also the surface area and the pore volume would decrease upon increasing the chain length of the ligands using the same reference silica support. This would also mean that the commonly used phase ratio (volume of stationary phase/volume of mobile phase) would not change significantly as the carbon number of the alkyl functions is increased. The surface concentration of the alkyl ligands is usually no more than $4 \mu\text{mol}/\text{m}^2$. This value is much smaller than the surface concentration of silanols on the surface before bonding that is typically taken as $8 \mu\text{mol}/\text{m}^2$. Therefore, this picket fence configuration observed in Figure 5-4 is unlikely due to the low surface concentration of the ligates. Retention in reversed phase is believed to be governed solely by the adsorption mechanism when the density of bonded nonpolar functions is high enough for the chains to interact laterally among themselves and to disallow penetration of the solutes into the hydrocarbon layer at the chromatographic surface^[14].

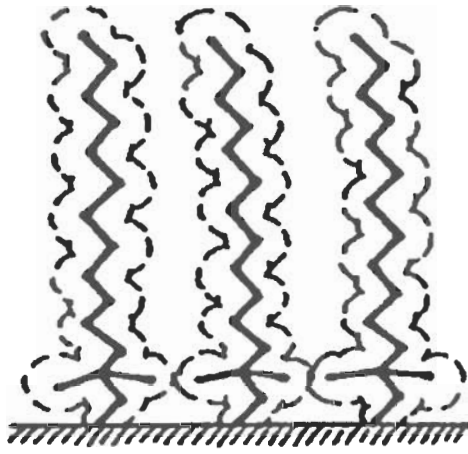


Figure 5-4. Schematic of the "Picket fence" conformation ^[30]

Solvated Hydrocarbon chains models

Depending on the nature of the eluent, it is proposed that two extreme stationary phase configurations are possible fur and “stacked” [14]. The discussion regarding these models describes retention in reversed phase chromatography and does not address a distinction between the adsorption or partition mechanisms. One configuration known as the “fur “ type implies that the distance between the alkyl chains perpendicular to the surface is such that certain solute molecules may actually be able to partition in between and bind to the chains laterally. The phase ratio in the “fur” phase would in essence be larger than that of the “picket fence” phase of the same bonded ligand since the accessible surface area would be greater due to the increased availability of space between the chains for the solutes, as well as for mobile phase components. The penetration of the organic solvent of the eluent in between the chains is denoting the solvation of the bonded layer, which is also another area of great controversy, as will be discussed later. Therefore, a linear increase in the phase ratio would be expected after increasing the chain length in this “fur” type bonded phase, assuming a constant bonding density. However, this is usually not the case, since the bonding density is usually higher for smaller alkyl ligands bonded to the same reference silica. This may be attributed to steric effects of the pore size and the ability to bond the same number of ligands of different chain lengths per unit surface area. Typically the bonded phase is thought to be in this fur conformation if the alkyl chains are able to be wetted or solvated by the organic eluent components. The retention according to the partition model in RPC occurs by penetration of the solute molecules within the interligate space; its interaction with the lateral surface of the ligates; or its association with the tips of the bonded chains or both.

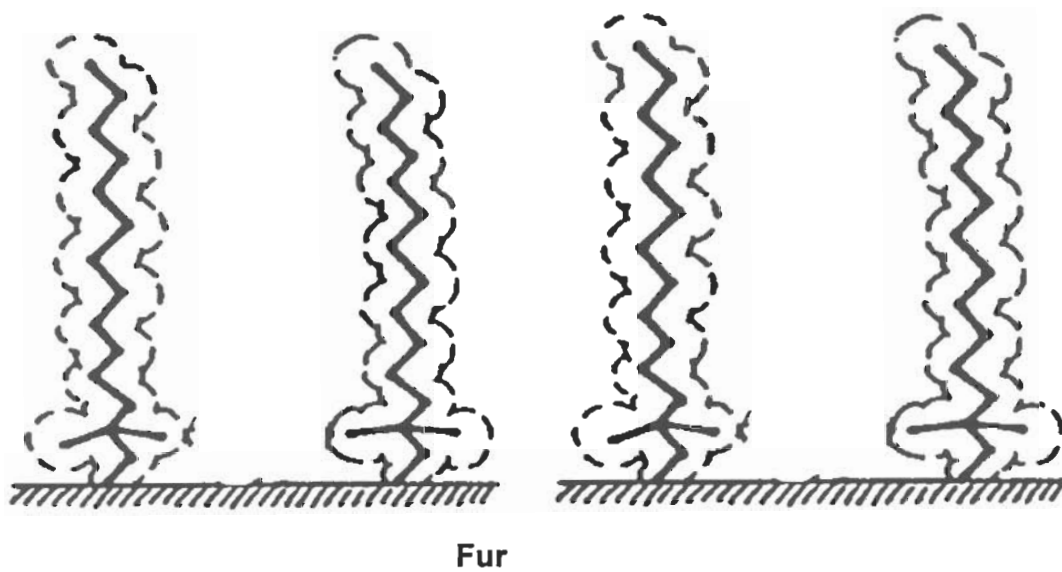


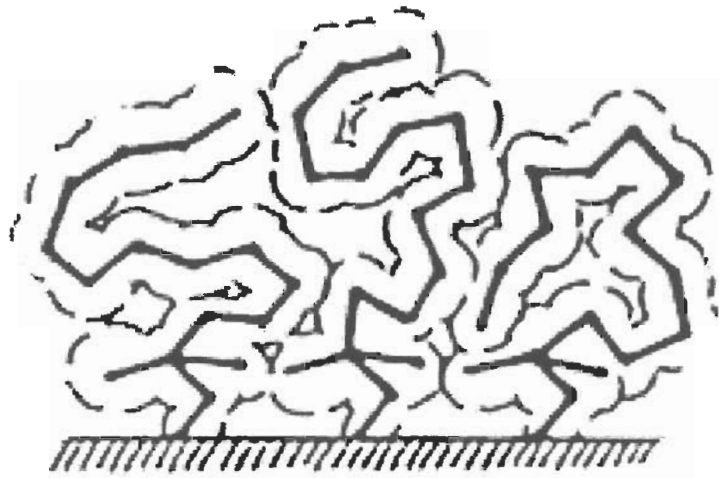
Figure 5-5. Schematic of the “fur” conformation of the stationary phase ^[30]

The “stack structure” assumes that the alkyl chains are not perpendicular to the surface and actually are self interacting with each other. The bonded layer is assumed to be in this configuration when the bonded layer comes in contact with a mobile phase that is incapable of solvating the ligands such as an aqueous phase. The hydrophobic association of the alkyl chains would be more energetically favorable than solvation with the more polar mobile phase. Many authors suggest that the configuration of the bonded layer is dependent upon the nature of the mobile phase indicating that the bonded layer is in the fur configuration at high organic compositions and is in the stacked configuration at high aqueous compositions. It was stated by Valiaya ^[14]

“ In view of the various ways the solute binds at the chromatographic surface, it is noted that the retention in RPC is due to the statistical average of such binding configurations and the measured retention factors represent average values of the corresponding free energy of binding. Therefore the two stationary phase configurations fur and stacked reflect the belief that retention in RPC is governed by the magnitude of the contact area that is formed upon binding of the elute molecule with the isolated solvated ligates of the stationary phase.”

Collapsed configuration

However, another model assumes that the bulk conformation of the chains is in the collapsed state and that their conformation is independent of the type and amount of organic solvent present in the eluent. Based on this assumption, the bonded ligands in this model are in their densest conformation on the silica surface and have a liquid like structure. However, since the maximum amount of coverage of the bonded ligands on



Stacked

Figure 5-6. Schematic of the stacked conformation of the stationary phase ^[21]

the silica surface cannot be achieved, there should also be some patches or areas of exposed residual silanols. Clearly, assuming this model one of the mechanisms to be considered involves adsorption on top of the collapsed dense molecular arrangement of alkyl chains. Therefore, in an attempt to understand the solute retention process in reversed phase liquid chromatography, there is a need for proper surface characterization of n-alkyl bonded phases. The results presented within this chapter discuss void volume and suggest that the bonded phase in reversed phase chromatography actually is independent of type and amount of organic modifier present in the mobile phase and is in this collapsed conformation. The characterization of the adsorbed layer, or the preferentially adsorbed organic eluent on top of the bonded layer is also presented.

Bonded phase stability

The extent of coverage may actually have an effect on the bonded phase stability. For example, at high pH values, cleavage of the Si-O-Si group connecting the silane to the silica support is attacked as well as loss of the silane bonded phase by dissolution [31]. Typically, reversed phase packing materials that are currently available are stable up to pH around pH=8.5. Silica is soluble at high pH and this may cause a steady dissolution of the column packing. Therefore, retention time reproducibility will be affected due to the steady degradation of the stationary phase. For acidic and basic components there may be a decrease in retention on a column that has been exposed to high pH. However, it is still possible to work at these high pH. Recently reversed-phase packings have been made more stable under high pH conditions. Bonding density of these packings is greater and the dissolution of the reversed phase material is less

pronounced. Also, decreased operating temperatures less than 40°C, is suggested when working at high pH. Therefore, higher bonding density silica and lower temperatures would permit the chromatographer the opportunity to work at high pH for the analysis of basic and acidic components if needed.

In an acidic environment the siloxane-bonded phases are more stable, but at extreme acidic pH values the nucleophilic attack of the Si-O-Si bond that binds the silane to the support may be prominent, leading to the hydrolysis of the bonded phase. The process is assumed to be kinetically much slower than attack in basic eluents. Therefore the analysis of basic compounds in reversed phase HPLC should be carried out in acidic media owing to the greater stability of the packing and also suppress any detrimental effects from interactions with residual silanols since the silanols are protonated at these low pH values.

Effect of chain length

In reversed phase chromatography, generally for packings of the same bonding density, the longer the chain length of the R group the greater is chromatographic retention. Generally as the length of the alkyl chain is increased the underlying polar surface is more effectively shielded giving increased hydrophobic character of the total surface. It is interesting to note that there is not a linear increase in retention of neutral solutes with an increase of the length of the bonded ligand. It has been shown that several compounds increase their retention on C₁ to C₈ phases and greater chain length phases generally show similar retention to those of C₈ [17]. These include the most popular reversed phase packing, C₁₈ phase. For the shorter chain lengths the pore size of the packing may not be important, but as the length of the chain increases the pore size of

the support must be adjusted to the size of the bonded appendage^[32]. For example one would not bond a C₃₀ ligand using 60Å pore size silica. If the pores are small enough, they could be blocked by these alkyl ligands and the effective surface area available to the analytes may be decreased leading to a decrease in chromatographic retention. In the past few years with the development of longer alkyl chain phases, including C₃₀, this may become increasingly important.

Void Volume

The most important parameter in liquid chromatography is the void volume. This is not to be confused with the hold up time which is a sum of the void volume and the system volume. The void volume, V_0 , is the total volume of the liquid phase in the column. The values of the capacity factor, selectivity and resolution are dependent on V_0 . These data are important for the optimization of the separation conditions of complex mixtures and for comparison of chromatographic data from different laboratories. However, there is no universally accepted method for the accurate measurement of this parameter. The methods that have been used to determine the void volume include the retention volume of radioactively labeled components, deuterated components, injection of “non-retained” components, injection of modified mobile phase of slightly higher concentration than equilibrated conditions, static weighing methods, frontal chromatography using breakthrough curves, and mathematical determinations based on the retention characteristics of members of various homologous series. We will give a general overview of these methods and then use some of the described methods to determine the void volume on 20 different columns of different geometric parameters

using a variety of organic/water eluents. The void volumes determined with the different methods and eluent systems will be compared.

Definition of the void volume

The void volume can be defined as the total volume of the liquid phase inside the column. This volume is comprised of the pore volume and the interstitial volume (volume around the particles) shown in equation 5-2. However, the volume of the mobile phase may be different than the void volume. It has been shown by many chromatographers^[33-34] that eluent molecules that are adsorbed on the solid surface form a stationary layer of mobile phase components and that reduces the column void volume shown in equation 5-3.

$$V_o = V_p + V_{ex} \quad [5-2]$$

$$V_m = (V_p - V_a) + V_{ex} \quad [5-3]$$

where V_m = volume of the mobile phase

V_p = pore volume

V_a = Volume of any adsorbed eluent

V_{ex} = Exclusion volume (interstitial volume) volume of eluent outside the pores of the column packing.

Static methods

This method involves filling the column with two solvents of different density and then weighing it after each filling. The total volume taken up by the mobile phase (V_o) can be calculated from the following equation^[35].

$$V_0 = \frac{w_a - w_b}{d_a - d_b} \quad [5-4]$$

First, the column was flushed with an eluent of a certain density, d_a , and weighed, w_a . Then a second eluent of different density, d_b was flushed through the column and the column was reweighed, w_b . The void volume was determined from the following equation 5-4 using the two column weights filled with the different liquids and the corresponding densities of liquids. In the literature, various combinations of solvents have been reported. In one report, Slaats et. al.^[36] weighed a column that was dried with a stream of nitrogen and then filled the same column with tetrachloromethane. In a later report Slaats et. al. used pure acetonitrile and methanol^[33]. Another author, Krstulovic^[37] used acetonitrile and carbon tetrachloride, owing to their large differences in densities, and also measured the difference in weight between a dry column which was purged with pentane and dried overnight at 60°C in a stream of helium and the same column filled with solvent. Others have used methanol and carbon tetrachloride also owing to their large differences in densities^[34,38-39]. Fin et. al.^[40] weighed the column plus the mobile phase and then removed the stationary phase and reweighed the empty column.

The limitation of this method is that it does not account for the possibility that the stationary phase is solvated by the eluent components and/or preferential adsorption of the eluent components on top of the stationary phase. Slaats^[36] proposed subtracting the volume of the adsorbed mobile phase layer (V_a) on the silica surface; this volume has been determined by using breakthrough curves^[41] and by using the minor disturbance method^[33]. Hence, without the correction ($V_m=V_o-V_a$), this may lead to erroneous values for the mobile phase volume and lead to negative k values. This correction factor was

supported by Riedo and Kovats^[42] assuming that the 1) density (specific volume) of the liquid that may be adsorbed is the same in the bulk as in the adsorbed state and 2) that the boundary between the liquid and solid is independent of the nature of the liquid and that exclusion can be ignored and 3) the partial molar volumes of the components should remain the same at the composition of the mixture in the surface phase as they are in the bulk.

Inorganic salts

Inorganic salts have been used to measure void volume which include sodium nitrate^[43], potassium iodide^[44], potassium dichromate^[45], potassium nitrate^[46], sodium chloride^[47], and sodium nitrite^[48] however this technique is faced with many difficulties. It has been found by Berendson^[38] and Slaats^[33] that the elution behavior of ionic solutes is extremely dependent on the background electrolyte concentration in the mobile phase. Therefore, it can be said the retention volumes of the salts vary with the salt concentration of the injected solutions presenting two limiting cases. 1) At low electrolyte concentrations the salt is excluded from the pores of the packing due to an ion exclusion effect as a result of electrical charges on the surface. 2) At high electrolyte concentrations or injections of highly concentrated solutions of a salt, the pores become accessible to the salt. Also, it was found that inorganic salts only give a fair estimation of the void volume when the mobile phase is comprised of methanol/water mixtures of 40 – 60% methanol. Other studies^[49] showed that the void volume is dependent on the degree of penetration of the salt into the pores of the column packing and that penetration may vary from zero, which is total exclusion (Donnan effect), to complete penetration. Using inorganic salts for the determination of V_0 is dependent on many variables such as the

nature of the mobile phase, type of salt, amount of the salt injected and the presence or absence of background electrolyte. Given all these issues, the use of inorganic salts may not give a true measure of the void volume, contrary to the belief of many authors such as Berendson^[38] and Roses^[50].

Organic compounds

Many authors have suggested the use of organic salts and unretained organic compounds including sodium benzene sulphonate^[51], nitrobenzene^[50], benzoic acid^[47], fructose^[53], uracil^[54] and phloroglucinol for the determination of the void volume. These compounds however may not serve as true measures of the void volume since it has been shown that different components were found to be dependent on a variety of factors. The void volume measured with these components was found to be dependent upon the mobile phase composition and/or concentration and, in some cases, dependent on the concentration of the salts. However, the best probe for the measurement of the void volume was stated in the literature to be phloroglucinol since it was found to be nearly constant for different mobile phase compositions and independent of the amount injected^[48]. Kazakevich^[55] showed that the retention of phloroglucinol changes across the entire concentration region of acetonitrile/water. This was shown by plotting the retention of phloroglucinol with the retention of minor disturbance peaks over the whole concentration range of acetonitrile in water. It was shown that phloroglucinol actually moves faster than the eluent components in mobile phases that contain greater than 30% acetonitrile, and negative values were obtained for the retention factor for phloroglucinol. Thiourea and urea^[40] have also been recommended as good probes but unless studies are performed that compare the retention volumes of these components versus the retention

volumes of minor disturbance peaks, there still will be some doubt in these measurements. However, it can be seen that organic compounds offer no real advantage over the inorganic salts due to the conflicting evidence among many authors and also may be dependent upon the particular experimental conditions being used.

Isotopically labeled components

The void volume measured with isotopically labeled components can be broken into two classes of components: radioactively labeled and deuterated components. Riedo and Kovats^[42] determined the void volume with compounds containing radioactive carbon and advocated their use over deuterated components. They reported that deuterated components yield less satisfactory determinations of the void volume due to small changes in the physical properties over their unlabelled counterparts (isotope effect). However, they suggested using a series of compounds with increasing degrees of deuteration, and upon assuming a linear change in properties, the retention volumes of compounds deuterated to different degrees could be extrapolated to 0% deuteration. This value would give the “apparent retention volume” of a labeled component and not a deuterated compound.

Radioactively labeled compounds

Knox^[56] used this method to determine the retention times of radioactively labeled compounds of the eluent where V_o is obtained by

$$V_o = V_A^* X_A + V_B^* X_B + \dots \quad [5-5]$$

where V_A^* etc. are the elution volumes of radioactively labeled eluent components A etc., and X_A etc. are the volume fractions of A etc. in the eluent going into the column. For $(N+1)$ component eluents there will be $(N+1)$ such peaks. If a mixture of the same eluent

components with different composition is injected into the column (as described below in minor disturbance method), N solvent disturbance peaks will be obtained which, in general, may or may not coincide with the peaks for radioactively labeled eluent components. The disadvantage of this method is the problem of detection. The same equation may be used to measure the void volume with the deuterated components. The void volume may be determined directly by running pure acetonitrile as the mobile phase and injecting 100% CD₃CN or running pure water and injecting 100% D₂O and the peaks obtained correspond directly to the measured void volume. For the intermediate compositions the void volume is determined by simple addition. For example if the mobile phase composition was 30% acetonitrile and 70% water, and a mixture of 70% D₂O and 30% CD₃CN was injected, and the retention volumes were 2 min and 1 min, respectively, the void volume would be : $V_o = (0.3*1)+(0.7*2)$.

Deuterated compounds

D₂O is the most popular of all deuterated components for the determination of the void volume. However, authors^[34] have also used deuterated acetonitrile, methanol and THF. Generally if a solution of the deuterated water to be injected has the same composition as in the mobile phase, one peak will be obtained with a refractive index detector. However, if the composition of the injected deuterated mixture is different than the mobile phase composition than 2 peaks may be obtained. The second peak is called a vacancy peak^[34]. McCormick and Karger^[34] explained that when equilibrium is established between the mobile phase and stationary phase in a RPLC column, the organic modifier is preferentially extracted into the stationary phase by virtue of its hydrophobic expulsion from the mobile phase. If this equilibrium is disturbed by the

injection of solute components, the composition of the extracted organic modifier system will vary in order to accommodate changes in the mobile phase stationary phase equilibrium. This will cause the appearance of an extra displacement or vacancy band in addition to the deuterated solute band. Colin and other authors^[57] have determined the V_0 using this method with much success. Berendson^[38] compared the retention times of water and methanol with their deuterated analogues using various aqueous methanol concentrations and concluded that all four compounds elute from the column in the same time. Also, they found the elution time to be dependent on the mobile phase composition with a minimum at 70% methanol and temperature dependence of the retention volume. A more intensive study was done by Karger who used deuterated water, methanol, acetonitrile, and THF as the void volume markers. Karger et.al.^[34] concluded that deuterated modifiers are not suitable as a measure of the void volume since they obtained retention volumes greater than the maximum column porosity at all compositions, with the exception at high modifier concentrations. However, they concluded that D_2O gives a good estimate of the column void volume; that these molecules have full access to the pore volumes; and that D_2O does not interact with the residual water-deactivated silanols. This is in contrast to what Slaats^[33] observed at 100% water. He observed a significant decrease in the void volume, which was attributed to poor wetting of the stationary phase and inability of water molecules to penetrate the internal pore structure. At 100% organic the void volume they obtained was greater and this effect was attributed to increased interactions with the residual silanols.

Minor disturbance method

Another way to measure the dead volume is to use the retention volume of the disturbance peaks of a component of the eluent^[34]. The definition of the dead volume using this thermodynamic approach will be that the dead volume is the total volume in the liquid phase in the column, and this is a direct consequence based on Gibbs theory. The Gibbs definition has been used as the basis for the mathematical treatment of the chromatographic process. Wang, Duda and Radke^[58] considered the mass transfer through the column using the following for a two component system:

$$u = \frac{FL}{V_o + S\left(\frac{d\Gamma}{dc}\right)} \quad [5-6]$$

where F is the eluent flow rate, L is the column length, u is the linear velocity of the chromatographic zone, V_o is the dead volume of the column (total liquid phase present in the column), S is the surface of the adsorbent in the column, and $(d\Gamma/dc)$ is the derivative to the excess adsorption isotherm. Since $LF/u = V_R$ which represents the retention volume we can write equation 5-6 as follows:

$$V_R = V_o + S\left(\frac{d\Gamma}{dc}\right) \quad [5-7]$$

Equation 5-7 can only be applied to a two component system. In RPLC, aqueous (water) and organic (Methanol, Acetonitrile, or Tetrahydrofuran) make up the two components. For a binary system, the column is equilibrated with a two-component solution, and then a small amount of the same solution with a small difference in concentration is injected (introduction of minor disturbance in the system). The minor disturbance method, also allows the simultaneous determination of the excess adsorption

isotherms of eluent components. Karger^[34] suggested that the dead volume could be measured by using the data for the retention of the **minor disturbance** peaks of a component in the eluent. Therefore the excess adsorption for any pure component is **always equal** to zero since it assumed that the specific molar volumes are the same in both the bulk phase and on the surface. This minor disturbance peak for each component will have retention volume corresponding to Equation 5-7. If we integrate Equation 5-7 **through the entire concentration range**

$$\int_{C_{\min}}^{C_{\max}} V_r(C)dc = \int_{C_{\min}}^{C_{\max}} V_o dc + S \int_{C_{\min}}^{C_{\max}} \left(\frac{d\Gamma}{dc} \right) dc \quad [5-8]$$

V_o is a constant and by definition, $\Gamma_{C_{\min}(0)} = \Gamma_{C_{\max}(100)} = 0$, hence

$$V_o = \frac{\int_{C_{\min}}^{C_{\max}} V_r(C)dc}{C_{\max} - C_{\min}} \quad [5-9]$$

Equation 5-9 gives us a simple method to calculate V_o from data generated.

It has been shown that the dead volume of a column is independent of the different types of mobile phase components. Many authors including, Kazakevich,^[55] Alvarez-Zepeda,^[59] and Karger,^[34] have used the minor disturbance method to determine void volume.

Some authors, Alvarez-Zepeda, have shown that the V_o values are independent of temperature while others have noticed a difference, Kazakevich^[60]. Scott and Kucera^[61] also used this method and found that the void volume obtained is the same as the value obtained by injecting samples of potassium nitrate. Using this technique, Colin^[57] recommended that the injection of the smallest detectable amount of component should be injected. Kazakevich^[55] showed that there is actually a dependence of the retention

volume of the minor disturbance peak as a function of concentration. If one injects more than a minor disturbance into the system, the equilibrium will be destroyed and the retention volume of that eluent component will not correspond to that of a minor disturbance peak. Therefore, the injection volume or concentration injected should be optimized and the most sensitive RI detector should be used. Using this method Karger determined the elution behavior of water enriched samples is similar to that for the corresponding modifier rich samples except that the differential refractive index detector response is opposite in direction.

As can be seen there is a large discrepancy between the various methods to determine V_0 . Hence, in order to elucidate the accuracy of the measurement of V_0 we had measured it using three different methods: 1) Weighing method (Pycnometry), 2) Deuterated component over the whole concentration range and 3) Minor disturbance method. Accurate determinations of the void volumes allow the analysis of the other geometric parameters of the modified silica at HPLC conditions.

We must note that the void volume is the sum of the pore volume and the interstitial volume. It is expected that bonding of a significant amount of relatively large alkyl groups on the silica surface should noticeably alter adsorbent geometry and ultimately influence the mechanism of separation ^[62]. Bonded alkyl chains occupy volume inside the pore space and are expected to decrease original silica pore volume. One also may expect a corresponding decrease of the adsorbent surface area and average pore diameter upon bonding of the alkyl ligands. Unfortunately, these effects have been addressed in the literature very lightly and the experimental results obtained are controversial ^[18,62-67].

Bass^[5] et al. have studied the effect of surface modification on adsorbent geometry for four different silica gels. Their results clearly show the decrease of pore volume, surface area, and mean pore diameter with an increase of the chain length of bonded alkyl moiety. Other investigators^[63,67] reported the same effect of decreasing geometric parameters with increasing length of bonded chain.

If one assumes that bonded n-octadecyl chains occupy approximately the same molecular volume as they do in the liquid phase ($\sim 600 \text{ \AA}^3/\text{molecule}$ or 361 ml/mole), then it is possible to calculate a theoretical decrease of the pore volume after surface modification. For example, for an adsorbent with surface area of $300 \text{ m}^2/\text{g}$ bonded with octadecylchlorosilane with bonding density of 3 \mu mole/m^2 and a molecular volume of 361 ml/mole , one would expect a pore volume decrease of approximately 0.33 ml/g ($300 \text{ [m}^2/\text{g}] \times 3 \text{ [\mu mole/m}^2] \times 361 \text{ [ml/mole]} = 0.325 \text{ [ml/g]}$ per one gram of original silica). If the original silica had 1 ml/g original pore volume, the decrease would be 33% and considered a very significant change.

Experimental data^[18,32,67] allow the evaluation of the decrease of the adsorbent pore volume. The recalculated data are shown in Figure 5-7. As can be seen from Figure 5-7, the decrease of the adsorbent pore volume of different silica gels chemically modified with various dimethylalkylchlorosilanes is consistent for five different research groups. The average slope for all three dependencies is 19 \mu l per gram per one CH_2 group and the standard deviation is less than 15%.

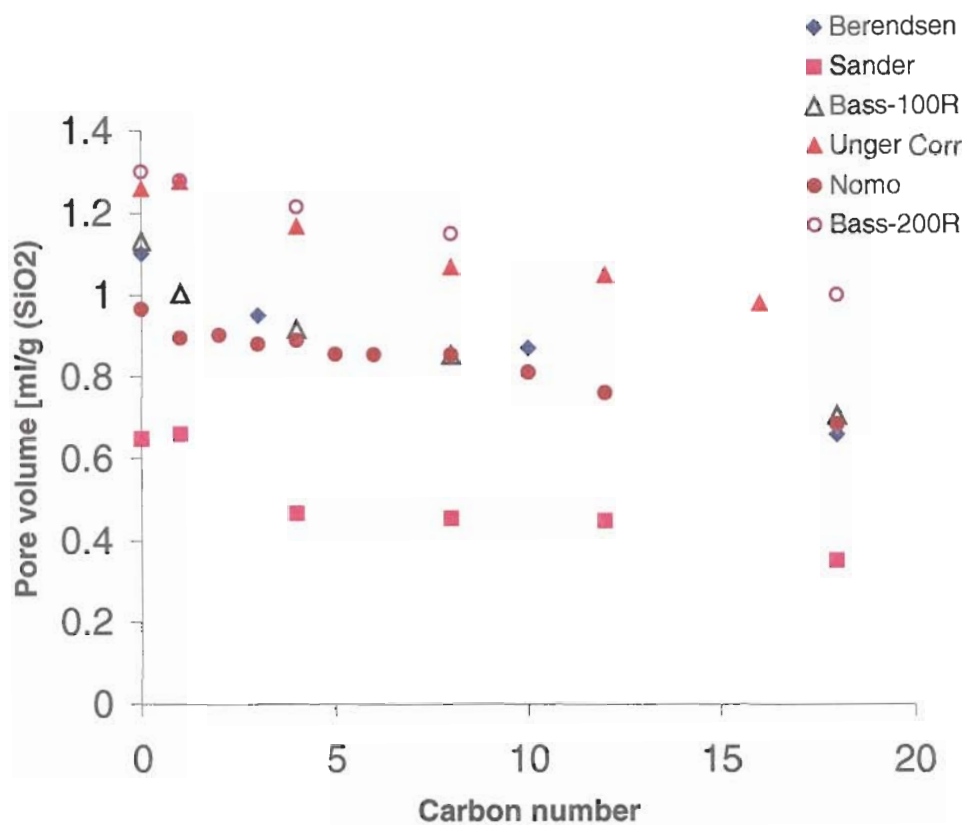


Figure 5-7. Decrease of the adsorbent pore volume with increase of the chain length of the bonded ligands. Data taken from Berendsen et al^[18] Sander^[67], and Bass et al^[56] and Unger^[32] Squares – data from G.E. Berendsen; Rombs – data from Sander; squares – data from Bass, open circles and triangles- data from Unger; closed triangles, - data from our research group, closed circles.. All data were corrected for the weight of silica.

The pore volume determined using LTNA is measured as a volume of the liquid nitrogen necessary to fill all pores in the adsorbent. This parameter is the least dependent on any assumptions. On the other hand, surface area calculations are based on the assumption of the nitrogen molecular area, and the pore diameter calculation is based on the assumption of the applicability of the Kelvin equation and the thickness of the liquid film adsorbed on the pore walls [68].

The molecular arrangement on the organic bonded layer exposed to the HPLC eluent at ambient temperature could be significantly different from that in vacuum at liquid nitrogen temperature. Could then the geometric characteristics of the porous reversed-phase adsorbent measured with LTNA be used for HPLC calculations? The answer could be found in comparison of the LTNA measured pore volume and the pore volume measured by HPLC. The pore volume at HPLC conditions can be determined by obtaining correctly measured column void volume, V_o , exclusion volume, V_{ex} , (interparticle volume) and actual mass of adsorbent in the column, m_a .

The purpose of this work is the evaluation of chromatographic validity of the geometric parameters of reversed-phase adsorbents determined by the LTNA method. Studies were performed for determination of the geometric parameters of ten adsorbents modified with ligands of different chain lengths and original silica by LTNA and compared to various chromatographically obtained parameters. These adsorbents will be denoted as the **Nomo** silicas.

Experimental

Adsorbents and Columns High purity porous silica was used in this study. This same silica was chemically modified with the alkyldimethylchlorosilanes of different alkyl chain lengths including C₁-C₆, C₈, C₁₀, C₁₂ and C₁₈ and these will be called Nomo silicas. Adsorbents were packed into 150 x 4.6 mm stainless steel columns using the slurry packing procedure. Two sets of Nomo columns were studied. The first set included all adsorbents (ten columns), and the second set (packed separately, two months later) included columns packed with C₁, C₂, C₄, C₈, and C₁₈ modified adsorbents. Other columns studied included Luna C₁₈, Jupiter C₁₈, Kovasil C₁₄, Waters Symmetry, Luna C₁₈-2, Zorbax Eclipse XDB-C₁₈, Prodigy ODS-2.

Low Temperature Nitrogen Adsorption (LTNA)

Bare silica and chemically modified Nomo samples were characterized using a low temperature nitrogen adsorption system ASAP model 2010 (Micromeritics, Norcross, GA). These experiments were performed at Phenomenex.

Adsorbents were degassed under vacuum (10^{-5} torr) at 350°C (for bare silica) and at 150°C for chemically modified silica for 12 h in the instrument vial. After cooling, the vial was weighed and placed into the adsorption instrument.

A static adsorption mode was used (full equilibration after each adsorbate load). The instrument temperature (manifold) was 28 °C. Chemically modified silica samples were measured on the same LTNA system at the same conditions.

Geometric parameters including surface area, pore volume, and pore size distribution for all adsorbents measured with LTNA are shown for the Nomo silicas in Table 5-I. Representative desorption isotherms for original silica and Nomo C₁₈

modified adsorbent are shown in Figure 5-8. Adsorbents pore volume was calculated from the upper plateau of the adsorption isotherm, which corresponds to complete pore filling^[69]. The pore size distribution and the resulting pore diameter were obtained from the desorption isotherms using the Kelvin equation^[69]. Surface area values were calculated using the BET method^[68].

The carbon load was derived from elemental analysis of the chemically bonded phases (Nomo). Weight percent of carbon and hydrogen on chemically modified silicas was measured according to the procedure described by Berendsen^[19]. The bonding densities of the chemically modified silicas were calculated from the weight % carbon and the specific surface area of bare silica.

HPLC systems

Experiments for the void volume and the excess adsorption determination were performed on two different HPLC systems. System I: HP model 1050 pump and autosampler (Hewlett-Packard, Wilmington, DE) equipped with refractive index detector ERC-7510 (Erma, Kingston, MA) and UV detector Spectroflow 783 (Kratos, Munich, Germany). System II: PE model 410 pump (Perkin-Elmer, Norwalk, CT); HP model 1050 autosampler (Hewlett-Packard, Wilmington, DE) and 2 different models of RI detectors used: 401RI and 410 RI detector (Waters, Millford, MA). The column temperature was set at 25°C and controlled by a circulating water-bath (Brinkman Model

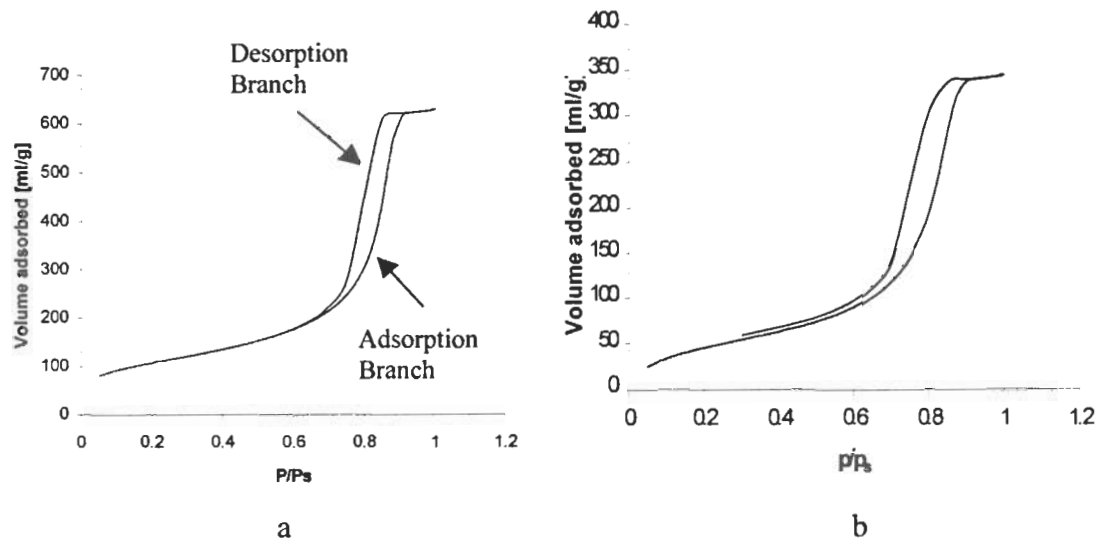


Figure 5-8. Nitrogen adsorption and desorption isotherms on bare silica (a) and on the C18 modified adsorbent (b).

RC6, Lauda, Lauda-Konigshofen, Germany). All eluents were degassed with a degasser unit (Phenomenex, Torrance, California).

GPC experiments for the determination of the exclusion volume was performed on the third system, consisting of a PE-410 pump, an ISS-100 autosampler (Perkin-Elmer, Norwalk, CT), and a model 785A variable UV detector (Applied Biosystems, Sunnyvale, CA). A series of high molecular weight polystyrene standards of low polydispersity (Polymer Laboratories Ltd, Church Stretton, Shropshire) were dissolved in HPLC grade THF (Sigma, Milwaukee, WI). The GPC experiments were not carried out on the Luna C18, Jupiter C18, Kovalsil C14, Waters Symmetry, Prodigy ODS-2, and Zorbax Eclipse XDB-C18 columns.

All systems were equipped with the Turbochrom-4 data acquisition system (Perkin-Elmer, Norwalk, CT). Extra-column volumes of all systems were determined by direct connection of column inlet and outlet capillaries. The volumes were 53 μL for Waters 401 RI detector; 137 μL for Waters 410 RI detector; 117 μL for the Erma Detector; 17.7 μL for the 785A variable UV detector and 83 μL for the Kratos UV detector. The average retention volume of a 1 μL injection of 100 ppm benzene solution at 5 different flow rates was used.

Geometric parameters of HPLC columns packed with above-mentioned adsorbents were studied using a GPC method (for determination of interparticle volume) and the minor disturbance method (for determination of the column void volume). The void volume was determined using three different eluent systems: acetonitrile/water; methanol/water; and tetrahydrofuran/water at 25°C for the Nomo set 1 and set 2 columns.

The void volume was determined using three different eluent systems: acetonitrile/water; methanol/water; and benzene/acetonitrile at 5-55°C for the Prodigy ODS-2 columns. For the Luna C₁₈, Jupiter C₁₈, Kovalis C₁₄, Waters Symmetry C₁₈ and Zorbax Eclipse XDB-C₁₈, the void volume was determined using acetonitrile/water system at 25°C.

Consistency of the void volume measurement was checked with three different methods: minor disturbance; injection of isotopically labeled component and pycnometry for all the Nomo columns and a selected set of the other columns.

After completion of all experiments, the second set of Nomo columns were purged with acetonitrile and unpacked. Then the adsorbent was dried at 85°C under slow nitrogen flow and followed by vacuum until a constant weight was obtained.

All solvents and reagents used were high purity HPLC grade (Sigma, Milwaukee, WI). Experimental values for the retention of acetonitrile/water minor disturbance peaks were corrected for extra-column volume for the first and second Nomo column sets (see Addendum, Tables A5-I and A5-II). Corresponding values for minor disturbance peaks for methanol/water for the first and second column set are shown in Addendum Tables A5-III and A5-IV, and values for tetrahydrofuran/water for the second set of columns are shown in Addendum Table A5-V. Representative dependencies of the minor disturbance peaks for different eluent types on Nomo-C1 and Nomo-C18 columns are shown in Figure 5-9. Corresponding values for deuterated peaks for acetonitrile/water for the C₁₈, C₁₂ and C₈ columns of the first set are shown in

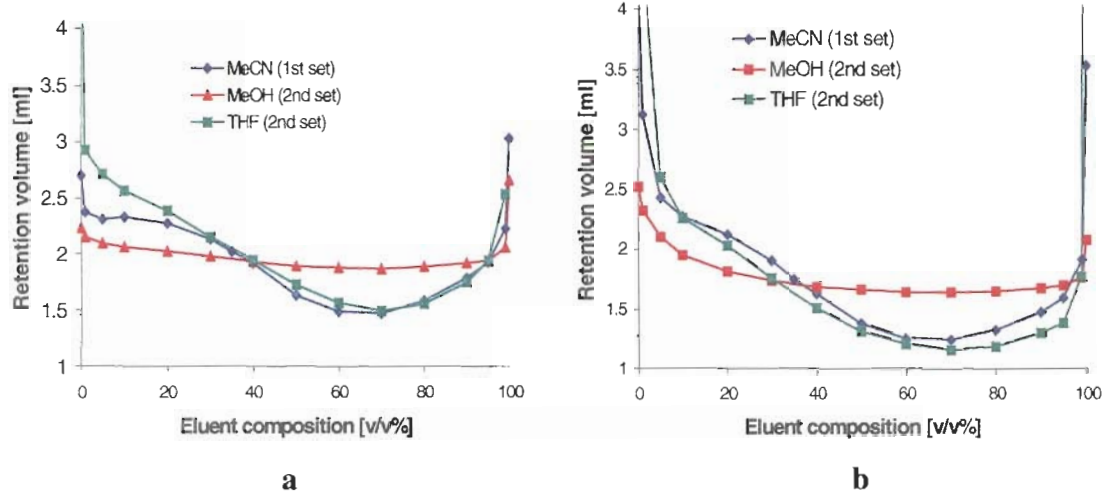


Figure 5-9. Representative dependencies of the minor disturbance peaks for different eluent types on C1 columns (a) and on C18 columns (b)

Addendum Tables A5-VI - A5-VIII respectively. Experimental values for the retention of acetonitrile/water minor disturbance peaks for the Symmetry C₁₈, Eclipse-XDB-C₁₈, and Luna C₁₈-2 are shown in Addendum Table A5-IX. Experimental values for the retention of acetonitrile/water minor disturbance peaks for the Kovsil-C₁₄, Jupiter C₁₈ and Luna C₁₈ are shown in Addendum Table A5-X.

RESULTS AND DISCUSSION

Analysis of the geometrical parameters of modified silicas (Nomo set 1 and set 2)

Pore Volume

The adsorbent pore volume is significantly dependent on surface chemical modifications. The adsorbent pore volume decreases as the length of bonded alkyl chains increases (Figure 5-7, Table 5-I). Low temperature nitrogen adsorption (LTNA) measurements gave specific pore volume values related to one gram of the actual sample used (Table 5-I, col. 2). The specific pore volumes for the modified adsorbents are denoted as V_p . Valid comparisons of the pore volume change due to the surface modification could be done if measured values are related to the same amount of original silica (one gram). These corrected values are denoted as V_p^{Si} and are shown in Table 5-II (column 3). The correction factor for each modified silica was calculated from the experimental value of bare silica surface area, bonding density, and type of attached ligands. The product of bonding density (d_{bond}), specific surface area of silica (S_{SiO_2}), and molecular weight of bonded ligands (MW_{ligand}) represents the weight of the bonded layer on one gram of bare silica. The correction factor for the calculation of the amount of bare silica in one gram of modified adsorbent will be:

$$f_{corr} = \frac{1}{1 + d_{bond} \cdot S_{SiO_2} \cdot MW_{ligand}} \quad [5-10]$$

The difference between the specific pore volume of bare silica (V_p) and the specific pore volume of modified adsorbent corrected to the bare silica weight (V_p^{Si}) represents the specific bonded layer volume (shown in column 4 of Table 5-II).

When the specific bonded layer volume is divided by the surface area of bare silica, the volume of the bonded layer per unit area of original bare silica can be calculated (Table 5-II, column 5). The bonded layer consists of anchored alkyl moieties. Since the average bonding density is known (Table 5-I, column 6), it is possible to calculate the effective molecular volume of the bonded chains. This was calculated by dividing bonded layer volume per unit area (Table 5-II, column 5) by its corresponding bonding density value (Table 5-I, column 6). These results are shown in Table 5-II, columns 6 and 7.

It is interesting to compare these values with the standard molecular volumes of liquid n-alkanes. Each bonded alkylsilane ligand consists of a silicon atom, two side methyl groups, and a corresponding alkyl chain. For example, ligands in the bonded phase, denoted as C4, contain a total of 6 carbon atoms (butyl chain and two side CH₃ groups).

Figure 5-10 shows a comparison of effective molecular volumes of bonded chains (from column 7, Table 5-II) with molecular volumes for corresponding (n+2)-alkanes calculated from their density.

Table 5-I**Geometric parameters of bare porous silica and alkylsililated gels**

1	2	3	4	5	6
Adsorbent	BET surface area	Total pore volume	Mean pore diameter	"Carbon" Load	Bonding density
	[m ² /g]	[ml/g]	[Å]	CH% w/w	[μmole/m ²]
Si	374	0.965	97	0	0
C1	292	0.804	88.6	6.3	4.16
C2	301	0.804	88.2	7.4	3.76
C3	295	0.781	87.1	8.2	3.38
C4	299	0.778	86.4	9.5	3.33
C5	288	0.746	84.8	10.0	3.03
C6	288	0.736	83	11.1	2.99
C8	287	0.726	81	12.4	2.72
C10	264	0.687	80	13.2	2.44
C12	236	0.623	78	15.9	2.61
C18	182	0.531	79	20.6	2.51

Table 5-II

Corrected pore volume and the volume of bonded phase

1	2	3	4	5	6	7
Carbon number	Measured pore volume V_p	Corrected pore volume V_p^{Si}	Bonded layer volume		Effective molecular volume	
	[ml/g]	[ml/g] _(SiO₂)	[ml/g] _(SiO₂)	$\mu\text{l/m}^2$	L/Mole	$\text{\AA}^3/\text{molecule}$
0	0.965	0.965	0			
1	0.804	0.894	0.071	0.189	0.045	75
2	0.804	0.901	0.064	0.172	0.046	76
3	0.781	0.880	0.085	0.227	0.067	112
4	0.778	0.889	0.076	0.204	0.061	102
5	0.746	0.854	0.111	0.297	0.098	163
6	0.736	0.853	0.112	0.299	0.100	166
8	0.727	0.853	0.112	0.300	0.110	183
10	0.687	0.811	0.154	0.413	0.169	281
12	0.623	0.760	0.205	0.549	0.210	350
18	0.531	0.685	0.280	0.748	0.298	494

Both dependencies show very similar slopes (almost parallel). Experimental effective molecular volumes in the bonded phase are slightly lower than those for liquid alkanes. This indicates a compact molecular arrangement of bonded ligands on the silica surface similar to what is observed in the liquid state.

Equivalent slopes indicate that the shortest ligand (C₁) has a very dense arrangement, although its effective volume is mainly determined by bonding density and not by its conformational freedom, which is minimal. However, longer ligands (C₈ - C₁₈) have lower bonding density values (Table 5-I, column 6) and greater conformational freedom. Their effective volumes are determined not only by their bonding density, but also by their conformation. The fitness of the longer ligands to the line in Figure 5-10 indicates that these flexible chains may actually fill “gaps” in the surface, since the molecular arrangement of the bonded layer also corresponds to that in the liquid phase.

These experimental dependencies actually represent molecular arrangement of alkyl chains in vacuum, since adsorbent samples have been vacuumed first at elevated temperature and then submerged to liquid nitrogen temperature (77 K), which restricts the chain mobility. The estimation shown above has been done solely using the surface area of bare silica and the total pore volume of modified adsorbents without any assumptions being made in reference to the pore shape, structure and the pore size distribution. Data from several authors^[18,32,63,67] allow correct recalculation of the

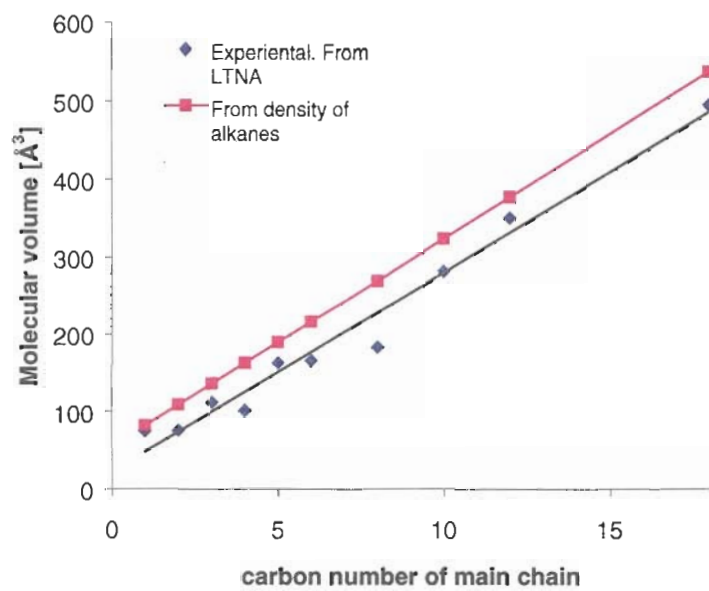


Figure 5-10. Comparison of the molecular volumes of bonded ligands with that calculated from the density of corresponding liquid.

molecular volume of attached ligands. These molecular volumes together with those from liquid density are shown in Figure 5-11. As can be seen, these data also show good correlation of surface molecular arrangement with that of the liquid alkanes.

The calculated effective molecular volume for bonded alkyl-chains for six different research groups correlates fairly well, in spite of the possible experimental errors involved in the determination of the adsorbent pore volume, surface area of silica, and carbon load. It is reasonable to say that effective molecular volume of alkyl chains bonded to the silica surface corresponds well to the volume of neat liquid alkanes. This treatment leads to the conclusion that alkyl chains under vacuum are “collapsed” on the surface, so they occupy minimum possible volume, which also minimizes surface energy. These ligands maybe in several conformations (or bulk molecular arrangement) after being exposed to the mobile phase under HPLC conditions. We will address the arrangement of the bonded layer at HPLC conditions later in this chapter.

Bonded Layer Thickness and Bonding Density

In the previous section, it was shown that the bonded layer has a liquid-like molecular arrangement. The thickness of that layer could be obtained from the bonded layer volume per unit area (column 5, Table 5-II) by simple unit conversion.

The dependence of the bonded layer thickness on the number of carbon atoms is shown in Figure 5-12 for the Nomo columns. The theoretical maximum bonded layer thickness, estimated as a length of the corresponding alkyl chains in an all-trans conformation, is also plotted in Figure 5-12. Other authors’ data for the dependence of the bonded layer thickness on the number of carbons is shown in Figure 5-13.

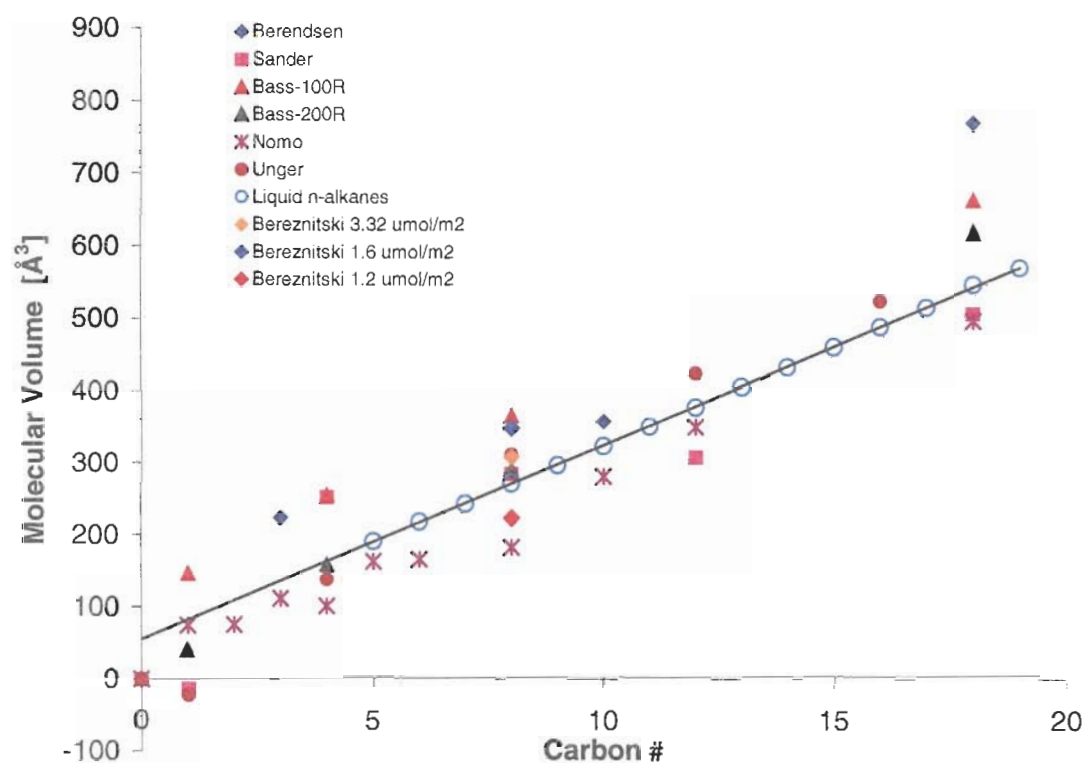


Figure 5-11. Comparison of the molecular volumes of bonded ligands with the molecular volumes of liquid n-alkanes. (n-alkanes volumes are plotted in n+2 scale to account for the two additional methyl groups of the bonded ligands). Open circles – calculated from density of liquid n-alkanes; closed red triangles– Bass^[5] closed black triangles - Bass data^[5] Blue diamonds- Berendsen^[18], Pink squares-Sander^[67], Burgundy closed circle-Unger^[32], Orange, blue and red diamonds –Berenitzki^[63]. Purple star, Our data Nomo columns, set 1.

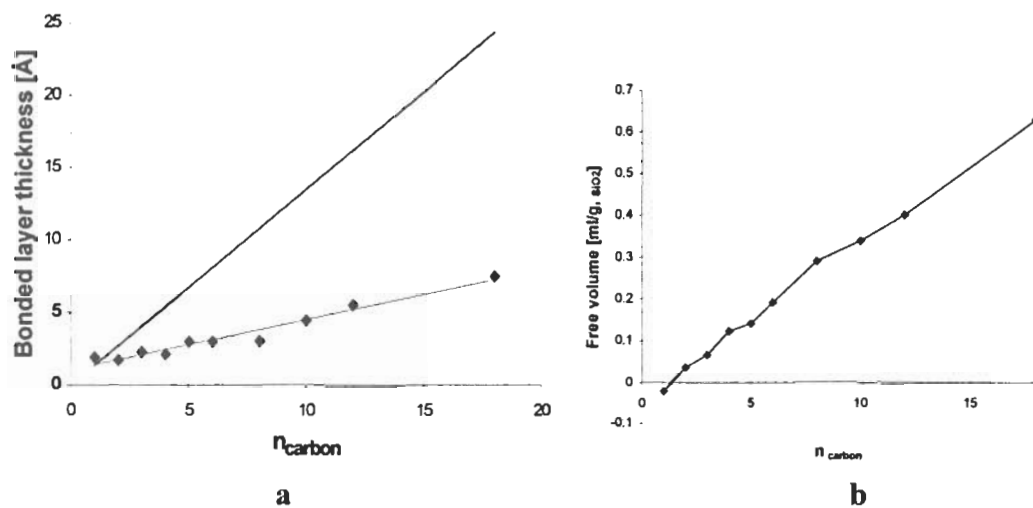


Figure 5-12. Bonded layer thickness versus carbon number. (a) Comparison of experimental bonded layer thickness dependence (bottom line) on the number of carbon atoms with theoretical (top line) calculated for all-trans alkyl chains conformation. (b) Hypothetical “free volume” in the bonded layer calculated as a difference between theoretical and experimental thickness multiplied by specific surface of silica.

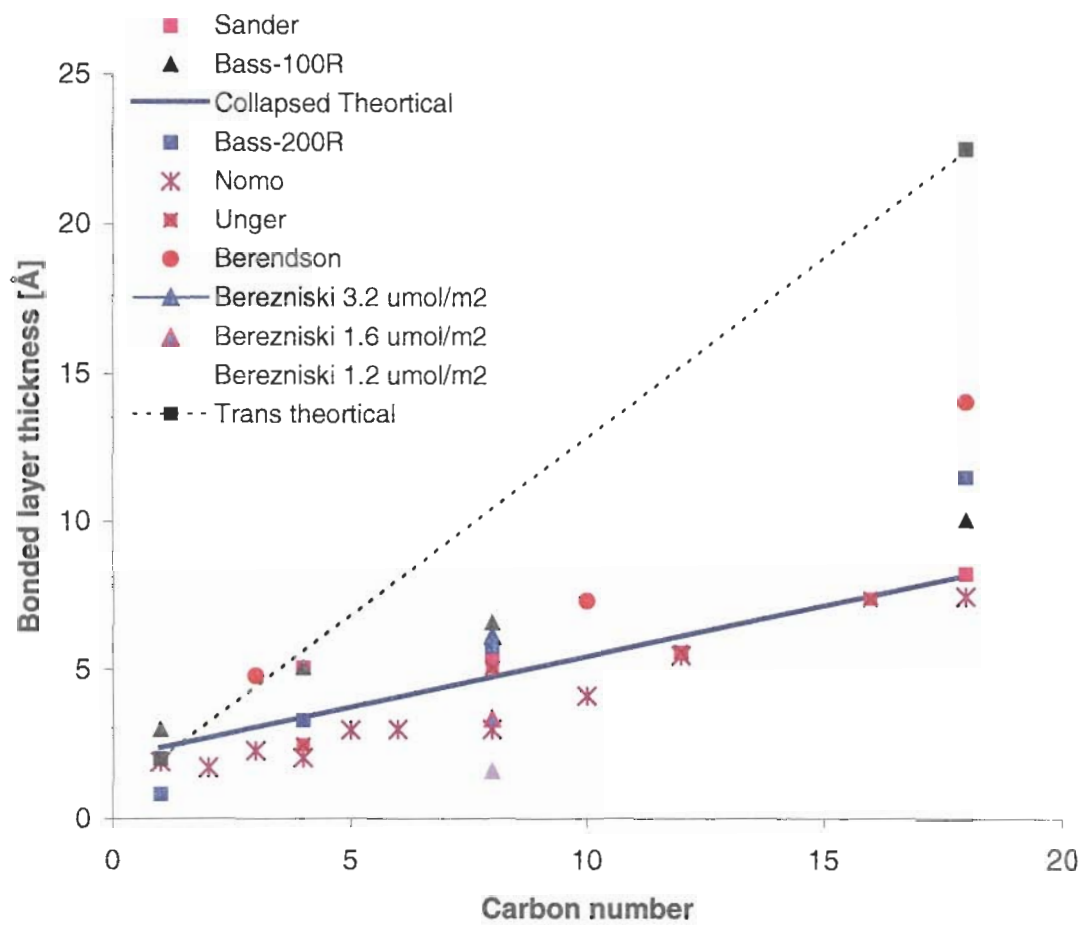


Figure 5-13. Bonded Layer thickness versus carbon number. References for authors are same as Figure 5-11.

As is seen in Figure 5-12A, the theoretical and experimental thickness of the bonded layer is the same for trimethylsilane (C_1) bonded on the surface. This is logical since there is minimal variation in the conformation of this ligand. All other ligands due to their conformational freedom may “collapse” to form the most compact layer and hence show a reduced bonded layer thickness compared to theoretical values.

The difference between the theoretical maximum thickness of the bonded layer and the experimental thickness (obtained from LTNA), multiplied by the surface area of silica, represent the free volume theoretically available for analyte molecules to penetrate (Figure 5-12B). As is observed on the adsorbents modified with the short-chain ligands (C_1 to C_4), analytes can not have any noticeable partitioning-based retention since there are not enough of the free volume between bonded chains. Although for C_{18} modified adsorbents partitioning in principle could be significant, provided that the bonded chains prefer to interact with the eluent and analyte molecules rather than with each other.

There should be a significant difference in the retention mechanism between short- and long-chained reversed-phase adsorbents if partitioning within these chains were a major retention mechanism. Partitioning of analytes into the alkyl chains can only occur if these chains are highly solvated and are extended away from the surface. If not, the predominant retention mechanism would be adsorption on top of the collapsed bonded layer and would be independent of the alkyl chain length. However, even if the chains were collapsed, the retention process may be dependent on the degree of shielding of underlying polar silanols, which would be greater for longer bonded alkyl chains.

An alkyl bonded layer exposed to different organic solvents should have different conformational configurations. For example, one can expect strong interactions of alkyl chains with tetrahydrofuran, less interactions with acetonitrile, and weaker interactions with methanol molecules. The bonded layer would be most likely more compact when in the contact with methanol than with acetonitrile. Methanol is more polar than acetonitrile, is capable of forming hydrogen bonds, and can self interact to a greater extent than acetonitrile. Since, acetonitrile is more hydrophobic, it may be able to penetrate the alkyl layer, and this effect could be even more pronounced with THF.

To evaluate these possibilities, one needs to measure the porosity of modified adsorbents at HPLC conditions and compare them with those measured at LTNA conditions. The total volume of the liquid phase in the column (void volume, V_0) is the sum of the volume inside the adsorbent pores (V_p) and the volume between adsorbent particles (V_{ex}). V_{ex} could be measured as an exclusion volume by GPC technique with high molecular weight polymers. The difference between the void volume and the exclusion volume would be a measure of the pore volume in the column.

Determination of the void volume

Void volume of each column was obtained using three different methods: (a) minor disturbance method, ^[34,60] (b) deuterated eluent components ^[42,56] and (c) pycnometry ^[70]. Emphasis must be made that with minor disturbance method we are measuring the total volume of the liquid phase in the column (V_0). The void volume measured with the minor disturbance method actually is an integral average of the retention dependence of minor disturbance peaks throughout the entire concentration range. The void volume for each column was also obtained by **determination of the**

retention of deuterated acetonitrile (CD_3CN) eluted with pure acetonitrile as was shown by Kovats^[42] and Knox^[56]. According to retention volume of a deuterium-labeled compound of a single component eluent should correspond to the column void volume. A representative set of retention volume data obtained on three columns, Nomo set 1, is provided in Tables A5-VI –A5-VIII of the Appendix. It was shown that the V_0 values calculated (using equation 5-5) at each mobile phase composition throughout the entire concentration range using the retention of volumes of the deuterated components at the corresponding eluent composition agreed within 0.3%. The validity of the determination of the V_0 was also tested by comparison of the void volume determined by pycnometry, “weighing method”, used by McCormick and Karger and Slaats et al. The void volume using the weighing method were determined with two different sets of eluents: 1) acetonitrile and methylene chloride and 2) THF and acetonitrile.

The minor disturbance measurements were performed using acetonitrile/water; methanol/water; and tetrahydrofuran/water eluents for all columns studied (experimental data are shown in Addendum Tables A5-I – A5-V). Comparison of the minor disturbance retention dependencies for all three eluent systems is shown in Figure 5-9. Void volume values were calculated as an integral average of measured dependencies of the minor disturbance peaks, according to the procedure described by Riedo and Kovats^[42]. These values for the whole series of the columns as well as the values determined by the labeled component are shown in Table 5-III. Comparison of the minor disturbance retention dependencies and deuterated components are shown in Figure 5-14. Table 5-IV shows the void volume values calculated for 2nd set of columns using the minor disturbance method, pycnometry and deuterated-labeled component.

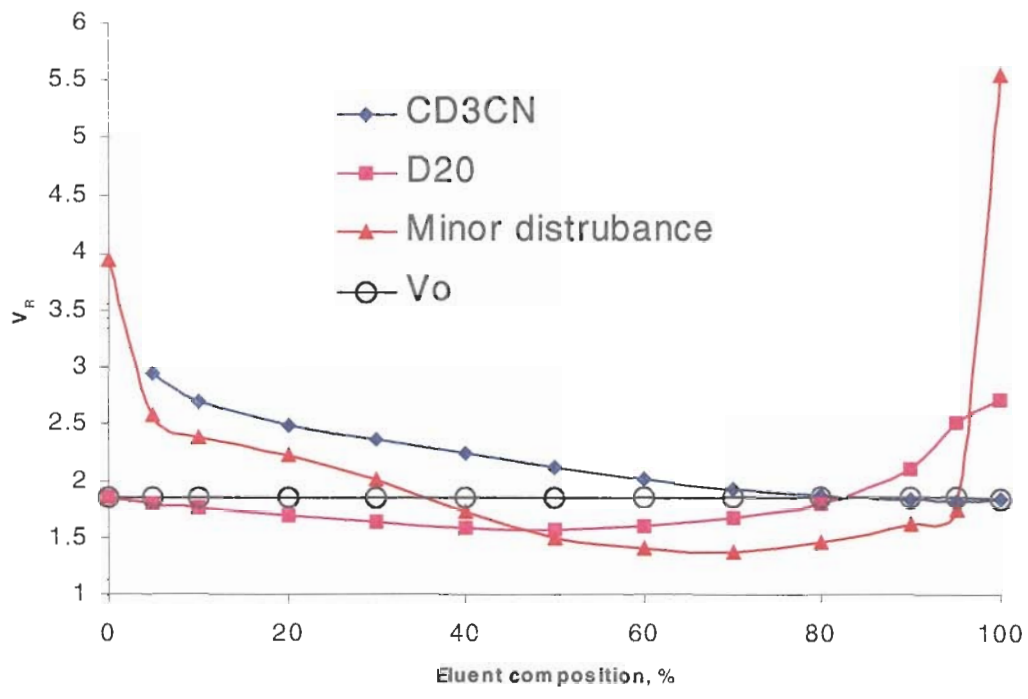


Figure 5-14. Comparison of the retention volumes obtained using deuterated components and minor disturbance method on Nomo Set 1-C₁₈.

Table 5-III**Void volume values measured with MeCN/Water, MeOH/Water and THF/Water and labeled component for 1st set of columns**

	V _{labeled}	V _o			RSD%
	From MeCN	MeCN/Water	MeOH/Water	THF/Water	
1	1.914	1.893	1.954	2.015*	2.76
2	1.895	1.909	1.951	1.974*	1.90
3	1.850	1.838	1.86		0.6
4	1.885	1.876	1.898	1.910*	0.79
5	1.860	1.846	1.880		0.92
6	1.833	1.818	1.847		0.79
8	1.827	1.814	1.869	1.865*	1.49
10	1.811	1.797	1.825		0.77
12	1.770	1.765	1.807		1.29
18	1.723	1.713	1.751	1.718*	0.98

**Data from 2nd set of columns*

Table 5-IV

Void volume values measured with MeCN/Water, MeOH/Water and THF/Water, pycnometry, labeled component for 2nd set of columns

	Pycnometry (MeCN/MeCl ₂)	Pycnometry (MeCN/THF)	V ^{labeled} From MeCN	MeCN/Water	MeOH/Water	THF/Water	%RSD
1	1.913	1.917	1.975	1.956	1.978	2.015	1.87
2	1.884	1.880	1.937	1.955	1.951	1.974	1.90
4	1.827	1.815	1.884	1.912	1.898	1.910	2.11
8	1.777	1.800	1.834	1.845	1.830	1.865	1.61
18	1.648	1.709	1.691	1.693	1.694	1.718	1.31

As can be seen in Table 5-III, void volume values measured with different eluents correlate very well for each studied column. Table 5-III also shows column void volumes consistently decrease with an increase of the bonded chain length. The dependence of the void volume on the number of carbon of the alkyl modifier in three different eluents is shown in Figure 5-15.

Figure 5-15 shows the difference between the void volumes of C₁ and C₁₈ columns to be about 0.3 ml which correlates well with the value theoretically estimated in the introduction section, for the expected pore volume decrease after surface modification with alkyloctadecylsilane.

Differences in column packing (packing density) could also account for differences in the void volumes for different columns. In order to determine if the decrease of the void volume is due to a decrease in the pore volume or due to differences in the packing density, the packing density must be determined.

Determination of column exclusion volume and packing density

Total exclusion volume (V_{ex}) obtained from GPC experiments is actually a measure of the interparticle volume in the column. The original porous silica used for these experiments had an average pore diameter of 97 Å. In order to obtain a true value of the total exclusion volume, a series of GPC experiments with polystyrene standards (PS) of different molecular weight were run. The chosen PS standards had high molecular weights to ensure their exclusion from the adsorbent pores. Polystyrene standards used for GPC experiments were 97.2K, 194K, 470K, 860K, 1840K, and 2.7M molecular weight, and the solvent used was THF. Globular polymer molecules in this

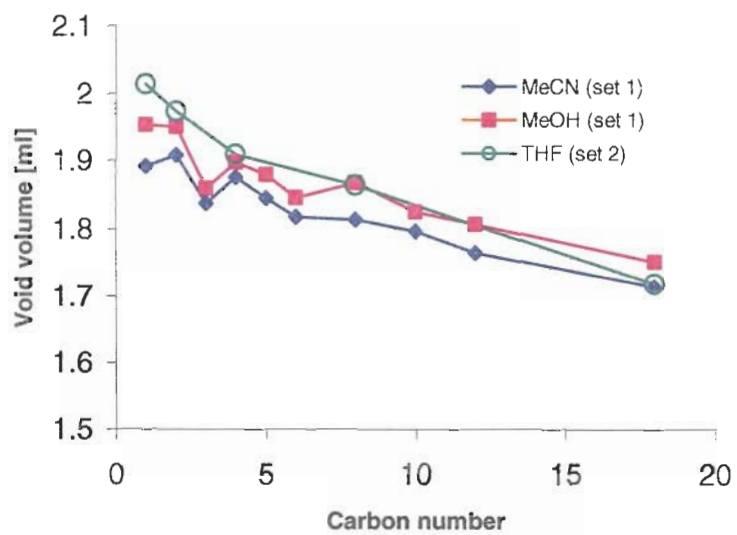


Figure 5-15. Decrease of the column void volume with the increase of the alkyl modifier chain length bonded on the silica surface.

region are too large to penetrate into the adsorbent pores with tetrahydrofuran used as an eluent. Normally, the higher the molecular weight of a standard, the lower its retention volume even for the total exclusion region. This relationship is associated with the fact that the measurement of volume, corresponds to all possible positions of the middle mass points of the molecular globe (excluding the globe radius). A schematic representation of the position of different polymer molecules of various molecular sizes on the surface is shown in Figure 5-16.

We can assume that gyration radius of a polymer molecule in the solution is proportional to the cubic root of its molecular weight. The dependence of the retention volume versus the cubic root from the molecular weight of corresponded excluded polymer should be linear. It was found to be linear for all studied columns (Figure 5-17).

The exclusion volume was found by the extrapolation of the exclusion branch of the GPC curve to zero mass point, and is shown in Figure 5-17. The exclusion volumes values were calculated as shown in Equation 5-11a. and these values for the Nomo set 1 columns are given in Table 5-V. Using these exclusion volumes the packing density was calculated as shown in Equation 5-11b.

$$V_{ex} = \frac{-\text{Intercept}}{\text{slope}} \quad [5-11a]$$

$$d_{packing} [\%] = \frac{V_{column} - V_{ex}}{V_{column}} 100 \quad [5-11b]$$

where V_{column} is the volume of the empty column and V_{ex} is the measured exclusion volume. The packing density of all columns (Table 5-V) is very consistent and has an average value of 58.6% of the column volume with a 0.7% RSD. These findings confirm that the decrease of the column void volume with the increase of the bonded chain length is solely due to the decrease of the adsorbent pore volume. Figure 5-18 is a plot of void

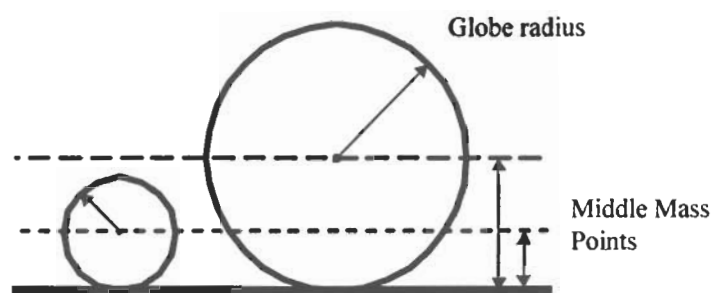


Figure 5-16. Schematic representation of the position of different polymer molecules on the outer surface of silica particles.

Table 5-V

Column exclusion volumes and packing density

	V_{ex} [ml]	d_{packing} [%] v/v
1	1.034	58.5
2	1.034	58.5
3	1.013	59.3
4	1.029	58.7
5	1.041	58.2
6	1.026	58.8
8	1.037	58.4
10	1.030	58.7
12	1.031	58.6
18	1.032	58.6
RSD%	0.729	0.703

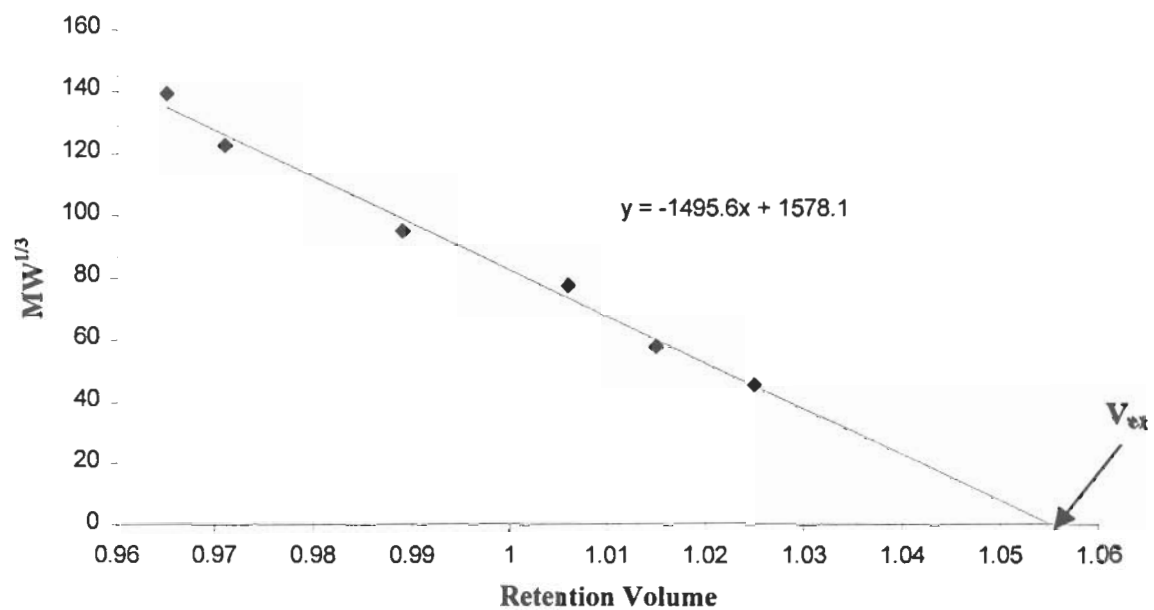
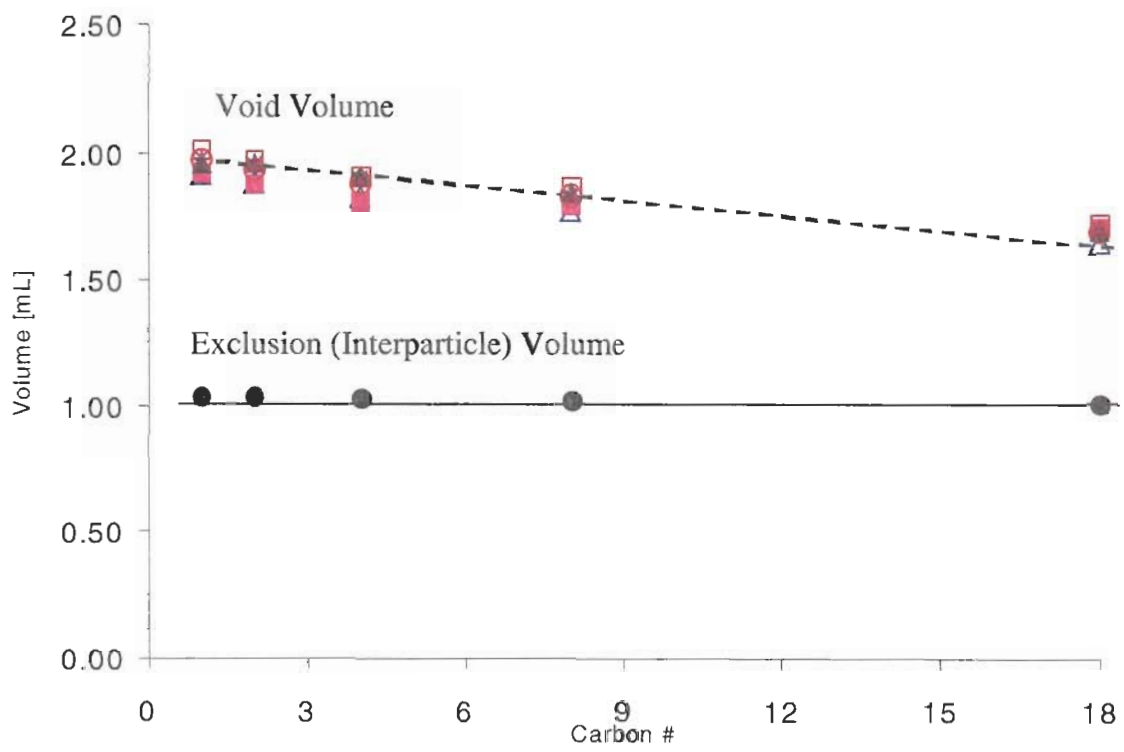


Figure 5-17. Decrease of the retention volume due to the molecular size on C₈ modified silica. V_{ex} represents the exclusion volume.



$$V_0 = V_{pore} + V_{ex}$$

Figure 5-18. Dependence of the void volume and exclusion volume of the column versus carbon number.

volume and interparticle volume versus the carbon number for the set 2 Nomo columns. It is apparent that the exclusion volume remains constant and the void volume decreases. The decrease of the void volume is attributed to the decrease of the pore volume. The void volume data was plotted from all the void volume determinations obtained by the three different methods; the data from all three independent coorelates well.

Comparison of the column void volume with the adsorbent pore volume

Modification of the silica surface does not significantly change the diameter of adsorbent particles. For example, the length of a C₁₈ chain in its all-trans conformation is about 25Å. (A 25 Å increase on the outside surface of a 5 µm particle makes only a 0.05% difference). The difference of the volume of the empty column (V_{col}) and the exclusion volume (V_{ex}) represent the total volume of all adsorbent particles in the column ($V_{part. tot}$), shown in equation 5-12. The difference of the column void volume (V_0) and interparticle volume represent the total pore volume (V_p^{tot}) in these particles and is shown in equation 5-13]

$$V_{col} - V_{ex} = V_{part. tot} \quad [5-12]$$

$$V_0 - V_{ex} = V_p^{tot} \quad [5-13]$$

The ratio of the total pore volume per column to the total particle volume represents adsorbent porosity assessed by HPLC; these values are shown in table 5-VI (column 4).

On the other hand, total volume of adsorbent particles in the column is proportional to the mass of silica in the column. It was discussed above that chemical surface modification alters only the pore volume and not the particle volume. This allows the porosity assessed from HPLC to be compared with the porosity assessed from LTNA.

If the conformation of the bonded alkyl chains at HPLC conditions is the same as it is under LTNA conditions, the pore volume (from LTNA) in reference to silica (V_p^{Si}) is proportional to the total pore volume (from HPLC), and the proportionality coefficient should be the same for all adsorbents. Indeed, for C₁ the pore volume should be the same for HPLC and LTNA, due to the lack of conformational freedom of the alkyl group. However, for a C18 modified adsorbent the situation may be different, since long alkyl chains may have different conformation under LTNA and HPLC conditions and organic eluents may show preferential solvation of the bonded layer. The ratio of the total pore volume assessed by HPLC (Table 5-VI, col. 3) and the pore volume determined by LTNA per gram of SiO₂, V_p^{Si} , (Table 5-VI, col. 5) is shown in column 6 of Table 5-VI. The ratio of HPLC to LTNA pore volume is very consistent for all columns, with a 2.5 %RSD. The graph for these experimental pore volume ratios versus carbon number, is shown in Figure 5-19. Theoretical pore volume ratios were also calculated assuming that the bonded layer would be solvated. If the bonded layer was solvated and the chains are extended, the HPLC pore volume would decrease. Hence, the pore volume ratio of LTNA/HPLC would be greater as the carbon number of the chain increased. This however is not the case and the pore volume ratio remains constant and is independent of the alkyl chain length bonded to the silica surface.

Table 5-VI

Comparison of the adsorbents porosity measured by LTNA and HPLC methods

1	2	3	4	5	6
Adsorbent	$V_{\text{part.}}^{\text{tot.}}$	$V_{\text{pore}}^{\text{tot.}}$	Adsorbent Porosity	V_p^{st}	LTNA/HPLC pore volume ratio
	$V_{\text{col}} - V_{\text{ex}}$	$V_o - V_{\text{ex}}$ (per column)	HPLC	LTNA (per g)	
C1	1.458	0.860	0.590	0.894	1.040
C2	1.458	0.875	0.600	0.901	1.030
C3	1.479	0.825	0.558	0.880	1.067
C4	1.463	0.847	0.579	0.889	1.049
C5	1.451	0.805	0.555	0.854	1.061
C6	1.465	0.792	0.540	0.853	1.077
C8	1.454	0.776	0.534	0.853	1.098
C10	1.462	0.767	0.525	0.811	1.056
C12	1.460	0.734	0.502	0.760	1.036
C18	1.459	0.681	0.466	0.685	1.007
RSD %					2.5

** V_o values used were from minor disturbance method with MeCN/Water*

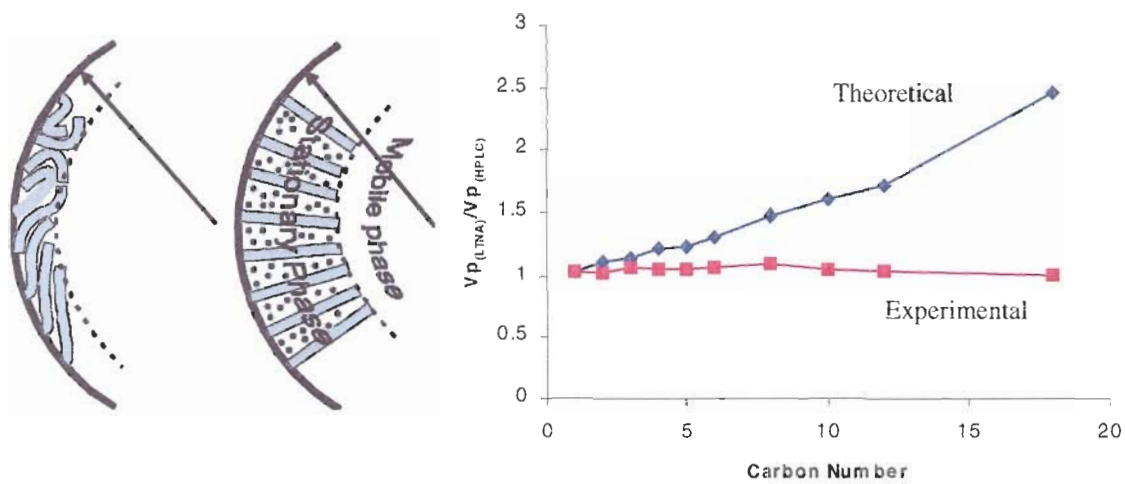
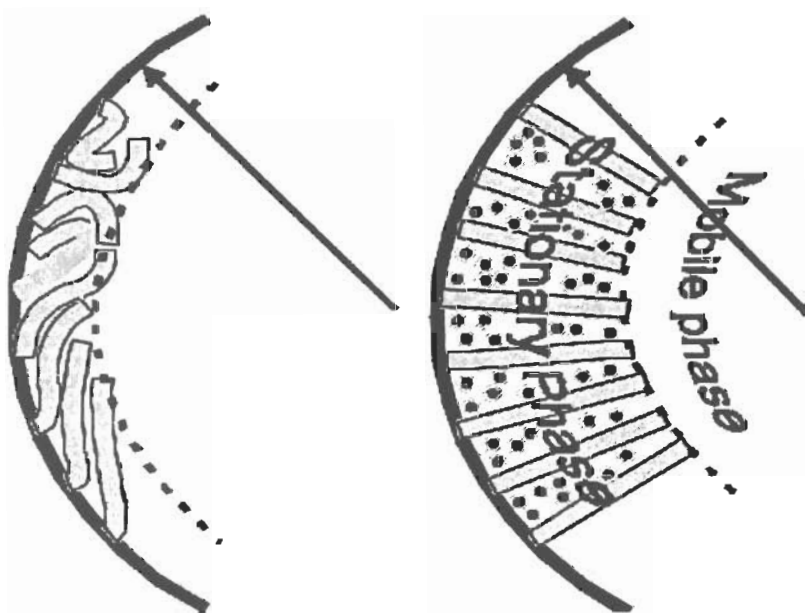


Figure 5-19. Dependence of the pore volume ratio (LTNA/HPLC): Theoretical (solvated bonded chains) and experimental (collapsed bonded chains).

The consistency of the proportionality constant over the large range of alkyl modified packings clearly indicates that the prevalent alkyl chain conformation of the bonded phase exposed to HPLC eluent is practically the same (in terms of occupied volume) as it is at LTNA conditions. Namely, alkyl chains tend to occupy lowest possible volume (“collapse”) since their own intermolecular interactions are prevalent over eluent – bonded chain interactions. The collapsed bonded layer is shown on the left and the solvated bonded layer with the eluent components is shown on the right in the schematic below.



This statement is also confirmed by the comparison of the void volume values obtained for three different eluent systems. As shown in Table 5-III, V_o values measured with methanol, acetonitrile, and tetrahydrofuran match for each column studied and are independent of the type of eluent used.

Relationship of the column void and exclusion volume with the adsorbent pore volume

The relationship among the void volume, exclusion volume, and the adsorbent pore volume also could be expressed in the form of the following equation below if the mass of the adsorbent in the column is known. The column void volume is equal to the sum of the exclusion volume and the product of the adsorbent specific pore volume and the mass of the packing material in the column.

$$V_p \cdot m_a + V_{ex.} = V_0 \quad \text{or} \quad m_a = \frac{V_0 - V_{ex.}}{V_p}, \quad [5-14]$$

where V_p is the specific pore volume of used adsorbent, $V_{ex.}$ is column exclusion volume obtained from GPC experiments, V_0 is a column void volume, and m_a is a mass of adsorbent packed in the column. When this equation is used, the actual specific pore volume of the modified material determined by LTNA must be used.

As mentioned above, adsorbent pore volume measured with LTNA may or may not represent the pore volume, which appear at HPLC conditions. However, very good correlation of the void volume values measured with three different eluents suggests that the conformation of the alkyl chains on the surface does not change much and most probably mainly maintain the conformation as it was under vacuum conditions (LTNA). In order to perform additional examination of this supposition several of the studied columns (set 2) were unpacked, and the packing material was collected, dried to constant weight (under vacuum) and weighed.

Thus we obtained all four values in equation 5-14, each by a completely independent method. Adsorbent pore volume was measured by LTNA; column exclusion volume was measured using GPC; column void volume was measured using deuterated components

and minor disturbance method; and adsorbent mass was directly weighed. Table 5-VII summarizes all values and column 5 represents adsorbent mass calculated using equation 5-14 and column 6 of Table 5-VII represents actually measured mass of adsorbent in the HPLC column. For all these five adsorbents, the calculated mass of adsorbent in the column correlates with the measured mass very well, in fact the deviation does not exceed 2.5%.

Surface area of alkyl-modified adsorbents

As previously discussed, the surface area of alkyl-modified adsorbents measured with LTNA is significantly dependent on the assumed molecular area which nitrogen molecules occupy on the surface. Besides that one could expect significant heterogeneity of the surface due to the different conformation which bonded chains may possess. This leads to the significant uncertainty in the calculation of the surface area of modified adsorbent.

The calculation of the adsorbent surface area using BET theory involves the estimation of the molecular cross-sectional area of nitrogen molecule. In general it is assumed to be equal to 16.2 \AA^2 per nitrogen molecule on the surface, but this value has been the subject of intense criticism in the past 30 years^[71].

It has been shown that nitrogen occupies a larger area on hydrophobic surface than on polar surfaces. Nitrogen molecular area on hydrophobic surfaces is estimated to be between $19 - 22 \text{ \AA}^2$ ^[69].

Adsorbent surface area is calculated as the product of the monolayer capacity, estimated from BET equation, and nitrogen molecular area, ω_{N_2} . If the specific surface area of hydrophobic adsorbent was determined using the value of $\omega_{N_2}=16.2 \text{ \AA}^2$, then total

Table 5-VII.

Correlation of the calculated and measured mass of the adsorbents in the column

1	2	3	4	5	6
Adsorbent	*V _o	V _{ex}	V _p	Adsorbent mass [g]	Adsorbent mass [g]
	[ml]	[ml]	[ml/g]	<i>Calculated</i>	<i>Measured</i>
C1	1.956	1.035	0.804	1.145	1.117
C2	1.955	1.041	0.804	1.138	1.142
C4	1.912	1.030	0.778	1.134	1.125
C8	1.845	1.026	0.727	1.127	1.150
C18	1.693	1.005	0.531	1.296	1.269

**The V_o used was determined with the minor disturbance method using MeCN/Water*

adsorbent area would be underestimated. Correct comparison of the surface area of different modified adsorbents also should be done relative to one gram of bare silica adsorbent.

The surface area dependencies on the number of carbons of the modified adsorbents measured with LTNA corrected for the different factors described above are shown in Figure 5-20. A plot of the directly measured surface area values shows a significant drop of the surface area between bare silica and C₁ modified adsorbent (Figure 5-20, line 4). Bonding a monolayer of relatively small trimethylsilane molecules could not cause this (almost 70 m²/g) drop in a surface area value. Although the increase of the effective molecular area of nitrogen from 16.2 to 20.5 Å² will cause exactly this error in the adsorbent surface measurement. The measured surface area values were corrected using nitrogen molecular area of 20.5 Å² (Figure 5-20, line 2).

On the other hand, a correct comparison of the change in the surface area due to its modification should be done by relating measured values to the same original silica weight (Figure 5-20, line 3). These values could also be corrected on the molecular area of the nitrogen shown in Figure 5-20, line 1. This leads to the significant increase of the surface areas for adsorbents modified with relatively short alkyl chains.

Although it looks strange, a restricted mobility of anchored short alkanes may actually cause an appearance of significant surface heterogeneity (roughness) which leads to the increase of the “monolayer” capacity and results in an increase of the total surface area. This is probably not the true surface area value, which will play any role in the

HPLC process, and it is doubtful that any of these values may be relevant for the description of HPLC retention.

The assessment of the surface area of modified adsorbent is **extremely uncertain**. Accounting for different types of corrections may lead to the significant differences in the calculated surface areas of the same material. The dominating factor is probably the roughness of the surface of modified silica. Differences in the alkyl chain conformations may lead to the completely different values of the same material. Possible occlusion of nitrogen molecules between alkyl chains adds additional uncertainty ^[72].

One definite surface parameter, the surface area of original bare silica, also is common to all related modified adsorbents. It is probably most appropriate to relate all processes to the surface of bare silica (making corresponding corrections for modified adsorbents on the fraction of the silica in 1 gram of actual material).

Total surface area of silica in the HPLC column could be calculated using the following equation, provided that V_0 , V_{ex} , V_{pore} , S_{SiO_2} , and bonding density (d_b) are known.

$$S_{SiO_2}^{total} = \frac{S_{SiO_2} (V_0 - V_{ex})}{V_{pore} [1 + S_{SiO_2} d_b (58 + 14n_c)]} \quad [5-15]$$

where n_c is the number of carbons in the main alkyl chain of the bonded phase.

Determination of void volumes of 8 other columns

Void volumes were determined for six other columns from different manufacturers using the minor disturbance method and deuterated components. These columns were all different in their geometric properties: Kovasil-C14 silica is non porous

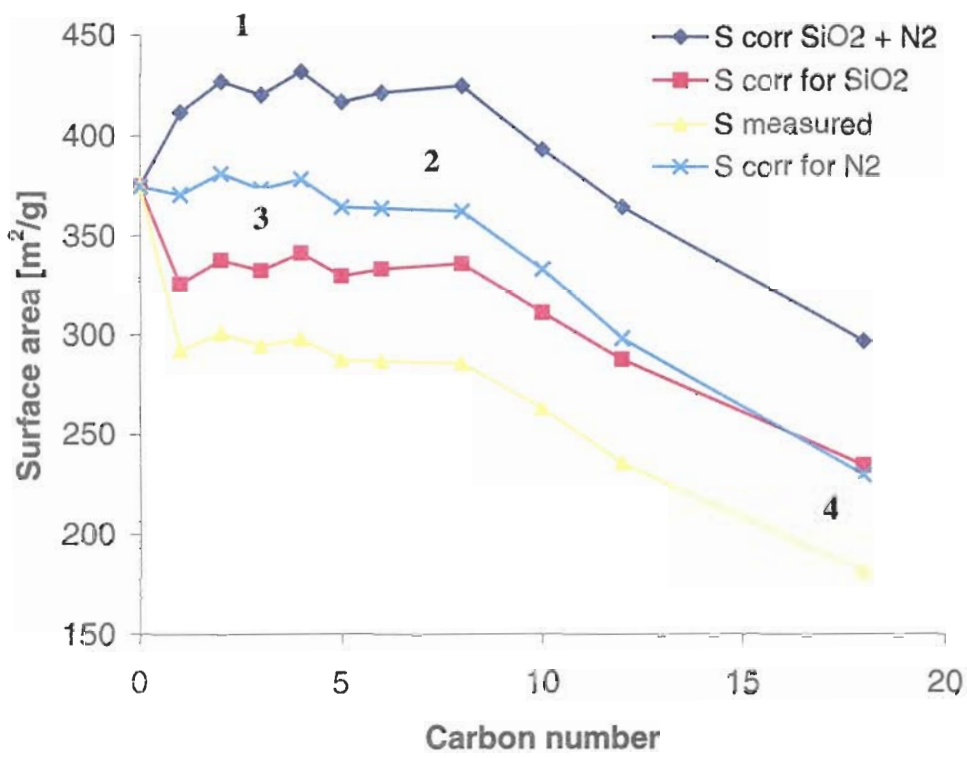


Figure 5-20. Measured and corrected surface area values of studied adsorbents.

Table 5-VIII

Void volume values of 6 commercial columns

Manufacturer	Column	*V_o
Phenomenex	Luna C18	1.586
Phenomenex	Jupiter C18	1.941
Phenomenex	Luna C18-2	1.578
Uketron	Kovasil C14	0.447
Waters	Symmetry C18	1.441
Hewlett Packard	Zorbax Eclipse XDB-C18	1.392

* All corrected for system volume, 0.053 μ L

and Jupiter C₁₈ has 300 Å pore size. Table 5-VIII shows a comparison of void volumes of those columns determined by the minor disturbance method. The retention volumes are shown in Appendix Table A5-IX and Table A5-X. The void volumes were also determined by using a mobile phase of 100% acetonitrile and injecting pure CD₃CN. The void volume value was 1.409 mL for Zorbax Eclipse XDB-C₁₈ and was 1.577 mL for the Luna C₁₈. The void volume values determined using the two methods (minor disturbance and deuterated components) agree well. The excellent correlation was also observed with the Nomo Set 1 and Set 2 data.

Effect of temperature on void volume

The retention of minor disturbance peaks of the eluent components at different temperatures for three types of organic modifiers in the eluent are compared: acetonitrile-water, methanol-water and benzene-acetonitrile. Figure 5-21 shows the dependence of the retention of the minor disturbance peaks for methanol (from a methanol-water eluent) on the eluent composition for a Prodigy ODS-2 column at different temperatures (5, 10, 20, and 28°C). Figure 5-22 shows the dependence of the retention of the minor disturbance peaks for acetonitrile (from an acetonitrile-water eluent) on the eluent composition for a Prodigy ODS-2 column at different temperatures (10, 20, 30, 40, and 50°C). Figure 5-23 shows the dependence of the retention of the minor disturbance peaks for benzene (from an acetonitrile-benzene eluent) on the eluent composition for a Prodigy ODS-2 column at different temperatures (5, 15, 25, 35, 45, and 55°C). It is observed that they all show a significant difference in the shape of the curve. The temperature stability was better than 0.1 °C, and the percent relative standard deviations for the retention times was better than 0.6% (at least 4 injections per point). The calculated V_o values in Tables

5-IX, 5-X and 5-XI indicate the linear dependence of temperature. Figure 5-24 shows the void volume dependence on temperature with the three different eluent systems and the data correlate well at all temperatures, %RSD less than 2% at all temperatures. The void volume was also determined for the Prodigy and Prodigy ODS-2 columns with deuterated acetonitrile at 30°C: Prodigy, 1.969 mL and Prodigy ODS-2, 1.679 mL. These data correlate well with the void volumes determined by the minor disturbance method which were 1.688 mL at 30°C for Prodigy ODS-2, and 2.055 mL at 25°C for Prodigy. The void volume measured with deuterated acetonitrile was about 90 μ L less than the value obtained using the minor disturbance method. This can be attributed to the trace water in the acetonitrile that may be adsorbed on the silica surface. The level of water was not determined in the acetonitrile for the deuterated experiments. The acetonitrile used for the minor disturbance experiments was dried under molecular sieves and had a Karl Fisher titration value of less than 30 μ g/mL.

The V_o values determined with the minor disturbance method indicate that the higher the temperature, the lower the dead volume (Void Volume + system volume). However, thermal expansion of the column tubing should give greater values for the dead volume. A possible explanation in the literature was given that there could be thermal expansion of the volume of the bonded phase^[60]. The change in V_o for the methanol-water system was calculated to be 25.3 μ L/10 °C, which is about 1.5% of the void volume. The total surface area of the adsorbent in the column was 340 m². The expansion coefficient (25.3 μ L/10 °C) divided by the surface area gives the possible effective linear expansion of the alkyl chains on the surface which is, 0.81 Å/10°C. In the acetonitrile-water system, there was also a decrease in the void volume upon increasing

temperature; the expansion coefficient was $17.6 \mu\text{L}/10^\circ\text{C}$, which is about 1.2% of the void volume, and corresponds to a possible linear expansion of $0.56 \text{ \AA}/10^\circ\text{C}$ for the alkyl chains. In the acetonitrile-benzene system, there also was a decrease in the void volume upon increasing temperature: the expansion coefficient was $22.5 \mu\text{L}/10^\circ\text{C}$, which is about 1.4% of the void volume, and corresponds to a possible linear expansion of $0.72 \text{ \AA}/10^\circ\text{C}$ for the alkyl chains.

Figure 5-25 shows the dependence of the retention of the minor disturbance peaks for acetonitrile (from an acetonitrile-benzene eluent) on the eluent composition for a Prodigy Silica column at different temperatures (5, 15, 25, 35, and 50°C). The calculated V_o values in Table 5-XII indicate the linear dependence of temperature as previously seen for the chemically modified C18 silica, Prodigy-ODS-2. The decrease in void volume was noted and a slope of $25.4 \mu\text{L}/10^\circ\text{C}$, which corresponds to about 1.5% of the void volume, was calculated. This corresponds to a possible linear expansion coefficient of $0.80 \text{ \AA}/10^\circ\text{C}$. Therefore, since we saw approximately the same increase in the thermal expansion coefficient with the unmodified silica, the decrease in the void volume cannot be attributed to the linear expansion of the alkyl chains. However, it is possible that upon increasing the temperature the silica may swell. However, we speculate that amorphous silica may swell upon heating. This would account for the decrease in the void volume of the two different columns, modified and unmodified adsorbents, with increasing temperatures.

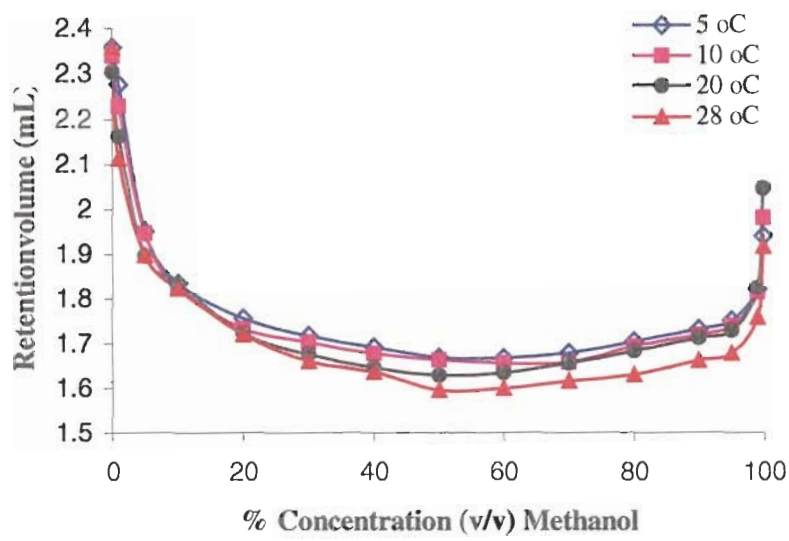


Figure 5-21. Dependencies of the minor disturbance peaks for the same eluent at different temperatures. Prodigy ODS-2 Methanol/Water at different temperatures.

Table 5-IX**Retention volume dependence for methanol disturbance peak from 5 – 28 °C**

Conc. MeOH (v/v%)	Retention (V_R) mL			
	5 °C	10 °C	20 °C	28 °C
0	2.3585	2.34	2.3045	2.358
1	2.277	2.23	2.163	2.113
5	1.952	1.9475	1.898	1.8985
10	1.836	1.823	1.833	1.823
20	1.7575	1.735	1.7235	1.722
30	1.719	1.7045	1.676	1.662
40	1.6935	1.6785	1.646	1.637
50	1.6705	1.6645	1.629	1.597
60	1.6695	1.657	1.634	1.602
70	1.681	1.6595	1.6555	1.617
80	1.7065	1.694	1.6825	1.631
90	1.7335	1.7205	1.7125	1.663
95	1.752	1.7405	1.729	1.679
99	1.8215	1.8145	1.8245	1.7585
100	1.942	1.982	2.046	1.9195
$V_o =$	1.748	1.734	1.715	1.687

Prodigy ODS-2, Methanol/Water, Temp: 5- 28°C, Decrease in void volume: slope 25.3 $\mu\text{L}/10^\circ\text{C}$, 1.5% of the void volume, Corresponds to a 0.81 $\text{\AA}/10^\circ\text{C}$ change.

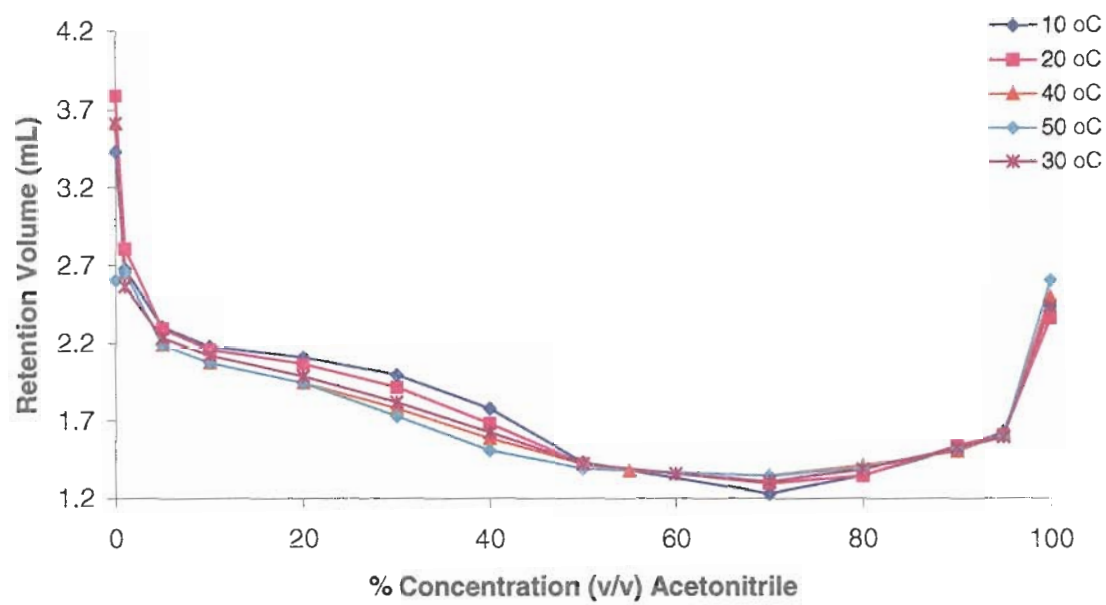


Figure 5-22. Dependencies of the minor disturbance peaks for the same eluent at different temperatures. Prodigy ODS-2 MeCN/Water at different temperatures.

Table 5-X

Retention volume dependence for acetonitrile disturbance peak from 10 – 50 °C

Conc. MeCN	10 °C	20 °C	30 °C	40 °C	50 °C
0	3.431	3.79	3.611	3.61	2.60
1	2.674	2.803	2.561	2.65	2.65
5	2.301	2.293	2.233	2.19	2.19
10	2.181	2.159	2.119	2.07	2.07
20	2.106	2.064	1.985	1.94	1.94
30	1.993	1.914	1.815	1.78	1.73
40	1.779	1.681	1.624	1.59	1.51
50	1.434	1.423	1.425	1.42	1.40
55				1.377	
60			1.362		
70	1.23	1.298	1.307	1.35	1.35
80	1.35	1.347	1.39	1.41	1.40
90	1.526	1.538	1.527	1.51	1.52
95	1.629	1.612	1.602	1.61	1.60
100	2.443	2.367	2.443	2.50	2.60
V ₀ =	1.731	1.718	1.688	1.679	1.662

Prodigy ODS-2, Acetonitrile/Water, Temp: 10- 50°C, Decrease in void volume: slope 17.6 $\mu\text{L}/10^\circ\text{C}$, 1.2% of the void volume, Corresponds to a 0.56 $\text{\AA}/10^\circ\text{C}$ change.

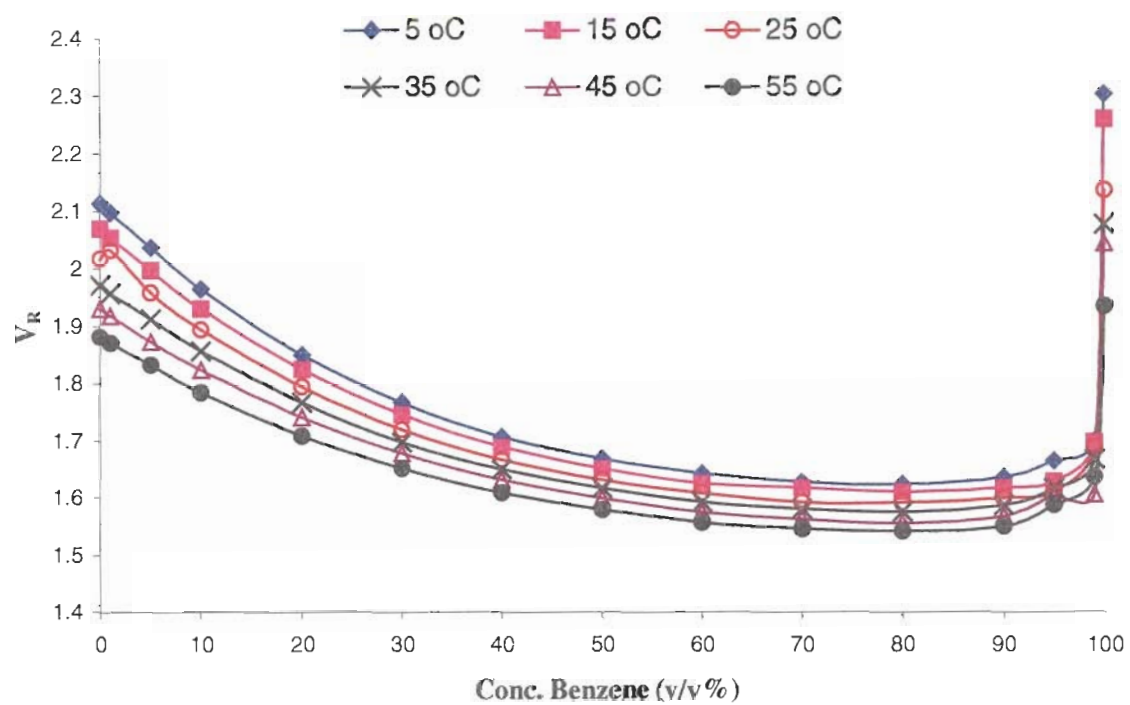


Figure 5-23. Dependencies of the minor disturbance peaks for the same eluent at different temperatures. Benzene minor disturbance peaks. Prodigy ODS-2 Benzene/Acetonitrile at different temperatures.

Table 5-XI

Retention volume dependence for benzene disturbance peak from 5 – 55 °C

Conc. Benzene	5 °C	15 °C	25 °C	35 °C	45 °C	55 °C
0	2.115	2.071	2.017	1.972	1.93	1.882
1	2.098	2.055	2.033	1.958	1.918	1.871
5	2.038	1.997	1.959	1.913	1.873	1.832
10	1.965	1.93	1.894	1.856	1.823	1.784
20	1.849	1.824	1.794	1.766	1.741	1.709
30	1.766	1.746	1.72	1.698	1.678	1.651
40	1.708	1.69	1.667	1.65	1.632	1.609
50	1.669	1.652	1.632	1.617	1.599	1.579
60	1.643	1.626	1.608	1.592	1.575	1.557
70	1.628	1.618	1.592	1.58	1.563	1.546
80	1.624	1.611	1.591	1.575	1.556	1.542
90	1.636	1.618	1.599	1.586	1.568	1.55
95	1.665	1.629	1.611	1.616	1.602	1.587
99	1.701	1.699	1.689	1.667	1.606	1.637
100	2.306	2.262	2.14	2.08	2.047	1.938
$V_o =$	1.742	1.721	1.697	1.676	1.653	1.630

Prodigy ODS-2, Benzene/Acetonitrile, Temp: 5- 55°C, Decrease in void volume: slope 22.5 $\mu\text{L}/10^\circ\text{C}$, 1.4% of the void volume, Corresponds to a 0.72 $\text{\AA}/10^\circ\text{C}$ change.

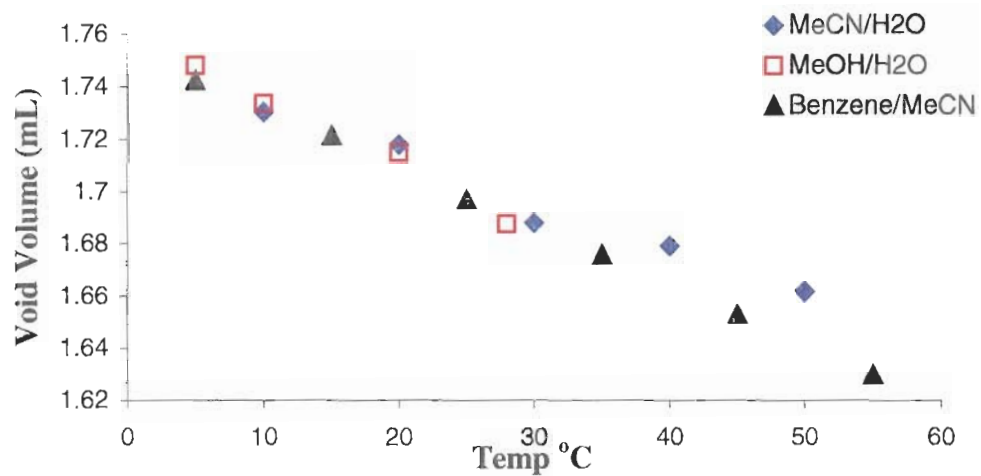


Figure 5-24. Comparison of the void volumes. Void volumes determined for Prodigy ODS-2 with three different eluent systems using the minor disturbance method.

MeCN/Water and methanol/water corrected for system volume of 0.053 μL , 401 RI detector. MeCN/Benzene corrected for system volume, 0.083 μL , UV detector.

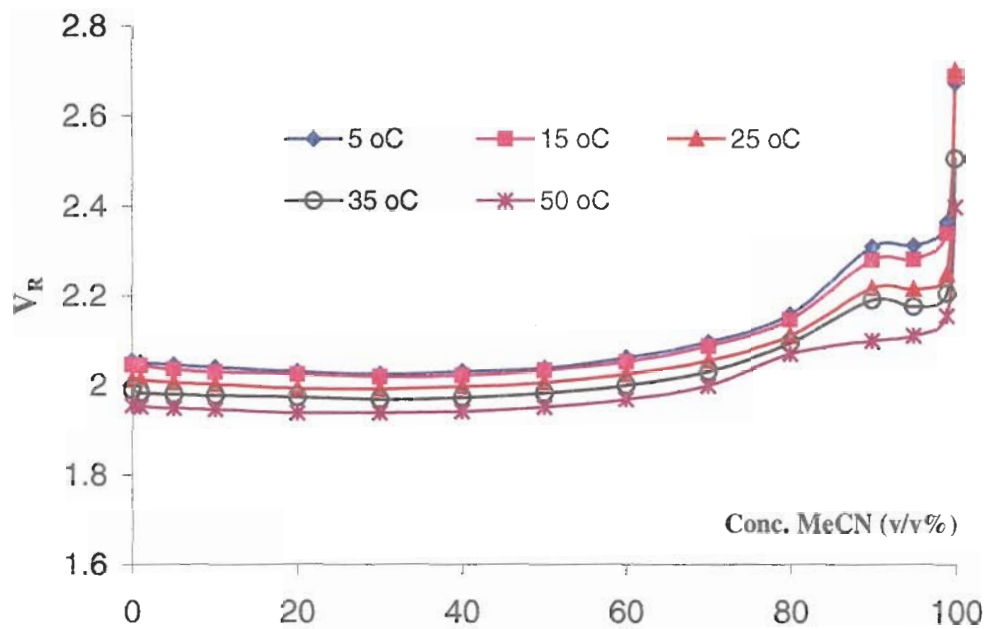


Figure 5-25. Dependencies of the minor disturbance peaks across the entire concentration range of acetonitrile at different temperatures. Column: Prodigy Silica, Acetonitrile/Benzene at different temperatures.

Table 5-XII

Retention volume dependence for acetonitrile disturbance peak from 5 – 50 °C

Prodigy Silica

Conc. MeCN	5 °C	15 °C	25 °C	35 °C	50 °C
0	2.055	2.046	2.014	1.99	1.956
1	2.051	2.045	2.013	1.983	1.953
5	2.047	2.037	2.007	1.981	1.95
10	2.041	2.031	2.004	1.978	1.948
20	2.032	2.026	1.995	1.974	1.94
30	2.026	2.021	1.993	1.969	1.94
40	2.032	2.023	1.999	1.973	1.943
50	2.039	2.035	2.007	1.983	1.953
60	2.062	2.054	2.026	2.001	1.971
70	2.096	2.088	2.056	2.031	2.001
80	2.157	2.146	2.11	2.092	2.069
90	2.309	2.279	2.216	2.188	2.098
95	2.312	2.28	2.214	2.174	2.11
99	2.363	2.339	2.247	2.204	2.154
100	2.672	2.687	2.699	2.506	2.397
$V_o =$	2.101	2.090	2.055	2.029	1.992

Prodigy Silica, Benzene/Acetonitrile, Temp: 5- 50°C, Decrease in void volume: slope 25.3 $\mu\text{L}/10^\circ\text{C}$, 1.5% of the void volume, Corresponds to a 0.81 $\text{\AA}/10^\circ\text{C}$ change.

It was shown that specific pore volume of alkyl modified HPLC adsorbents measured with LTNA method are consistent with pore volumes determined at HPLC conditions. The void volume, one of the most important characteristics of HPLC columns has been measured by three different methods (minor disturbance, retention of isotopically labeled components, and pycnometry). All three methods from six different experiments had shown similar results and RSD is less than 2%. These methods allow the measurement of the total volume of the liquid phase in the column without distinction if the liquid is moving, stagnant or retained at close proximity of the surface due to the viscosity or surface interactions. This approach is the most universal one, since it allows a comparison of different systems, and it is similar to the convention “Nothing is adsorbed” introduced by Riedo and Kovats^[42] for the description of adsorption systems.

Our results suggest that despite the existence of conformational freedom and definite presence of chain mobility (which had been shown in various studies in the literature^[20,23,73]) of bonded ligands, their average arrangement in bonded layer remains very dense “liquid like”. The possible penetration of significant amount of organic eluent in between these chains is very unlikely. This conclusion is drawn from the similarity of the geometric parameters assessed using LTNA (vacuum conditions) and HPLC. This similarity was observed for all studied chemically modified adsorbents, from C₁ to C₁₈.

Our study for the determination of the void volume has shown that the most practical and convenient method for the measurement of the total volume of the liquid phase in the column (void volume) is the injection of isotopically labeled sample of a single component eluent. Injection of the deuterated acetonitrile in the column with

regular acetonitrile as the eluent is probably the most practical procedure. One of the advantages of this method is that the measured void volume value is independent of the amount of acetonitrile injected.

Our study has also suggested a convenient method for estimating the actual amount of the adsorbent packed into the column, without actually unpacking it. This could be done by simply measuring the exclusion volume (GPC) and column void volume (labeled component), and obtaining adsorbent pore volume which may be obtained from the column manufacturer.

Excess Adsorption

The excess adsorption isotherms determined with the minor disturbance method using three different mobile phase systems were compared. The results indicate that methanol shows monomolecular adsorption and acetonitrile and THF show multilayer adsorption. The purpose of the second part of this chapter is to describe the characteristics of the organic adsorbed layer in three different eluent systems by obtaining the surface excess isotherms using the minor disturbance method. The description and thickness of this layer will be discussed. The thickness of the adsorbed organic and the bonded layer have been corrected for the curvature of the surface. Also, the total amount of organic portion of the eluent excessively adsorbed above equilibrium conditions determined using the surface excess isotherms from minor disturbance and deuterated components will be compared to demonstrate the validity of the two approaches.

Composition of the binary (water/organic) eluent in reversed phase HPLC shows great influence on the analyte retention. The effect of the type of the organic modifiers

and mobile phase compositions on the analyte retention may be a direct consequence of the adsorption of organic modifier on the adsorbent surface.

In an attempt to understand the solute retention mechanism(s) in reversed-phase liquid chromatography (RPLC), a large number of papers have been devoted to the surface characterization of n-alkyl bonded phases [74-75]. Knox and Pyrdé [76] were among the first to propose the importance of the uptake of the organic modifier in the stationary phase, and their hypothesis was experimentally verified by Scott and Kucera [46,77] and others [78-79]. In order to obtain more insight into the influence of the modifier chain length and the nature and concentration of the organic modifier, it is important to study the adsorption isotherms for organic modifiers on reversed-phase materials.

The amount of organic eluent component adsorbed on the stationary phase support can be determined only as the surface excess amount. General relationships for calculating the surface excess amount from chromatographic retention data have been given by Wang Duda and Radke [58]. The chromatographic methods to determine the surface excess were based on measurements of the retention volumes of concentration steps (frontal analyses) [58,80-81], isotopically labeled components of the eluent, and solvent disturbance peaks [33-34,56].

The surface excess amount depends upon the type of organic component and the composition of the mobile phase. The excess adsorption isotherm is also under the influence of the type of bonded phase. The type of bonding such as monomeric or polymeric has also shown to have an influence on the preferential adsorption of organic eluents in a binary system [82].

Adsorption isotherms have attracted great attention for many years as fundamental tools for investigation of the physical processes involved in chromatographic retention. McCormick and Karger^[34] studied the elution behavior of isotopically labeled solutes in three organic modifiers mixed with water: methanol, acetonitrile and THF. The interpretation of the elution data of the isotopically labeled solutes (ILS) and minor disturbance peaks (MD) was based on Helfferich's equation for the finite band migration in liquid chromatography^[83-84]. Slatts^[33] used ILS and MD to study the adsorption of solvent components of acetonitrile and methanol with aqueous binary mixtures, in a liquid-solid chromatographic column in terms of surface excess.

The first mathematical description of ideal equilibrium gas chromatography using a differential material balance was derived by Wilson^[85] and subsequently modified by DeVault^[86] Wang et. al.^[58] applied a similar approach for liquid chromatography.

Solution of the mass-balance equation requires mathematical description of analyte distribution between the surface and the liquid phase. This could be accomplished in two ways.

- 1). Use of the classical Gibbs approach requires the definition of the position of the imaginary dividing plane. Above this plane, the absence of the adsorbent influence is assumed and equilibrium analyte concentration is not disturbed. Space below this plane is considered as an adsorbed phase and the analyte is under the influence of adsorption forces.
- 2). If the existence of some small volume of the liquid phase where there is no influence of the adsorbent surface forces (in HPLC this is at the column outlet) is assumed, then the adsorption effect can be associated to the surface and excessive values can be used.

Excess adsorption is defined as the difference between the amount of the component that would be in a hypothetical system without the surface influence and the same system with the influence of the surface ^[55]. The first system corresponds to the two component solutions with the concentration of the solute (C_o), volume (V) and pressure (P) without any influence from the adsorbent surface. The second system is essentially the same as the first one except that the solution is in contact with the adsorbent surface. The volume V_o^i of a binary solution contains, before adsorption, a concentration C_o^i of the i^{th} component, which decreases to C_e^i , when the solution is brought into contact with the adsorbent. Owing to the effect of adsorption forces, an excess of $\Gamma_i^{(v)}$ moles (per unit area of the surface mS) is created in the adsorption volume close to the surface. Therefore, excess adsorption, Γ , in general, can be defined as the following:

$$\Gamma = \frac{(C_o - C_e)V_o}{mS} \quad [5-16]$$

Where V_o is total volume of liquid phase in the system, m is the mass of adsorbent; S is the specific surface area; C_o is the initial concentration; and C_e is the concentration after equilibrium. In this approach, adsorbed layer on the surface is a part of the liquid phase and does not need to be defined. Excess adsorption is an experimentally accessible quantity and is advantageous since no model is required to interpret the experimental data. The data can be obtained experimentally without being limited to any abstract boundary concept, such as the Gibbs dividing surface ^[87].

The definition [5-16] of excess adsorption and its relationship with the HPLC retention volume allow the direct chromatographic measurement of excess adsorption

isotherms without assuming any specific model, save the assumption on the thermodynamic equilibrium in the column. Further interpretation of these isotherms will require the introduction of some type of retention model.

This approach is useful in the physico-chemical description of adsorption from the liquid phase and allows the calculation of the amount of organic modifier adsorbed on the surface. The preferentially adsorbed layer may be denoted as V_a . The volume of liquid mobile phase within the column, V_m , is equal to the difference between V_o , the void volume, and V_a , the volume of the adsorbed layer. This is essentially an introduction to the Gibbs dividing plane for the model of the finite thickness adsorbed layer.

According to the definition given by Gibbs for excess adsorption, it must be assumed that the adsorption process is isochoric; no volume contractions or expansions occur near the solid surface due to changes in molecular configuration, orientation, or force fields.

Quantitative definitions for adsorption of mixtures at solid-liquid interfaces in terms of surface excess amounts were given by Everett,^[88] and general relationships for calculating the surface excess amount from chromatographic retention data were given by Riedo and Kovats^[42]. In 1962 Kiselev and Pavlova^[89] showed different ways to express excess amount, Γ , (Equation 5-16) related to the solution mass, volume, mole fraction, or concentration per surface area. Precautions should be taken when dealing with concentration. Calculating the surface excess based upon concentration introduces an uncertainty because volume changes may occur on adsorption and the partial molar volumes may also vary with composition. Insufficient wetting leads to incomplete pore

filling, and void volume is not constant. In other words, the additivity of volumes is no longer valid, and the concentration-based excess is not valid for chromatographic data. The actual form, volume, is preferred because volume is the measured quantity in chromatographic experiments (V_r). It also should be noted that by using the volume notion as a basis for excess measurement, one calculates volume of the adsorbed layer directly from the excess isotherm^[42]; this will be discussed later in this chapter.

Measurement of excess adsorption

The experimental measurement of excess adsorption can be performed by static or dynamic methods. In the static method, the difference of concentrations of one of the components of a binary system, component 1, in the initial solution and in the solution in equilibrium with the adsorbent is measured. The method of measurement of adsorption from solution entails immersing a known weight of adsorbent in solutions into closed vessels each containing a solution of a different concentration. When the adsorption equilibrium is established (usually after many hours), the equilibrium concentration of the solution of the adsorbent is measured.

$$\Gamma = \frac{(C_o - C_e)V}{mS} \quad [5-17]$$

where V is the volume of the solution used in the measurement, and C_o and C_e are the volume concentrations of component 1 in the initial and adsorption equilibrium solutions, respectively. Kurbanbekov^[90] applied this static method where a solution is pumped through a bed of adsorbent in a closed cycle until adsorption equilibrium is reached to determine adsorption from solution.

Determination of excess amount using labeled components

Theoretical basis for this method was previously given by Riedo and Kovats^[42]. They showed that excess amount can be calculated from retention volume of labeled components using Equation 5-18.

$$V_{r,A}^* = V_o + S \left(\frac{\Psi_A}{\Phi_A} \right)_{\Phi_A} \quad [5-18]$$

Where $V_{r,A}^*$ is retention volume of labeled component A , ψ_A is excess amount of component A in terms of volume ($\mu\text{mol}/\text{m}^2$), θ_A is volume fraction of component A , and V_o is the void volume determined by the retention volume of the deuterated component in the corresponding nondeuterated eluent. The two assumptions made when using Equation 5-18 are that the mixture is ideal and that isotopic exchange is ignored^[91].

Determination of excess amount using minor disturbance method

Excess adsorption, Ψ (in terms of volume), can be calculated from Equation 5-7 using its integral form.

$$\Psi_{\Phi} = \int_{\Phi_{\min}}^{\Phi_{\max}} \left(\frac{Vr - V_o}{S} \right) d\Phi \quad [5-19]$$

Surface area and void volume are properties of the chromatographic column. Measurement of the dependence of the minor disturbance peak retention through the entire range (volume fraction) allows the calculation of the excess adsorption, in terms of volume, of the component using Equation 5-19.

Comparison of minor disturbance method and labeled components

The void volume is constant for any given column and should not be method specific. A few authors^[33-34] have obtained similar values for void volume of a column determined by either minor disturbance method or labeled components gives similar values. Even though the results were presented to show the similarities, there was no mathematical relationship given to explain the correlation. By rearranging equation 5-16 we get equation 5-20 an equation that shows the fundamental relationship of the two methods for the determination of the void volume.

$$\Gamma mS = C_oV_o - C_eV_o \quad [5-20]$$

According to the definition of excess adsorption, C_oV_o is the amount of the component 1 in the system in the absence of adsorption forces. In the presence of adsorption forces, analyte concentration on the mobile phase will be C_e . Since it is assumed that the isotopically labeled component injected into the column has the same behavior as the component of the liquid phase, then in the presence of adsorption forces its retention V_R could be written as follows

$$V_R C_e = C_o V_o \quad [5-21]$$

This equation shows that the process in a column follows first law of thermodynamics; conservation of mass. After substituting $V_R C_e$ for $V_o C_o$ in equation 5-20, equation 5-22 is obtained:

$$V_R C_e - V_o C_e = \Gamma mS \quad [5-22]$$

This equation can be used to determine the excess adsorption isotherms in terms of $\mu\text{mol}/\text{m}^2$ using deuterated components. This equation is also consistent with equation 5-34 in which the excess amount at each mobile phase composition was calculated directly for the deuterated component.

Excess adsorption determined using minor disturbance and deuterated components

We can assume that analytes in the mixture are in very low concentration and after being injected into the column they are separated from each other and do not show any analyte – analyte interactions. Considering isocratic conditions binary eluent is in the equilibrium with the column prior the analyte injection. It has been shown that water-organic eluents show the excess adsorption of the organic component of the reversed-phase adsorbent^[88], which means there is some type of layer with different water-organic composition at the adsorbent surface. Is this layer monomolecular or does it have a greater thickness?

Unfortunately the answer to this question is difficult to obtain since all publications on the adsorption of the eluent components represent the experimental data in moles of the adsorbed component per gram of the adsorbent. This is in fact related to the difficulty of measuring the actual surface area of the adsorbent inside the column.

D.H.Everett^[92] had described the interpretation of the excess adsorption isotherm of binary mixtures. The procedure proposed by D. Everett^[92] allows the estimation of the maximum amount of organic component which could be accumulated in the adsorbed layer. As illustrated in Figure 5-26, Everett showed that for the monomolecular adsorption model, the crossing of the tangent to the slope of the excess adsorption isotherm in the saturation region with the y-axis represents the reciprocal value of the

adsorbate molecular area. According to Everett, when the y values are represented as $[\mu\text{Moles}/\text{m}^2]$ and are plotted versus mole/L of the excessively adsorbed they represent the total number of molecules accumulated on the unit of surface. The molecular area of the acetonitrile may be obtained by dividing the reciprocal maximum amount adsorbed by Avogadro's number. Multiplication of the maximum adsorption value ($\mu\text{mol}/\text{m}^2$) by the molecular volume of acetonitrile (\AA^3) and Avogadro's number allow us to estimate the thickness of the adsorbed acetonitrile phase. The multiplication of this thickness by the adsorbent surface area relative to bare silica will yield the estimated volume of the adsorbed acetonitrile layer.

Everett's approach assumes the monomolecular adsorption from the binary system. As we discussed above, in our measurements of excess adsorption isotherms, no specific assumptions on the adsorption model has been made.

If we assume a finite thickness adsorption model and constant molecular volumes of components of the liquid phase (same in bulk and adsorbed phase), then Everett's method allows us to estimate the actual thickness of adsorbed layer.

The linear decrease of the excess adsorption with the increase of the equilibrium concentration are associated with the saturation of the adsorbed layer. Propagation of this slope towards the y-axis will give maximum possible (absolute) amount of adsorbed component which could be accumulated in the adsorbed layer. The multiplication of that amount by the component molecular volume gives the adsorbed layer volume, and division of this volume of the adsorbent surface area will give the adsorbed layer thickness.

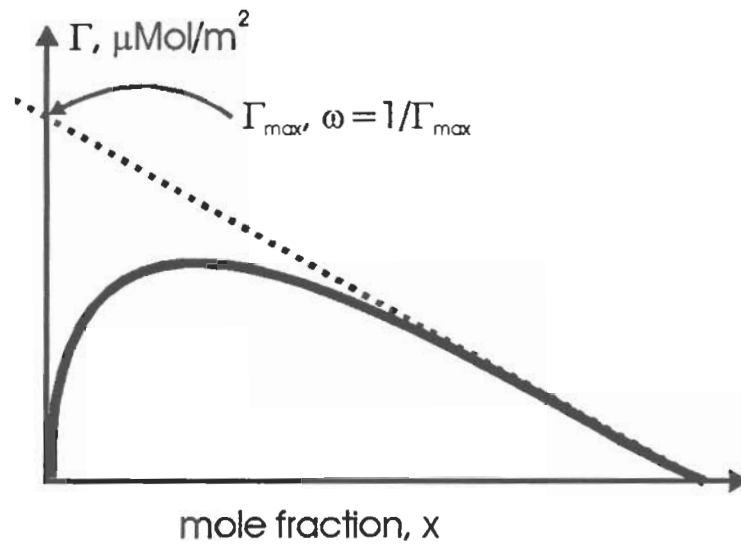


Figure 5-26. Determination of the adsorbate molecular area from the excess adsorption isotherm for monomolecular adsorption model.

Excess adsorption isotherms of acetonitrile from water have been measured by means of the minor disturbance method. The retention volume values over the entire composition range are given in the Addendum, Tables A5-I – A5-V. Excess adsorption values [$\mu\text{mole}/\text{m}^2$] were calculated using the corrected surface area and total mass of the adsorbent in the column (as previously discussed). The excess adsorption isotherms have also been measured using deuterated components. The retention volume values over the entire composition range are given in the Addendum, Tables A5-VI – A5-VIII.

We measured the excess adsorption of acetonitrile from water using a series of reversed-phase columns (Nomo Columns) packed with the adsorbent of the same silica structure shown in Figure 5-27. We also measured the excess adsorption isotherms in methanol/water and THF/water shown in Figure 5-29 and Figure 5-30 respectively. All these isotherms were plotted as amount per unit area at each molar concentration of acetonitrile/water, methanol/water, and THF/water. However, in Figure 5-28 the amount is expressed in volume units per unit area ($\mu\text{L}/\text{m}^2$) at each mole fraction. Since, it is assumed that the molecular volume of the adsorbed species does not change upon adsorption, for sake of convenience, we determined from the intercept the maximum surface excess amount adsorbed (thickness of the adsorbed layer). Surface excess isotherms were measured over the entire composition range of the three binary systems of Acetonitrile, Methanol and Tetrahydrofuran from water, using minor disturbance method. The surface excess isotherms were only determined with acetonitrile from water using the labeled eluent components and are shown in Figure 5-31, Figure 5-32, and Figure 5-33. Table 5-XVI shows a comparison of the excess adsorption isotherms for 3 columns (

Nomo set 1) , C₈, C₁₂, and C₁₈ obtained using the minor disturbance and deuterated components.

The excess adsorption isotherms of all bonded phases are compared for different organic modifiers. Excess adsorption isotherms determined by the minor disturbance method are shown to be highly reproducible (day to day, instrument to instrument and analyst to analyst). The main aim of this work was to gain some understanding, on a molecular level, of the rich organic adsorbed layer and to measure dead volume of a column by different methods (minor disturbance and isotopically labeled eluents). Comparing excess adsorption isotherms obtained from different bonded ligands which are attached to the same starting silica can provide a better understanding of the adsorbed layer on top of the bonded ligand. Performing this study will also help to clarify the retention mechanism in RPLC, since it has been shown that there is an organic rich phase adsorbed on the bonded phase (which is different than the mobile phase) suggesting a complex retention mechanism.

Calculated values for the adsorbed layers using the retention volume dependence from the minor disturbance method are shown in Table 5-XIII for acetonitrile, Table 5-XIV for methanol, and Table 5-XV for THF. Column 2 includes the corrected surface areas of the modified adsorbent related to the same amount of original silica. Column 3 shows the total amount adsorbed, Γ_{\max} , obtained using the Everett approach. Column 4 includes the apparent molecular area, which is obtained by multiplication of the reciprocal of Γ_{\max} and reciprocal of Avogadro's number. Column 6 includes the adsorbed layer thickness, τ_a , which is obtained by multiplication of the Γ_{\max} by the molecular volume of the component and Avogadro's number. Column 5 shows the

volume of the adsorbed layer is obtained by multiplying the τ_a and the surface area of the modified adsorbent in reference to the bare silica. Column 7 lists the corrected values (for the surface of curvature) for the bonded layer. The experimental adsorbed layer values, as well as the bonded layer values, were corrected for curvature of the radius in the pore. This procedure for the correction for curvature is described in the Appendix. Also, the adsorbed layer was determined using deuterated components for the C₈, C₁₂ and C₁₈ Nomo Set 1 columns and correlate well with the adsorbed layer determined by using the minor disturbance peaks shown in Table 5-XVI.

Table 5-XIII**Characteristics of the acetonitrile adsorbed layer**

Determined using retention volumes from minor disturbance method (Set 1 columns).

1	2	3	4	5	6	7
Adsorbent	Corrected surface area	Γ max	Apparent molecular area	Volume of ads. layer	*Adsorbed Layer thickness	*Volume of alkyl bonded layer
	m ² /g	μ Mole/m ²	Å ²	ml/column	[Å]	ml/column, Å
C1	359	16.4	10.1	0.31	9.9	1.94
C2	363	18.8	8.8	0.35	11.5	1.74
C3	351	19.0	8.7	0.35	11.9	2.33
C4	357	19.8	8.4	0.37	12.4	2.08
C5	353	20.0	8.3	0.37	12.9	3.06
C6	347	20.5	8.1	0.37	13.3	3.09
C8	340	21.0	7.9	0.37	13.7	3.09
C10	354	20.9	8.0	0.38	14.1	4.31
C12	361	20.8	8.0	0.39	14.7	5.83
C18	371	19.4	8.6	0.37	14.8	8.17

*Corrected for curvature and related to the same amount of original silica (one gram)

Table 5-XIV

Characteristics of the methanol adsorbed layer

Determined using retention volumes from minor disturbance method (Set 1 columns).

1	2	3	4	5	6	7
Adsorbent	Corrected surface area	Γ max	Apparent molecular area	Volume of ads. layer	*Adsorbed Layer thickness	*Volume of alkyl bonded layer
	m ² /g	μ Mole/m ²	Å ²	ml/column	[Å]	ml/column, Å
C1	359	4.0	41.2	0.063	1.73	1.94
C2	363	4.9	33.6	0.073	2.1	1.74
C3	351	5.0	33.1	0.073	2.2	2.33
C4	357	4.9	34.0	0.073	2.1	2.08
C5	353	5.7	29.3	0.084	2.5	3.06
C6	347	6.1	27.2	0.090	2.7	3.09
C8	340	6.4	26.0	0.099	2.8	3.09
C10	354	6.3	26.4	0.095	2.9	4.31
C12	361	5.9	28.3	0.098	2.8	5.83
C18	371	5.3	31.3	0.095	2.7	8.17

*Corrected for curvature and related to the same amount of original silica (one gram)

Table 5-XV

Characteristics of the Tetrahydrofuran adsorbed layer

Determined using retention volumes from minor disturbance method (Set 2 columns).

Adsorbent	Corrected surface area	Γ max	Apparent molecular area	Volume of ads. layer	*Adsorbed Layer thickness	*Volume of alkyl bonded layer
	m ² /g	μ Mole/m ²	Å^2	ml/column	[Å]	ml/column, Å
C1	359	11.1	14.9	0.37	10.6	1.94
C2	363	12.3	13.5	0.39	11.9	1.74
C4	357	13.5	12.3	0.41	13.4	2.08
C8	340	14.3	11.6	0.44	14.8	3.09
C18	371	12.0	13.8	0.43	14.3	8.17

**Corrected for curvature and related to the same amount of original silica (one gram)*

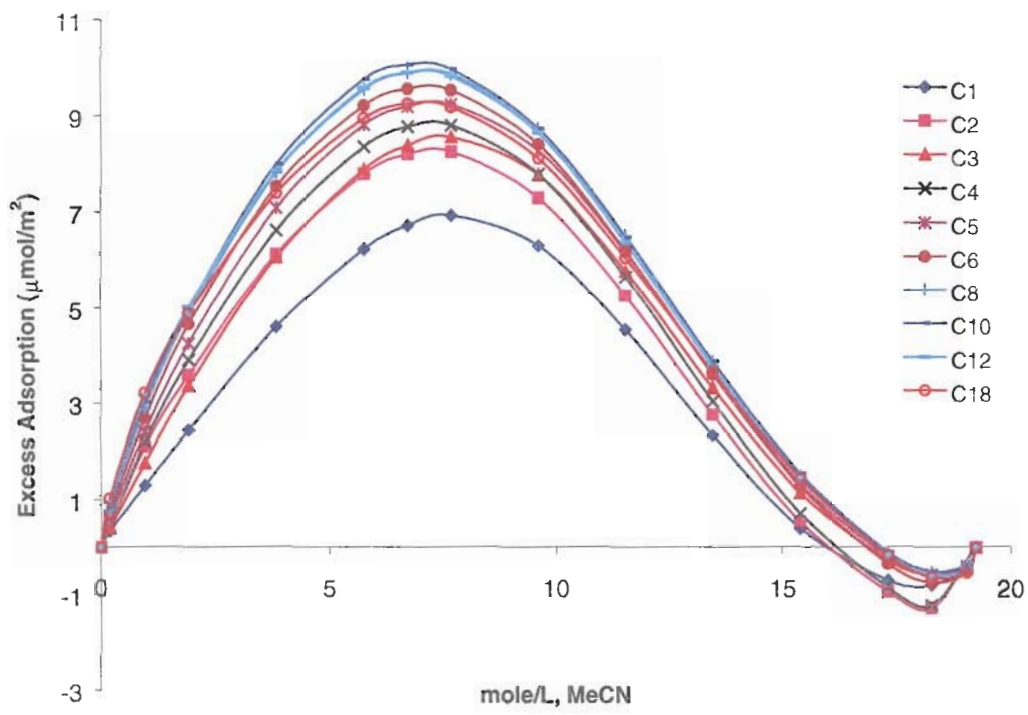


Figure 5-27 Overlay of all excess adsorption isotherms of acetonitrile from water at 25°C versus mole/L MeCN. Intercept is in $\mu\text{Mol}/\text{m}^2$, molecular volume of acetonitrile and Avogadro's number must be multiplied to get, \AA , thickness (τ_{ads}).

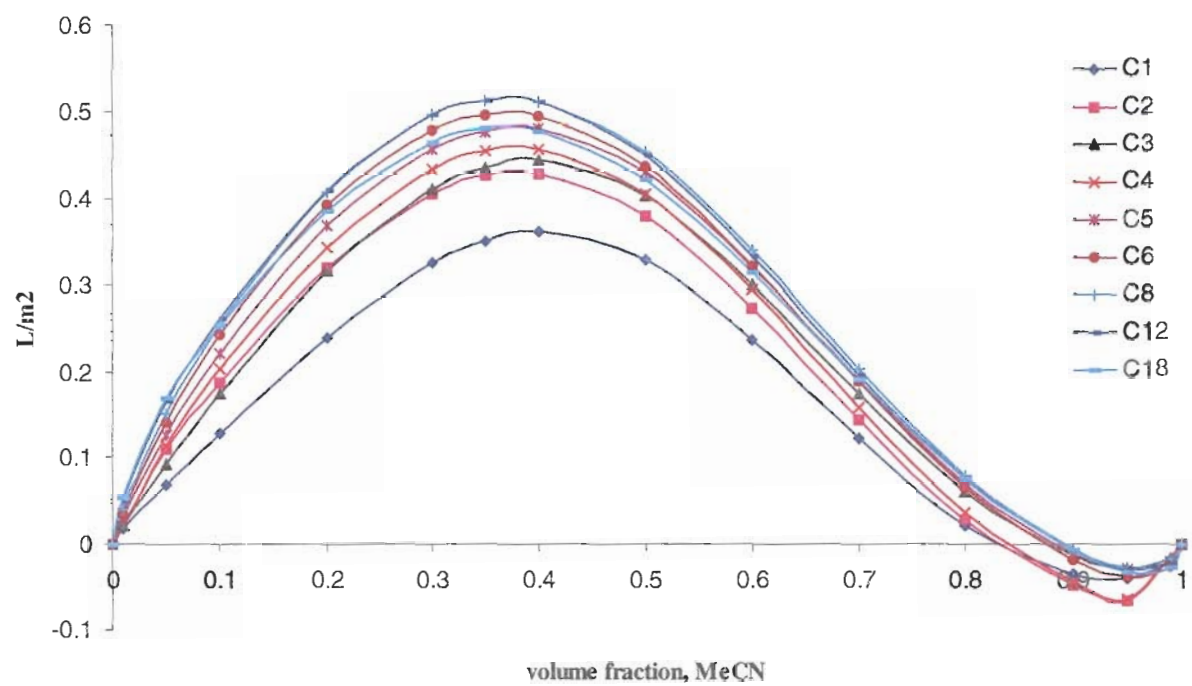


Figure 5-28 Overlay of all excess adsorption isotherms of acetonitrile from water at 25°C versus mole fraction. Intercept is in $\mu\text{L}/\text{m}^2$, The thickness (τ_{ads}), \AA , is directly determined from the intercept.

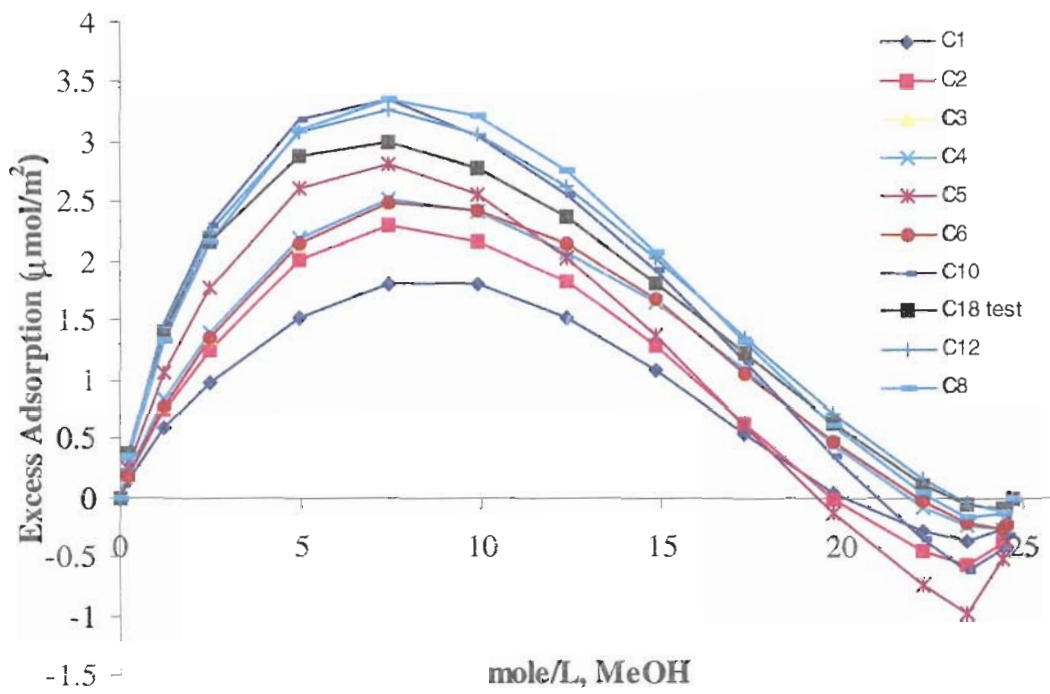


Figure 5-29 Overlay of all excess adsorption isotherms of methanol from water at 25°C versus mole/L MeOH. Intercept is in $\mu\text{Mol}/\text{m}^2$, molecular volume of methanol and Avogadro's number must be multiplied to get, \AA , thickness (τ_{ads}).

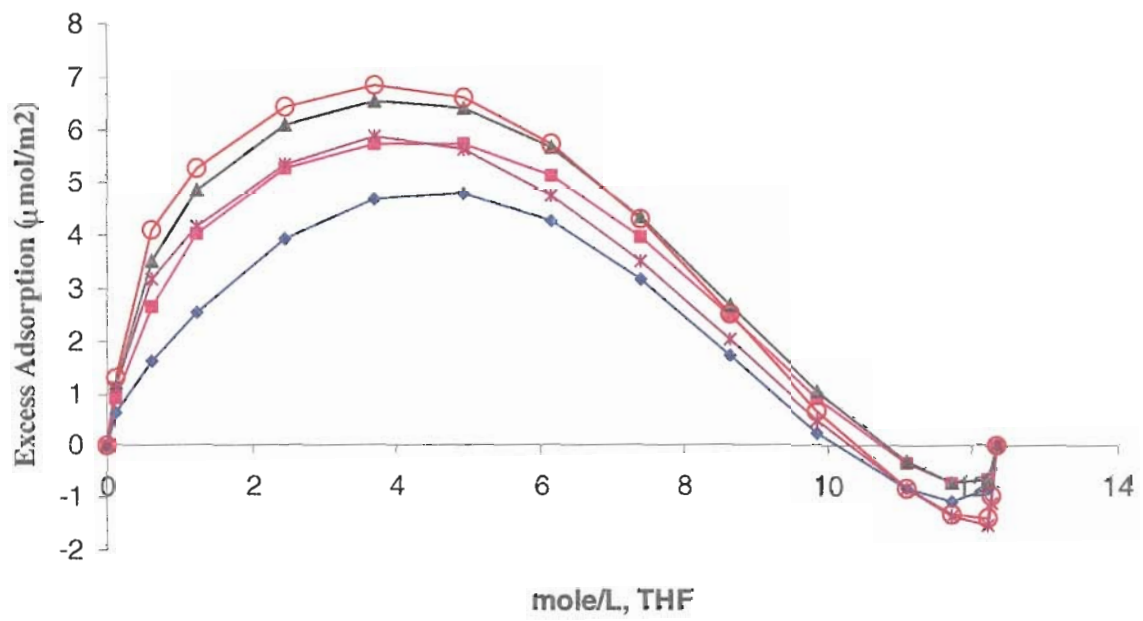


Figure 5-30 Overlay of all excess adsorption isotherms of THF from water at 25°C versus mole/L THF. Intercept is in $\mu\text{Mol}/\text{m}^2$, molecular volume of THF and Avogadro's number must be multiplied to get, \AA , thickness (τ_{ads}).

Table 5-XVI

Comparison of adsorbed layer thickness obtained with V_R from deuterated component and V_R from Minor disturbance method.

	*Thickness of Adsorbed Layer (Å)		
	CD₃CN	Minor Disturbance	Difference
C8	10.3	10.9	0.6
C12	9.9	10.8	0.9
C18	9.1	10.1	0.9

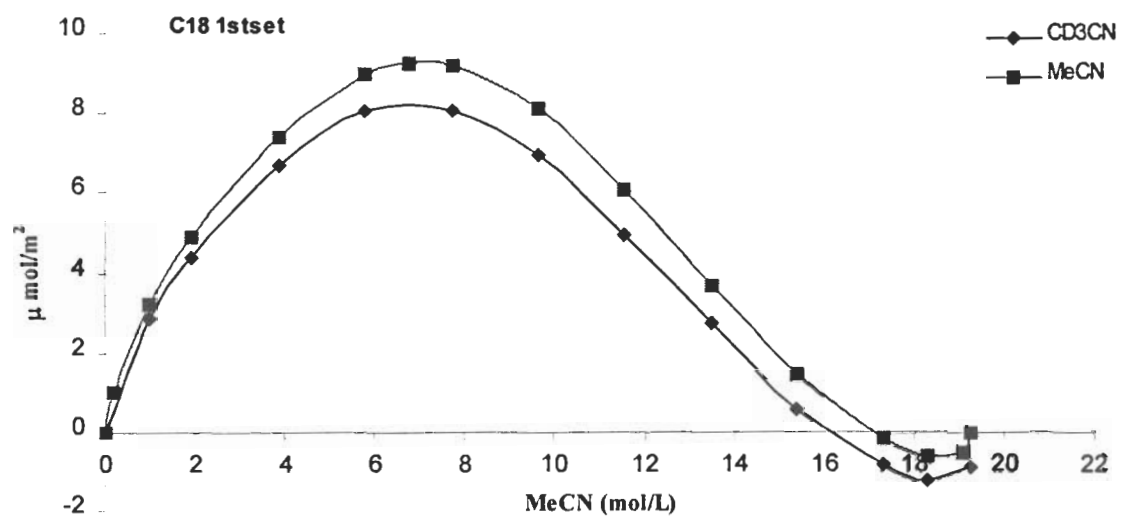


Figure 5-31 Excess adsorption isotherms obtained using minor disturbance peaks (top) and deuterated components, CD₃CN and D₂O (bottom) on Nomo C₁₈, 1st set.

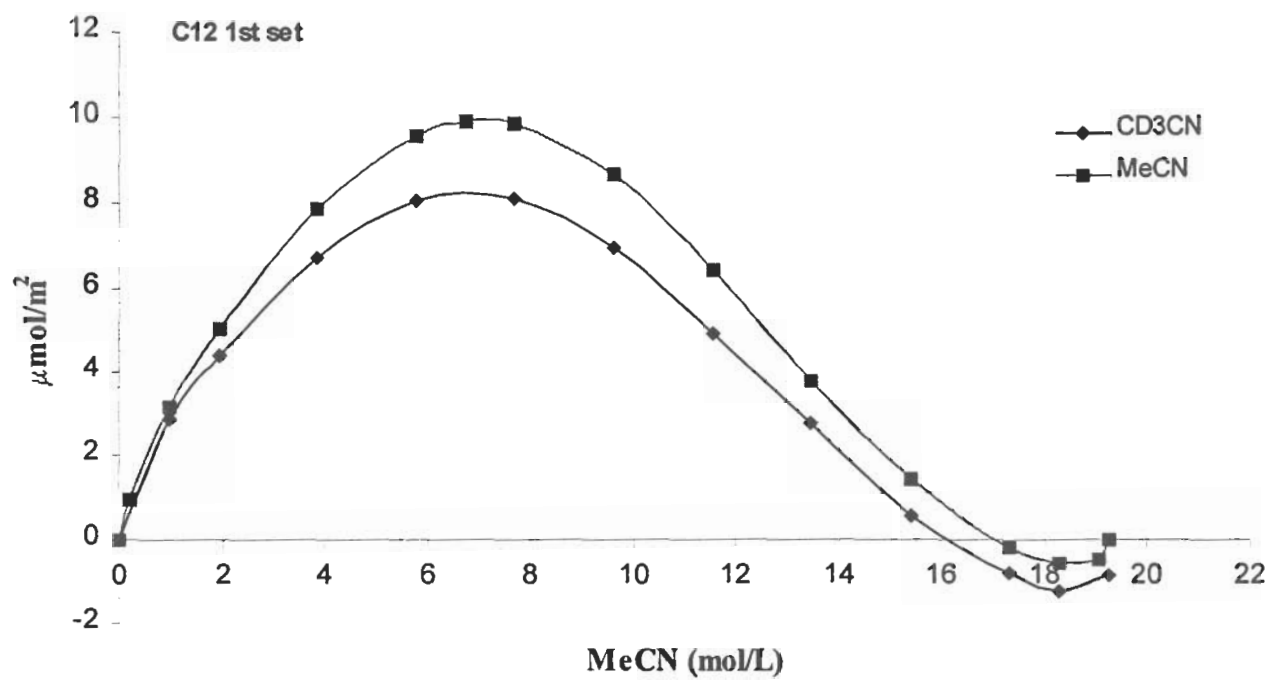


Figure 5-32. Excess adsorption isotherms obtained using minor disturbance peaks (top) and deuterated components, CD₃CN and D₂O (bottom) on Nomo C₁₂, 1st set.

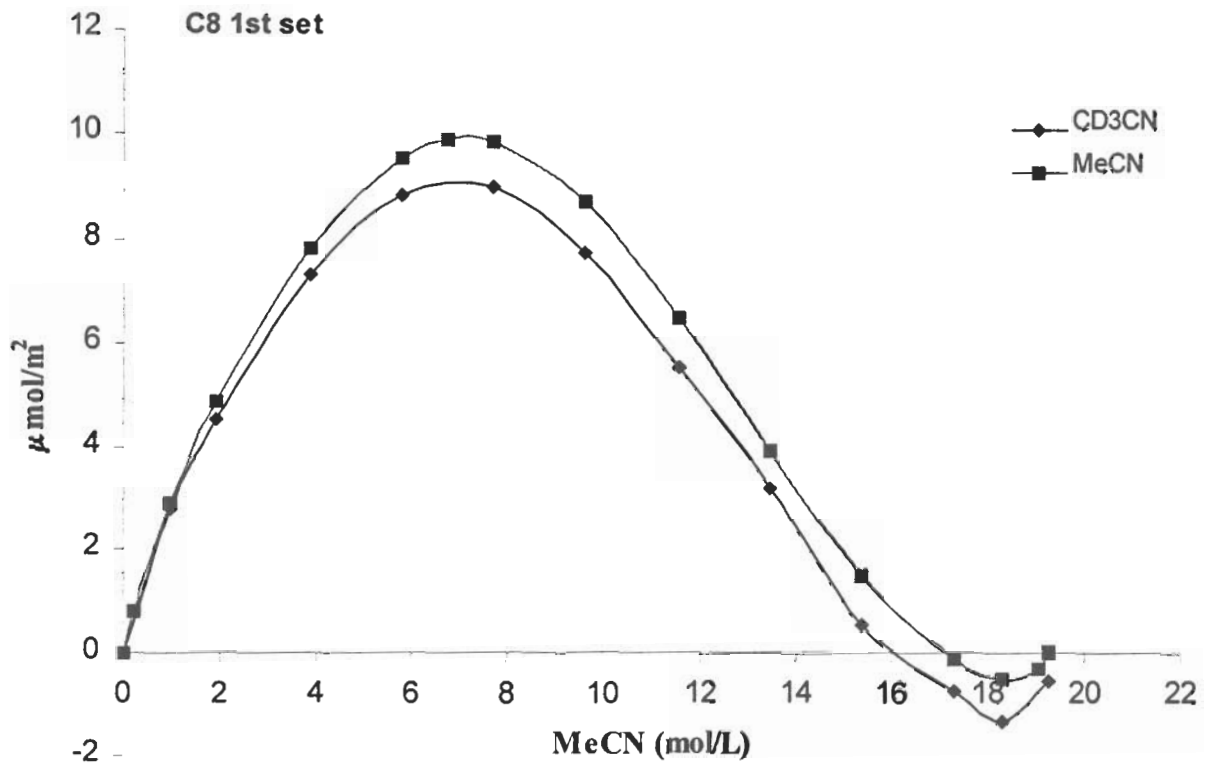


Figure 5-33. Excess adsorption isotherms obtained using minor disturbance peaks (top) and deuterated components, CD₃CN and D₂O (bottom) on Nomo C_{8,1}st set.

Adsorbed Layer Thickness

Analysis of the actual molecular area of the eluent component adsorbed on the surface may be useful for the understanding of the eluent behavior inside the adsorbent pores. These calculations actually lead to unusually low values of acetonitrile molecular areas. These calculated values are shown in Table 5-XIII, column 4. That area is actually smaller than even the area occupied by nitrogen on polar surfaces at very low temperature (16.4 \AA^2). The apparent molecular area decreases remains constant with an increase in the bonded alkyl chain length. For the acetonitrile adsorption on all types of reversed phases of different polarity from $C_1 - C_{18}$, the average molecular area occupied by one acetonitrile molecule is about 8.5 \AA^2 . It can be seen that the thickness of the adsorbed layer does not increase significantly with the increase of the chain length. Also, the volume of the adsorbed acetonitrile layer does not changing significantly.

Kuznetsov, et.al^[93] have studied the adsorption of the acetonitrile from the vapor phase and found that molecular area of acetonitrile is approximately 40 \AA^2 . Based on this estimation of that area from excess adsorption, we believe we have a supposition of monomolecular adsorption of acetonitrile. It is logical to conclude that this adsorption is not monomolecular. Acetonitrile forms an adsorbed layer of certain thickness on the hydrophobic surface. The formation of the layer seems to be independent of the alkyl chain length. Even with the increased hydrophobicity of the surface the layer thickness still remains constant. However, with the lower alkyl chains the influence of the underlying polar silanols may be suppressing some adsorption of the organic eluent components from $C_1 - C_4$ and leading to slightly lower values of the thickness of the adsorbed layer. If the actual area occupied by acetonitrile molecule is 40 \AA^2 then the

apparent area of $\sim 8.5 \text{ \AA}^2$ actually means that about four acetonitrile molecules stack on the top of each other on the surface. The number of molecules in the stack could be estimated as a ratio of the actual area to the apparent one.

The thickness of the adsorbed layer also could be estimated as a product of the number of molecules in the stack and the thickness of a single layer. Effective volume of a single acetonitrile molecule (estimated from acetonitrile density) is equal to 86.3 \AA^3 . Ratio of that molecular volume to the molecular area (40 \AA^2) gives the effective thickness of a single adsorbed layer which is about 2.2 \AA . The effective thickness of the adsorbed acetonitrile layer on all studied adsorbents is shown in table 5-VIII above. The product of that thickness and the adsorbent surface area in the column gives a total volume of the adsorbed acetonitrile layer in the column. As one can see, the value for C18 bonded phase is very significant (0.37 ml) and is approximately $1/5$ of the total volume of the liquid phase in the column, $V_o=1.713 \text{ ml}$, (Table 5-III).

The average area calculated for Tetrahydrofuran adsorption on the basis of van der Waals atom radii is about 40 \AA^2 , and does not correspond to the calculated cross sectional area of the molecule of $\sim 13 \text{ \AA}^2$. If THF laid flat on the surface it would occupy an area of 40 \AA^2 , but if one assumes that THF molecules are stacked vertically on the surface, then THF shows multilayer formation.

For methanol adsorption, the average area calculated in the same manner as for THF was 30 \AA^2 ; this value corresponds well to the theoretical cross sectional area of the molecule (25 \AA^2). This observed effect shows that methanol obeys monomolecular adsorption on all the bonded phases, Nomo, set C₁ –C₁₈. The adsorbed layer thickness

for the different organic systems plotted versus carbon number of the alkyl chain bonded to the silica surface is shown in Figure 5-34.

This acetonitrile molecules could either accumulate on the top of the surface or could get embedded between the alkyl chains. If all acetonitrile molecules are embedded between the alkyl chains of bonded phase, then the increase of the adsorption values should be proportional to the increase of the carbon number of the bonded ligands. Figure 5-35 represents the thickness of the bonded layer and the adsorbed layer of increasing alkyl chain length. It can be seen that at the lower chain lengths there is not enough volume, to accommodate the volume of the adsorbed layer. This confirms that the volume of that adsorbed layer is on top of the collapsed bonded layer. However, at higher alkyl chain lengths, C₁₂ and C₁₈, there is ample room for the acetonitrile molecules to penetrate. However, we observed that the adsorbed layer thickness is independent of the alkyl chain length. It can be assumed that since the adsorbed layer is on top of the smaller less hydrophobic alkyl chains that it is still on the top of the more hydrophobic ligands. One assumption we are making though is that if solvation of the alkyl chains is occurring, the kinetics of the process of solvating the chains with the organic solvent is very slow.

Filling of Adsorption Layer

Negative excess observed in excess adsorption isotherms in binary eluent system such as acetonitrile from water on reversed phase packing materials means actual accumulation of the water molecules, probably on the residual silanols. This negative excess is usually seen at high concentrations (v/v%) of the organic eluent where the

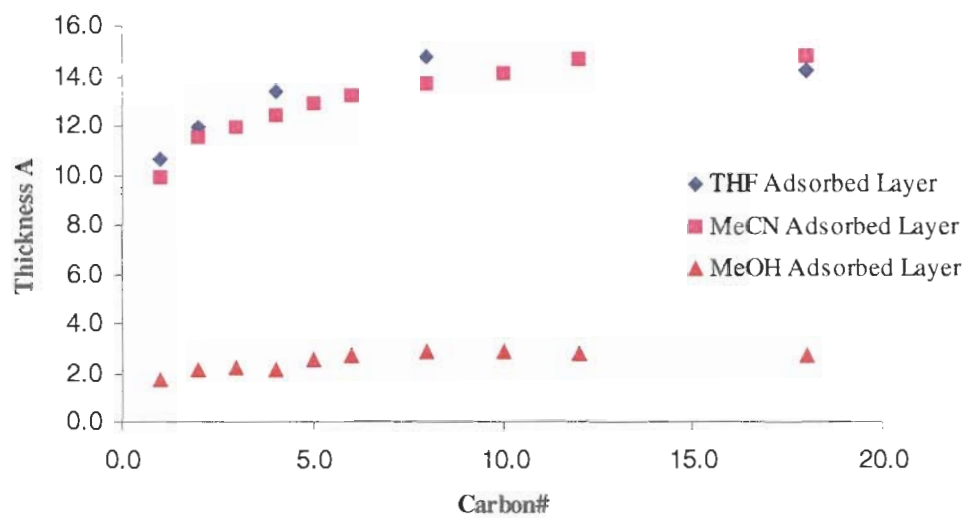


Figure 5-34. The relationship between increasing carbon number and thickness of the adsorbed layer. MeCN and MeOH adsorbed layers on Nomo Set 1 columns. THF adsorbed layers on Nomo Set 2 columns.

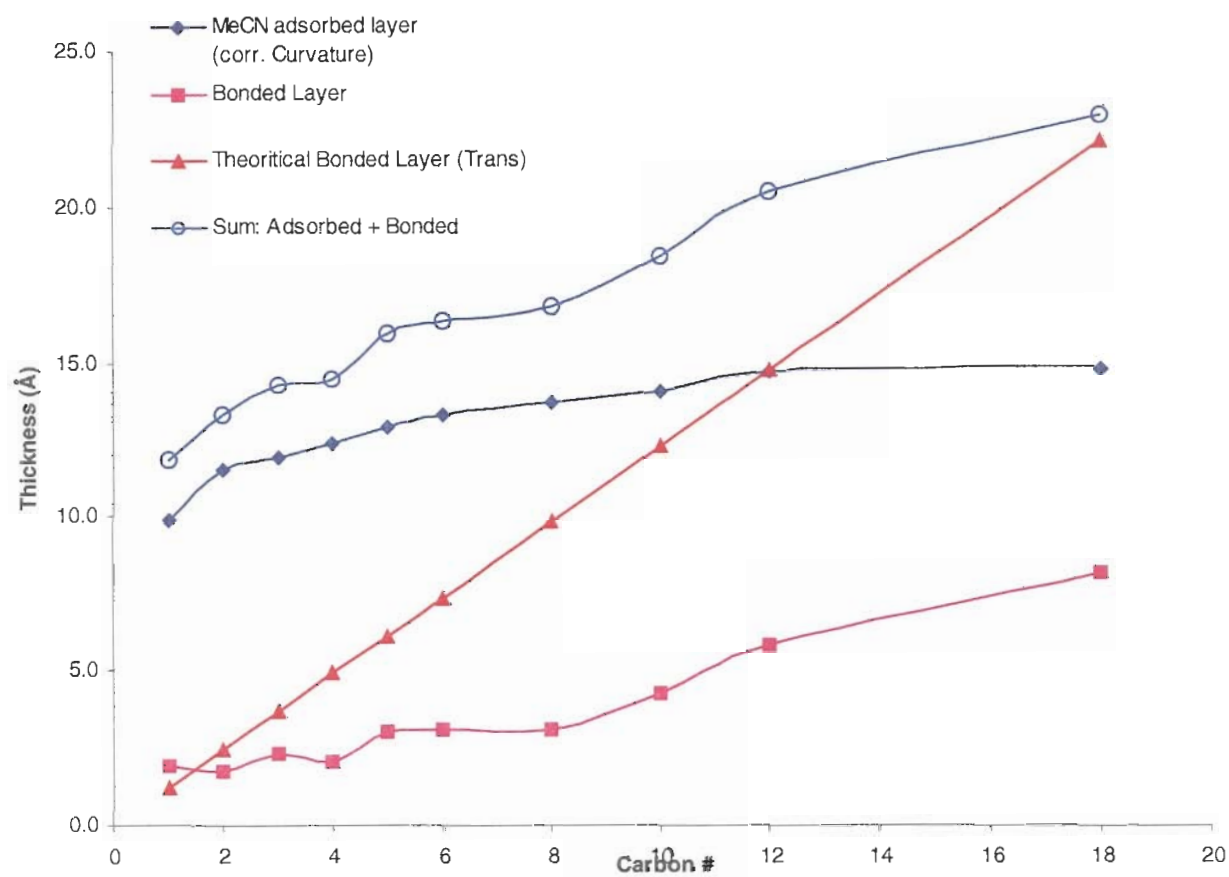


Figure 5-35. Comparison of the bonded layer and adsorbed layer thickness versus carbon number of the alkyl chain bonded to the silica surface

interactions with the silanols are enhanced. The region between 40 and 90% of acetonitrile on Figure 5-36 is where all isotherms have negative slope actually represent maximum filling of available hydrophobic adsorbent surface with acetonitrile (maximum total adsorption). If we apply the Everett's approach we can calculate the acetonitrile molecular volume occupied on the surface actually and concentration of the surface adsorbed layer at any composition shown in Figure 5-36.

The total amount of a component, T_a , on the surface layer per unit area of the adsorbent may be obtained from the following equation:

$$T_a = \Gamma + V_a * x \quad [5-23]$$

where Γ is the surface excess amount; V_a is the volume of the surface layer of 1 g of the adsorbent; and x is the mole fraction of acetonitrile. The value of T_a will increase with increase of x only up to a certain limit, since the isotherms for completely miscible liquids achieve a maximum value and then decrease, often linearly to zero. The values for T_a are represented in Table XVII, column 5. The values for surface excess amount adsorbed above the equilibrium concentration is represented in Table XVII, column 2. The values for the volume of acetonitrile at a certain equilibrium mole fraction of the binary eluent mixture is represented in Table XVII, column 4. This value of $V_a * x$ can be denoted as a_e . The total concentration at each mole fraction is shown in column 7 of Table XVII and was calculated as follows.

$$\frac{a_e + \Gamma}{V_a} = \text{Conc.}(v/v\%) \quad [5-24]$$

It can be seen that a maximum filling of the adsorbed layer is reached at about 0.16 mole fraction acetonitrile, which corresponds to about 35(v/v%) acetonitrile. At mole fractions from 0 to 0.16, there is a filling of the adsorbed layer and the thickness of the layer is

shown in Table XVII, column 6. This suggests that at increasing acetonitrile content in the binary eluent, this layer increases suggesting that a layer of finite thickness is not established until about 35% acetonitrile. This maximum amount adsorbed is shown in Figure 5-36 as the dotted line. Once the thickness of this layer is calculated and we can define both the maximum amount adsorbed and the Gibbs dividing plane. Initially we postulated that we did have a Gibbs dividing plane, but we did not define where it was. Once, the position of the plane is determined, a description of a partition-adsorption model may be developed.

Adsorption-Partitioning Model

Earlier in this chapter it was shown that acetonitrile and THF are adsorbed on hydrophobic surfaces forming a layer of significant volume, which may be treated as a phase with a composition different from the mobile phase. Most likely there is no distinct boundary between the adsorbed acetonitrile layer and the eluent with set composition. There is supposed to be a distribution of the acetonitrile and THF along the perpendicular to the surface. Following the classical Gibbs approach, the boundary can be defined where only pure component (e.g. acetonitrile) is beneath that boundary and the equilibrated eluent composition is set above this boundary.

Let us consider now a hypothetical situation where we have a coexistence of partitioning and adsorption processes. The partitioning is not referred to as classical partitioning, but rather partition of the analyte from the mobile phase composition at equilibrium conditions into an adsorbed organic stagnant layer on top of the bonded layer. Our analyte may get distributed between those phases and the portion of

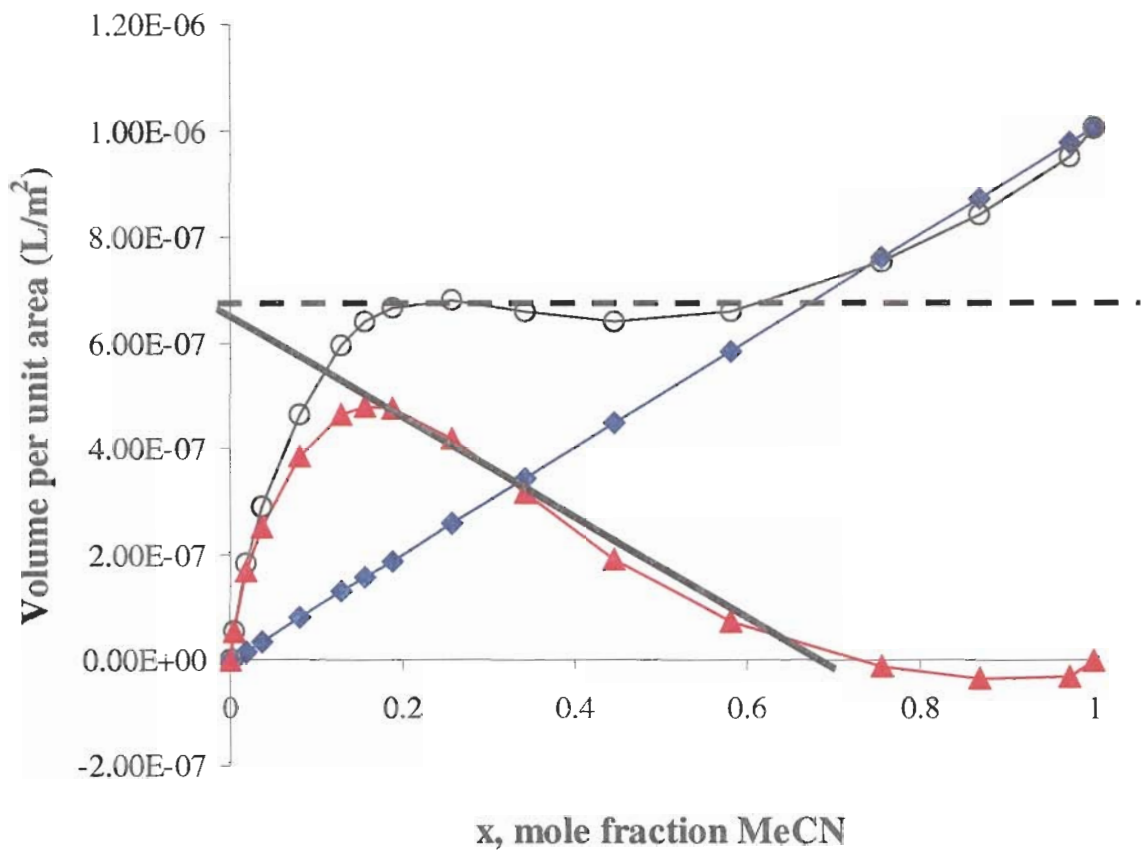


Figure 5-36. Filling of the adsorbed layer on a reversed phase surface. open circles represent total amount adsorbed ($\Gamma + V_a \cdot x$); closed triangles represent surface excess amount, Γ (vol); closed diamonds represent the amount of acetonitrile at equilibrated concentration ($V_a \cdot x$).

Table 5-XVII
Concentration of the adsorbed layer at different MeCN/Water compositions

1	2	3	4	5	6	7
MeCN	MeCN	MeCN	a_e	$\Gamma + a_e$		Conc.
C_e	Γ (vol)	x	$V_s \cdot x$	$\Gamma + V_s \cdot x$	Tau	$(\Gamma + a_e)/V_s$
Mol/L	L/m ²		L/m ²	L/m ²	A	v/v%
19.24	7.96E-22	1.00	1.01E-06	1.01E-06	10.07	100.0
19.05	-2.74E-08	0.97	9.78E-07	9.51E-07	9.51	94.4
18.28	-3.24E-08	0.87	8.74E-07	8.42E-07	8.42	83.6
17.32	-8.65E-09	0.76	7.62E-07	7.54E-07	7.54	74.9
15.40	7.55E-08	0.58	5.85E-07	6.60E-07	6.60	65.6
13.47	1.91E-07	0.45	4.50E-07	6.41E-07	6.41	63.7
11.55	3.16E-07	0.34	3.44E-07	6.60E-07	6.60	65.5
9.62	4.22E-07	0.26	2.59E-07	6.81E-07	6.81	67.6
7.70	4.78E-07	0.19	1.89E-07	6.67E-07	6.67	66.2
6.74	4.81E-07	0.16	1.58E-07	6.39E-07	6.39	63.5
5.77	4.66E-07	0.13	1.30E-07	5.96E-07	5.96	59.2
3.85	3.85E-07	0.08	8.02E-08	4.65E-07	4.65	46.2
1.92	2.54E-07	0.04	3.73E-08	2.92E-07	2.92	29.0
0.96	1.68E-07	0.02	1.80E-08	1.86E-07	1.86	18.5
0.19	5.33E-08	0.00	3.51E-09	5.68E-08	0.57	5.6
0.00	0.00E+00	0.00	0.00E+00	0.00E+00	0.00	0.0

Nomo Set 1 C18, MeCN from water

the analyte, which appears to be in the liquid stationary phase, could get adsorbed on the underlying surface. In essence this is a substitution of a complex tertiary adsorption system by a superposition of partitioning process and adsorption from binary system. A schematic representation of what may be happening inside the pore is given in Figure 5-37.

Summary

The adsorbed organic layer on top of the bonded phase may act as a real liquid stationary phase in reversed phase HPLC and suggest a complex retention mechanism for analytes in the HPLC column. Since there is an adsorbed layer of different composition than the bulk eluent being pumped, an analyte may partition from the bulk eluent into the adsorbed layer of a certain thickness. The layer thickness is dependent upon the concentration of acetonitrile in the binary eluent system. The overall HPLC retention process most likely consists of two processes: 1) distribution of the analyte into the adsorbed layer and 2) adsorption of the analyte onto the surface of the reversed phase material. This partition-adsorption model may allow explanation of some discrepancies from expected temperature and eluent composition effects. A solid foundation for the distinction between the different retention mechanisms in reversed phase chromatography must be established and should be considered when discussing the validity of the results obtained with a certain model prior to the description of any secondary processes such as ion-association equilibria.

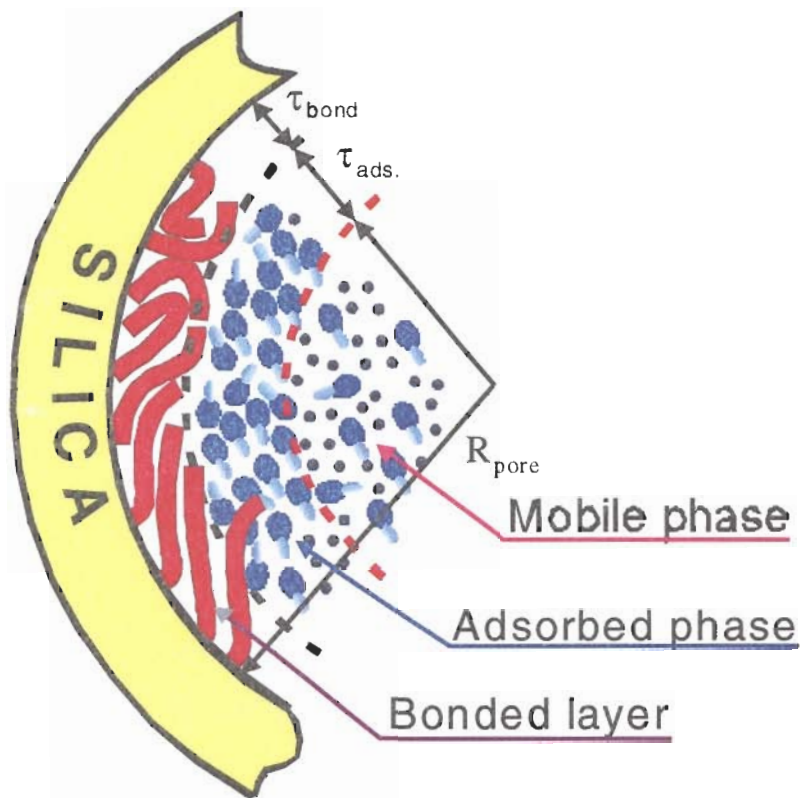


Figure 5-37. A schematic representation of the bonded layer, the adsorbed layer and the pumped mobile phase composition.

Appendix

Thickness of Bonded Layer corrected for surface of curvature

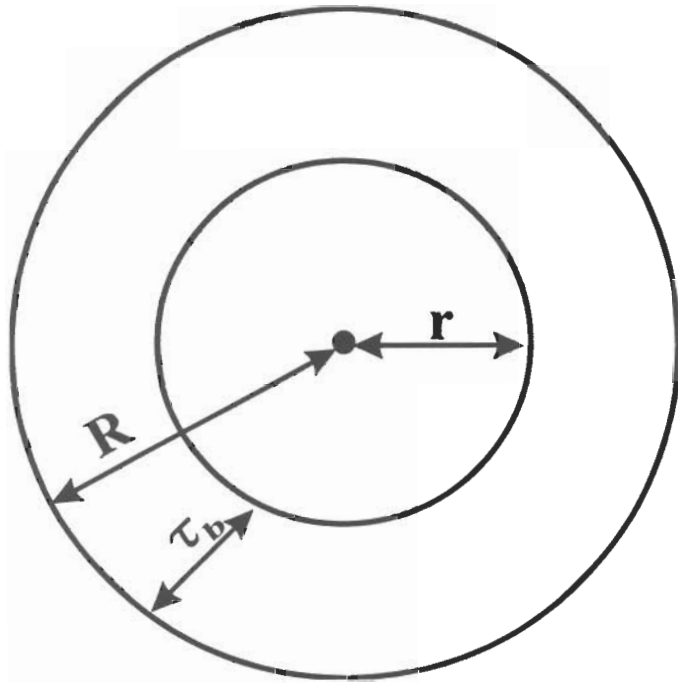


Figure 5-38. A schematic of the pore and bonded layer dimensions.

$$V_b = L(\pi R^2 - \pi r^2) \quad [5-25]$$

$$V_b = L\pi(R^2 - r^2) \quad [5-26]$$

$$V_b = L\pi(R - r)(R + r) \quad [5-27]$$

where $\tau_b = R - r$ and $r = R - \tau_b$

$$V_b = L\pi * (\tau_b) * (R + (R - \tau_b)) \quad [5-28]$$

$$V_b = L\pi\tau_b(2R - \tau_b) \quad [5-29]$$

Since the pores within the silica are assumed to be cylindrical the surface area is related to the length as the following.

$$S = 2\pi RL \cdots L = \frac{S}{2\pi R} \quad [5-30]$$

Substituting **L** we get

$$V_b = \frac{S}{2R} \tau_b (2R - \tau_b) \quad [5-31]$$

$$\frac{S}{2R} \tau_b^2 + S\tau_b - V_b = 0 \quad [5-32]$$

Using the quadratic formula we can solve for τ_b . The surface area value (**S**) used is the surface area of the modified silica corrected per gram of original silica; The **R** value is the radius of the original silica obtained from the median of the pore size distribution using LTNA. The volume of the bonded layer is obtained from the LTNA experiments using the pore volume of the original silica and the pore volume of the modified adsorbent.

Thickness of Adsorbed Layer corrected for surface of curvature

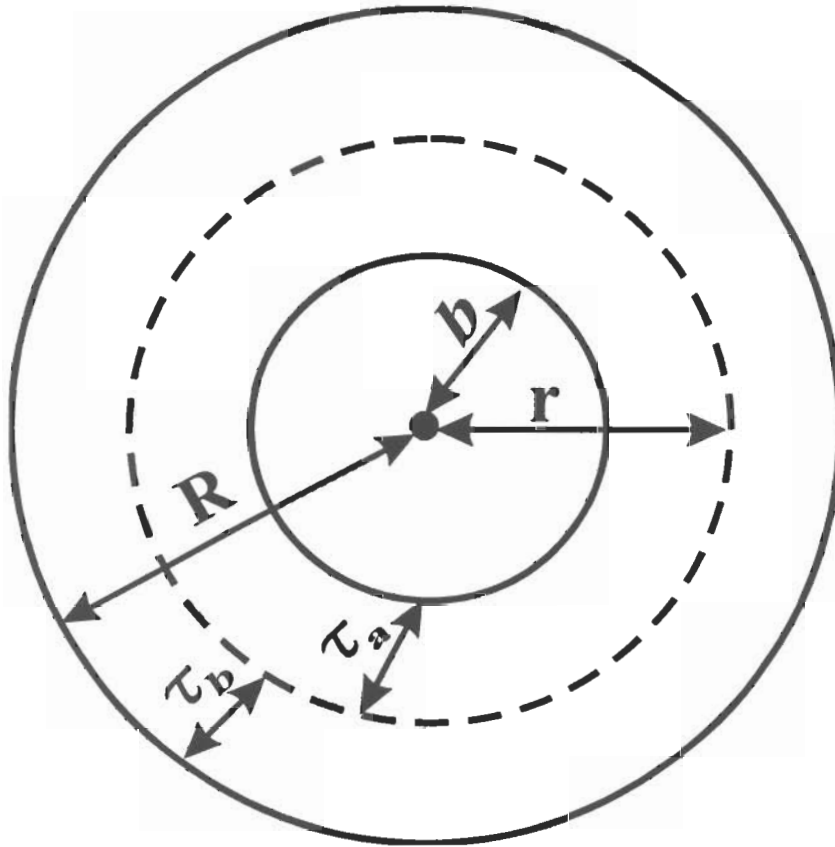


Figure 5-39. A schematic of the pore, bonded layer and adsorbed layer dimensions.

$$V_a = L(\pi r^2 - \pi b^2) \quad [5-33]$$

$$V_a = L\pi(r^2 - b^2) \quad [5-34]$$

$$V_a = L\pi(r - b)(r + b) \quad [5-35]$$

where $\tau_a = r - b$ and $b = r - \tau_a$

$$V_a = L\pi * (\tau_a) * (r + (r - \tau_a)) \quad [5-36]$$

$$V_a = L\pi\tau_a(2r - \tau_a) \quad [5-37]$$

$$S = 2\pi RL \dots L = \frac{S}{2\pi R} \quad [5-38]$$

Substituting L we get

$$V_a = \frac{S}{2R} \tau_a (2r - \tau_a) \quad [5-39]$$

However, since r is unknown we can substitute $R - \tau_b$ for r .

$$V_a = \frac{S}{2R} \tau_a (2(R - \tau_b) - \tau_a) \quad [5-40]$$

$$-\frac{S}{2R} \tau_a^2 + (S - \frac{S\tau_b}{R})\tau_a - V_a = 0 \quad [5-41]$$

Using the quadratic formula we can solve for τ_a . All the values are known and were previously described in the calculation of the bonded layer thickness corrected for surface of curvature. The τ_b value used in the text is the one that has been corrected for surface of the curvature.

ADDENDUM

Experimental results of minor disturbance and deuterated retention volumes with different eluents (Tables A5-I to A5- X)

Table A5-I

MeCN/Water Minor disturbance retention volumes for 1st set of columns

Conc. MeCN	C1	C2	C3	C4	C5	C6	C8	C10	C12	C18
0	2.694	2.927	2.659	2.817	3.059	3.282	3.496	3.671	4.020	4.258
1	2.373		2.480		2.776	2.836	2.906	3.019	3.089	3.125
5	2.309	2.481	2.438	2.557	2.582	2.607	2.589	2.586	2.530	2.432
10	2.328	2.464	2.406	2.467	2.466	2.447	2.438	2.451	2.386	2.274
20	2.270	2.316	2.259	2.297	2.267	2.230	2.236	2.255	2.210	2.122
30	2.131	2.125	2.074	2.097	2.053	2.011	2.001	1.983	1.964	1.903
35	2.022	2.001	1.966	1.967	1.918	1.872	1.865	1.833	1.800	1.751
40	1.918	1.852	1.837	1.807	1.805	1.746	1.742	1.696	1.683	1.628
50	1.636	1.606	1.552	1.567	1.533	1.486	1.491	1.448	1.410	1.381
60	1.488	1.445	1.397	1.397	1.390	1.354	1.352	1.318	1.268	1.256
70	1.473	1.431	1.387	1.387	1.373	1.350	1.342	1.322	1.283	1.244
80	1.589	1.543	1.491	1.497	1.473	1.442	1.439	1.409	1.376	1.324
90	1.789	1.721	1.667	1.677	1.648	1.607	1.609	1.580	1.543	1.476
95	1.927	1.839	1.790	1.797	1.776	1.747	1.736	1.715	1.673	1.597
99	2.227		2.090		2.075	2.088	2.063	2.005	1.985	1.921
100	3.027	2.932	2.838	2.867	3.097	3.415	2.770	2.934	3.224	3.540

Table A5-II.**Acetonitrile/Water Minor disturbance retention volumes for 2nd set of columns**

Conc. MeCN	C1	C2	C4	C8	C18
0	2.957	2.995	3.014	3.715	4.316
1	2.440	2.530	2.669	3.044	3.041
5	2.388	2.523	2.568	2.640	2.379
10	2.388	2.506	2.483	2.478	2.204
20	2.324	2.371	2.309	2.229	2.069
30	2.176	2.177	2.105	1.999	1.871
35	2.078	2.061	1.975	1.855	1.723
40	1.949	1.920	1.836	1.717	1.583
50	1.683	1.637	1.567	1.473	1.361
60	1.528	1.484	1.415	1.333	1.253
70	1.525	1.482	1.406	1.325	1.244
80	1.655	1.595	1.531	1.434	1.325
90	1.858	1.779	1.709	1.601	1.478
95	2.023	1.933	1.877	1.776	1.624
99	2.508				2.062
100	3.170	3.126	3.580	3.434	3.360

Table A5-III.**Methanol/Water minor disturbance retention volumes for 1st set of columns**

Conc. MeOH	C1	C2	C3	C4	C5	C6	C8	C10	C12	C18
0	2.229	2.187	2.152	2.222	2.280	2.339	2.434	2.431	2.492	2.521
1	2.149	2.149	2.110	2.178	2.235	2.285	2.339	2.342	2.359	2.324
5	2.093	2.069	2.051	2.093	2.132	2.140	2.174	2.139	2.151	2.103
10	2.059	2.045	2.002	2.049	2.055	2.042	2.078	2.020	2.013	1.947
20	2.021	1.992	1.954	1.985	1.949	1.914	1.945	1.896	1.877	1.812
30	1.977	1.901	1.871	1.904	1.876	1.825	1.874	1.803	1.802	1.736
40	1.929	1.870	1.830	1.862	1.807	1.780	1.819	1.759	1.747	1.688
50	1.892	1.840	1.810	1.836	1.794	1.764	1.779	1.740	1.718	1.664
60	1.875	1.809	1.774	1.829	1.768	1.734	1.753	1.720	1.696	1.643
70	1.867	1.802	1.766	1.797	1.764	1.732	1.747	1.697	1.693	1.642
80	1.889	1.826	1.784	1.808	1.780	1.736	1.771	1.711	1.706	1.649
90	1.917	1.853	1.796	1.829	1.801	1.758	1.793	1.727	1.730	1.677
95	1.935	1.881	1.820	1.876	1.811	1.792	1.816	1.769	1.751	1.701
99	2.060	1.963	1.857	1.893	2.292	2.118	1.946	2.022	1.802	1.764
99.5					2.382	2.379		2.261		
100	2.654	3.105	2.363	3.173	3.543	3.226	2.202	3.321	2.176	2.083

Table A5-IV.

Methanol/Water minor disturbance retention volumes for 2nd set of columns

Conc. MeOH	C1	C2	C4	C8	C18
0	2.247	2.244	2.250	2.436	2.435
1	2.201	2.222	2.245	2.376	2.364
5	2.105	2.125	2.186	2.173	2.012
10	2.065	2.090	2.073	2.035	1.879
20	2.02	2.034	1.985	1.901	1.744
30	1.998	1.974	1.911	1.819	1.676
40	1.935	1.912	1.844	1.755	1.629
50	1.918	1.881	1.804	1.740	1.601
60	1.906	1.848	1.788	1.706	1.582
70	1.906	1.844	1.785	1.705	1.576
80	1.916	1.860	1.798	1.715	1.584
90	1.943	1.886	1.834	1.748	1.607
95	1.972	1.931	1.873	1.783	1.635
99	2.042	2.049	1.987	1.893	1.785
100	3.389	3.531	2.794	3.010	2.792

Table A5-V.**THF/Water minor disturbance retention volumes for 2nd set of columns**

Conc. THF	C1	C2	C4	C8	C18
0	5.428	6.138	6.863	8.63	5.884
1	2.922	3.568	4.334	5.161	4.485
5	2.710	3.127	3.039	2.856	2.605
10	2.561	2.539	2.416	2.344	2.264
20	2.384	2.197	2.139	2.084	2.030
30	2.151	2.050	1.960	1.893	1.759
40	1.950	1.89	1.782	1.696	1.514
50	1.731	1.685	1.584	1.501	1.320
60	1.569	1.532	1.427	1.374	1.215
70	1.497	1.472	1.387	1.256	1.161
80	1.562	1.499	1.430	1.330	1.187
90	1.750	1.648	1.568	1.480	1.307
95	1.939	1.814	1.717	1.639	1.391
99	2.532	2.239	2.233	2.004	1.774
99.5				7.650	2.824
100	6.874	5.871	5.534	7.596	5.884

Table A5-VI.

Deuterated retention volumes for Nomo Set 1-C₁₈

				Corrected system volume	Corrected system volume	
		Deuterated	Deuterated	Deuterated	Deuterated	Calculated
		CD ₃ CN	D ₂ O	CD ₃ CN	D ₂ O	V _o
100	0	1.832	2.7	1.715	2.583	1.715
95	5	1.824	2.503	1.707	2.386	1.74095
90	10	1.831	2.092	1.714	1.975	1.7401
80	20	1.863	1.806	1.746	1.689	1.7346
70	30	1.925	1.668	1.808	1.551	1.7309
60	40	2.007	1.608	1.89	1.491	1.7304
50	50	2.117	1.576	2	1.459	1.7295
40	60	2.238	1.586	2.121	1.469	1.7298
30	70	2.367	1.63	2.25	1.513	1.7341
20	80	2.493	1.689	2.376	1.572	1.7328
10	90	2.696	1.755	2.579	1.638	1.7321
5	95	2.958	1.793	2.841	1.676	1.73425
0	100		1.845		1.728	1.728
					Avg. V _o	1.73173
					SD	0.006335
					%RSD	0.365791

Table A5-VII.

Deuterated retention volumes for Nomo Set 1-C₁₂

				Corrected system volume	Corrected system volume	
		Deuterated	Deuterate d	Deuterated	Deuterated	Calculated
		CD ₃ CN	D ₂ O	CD ₃ CN	D ₂ O	V ₀
100	0	1.895	2.7	1.778	2.583	1.778
95	5	1.878	2.414	1.761	2.297	1.788
90	10	1.888	2.095	1.771	1.978	1.792
80	20	1.916	1.835	1.799	1.718	1.783
70	30	1.978	1.71	1.861	1.593	1.781
60	40	2.069	1.636	1.952	1.519	1.779
50	50	2.183	1.609	2.066	1.492	1.779
40	60	2.334	1.601	2.217	1.484	1.777
30	70	2.464	1.651	2.347	1.534	1.778
20	80	2.591	1.725	2.474	1.608	1.781
10	90	2.773	1.804	2.656	1.687	1.784
5	95	2.978	1.844	2.861	1.727	1.784
0	100		1.896		1.779	1.779
					Avg. V ₀	1.782
					SD	0.004
					%RSD	0.240

Table A5-VIII.

Deuterated retention volumes for Nomo Set 1-C₈

MeCN (v/v%)	H ₂ O (v/v%)	Deuterated		Corrected for system volume		Calculated V _o
		CD ₃ CN	D ₂ O	CD ₃ CN	D ₂ O	
100	0	1.947		1.83		1.830
95	5	1.932	2.52	1.815	2.403	1.844
90	10	1.942	2.188	1.825	2.071	1.850
80	20	1.969	1.913	1.852	1.796	1.841
70	30	2.038	1.784	1.921	1.667	1.845
60	40	2.12	1.705	2.003	1.588	1.837
50	50	2.232	1.671	2.115	1.554	1.835
40	60	2.356	1.685	2.239	1.568	1.836
30	70	2.478	1.73	2.361	1.613	1.837
20	80	2.605	1.795	2.488	1.678	1.840
10	90	2.759	1.868	2.642	1.751	1.840
5	95	2.936	1.909	2.819	1.792	1.843
0	100		1.958		1.841	1.841
					Avg. V _o	1.840
					SD	0.005
					%RSD	0.275

Table A5-IX.

**MeCN/Water minor disturbance retention volumes for Waters Symmetry C₁₈,
Eclipse XDB-C₁₈ and Luna C₁₈-2 columns**

	Waters	Zorbax	Phnomex
conc. MeCN	Symmetry C18	Eclipse XDB-C18	Luna C18-2
100	2.844	1.465	2.05
99	1.792	1.428	
95	1.432	1.371	1.507
90	1.342	1.325	1.423
80	1.222	1.247	1.299
70	1.15	1.19	1.218
60	1.156	1.198	1.235
50	1.24	1.267	1.342
40	1.403	1.405	1.542
35	1.513	1.474	1.661
30	1.623	1.567	1.796
20	1.793	1.711	1.991
10	1.92	1.806	2.131
5	2.025	1.884	2.264
1	2.324	2.077	
0	3.509	2.116	3.309

***These values are not corrected for system volume of 0.053 μ L**

Table A5-X

MeCN/Water minor disturbance retention volumes for Kovalsil-C₁₄, Jupiter C₁₈ and Luna C₁₈ columns.

	Uketron	Phenomenex	Phenomenex
Conc. MeCN	Kovalsil-C₁₄	Jupiter C₁₈	Luna C₁₈
100	0.5	2.7	2.56
99	0.498	2.3	1.93
95	0.495	1.95	
90	0.492	1.89	1.4
80	0.495	1.8	1.25
70	0.495	1.74	1.15
60	0.495	1.72	1.13
50	0.498	1.8	1.27
40	0.500	2	1.53
30	0.500	2.11	1.85
20	0.500	2.18	2.06
10	0.505	2.24	2.22
5	0.51	2.33	2.38
1	0.515	2.8	3.18
0	0.523	3.21	3.9

*These values are not corrected for system volume of 0.053 μ L.

Literature Cited

Chapter 5

1. J. Nawrocki, *J.Chromatogr.A.*, 779, 1997, 55
2. E. Papp and Gy. Vigh, *J.Chromatogr.*, 259, 1983, 49
3. E. Papp and Gy.Vigh. *J.Chromatogr.*, 282, 1983, 59
4. L.L. Synder. Principles of Adsorption Chromatography, New York: Marcel Dekker, Inc., 1968
5. J.L. Bass, B.W. Sands and P.W. Bratt, Silanes Surfaces and Interfaces, Proceedings of the Silanes Surfaces and Interfaces Symposium, June 1985. 267
6. J. Dorsey, and W.T. Copper, Analytical Chemistry, 66, (17), 1994, 858A
7. K.K. Unger, Packings and Stationary Phases in Chromatographic Techniques, Marcel Dekker, Inc., New York, 1990
8. E. Heftmann. Chromatography, 2nd ed., New York: Reinhold Publishing Corp., 1961
9. U.D. Neue, HPLC Columns, Wiley-VCH, 1997
10. M. Jaroniec, *J.Chromatogr.A*, 656,1993, 37
11. C.H. Lochmuller, and D.R. Wilder *J.Chromatogr. Sci.*, 17, 1979, 574
12. J.G. Dorsey, and K.A. Dill *Chem.Rev.*, 1989, 331
13. D.E. Martire, and R.E. Boehm, *J.Phys.Chem.*, 84,1980, 3620
14. A. Vailaya, and Cs. Horvath, *J.Chromatogr.A.*, 829, 1998, 1
15. Y.V. Kazakevich, HPLC 1999, Granda, Spain, June 1999
16. C. Eaborn, "Organosilicon Compounds." Butterworths, London, 1960

17. D.A. Barrett, V.A. Brown, P.N. Shaw, M.C. Davies, H. Ritchie, P. Ross, *J.Chrom.Sci.*, **34**, **1996**, 146
18. G.E. Berendsen, K.A. Pikaart, L. de Galan, *J.Liq.Chromatogr.*, **3**, (10), **1980**, 1437
19. G.E. Berendsen, K.A. Pikaart, L. de Galan, *J.Liq.Chromatogr.*, **1**, (5), **1978**, 561
20. S.M. Staroverov and A.Y. Fadeev, *J.Chromatogr.* **544**, **1991**, 77
21. A.U. Fadeev and S.M. Staroverov, *J.Chromatogr.*, **447**, **1988**, 103
22. W. Cheng, and M. McCown, *J.Chromatogr.*, **318**, **1985**, 173
23. L.C. Sander, J.B. Callis L.R. Field, *Anal.Chem.*, **55**, **1983**, 1068
24. R.K. Gilpin, and M.E. Gangoda, *J.Chromatogr. Sci.*, **21**, **1985**, 428
25. K. Albert, B. Evers, E. Bayer, *J. Magn. Reson.*, **62**, **1985**, 428
26. E.C. Kelusky and C.A. Fyfe, *J. Am. Chem. Soc.* **108**, **1986**, 1746
27. M.E.Gangoda, R.K.Gilpin, B.N.Fung, *J. Magn. Reson.*, **74**, **1987**, 134
28. G.R. Hays, A.D.H. Clague, R. Huis, G. van der Velden, *Appl. Surf. Sci.*, **10**, **1982**, 247
29. L. Sander, C. Glinka, S. Wise, *Analytical Chemistry*, **62**, **1990**
30. C. Horvath, *High Performance Liquid Chromatography, Advances and Perspectives, Vol. 2*, Academic Press, New York, **1980**, 156
31. J.J. Kirkland, M.A. van Straten, H.A. Claessens, *J.Chromatogr.A.*, **797**, **1998**, 111
32. Proumeliotis and K.K. Unger, *J.Chromatogr.* **149**, **1978**, 211
33. E.N. Slaats, W. Markovski, J. Fekete, H. Poppe, *J.Chromatogr.*, **207**, **1981**, 299
34. R.M. McCormick and B.L. Karger, *Anal.Chem.* **52**; **1980**, 2249

35. J.J. Kirkland, *J.Chromatogr. Sci.*, **7**, 1969, 7
36. E.N. Slaats, W. Markovski, J. Fekete, H. Poppe, *J.Chromatogr.* **149**, 1978, 255
37. A.M. Krstulovic, H. Colin, G. Guiochon, *Analytical Chemistry*, **54**, 1982, 2438
38. G.E. Berendson, P.J. Schonmakers, L. D. Galan, *J.Liq.Chrom.*, **3**, 1980, 1669
39. A. Tchaplá, H. Colin, G. Guiochon, *Anal.Chem.*, **56**, 1984, 621
40. O. Fini, F. Brusa, L. Chiesa, *J.Chromaogr.*, **210**, 1981, 326
41. J.F.K. Huber and R.G. Gerritse, *J.Chromatogr.*, **58**, 1971, 137
42. F. Riedo, and E. Kovats, *J.Chromatogr.*, **239**, 1982, 1
43. C. Horvath, and H.J. Lin., *J.Chromatogr.* **149**, 1978, 43
44. J. de Jong, *J.Chromatogr.*, **322**, 1985, 43
45. P.J. Schoenmakers, *J.Chromatogr.*, **149**, 1978, 519
46. R.P.W. Scott. and P. Kucera, *J.Chromatogr.*, **175**, 1979, 51
47. A.N. Ageev, *Chromatographia*, **14**, 1981, 638
48. I.V.M. Popl and J. Fahrnich, *J.Chromatogr.*, **281**, 1983, 293
49. J.H. Knox, R. Kaliszan, G.J. Kennedy, Faraday Symposium of the Chemical Society, **15**, 1980 113
50. M. Roses, I. Canals, H. Allemann, K. Siigur, E. Bosch, *Anal.Chem.*, **68**, 1996, 4094
51. S.R Bakalyar, *J.Chromatogr.*, **142**, 1977, 353
52. H. Engelhardt, *J.Chromatogr.* **14**, 1981, 227

53. A. Nahum, *J.Chromatogr.* 203, 1981, 53
54. B.L. Karger, J.R. Gant, A. Hartkopf, P.H. Weiner, *J.Chromatogr.* 128, 1976, 65
55. Kazakevich, Y.K, McNair, H.M., *J.Chrom.Sci.*, 31, 1993, 317
56. Knox, J.H., R.Kaliszan, *J.Chromatogr.*, 349, 1985, 211
57. Colin, H.J., J.C. Diez-Masa, G.Guiochon, T.Gzajkivska, and I.Miedziak, *J.Chromaogr.* 167, 1978, 41
58. Wang, H.L., Duda, J.L., Radke, C.J., *J.Colloid and Interface Sci.*, 66 (1), 1978, 153
59. A.Alvares-Zepeda, B.N.Barman, and D.E.Martire, *Anal.Chem.* 64, 1992, 1978
60. Kazakevich, Y.V., and McNair, H.M., *J.Chrom.Sci.*, 33, 1995, 321
61. Scott,R.P.W. and Kucera,P., *J.Chromatogr.*, 125, 1976, 251
62. S. Kitahara, K.Tanaka, T. Sakata, H. Muraishi, *J. of Colloid and Interface Science*, 84, 1981, 519
63. Bereznitski Y., Jaroniec M., Gangoda M.E., *J. Chromatogr.* 828, 1998, 59
64. Jaroniec C.P., Gilpin R.K., Jaroniec M., *J. Phys., Chem. B*, 101, 1997 6861
65. Tani K., and Suzuki Y., *J. Chromatogr.* 515, 1990, 159
66. Guan-Sajons H., Guiochon G., Davis E., Gulakovski K., Smith D.W., *J. Chromatogr. A* 773, 1997, 33
67. Sander L.C., Glinka C.J., Wise S.A., Silanes, Surfaces, and Interfaces, Proceedings, Colorado, 1985, 431
68. K.S.W. Sing, D.H.Everett, R.A.W. Haul, *Pure & Appl. Chem.* 57, 1985, 603
69. Gregg S.J., Sing K.S.W., Adsorption, Surface Area and Porosity, Academic Press, London, 1982
70. E.N. Slaats, J.C. Kraak, W.J.T. Brugman, H.Poppe, *J.Chromatogr.*, 149, 1978, 519

71. Amati D., and Kovats E., *Langmuir*, 3, (5), 1987, 687
72. Y.V.Kazakevich, and R.LoBrutto, *J.Phys.Chem. B*, 104, 2000, 554
73. P.Claudy, J.M.Letoffe,C.Gaget, D.Morel, and J.Serpinet, *J.Chromatogr.*, 329, 1985, 331
74. H.Poppe, *J. Chromatogr. A*, 656, 1993, 19
75. L.C.Sander and S.A.Wise, *CRC Crit. Rev. Anal. Chem.*, 18, 1987, 299
76. J.H.Knox and A.Pyrde, *J.Chromatogr.*, 112, 1975, 171
77. R.P.W.Scott and P.Kucera, *J.Chromatogr.*, 142, 1977, 213
78. D.Westerlund and A.Theodorsen, *J.Chromatogr.*, 144, 1977, 27
79. A.Tilly-Melin, Y.Askemark, K.G.Wahlund and G.Schill, *Anal.Chem.*, 51, 1979, 976
80. F.Koster and G.H.Findenegg, *Chromatographia*, 15, 1982, 743
81. C.S.Koch, F. Koster, G.H.Findenegg, *J.Chromatogr.*, 406, 1987, 257
82. K.Tani, and Y.Suzuki, *J.Chromatogr.Sci.*, 27, 1989, 698
83. F.J.Helfferich, *J.Chem.Educ.*, 41, 1964, 410
84. D.L.Peterson and F.J.Helfferich, *J.Phys.Chem.*, 69, 1965, 1283
85. J.N.Wilson, *J. Amer. Chem. Soc.*, 62, 1940, 1583
86. D.DeVault, *J. Amer. Chem. Soc.*, 65, 1943, 532
87. K.S.Yun,C.Zhu, and J.F.Parcher, *Anal.Chem.* 67, 1995, 613
88. D.H.Everett, *Trans Faraday Soc.*, 60, 1964, 1803

89. Kiselev and Pavlova, 1962
90. E. Kurbanbekov, O. G. Laryonov, K. V. Chmutov, and M.D.Yubilevich, *Zh. Fiz. Khim.*, **43**, 1969, 1630
91. G.Foti, and E.Kovats, *Langmuir*, **5**, 1989, 232
92. D. H. Everett, *Pure Appl. Chem.* **58**, 1986, 967
93. B. V. Kuznetsov and A. K. Y.Mukhammed, *Russian Journal of Physical Chemistry*, **71**, 1997, 1054

Chapter 6

Discontinuous Head-Space Desorption Method for Characterization of Adsorbents

Summary

A headspace-GC (HSGC) method with multiple extractions from a single vial was developed for the measurement of desorption isotherms with any volatile organic component at any reasonable temperature. The geometric parameters of porous silica and chemically modified silica have been determined by this method.

The methodology and instrumentation for the determination of porosity and surface areas of solids at various temperatures are described. This methodology is based on the periodic withdrawal and gas chromatographic analysis of aliquots of vapors from a headspace vial containing the adsorbent spiked with a chemical of interest (adsorbate). The instrumentation is calibrated using the same chemical in a vial without adsorbent.

The desorption isotherm of the adsorbate on mesoporous silica was measured by headspace GC at 363°K up to $p/p_s = 1.00$ and by low temperature nitrogen adsorption at 77°K. On the basis of the desorption isotherms the pore size distribution was calculated by the Barrett, Joyner and Hallender ^[1] method where the pore shape was assumed to be cylindrical. The measurement of the total surface area was performed according to Brunauer-Emmett-Teller (BET) theory ^[2].

The isotherm obtained using benzene as the adsorbate was then used for the determination of the geometrical properties of the mesoporous silica. The surface area, pore volume, and average pore radius were determined to be 325 m²/g, 1.1 mL/g, and 77Å for Prodigy-Si (Phenomenex, Torrance, CA) using benzene with headspace-GC method. The

surface area, pore volume, and average pore radius determined by low temperature nitrogen adsorption were 326 m²/g, 1.2 mL/g, and 75 Å respectively.

In addition to geometrical characterization of surfaces, the methodology and instrumentation proposed provide information about specific interactions between the adsorbate and the surface of the adsorbent or catalyst under study. It also permits the determination of the energies involved in these interactions as well as the evaluation of the competitive sorption of mixtures.

Introduction

Porosity and surface area of porous materials play significant roles in many industrial and academic studies. Adsorption purification of industrial waste or contaminated ground water is largely dependent upon the adsorbent capacity. Many catalytic processes are dependent upon the active surface area of the catalyst and its accessibility. All high performance liquid chromatographic (HPLC) separations are performed on columns packed with highly porous adsorbents, and the pore size, surface area and pore size distribution are among the major parameters defining the chromatographic properties of these materials.

Characterization of adsorbents

Surface Area

The generally accepted method for surface area measurements is by low temperature nitrogen adsorption with interpretation based on the Brunauer, Emmet, Teller (BET) theory

[2].

$$\frac{p/p_s}{n(1-p/p_s)} = \frac{1}{n_m C} + \frac{C-1}{n_m C} p/p_s \quad [6-1]$$

where n is the adsorbate amount, n_m is the adsorbate amount in the completely filled monolayer, C is an energy parameter, and p/p_s is the ratio of the measured adsorbate pressure in the vapor phase to its saturation vapor pressure. The plot of $(p/p_s)/n(1-p/p_s)$ against p/p_s should be a straight line with a slope $s = (C-1)/n_m C$ and intercept $i = 1/n_m C$. Solution of these two simultaneous equations gives n_m and C . The BET plots are usually linear between relative pressures of about 0.05 and 0.3.

The experimental points are usually plotted as amount adsorbed against p/p_s , as shown in Figure 6-1. Figure 6-1 represents a typical type IV isotherm obtained for cylindrical pores. The low pressure region is attributed to monolayer-multilayer adsorption. In monolayer adsorption all the adsorbed molecules are in contact with the surface layer of the adsorbent. At point E, the point of inflection that is also known as the knee of the isotherm is often taken to indicate the stage at which monolayer coverage is complete and multilayer adsorption begins. The shape of the knee depends on the value of C , becoming sharper as the value of C becomes greater. In multilayer adsorption the adsorption space includes more than one layer of molecules and not all adsorbed molecules are in direct contact with the surface layer of the adsorbent.

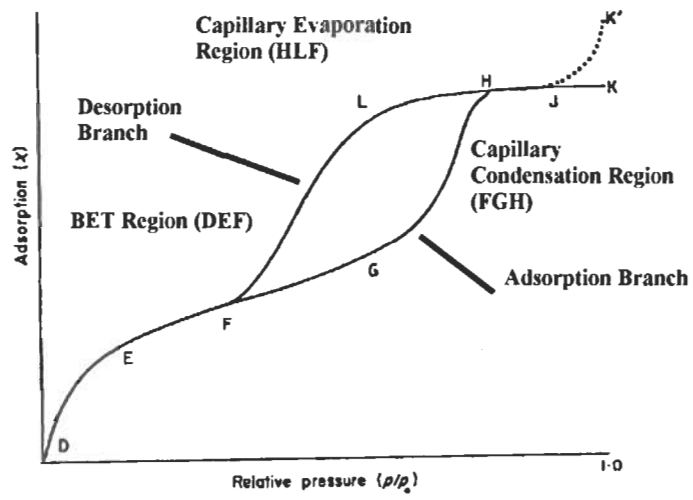


Figure 6-1. Typical type IV adsorption and desorption isotherms^[3]

The amount of adsorbate (in moles) on the monomolecular layer of the surface, n_m may be calculated from the BET equation. The specific adsorbent surface area can be calculated by multiplying this value by the adsorbate molecular area.

$$S = n_m \omega, \quad [6-2]$$

where ω is the area that one mole of adsorbate occupies on the surface.

Some criticisms of the BET model are 1) assume the adsorption sites on the surface to be energetically identical, and 2) only considers the forces between the adsorbent and the adsorbate molecules (vertical interactions) and neglects the forces between an adsorbate molecule and its neighbor in the same layer (horizontal interactions).

The applicability of the BET method using nitrogen adsorption has been the subject of intense discussion during the past 30 years. Several authors have suggested that the molecular cross-sectional area occupied by nitrogen is strongly dependent upon the surface chemistry [4-9]. It has been shown^[4] that the adsorption of nitrogen on silica gel is increased with an increase of silica gel hydration. This is due to the additional interactions of the quadrupoles of nitrogen with the dipoles of the surface hydroxyl groups. Chemical modification of the adsorbent surface by various organic groups decreases both the energy of adsorption interactions and the amount of adsorbed nitrogen [5-6]. This leads to an increase in the “effective” nitrogen molecular area on that surface.

It has been shown that there is a dependence of the nitrogen molecular area, $\omega(N_2)$, and the energy constant C of the BET equation [7-8]. According to Karnaukhov [7], the constant C and the adsorbate molecular area ω varies for different adsorbents at a given pressure for a given analyte. In other words, geometrical characterization of adsorbent

surfaces from sorption/desorption experiments using nitrogen does not generate true values of the surface area because the measurement itself is adsorbent dependent.

Moreover, the surface area accessible to nitrogen may not be representative of the surface area accessible to other molecules. Larger molecules may be excluded from sorption on the surfaces of smaller pores. The effective surface area in this case may differ significantly from that measured with nitrogen.

Capillary Condensation and Capillary Evaporation Region

Capillary condensation is associated with the formation of a hemispherical meniscus if a cylindrical pore model is assumed. The point at which the adsorption branch begins to deviate upward (FGH) of Figure 6-1 represents the capillary condensation region. This process begins in the residual pore space that remains after multilayer adsorption has occurred. As the pressure progressively increases the slope of the branch decreases as it reaches the saturation vapor pressure in the region (HK) of Figure 6-1. In this region, the entire pore system is full of condensate and the pore volume may be obtained.

The reverse process, known as desorption is the amount of adsorptive desorbed from the silica surface. The desorption branch represents the progressive withdrawal of N_2 or other adsorptive. As the pressure progressively decreases the adsorptive starts to evaporate from the pores and this is known as the capillary evaporation region (HLF) of Figure 6-1.

Adsorption hysteresis occurs when the adsorption and desorption curves do not coincide. The values for the adsorbed volumes for the adsorption isotherm lie at higher relative pressures than for the desorption part. This can be explained, since the process of condensation starts from the walls of the pore and evaporation from the ends of the

cylindrical pore. After enough condensate is evaporated and there is no more meniscus within the pores the desorption branch should coincide with the adsorption branch.

Pore volume

The determination of the pore size distribution is based upon the application of the Kelvin equation to capillary condensation region of the desorption isotherms ^[3].

$$\ln\left(\frac{p}{p_s}\right) = -\frac{2\gamma V_L}{RT r_k} \quad [6-3]$$

where γ is the adsorbate surface tension, r_k is the pore radius, V_L is the adsorbate molar volume, p_s is the adsorbate saturation pressure, and p is the adsorbate measured pressure.

The use of adsorbates other than nitrogen offers experimental advantages especially for macro- and meso-porous samples as well as catalysts. The value of $\gamma V_L / RT$ for benzene at 298 K is 2.2 times larger than that for nitrogen at 77 K. This means that benzene starts to condense at lower relative pressures than nitrogen. The adsorption of benzene allows a more precise determination of the pore size distribution ^[10].

Apparently, the characterization of adsorbents would be more complete if conducted with several adsorbates of different dimensions and different functional groups. This work offers a headspace gas chromatographic (HSGC) methodology for the generation of such data with precision equal or better than classical nitrogen sorption measurements.

Headspace techniques for measurement of adsorption/desorption isotherms

A static headspace GC (HS-GC) method is a logical choice for the generation of sorption/desorption data with many volatile chemicals. Its major advantage is that it functions as a partial vapor pressure “gauge” unlike the total vapor pressure measurements used in BET methods. This means that the sorption isotherms of an analyte can be generated in the presence of other volatile components.

Overview of Static Headspace Technique

Several authors have used HS-GC for the generation of adsorption isotherms and the subsequent measurements of surface areas ^[11,12]. This method involves the determination of the difference of adsorbate concentrations in the vapor phase from two vials of equal volume. One vial is filled with only adsorbate and the other is filled with adsorbate equilibrated with a known amount of adsorbent. The amount of adsorbate trapped on the adsorbent surface can then be calculated as the difference between the adsorbate vapor concentrations of these two vials. By measuring samples with differing amounts of adsorbate, one can plot an adsorption isotherm and calculate the surface area using the BET method. This method assumes that oxygen and nitrogen in the vial do not interfere with the adsorbate adsorption on the surface.

This method offers some advantages over classical low temperature nitrogen adsorption: (1) adsorption measurements can be performed at any desirable temperature and are not restricted to 77°K; (2) any compound with measurable vapor pressures can be used; and (3) this technique allows an indirect measurement of the amount of analyte adsorbed on a catalyst or other adsorbents.

This method also has disadvantages. The accurate measurement of the adsorption isotherm requires a large amount of adsorbent because each experimental point requires a separate sample. Vial to vial volume variations may have an effect upon the precision of the measurements. Moreover, desorption measurements cannot be made in this mode.

Overview Headspace-GC with Multiple Adsorbate Extraction (HS-MHE)

The advantage of the HS-GC method using multiple adsorbate extraction for characterization of porous materials is the use of a single vial for the whole span of p/p_s values needed for construction of the isotherm.

In principle, surface areas, pore volumes, and pore size distributions could be evaluated from the desorption branch of the isotherm using BET theory and the theory of capillary condensation^[3].

In order to obtain the experimental points needed for a desorption isotherm of a particular analyte, the pores of the adsorbent must be completely filled with adsorbate. A measured amount of the adsorbate vapor is then sequentially withdrawn from the vial. A dependence of the amount of adsorbate left in the vial and corresponding vapor pressure (p_s) is obtained. This is conducted until all of the experimental points are obtained from $p/p_s=1.0$ to $p/p_s=0.01$ and a plot of the number of moles per gram of adsorbent is plotted vs. p/p_s . This represents a desorption isotherm.

Sequential sampling from the same equilibrated vial is essential for multiple headspace extraction. This means that application of the MHE procedure to a single vial with

known amounts of adsorbent and adsorbate should generate the desorption isotherm. This could then be used to calculate pore volume, pore size distribution, and surface area,

This method has additional advantages. Headspace measurements can be performed at different temperatures, which allows calculation of the energy of adsorption. Since we are using HS-GC, we can measure multicomponent adsorption directly, and can study competitive desorption. It is also possible to rearrange the system to measure adsorption isotherms. Another advantage with this continuous headspace method is that a limited amount of adsorbent and only one sample vial is needed for the entire experiment.

Experimental

Sample preparation

The literature pays special attention to a proper preparation of the adsorbent surface prior to sorption experiments^[3]. Our experiments showed that after 1 hour heating of silica gel at 180 °C under slow nitrogen flow, no significant differences in adsorption values were obtained. Similar observations were made for the silica adsorbents with chemically modified surface after they were heated at 130 °C under slow nitrogen flow for one hour.

After adsorbent preparation, a known volume of an adsorbate was added to the sample vial. This amount must be sufficient to ensure the presence of free liquid phase after equilibration. This establishes the same reference point corresponding to the saturation vapor pressure of the free liquid phase in the vial throughout the whole experiment.

The following procedure was used to ensure a complete filling of the adsorbent pore space with the adsorbate at equilibration. The capped vial with both adsorbent and adsorbate

was heated in a GC oven at a temperature higher than that required for complete evaporation of the loaded adsorbate. After heating, the vial was cooled at 2 °C/min. The measurements showed that the experimental desorption isotherm profiles were repeatable for samples that went through at least three such equilibration cycles.

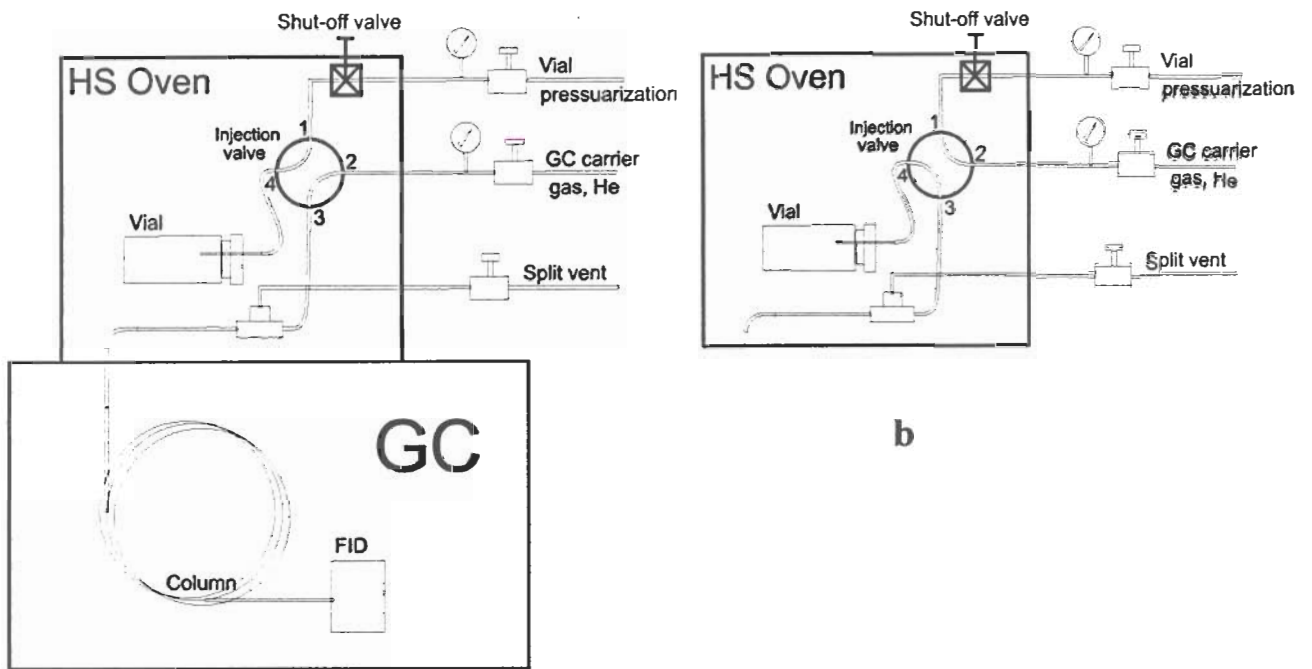
Low temperature nitrogen adsorption (static mode)

Nitrogen adsorption isotherms were measured on an Omnisorp-100CX system (Coulter, Hialeah, FL). Silica adsorbents were prepared by heating at 180 °C under vacuum for 2 hour. Organically modified silica based adsorbents (C-18) were heated at 130 °C under vacuum for 2 hour. All adsorption measurements were performed in the static mode to ensure proper equilibration. All measurements were performed according to the instrument manual, and calculations were made by the computer program included with the instrument^[13].

Headspace Methods

Headspace studies were carried out on HP model 5890 (Hewlett-Packard, Little Falls, DE) gas chromatograph equipped with a modified headspace autosampler (Asist-150HT, Asist Inc., Cleveland, OH).

A general schematic of the system is shown on Figure 6-2. Several modifications have been made to accommodate experimental requirements. The headspace sampler was placed on top of the GC instrument. The standard injection port was used as a transfer line heater for the column (HP-5, 30 m, 0.32mm, 1µm film thickness, Hewlett-Packard, Little Falls, DE) that was connected to the T-connector inside the headspace oven. High precision pressure regulators and flow controllers (Hewlett-Packard, Little Falls, MD) were used for



a

Figure 6-2. GC-Head-space system used for desorption experiments.

6-2a. In the “Load” position sample vial is connected to the pressurization line (ports 1 –4), and carrier gas is directed to the GC column (ports 2-3). Shut-off valve is always closed except the pressurization period at the beginning of the equilibration step (valve in “load” position).

6-2b. Injection valve is shown in the “Inject” position.

both carrier gas and pressurization lines to ensure flow stability and reproducibility of the injected volume in MHE mode. The column flow rate was 1.0 ml/min, the oven temperature was 80 °C, the column head pressure was 7 psi; and the split flow was 115 ml/min for all experiments. A solenoid shut-off valve (Valco, Houston, TX) was installed on the pressurization line to decrease diffusion during equilibration.

Discontinuous Headspace Desorption (DHD) Experiments

A known weight of adsorbent was placed in a vial. The adsorbates used in these experiments were Prodigy-Si, Prodigy-ODS2 from Phenomenex (Torrance, CA), Spherisorb-Si (Phase Separations, Glauppauge, NY), and Kovasil MS-H (C-14)(Uetikon, Lusanne, Switzerland). Adsorbate (benzene or cycloheptane) was loaded into the vials by microsyringe. The vial was capped immediately after adding the adsorbate.

Dynamic experiments were conducted by multiple extraction of vapor aliquots from the headspace vial. The total adsorbate placed in the vial exceeded the sum of the expected pore volume of the adsorbent plus any volume that evaporated inside the vial at the temperature of the experiment. The temperature for complete adsorbate evaporation was estimated using the following ideal gas law equation:

$$T = \frac{P_{s,T}V}{nR} \quad [6-4]$$

where $P_{s,T}$ is the adsorbate saturation pressure at chosen temperature, V is the vial volume, n is the amount of adsorbate added, R is the gas constant.

The sampling needle was inserted into the sample vial and kept there throughout the entire experiment. The three way valve connected the needle either to the pressurization line, or to the GC column. The vial and valve were placed in the same thermostat and kept at 60 °C .

A typical sampling cycle consist of the following steps:

1. Vial pressurization. The vial is pressurized for 3 min at 15 psi, which exceeded the partial vapor pressure of benzene and cycloheptane at the chosen temperature by at least 5 psi. This was necessary to ensure a reproducible injection volume. The pressurization value also exceeded the GC column head pressure (7 psi) to ensure that the sample will actually be transferred into the column.
2. Vial equilibration. The vial was kept under pressure with the pressurization line closed by the solenoid shut-off valve for at least 15 min. It has been shown^[14] that for most adsorbents and adsorbates about 95% of the equilibration values are reached within 10 - 15 min.
3. Injection. Connection of the pressurized and equilibrated vial to the GC column with the column head pressure lower than the vial pressure led to the transfer of some adsorbate from the vial. The injection valve was turned for a fixed time (0.4 sec). The amount of adsorbate transferred was detected as a peak and integrated. The experimental setup can be seen in Figure 6-2.

After each injection the vial was pressurized and equilibrated again. The total amount of adsorbate inside the vial decreased after each injection and the remaining adsorbate redistributed itself between the adsorbent pore volume and the vapor phase.

The number of cycles needed is dependent upon the adsorbate amount, its vapor pressure, injection time and other parameters. For most of our experiments eighty points for benzene and cycloheptane at 60 °C was sufficient to characterize the entire desorption isotherm from $p/p_s = 1$ to $p/p_s = 0.001$.

A typical experimental curve for benzene desorption is shown in Figure 6-3.

Measurement of the desorption isotherm from a single vial.

Placement of an excess of adsorbate at a particular temperature into the vial will cause saturation of the vapor phase at the beginning of the desorption experiment. At saturation conditions the peak areas of several consecutive injections should be the same (as shown in Figure 6-3) until the free liquid phase is exhausted. The decrease of the adsorbate concentration in the gas phase will cause its evaporation from the liquid phase. This will continue until the excess liquid adsorbate is depleted.

When the excess liquid phase is gone, the formation of a meniscus at the entrance of the adsorbent pores begins. This leads to the decrease of the adsorbate partial vapor pressure in the gas phase and consequently a decrease of the corresponding peak area. Sequential withdrawals of adsorbate from the vial will lead to adsorbate desorption from the adsorbent surface, which will be reflected by the adsorbates partial vapor pressure and its corresponding peak area.

Consistent pressurization of the vial to a fixed excess pressure and exact timing of its connection to the GC column allows control of the withdrawn volume of the gas phase. This ensures that the peak areas are representative of the adsorbate partial vapor pressure. The

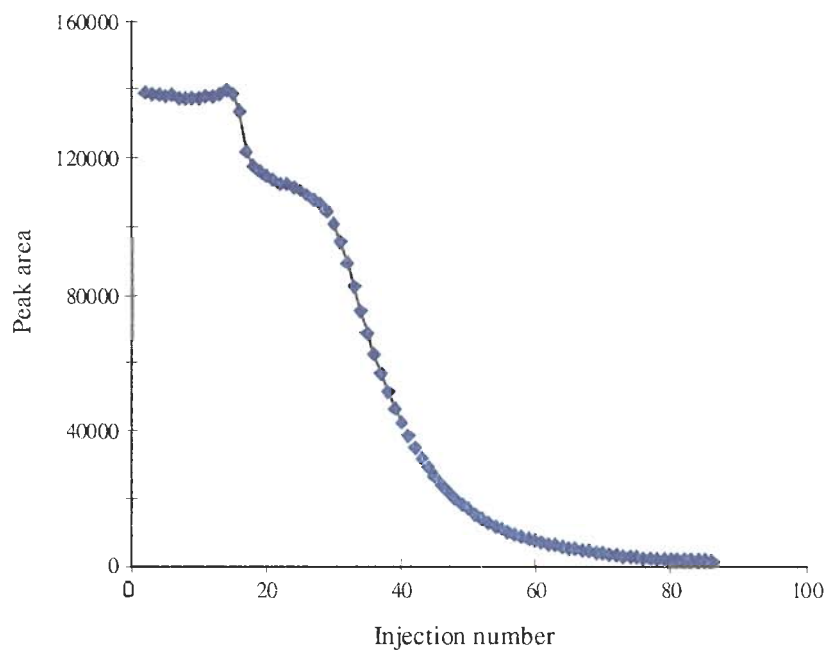


Figure 6-3. Headspace experimental profile for benzene desorption from Spherisorb Silica. Corresponding isotherm shown in Figure 6-5

ratio of peak areas at a certain point to the peak area at saturation conditions represents p/p_s values of the BET equation. The amount of adsorbate left on the adsorbent can be calculated by subtraction of the amount withdrawn at this step from the amount of adsorbate left in the previous step. This requires a calibration of the exact volume of gas phase transferred to the GC at each injection. At a fixed pressure this volume has shown to be stable. The calibration procedure is described below.

System calibration and desorption calculation procedure

The total volume of the HS vial was determined by weighing an empty vial and vial filled with deionized water on an analytical balance. The average vial volume was found to be 24.3 ml with a 1% RSD.

System calibration

It is assumed that during sampling, the withdrawal of the adsorbate does not disturb the established equilibrium within the vial. This assumption is more valid as the sampling time decreases.

The mass balance equation for the first withdrawal can be described as follows:

$$c_0V = c_1V + c_0V_w \quad [6-5]$$

where c_0 is the original concentration of the adsorbate in the vial, V is the vial volume, V_w is the volume withdrawn, and c_1 is the equilibrium concentration established in the vial after the first injection.

The change of adsorbate concentration in the vial during the continuous extraction is proportional to the concentration of the adsorbate left in the vial and can be described by the following differential equation:

$$\frac{dc(t)}{dt} = -kc \quad [6-6]$$

Integration of this equation gives:

$$\ln[c(t)] = -kt + M \quad [6-7]$$

where M is the integration constant .

At $t=0$ the adsorbate concentration within the vial is equal to c_0 , so from [6-7] we can assume that $M=\ln(c_0)$. At $t=1$ (first injection) we can write:

$$\ln(c_1) = -k + \ln(c_0) \quad [6-8]$$

From equation [6-5] we can express c_1 as a function of c_0 , and the withdrawn volume (V_w) and vial volume (V) and by substituting this in equation 8 we obtain:

$$\ln(c_0) + \ln\left(\frac{V - V_w}{V}\right) = -k + \ln(c_0) \quad \Rightarrow \quad k = -\ln\left(1 - \frac{V_w}{V}\right) \quad [6-9]$$

Substituting k and M into equation [6-7] we will get:

$$\ln[c(t)] = t \ln\left(1 - \frac{V_w}{V}\right) + \ln(c_0) \quad [6-10]$$

Since we are using an incremental withdrawal, the variable t is just the consecutive injection number (integer) and can be replaced by i (for convenience). Equation [6-10] could be written in the short final form as:

$$c_i = c_0 \left(1 - \frac{V_w}{V} \right)^i \quad [6-11]$$

Equation [6-10] is linear with respect to the dependence of $\ln(c)$ vs. i (injection number). This dependence allows us to use a simple method for the calibration of the system. A plot of the logarithm of the peak area versus the injection number for sequential withdrawals of adsorbate from the vial should be linear. Its intercept $\ln(C_0)$ represents the starting adsorbate concentration and its slope $\ln(1-V_w/V)$ represents the volume ratio.

This calibration was made using the data of multiple extraction of both benzene and cycloheptane without adsorbent. Vial pressurization, injection time, split ratio and oven temperature were the same. For the calibration experiments the amount of adsorbate loaded into the vial was chosen to ensure a complete evaporation at the HS oven temperature.

The slope of the calibration curve is dependent upon the HS oven temperature, vial pressure, and sampling time. Since we pressurized the vial after each injection up to the same pressure, the volume of the gas phase withdrawn at each injection was constant. The smaller the slope of the calibration curve, the smaller the amount of the adsorbate withdrawn from the vial at each injection.

Experimental calibration curves for benzene and cycloheptane are shown in Figure 6-4, and corresponding slope and intercept values are given in Table 6-1.

Isotherm calculations

Generation of the desorption isotherms from multiple extraction experiments were performed using the following procedure.

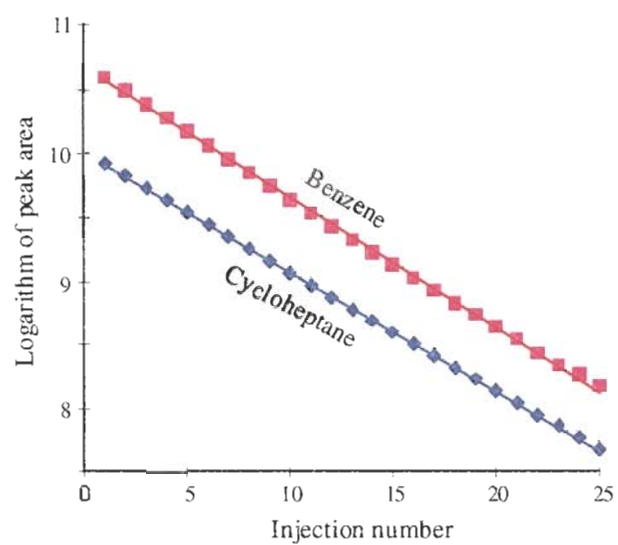


Figure 6-4 System calibration curves for benzene and cycloheptane. Calibration parameters are shown in the Table 6-1.

Table 6-I
Benzene and cycloheptane DHD calibration parameters

Analyte	Starting volume, μl	Slope	Intercept	Response factor, pl/area count	Correlation coefficient
Benzene	20	-0.102	11.196	29.5	0.99999
Cyclohexane	10	-0.090	9.961	41	0.99997

The amount of the adsorbate left in the vial after each DHD step was calculated ($m_i = m_{i-1} - k_{cal}A_i$). Amount of the adsorbate on the surface or condensed inside pores could be calculated as the difference of the total adsorbate amount (expressed in the number of moles) at the given DHD step and adsorbate in vapor phase.

$$n_{ads.} = n_i - \frac{24.3 \cdot P_s}{RT} \frac{P}{P_s} \quad [6-12]$$

where, P_s is the adsorbate saturation pressure; P/P_s is a ratio of the adsorbate partial pressure to its saturation pressure and this value is equal to the ratio of the adsorbate peak area at given DHD step to its peak area at saturation conditions; 24.3 is the vial volume (ml).

The dependence of the amount of the adsorbate adsorbed, $n_{ads.}$ on P/P_s is actually the desorption isotherm of the adsorbate on a given adsorbent (Figure 6-5).

Determination of Pore volume

Total pore volume of the adsorbent could be calculated from the experimental curve, Figure 6-3. The vertical drop of the peak areas starting at injection #17 corresponds to the beginning of the formation of meniscus at the adsorbent pores entrance. This means that all excess adsorbate has been withdrawn from the vial and the only liquid adsorbate left is inside the pore volume. Since $p/p_s=1$ at saturation conditions, than the total amount of adsorbate left after 17 injections can be expressed from [6-12] as:

$$V_{pore} = V_0 - 17 \frac{24.3 P_s MW}{RTd} \quad [6-13]$$

where V_{pore} is the adsorbate volume inside the pore volume, V_0 is the initial adsorbate volume, MW is the adsorbate molecular weight, d is the adsorbate density at temperature T .

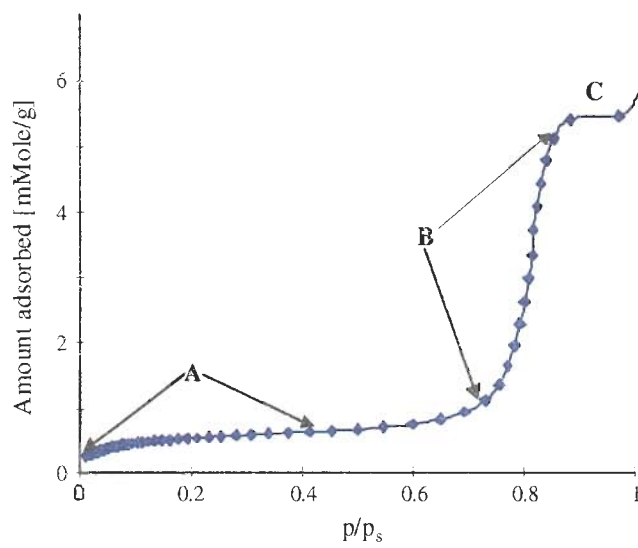


Figure 6-5. Benzene desorption isotherm measured by discontinuous headspace desorption method on Spherisorb silica. A – BET region; B – capillary condensation region; C – complete filling of the pore volume

The pore volume calculated for the Spherisorb-Si was equal to 0.49 ml/g. This value was obtained from the corresponding desorption isotherm (Figure 6-5) using the adsorption value for the horizontal portion (section C of the curve in Fig 6-5) of the isotherm. The calculated value of the pore volume was in a good agreement with that given in the manufacturers catalog, 0.5 ml/g which used low temperature nitrogen adsorption (LTNA) [15].

Pore size distribution calculations

Pore size distributions were calculated from the capillary condensation portion (section B of the curve in Fig 6-5) of the measured isotherms using the Kelvin equation [6-3], and the Barrett Joyner Hallender (BJH) method described by Gregg and Sing [3].

Results and Discussion

The method of discontinuous headspace desorption (DHD) was used to measure the pore volume, pore size distribution and surface area and was compared with classical low temperature nitrogen adsorption (LTNA) on the same adsorbent.

The adsorbent used was Prodigy-Si, which is high purity porous silica gel with an average pore diameter of 150 Å. Fig 6-6a represent DHD benzene desorption isotherm on Prodigy-Si; Figure 6-6b shows the full nitrogen isotherm on the same adsorbent. As it could be seen, the hysteresis loop is closed; adsorption and desorption branches coincide in the low pressure region. Calculation of the adsorbent surface area requires the estimation of the molecular area of the analyte. The generally accepted value for nitrogen is 16.2 Å² and 45 Å² for benzene [3]. The surface area values calculated from DHD with $\omega_{\text{benzene}}=45 \text{ Å}^2$ was 325 m²/g, and from LTNA with $\omega_{\text{N}_2}=16.2 \text{ Å}^2$ was 326 m²/g. These values are in good agreement.

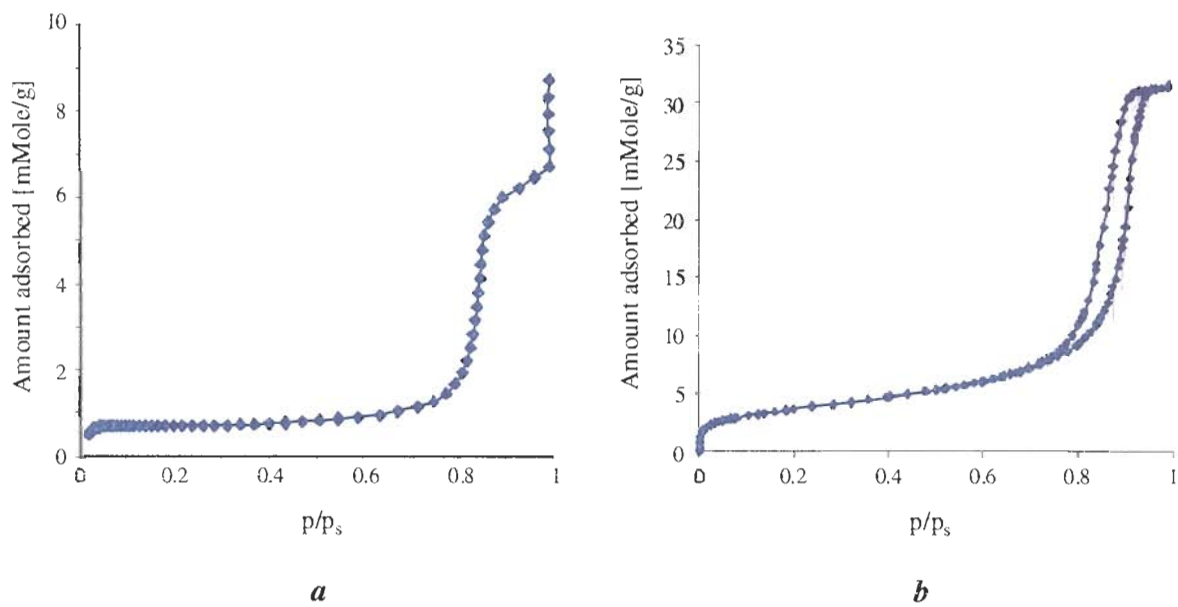


Figure 6-6. Benzene desorption isotherm measured by DHD on Prodigy-Si (a) and full nitrogen sorption isotherm on the same adsorbent (b).

The same porous silica with octadecyl modified surface (Prodigy-ODS2, Phenomenex, Torrance CA) was used for the desorption/adsorption experiments on hydrophobic surfaces. Figure 6-7b represents the full nitrogen isotherm measured with the classical LTNA method.

These measurements led to one unusual phenomenon. The desorption branch of the full isotherm for the C18 modified adsorbent (Figure 6-7b) did not coincide with its adsorption branch in the low pressure region as it did on polar silica surface (Figure 6-6b). This effect had been verified by repeated experiments. Complete calibration of the instrument had been done and the full isotherms measured four times. A good agreement had been obtained for all experiments. A possible explanation for the observed effect is that during the adsorption process some nitrogen molecules had been trapped between the C18 chains and did not desorb during the desorption process. Since the adsorption/desorption experiment is a cumulative one, trapping of some nitrogen molecules may result in the rise of the desorption branch. The calculated distance between both branches could be used for the estimation of the amount of trapped N₂ and the corresponding accessible volume between bonded ligands. It is shown to be a very small volume, 5.6 μl/g, which is about 1.5% of the total volume of C18 modified layer on the adsorbent surface. Possible explanation of the observed effect could be the restricted desorption of a small amount of adsorbed nitrogen molecules which appears to be occluded between the alkyl chains (slow desorption kinetics). This phenomenon needs to be investigated but is beyond the scope of this work.

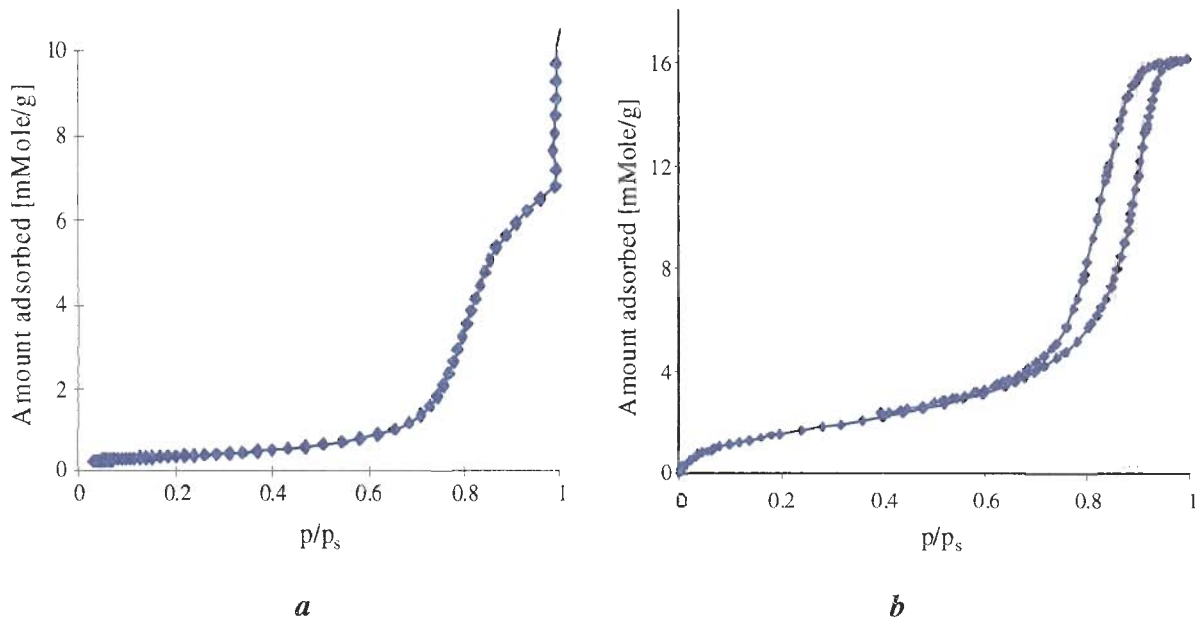


Figure 6-7 Benzene desorption isotherm measured with DHD system (a) and full nitrogen isotherm (b) on Prodigy-ODS2.

Surface area of chemically modified adsorbents

The interpretation of the LTNA data on chemically modified hydrophobic surfaces is not straightforward. It is possible to obtain high surface area values due to the roughness of the surface constructed by the attached organic ligands. Also, several authors [3,7-8] pointed out that the nitrogen molecule has a higher molecular area on a hydrophobic surface due to weaker surface interactions. This will lead to an underestimation of the adsorbent surface area.

Most silica based adsorbents show type IV nitrogen isotherms, which is usually associated with a cylindrical pore shape [3]. A cylindrical pore model allows a simple geometrical description of the pore structure. Chemical modification of the original silica surface leads to a decrease of the average pore size, pore volume and surface area. If the surface modification was made with the highest possible bonding density, then the decrease of the pore radius will correspond to the maximum length of the attached ligands. The pore radius of the original bare silica is denoted by R_0 . For example, a surface modification with octadecyl chains will lead to the decrease of the pore radius by 21 Å (average length of C18 chains in trans conformation). Therefore one CH₂ group occupies approximately 1.2 Å of an alkyl chain length. The following simple expressions could be written for pore volume, and surface area changes in relationship to the number of carbon atoms in the alkyl chain attached to the silica surface.

$$V_{pore} = \pi(R_0 - 1.2n_c)^2 L \quad [6-14]$$

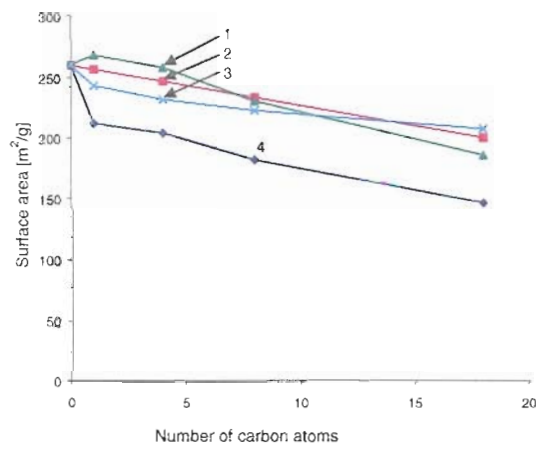
$$S = 2\pi(R_0 - 1.2n_c)L, \quad \Rightarrow \quad \frac{V_{pore}}{S} = \frac{R_0 - 1.2n_c}{2} \quad [6-15]$$

where R_o is an average pore radius of original silica; n_c is the number of carbon atoms of alkyl-modifier chain; L is the hypothetical length of all pores in 1 g of the adsorbent; V_{pore} is the pore volume; S is the surface area.

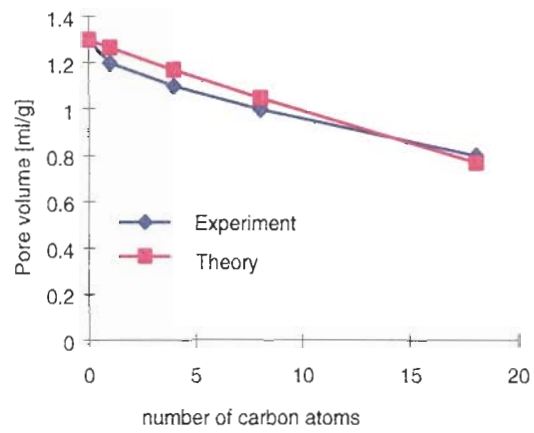
These equations were derived with the assumption of cylindrical pore structure and all-trans conformation for most of the bonded ligands. Pore network, pore size distribution, and bonding density may have a significant effect on the applicability of these equations.

The equations above predict a linear decrease of the surface area with an increase of the chain length of the attached ligands. This decrease has been experimentally observed and was reported in the literature ^[16]. A cylindrical pore model predicts a linear surface area decrease with an increase of the ligand size, but all reported experimental dependencies ^[16-18] show a sharp drop in surface area from bare silica to the modified silica.

The most obvious drop in linear surface area decrease with an increase in ligand size was seen from the LTNA experimental data obtained by Bass and Bratt ^[16] is represented by diamonds in Figure 6-8a. The cylindrical pore model is used for the evaluation of the adsorbents pore size. We applied this model for the estimation of the surface area from the experimentally measured pore volume using equations 6-14 and 6-15. Using this model, the surface areas were calculated from the estimated chain length and the experimental pore volumes determined by Bass and Bratt, shown by crosses in Figure 6-8a. The same dependence of the decrease in surface area with increase in length of the alkyl chains could be calculated from the estimated chain length and the experimental pore diameter values, shown by squares in Figure 6-8a. These two sets of surface area values estimated from the experimental pore volume and pore diameter were in good agreement. Though as one can



a



b

Figure 6-8. Theoretical and experimental ^[16] dependencies of the surface area (a) of chemically modified adsorbents vs. the number of carbon atoms of alkyl chains attached to the silica surface.

(a) 1 - measured surface area values corrected for nitrogen molecular area; 2 – Surface area calculated from cylindrical pore model; 3 – Surface area calculated from measured pore volume data; 4 – Experimental surface area values

(b) Pore volume dependence vs. the number of carbon atoms. (Experimental data taken from the Table II (p.272) of reference ^[16]).

see the surface areas of the modified silica gels calculated from the low temperature nitrogen adsorption do not agree with the surface areas calculated from the experimental pore volume and pore diameter data.

As mentioned before, nitrogen molecules occupy larger molecular areas on hydrophobic surfaces. This means that the formation of the adsorbed monomolecular layer of nitrogen on the hydrophobic surface requires a smaller amount of nitrogen. The use of 16.2 \AA^2 for the nitrogen molecular area in calculating the adsorbent surface area leads to significantly lower surface area values (see Figure 6-8a).

Ratios of the theoretically estimated areas to the measured ones are almost the same for all chain lengths; this suggests that these ratios are equal to the ratio of the actual nitrogen molecular area to the value used (16.2 \AA^2). Correction of the results reported in ^[16] by the suggested area ratio ($20.5/16.2$) lead to an excellent agreement with the two sets of data.

These results are represented by triangles in Figure 6-8a. An estimated value of the nitrogen molecular area (20.5 \AA^2) on a hydrophobic surface correlates well with the 19 - 22 \AA^2 values estimated in the literature ^[3,8].

It is important to note that the pore volume dependence did not experience such a sharp drop and is consistent with the theoretically predicted line (Figure 6-8b). The theoretical values were calculated using the estimated length of the pore, the estimated chain length of the modified silica and the experimentally determined pore size.

Table 6-II**Surface area and pore volume of Prodigy-ODS2**

	DHD (benzene) $\omega = 45 \text{ \AA}^2$	LTNA (N ₂) $\omega = 16.2 \text{ \AA}^2$	LTNA (N ₂) $\omega = 20.5 \text{ \AA}^2$
Surface Area	200 [m ² /g]	159 [m ² /g]	201 [m ² /g]
Pore volume	0.61 [ml/g]	0.64 [ml/g]	0.64 [ml/g]

Comparison of surface area measurements

In our experiments with Prodigy-ODS2 adsorbents, the surface area calculated by the standard program of our LTNA system was also about 25% lower than surface area obtained from DHD experiments. Table 6-2 shows the experimental and corrected surface area and pore volume values. We have to emphasize that pore volume values from both methods are in the good agreement. LTNA surface area values corrected for nitrogen molecular area are also in a good agreement with DHD data (Table 6-2).

Comparison of the pore volume and pore size distribution measurements

The proposed method is best used for pore size distribution measurements. Figures 6-9 and 6-10 represent the comparison of the pore size distribution curves calculated from both the LTNA and DHD experiments on Prodigy silica adsorbent. Pore size distribution profiles obtained by both methods on a polar porous adsorbent (silica gel) had shown a similar distribution. Positions of the maximum on both curves are 77 and 75 Å (radius) correspondingly. The only difference is in the small pore size region, where the DHD method indicates the presence of small pores (see Fig 6-9).

Pores with diameter lower than 20 Å are classified as micropores, and according to Gregg and Sing ^[3] the applicability of the Kelvin equation [6-3] for them is doubtful. There is also a possibility that benzene may show certain anisotropy in such narrow pores, which will have an affect on the meniscus shape and vapor pressure ^[7].

Measurement of the pore size distribution and cumulative pore volume on the same

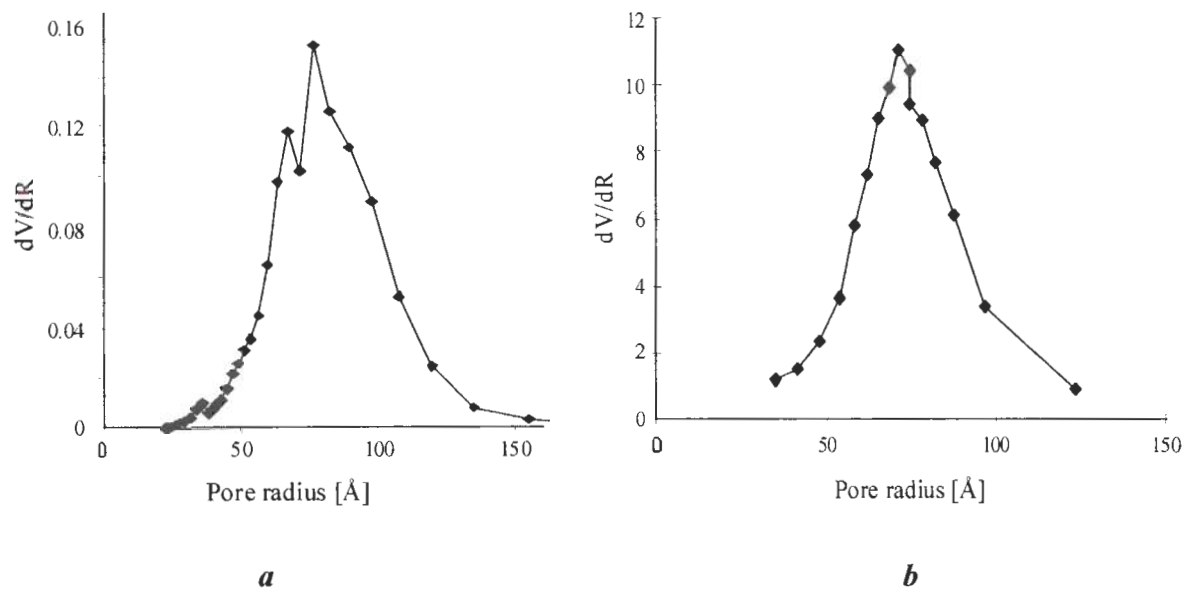


Figure 6-9. Pore size distribution measured with LTNA (a) and DHD (b) methods on Prodigy-Si adsorbent. Nominal average pore size is 150 \AA

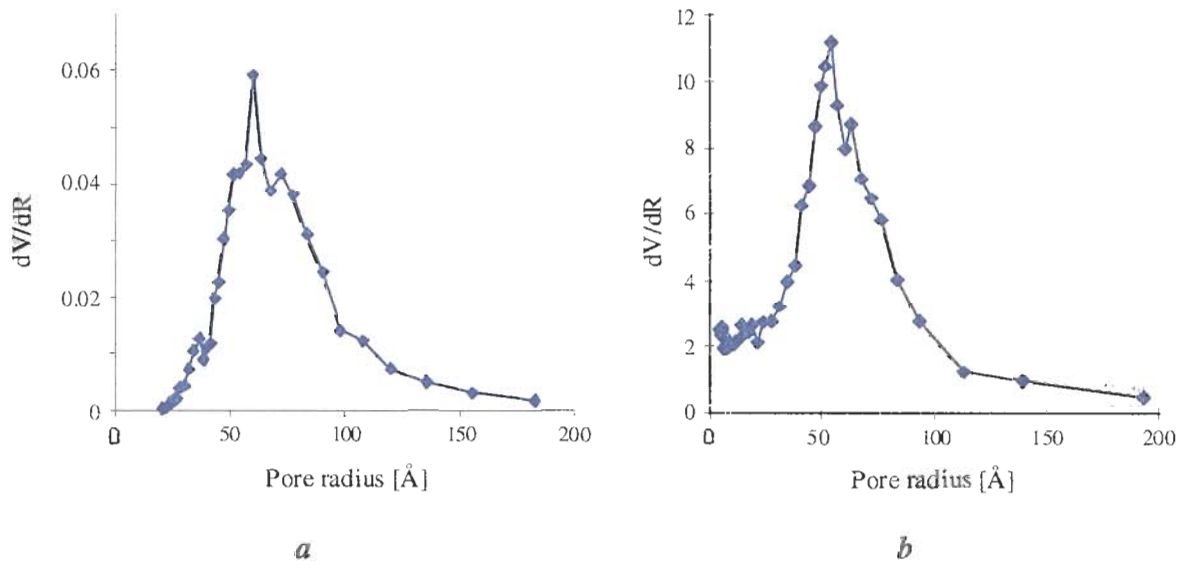


Figure 6-10 Pore size distribution of Prodigy-ODS2 measured with LTNA (a) and DHD (b) methods.

Table 6-III**Pore volume and average pore radius of Prodigy-Si and Prodigy-ODS2 adsorbents measured with LTNA and DHD methods**

	Prodigy- Si		Prodigy-ODS2	
	LTNA (N ₂)	DHD (Benzene)	LTNA (N ₂)	DHD (Benzene)
Pore volume [ml/g]	1.17	1.11	0.64	0.61
Average pore radius [Å]	75	77	60	58

adsorbent with the chemically modified surface (modified with dimethyloctadecylchlorosilane, bonding density $3.35 \mu\text{mole}/\text{m}^2$) has shown significant decrease of both the pore volume and average pore size (see Table 6-III, Figure 6-10).

Maximum of pore size distribution curves were 60 \AA by LTNA and 58 \AA by DHD respectively. Both methods have shown a consistent decrease of the pore size (radius) and pore volume of adsorbent with the alkylsililation of the silica surface.

Surface area of nonporous material

One of the main advantages of the proposed DHD method is the possibility to measure the effective surface area at almost any temperature. Since adsorbate surface interactions are strongly dependent upon the temperature, this has an obvious effect on the adsorbate effective molecular area. The stronger the interactions of the adsorbate molecules with the surface, the less mobility it has along the surface which will lead to a decrease of its effective molecular area.

There are several possible ways to overcome this problem. First is the application of the above mentioned relationships of S , V_{pore} and R (equation 6-15). This has the limitation that the adsorbent has to have a very narrow and symmetrical pore size distribution. Even this however is only an estimate since it does not account for a porous network structure.

Another way is to measure the adsorbate monolayer capacity on nonporous adsorbents with spherical particles and with the same surface chemistry. It is essential that this adsorbent has a very narrow particle size distribution, which will allow for the simple geometrical calculation of its surface area. This type of silica has been introduced by Kovats

^[9] and has been used for the estimation of the nitrogen molecular area. Alkyl-modified nonporous spherical silica particles have an average particle diameter of 1.5 μm and particle size distribution of less than 1%. This narrow distribution allows for a geometrical calculation of its surface area: $S = N \cdot 4\pi R^2$, where N is the total number of particles in 1 g of adsorbent. Density (d) of amorphous silica is 2.4 g/ml, thus $N = \frac{3}{d4\pi R^3}$, or $S = \frac{3}{Rd}$. For particles of 0.75 μm radius this leads to a surface area value of about 1.82 m^2/g . We should mention that chemical modification of this silica adsorbent will not change its surface area significantly. An increase of the particle radius by 2 nm due to the length of attached ligands will increase the particle surface area by less than 0.2%.

Figure 6-11 shows the desorption isotherm of benzene on an alkyl-modified nonporous adsorbent (Kovasil-C14) measured with the DHD method at 60 $^\circ\text{C}$.

The absence of porosity is confirmed by the shape of the isotherm. A drop at p/p_s over 0.99 confirms the absence of any pores less than 2000 Å in diameter. This is most probably capillary condensation in the inter-particle space. The surface area calculated using $\omega_{\text{benzene}} = 45 \text{ Å}^2$ was 3.9 m^2/g , which is two times higher than the geometrically calculated value of 1.82 m^2/g .

This suggests the actual molecular area for benzene is 22 Å^2 , which is too small for its flat orientation on the surface. This does correlate well with the area suggested for vertically stacked benzene molecules (25 Å^2 , p.81 ^[3]). At 60 $^\circ\text{C}$ adsorbate-adsorbate interactions (π - π interactions of benzene molecules) are more significant than its interactions with hydrophobic surface and it may cause stacking of the benzene molecules.

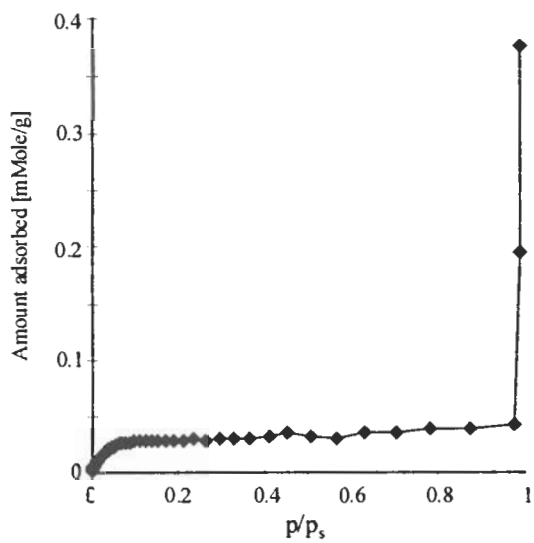


Figure 6-11. Benzene desorption isotherm from spherical nonporous silica particles (particle diameter - 1.5 μm)

On the other hand, the nonporous silica may not necessarily be perfectly spherical and the roughness factor should be taken into account. The less spherical the nonporous silica, the greater is the surface area. Studies with atomic force microscopy and additional headspace studies with temperature variations are being investigated but this is beyond the scope of this article.

Effect of different analytes

The significant advantage of the suggested DHD method that it is possible to measure the desorption isotherm of any volatile compound. This allows the measurement of the adsorbent porosity specific for any analyte with detectable vapor pressure. Some adsorbents or catalysts may show significant porous space accessible to small nitrogen molecules, but the pore space accessible for bigger molecules will be significantly smaller, especially in the presence of bottleneck type pores. This will lead to a decrease in the effective surface area, pore size distribution, and pore volume.

It is important to show that different adsorbates with similar molecular volume generate the same surface area and a very similar pore size distribution. Molecular area for cycloheptane was estimated from the molecular modeling with random-flat orientation of cycloheptane on the surface. Fig 6-12a represents the experimentally determined cycloheptane desorption isotherm from Spherisorb-Si. Figure 6-12b is the corresponding pore size distribution. The corresponding benzene desorption isotherm is shown in Figure 6-5. Geometrical parameters calculated from both adsorbates are given in Table 6-IV and were in good agreement.

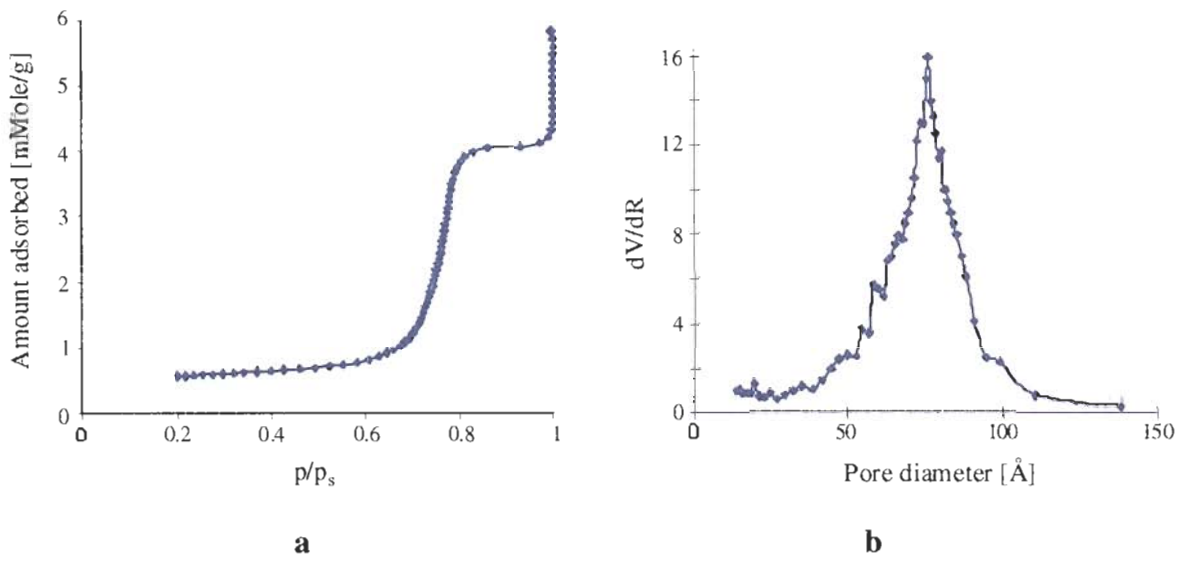


Figure 6-12. Desorption isotherm and pore size distribution of Spherisorb-Si measured by DHD of cycloheptane at 60°C. Surface area, $S = 212 \text{ m}^2/\text{g}$ (BET, $\omega_{\text{cycloheptane}}=95\text{Å}^2$), pore volume = 0.49 ml/g.

Table 6-IV

Surface area and porosity of Spherisorb-Si calculated from DHD experiments with benzene and cycloheptane

	Benzene	Cycloheptane
Pore volume [ml/g]	0.49	0.49
Median pore diameter [Å]	75	77
Surface area [m ² /g]	218	212

Conclusions

The DHD method allows the measurement of the pore volume and pore size distribution of porous materials and the calculation of the adsorbent surface area. This method also offers the possibility to characterize different adsorbents with many adsorbates of specific interest and is not restricted to nitrogen sorption with the LTNA method. Since, the interactions of nitrogen with the surface are normally different than that of the probe adsorbates, a more accurate determination of the geometrical parameters of the adsorbents may be obtained. Moreover, this method allows the measurement of energetic parameters for these interactions by conducting experiments at different temperatures. For certain applications, like the characterization of catalysts, the suggested method may eliminate the greatest uncertainty in BET-based area measurements - the estimation of the adsorbate molecular area. The ability to use any volatile compound allows the direct measurement of the adsorption capacity of porous material. This can be directly calculated from the monolayer capacity using the BET equation.

This unique GC-HS system has been designed for the measurement of desorption isotherms of any volatile adsorbate from adsorbent surfaces. Since, GC detection is used instead of the conventional pressure monitoring technique in LTNA, this method also offers additional advantages. It can be used not only to determine adsorption and desorption isotherms of single adsorbates, but it has the capability to study competitive adsorption and desorption of multiple adsorbates at a range of temperatures. Thus, it is possible to measure the competitive adsorption/desorption of several components from the porous material

presaturated with their mixture and the excess adsorption energies of the competing components than can be calculated.

Literature Cited

Chapter 6

1. Barrett, E.P.; Joyner, L.G.; Halenda, P.H. *J. Amer. Chem. Soc.*, **73**, **1951**, 373
2. Brunauer, S.; Emmet, P.H.; Teller, E. *J. Amer. Chem. Soc.*, **60**, **1938**, 309
3. Gregg, S.J.; Sing, K.S.W. *Adsorption, Surface Area, and Porosity*, Academic Press: NY, **1967**
4. Aristov, B.G.; Kiselev, A.V. *Zh. Fiz. Khim.*, **37**, **1963**, 2520
5. Kiselev, A.V.; Korolev, A.Ya.; Petrova, R.S.; Scherbakova, K.D., *Kolloidn Zh.*, **22**, **1960**, 671
6. Neimark, I.E. *Adsorption and Porosity*, Nauka: Moscow, 1976.
7. Buyanova, N.E.; Zagrafskaya, R.V.; Karnaukhov, A.P.; Shepelina, A.S. *Kinetika I Kataliz*, **24**, **1983**, 983
8. Amati, D.; Kovats, E. *Langmuir*, **3**, **1987**, 687-695
9. Jelinek, L.; Kovats, E. *Langmuir*, **10**, **1994**, 4225.
10. Naomo, H.; Hakuman, M.; Nakai, K. *J. Colloid & Interface Sci.*, **165**, **1994**, 532
11. Kolb, B.; Pospisil, P.; Auer, M. *Ber. Bunsenges. Phys. Chem.* **81**, **1977**, 1067
12. Pausch, J.B. *J. Chromatogr. Sci.* **22**, **1983**, 161
13. Coulter "Omnisorb" manual, Coulter: Hialeah, FL, **1991**
14. Marshall, D.B.; Conolly, D.E.; Flikinger, R.W.; McNew, E.B. *Silanes, Surfaces, and Interfaces*, Proceedings, ed. D.E. Leyden, N.Y. **1985**, p.319

15. Phenomenex Catalog, Phenomenex: Torrance, CA, **1999** p. 395
16. Bass, J.L.; Sands, B.W.; Bratt, P.W. *Silanes, Surfaces and Interfaces*. ed. Leydel D.E., 2, **1986**, 267
17. Bereznitski, Y.; Jaroniec, M.; Kruk, M. *J. Liq. Chrom. & Rel Technol.* **19**, **1996**, 2767
18. Sander, L.C.; Glinka, C.J.; Wise, S.A. *Silanes, Surfaces, and Interfaces*, Proceedings, ed. D.E.Leyden, N.Y. **1985**, 431

Chapter 7

Overall Conclusions

This dissertation has outlined several studies that positively contribute to the growing research effort focused on understanding the selectivity and retention of basic compounds in reversed phase HPLC, and to the expanding research effort focused on understanding the elucidation of the bonded layer structure and the overall retention mechanism.

1. We have determined that the pH of the aqueous eluent is not equivalent to the pH of an aqueous/organic eluent. The addition of the organic eluent changes the pH of the aqueous/organic eluent to higher values since it suppresses the ionization of the acidic pH modifiers. This effect was taken into account when correlating chromatographically and titrimetrically determined pK_a values of the basic analytes.
2. We determined that upon correcting for the pH shift of the aqueous/organic eluent, the chromatographically determined pK_a for some basic compounds still does not correlate to their pK_a values determined by titration. This represented a true pK_a shift. The pK_a shift for the basic analytes has been attributed to actual suppression of their ionization due to a change in the dielectric constant of the eluent and preferential solvation of the basic analyte by the eluent components.
3. Another observation is the increase of the basic analyte retention with the increase of the counteranion concentration of the acidic modifier. Without altering the pH this effect was enhanced by increasing the concentration of the counteranion with the addition of salt.

4. It was demonstrated that the increase in retention was dependent upon the counteranion concentration but not on the pH adjustment of the mobile phase. This was attributed to the solvation equilibria of the ionic species. The protonated (ionic) basic analyte is solvated with water molecules, and thus is relatively more hydrophilic. An increase of the counteranion concentration of the acidic modifier in the mobile phase disrupts the analyte solvation shell due to ion association. For all studied organic bases, a significant increase of the retention was observed with a decrease of mobile phase pH far below the analytes' pK_a 's. Disruption of the analyte solvation results in an increase in the analyte hydrophobicity and its retention.
5. A mathematical model was proposed for the description of the counteranion effect on the analyte solvation. The solvation constants, K , and limiting retention parameters k_s and k_{us} were calculated using the analyte retention dependencies as a function of counteranion concentration. These parameters were determined for more than 20 different basic analytes using conventional reversed-phase columns with two different types of acidic counteranions in a wide concentration range.
6. A method for the pore volume determination under HPLC conditions of reversed phase HPLC adsorbents was proposed. The adsorbent pore volume was determined as the difference of the experimentally determined void volume and the exclusion volume. The void volume of over 20 columns using 3 different experimental techniques was also performed, and the results from the three techniques correlated well. One of the techniques, applied for the determination of the void volume, the minor disturbance method, allowed the determination of the excess adsorption isotherms. The adsorbent

pore volume determined under HPLC conditions correlated well with the pore volume determined under LTNA conditions.

7. The determination of the adsorbent pore volume by LTNA (Low Temperature Nitrogen Adsorption), the exclusion volume by GPC (Gel Permeation Chromatography) and the void volume by the minor disturbance method allowed the calculation of the mass of the adsorbent in the column. The mass determined experimentally and the measured mass that was determined by unpacking and weighing the packing material correlated well. This conformation led to the validity of the three techniques for the determination of the void, pore and exclusion volumes of the studied adsorbents.
8. The determination of the adsorbent pore volume under LTNA conditions led to the determination of the bonded layer volume. Using the bonded layer volume of the particular modified adsorbent and its corresponding bonding density the apparent molecular volume of the bonded alkyl chains was calculated. The experimentally determined molecular volumes for the alkyl chains correlated well with the theoretical molecular volumes obtained from the density of liquid n-alkanes. This positive correlation led to the conclusion that the bonded layer structure on the surface is in its densest conformation and is in a collapsed state. The determination of the LTNA pore volume allowed comparison to the HPLC determined pore volume. Since the HPLC and LTNA pore volumes correlated very well, we stated that the bulk conformation of the bonded layer under HPLC conditions is also in the densest conformation on the surface of the silica. The bulk conformation of the bonded layer exposed in vacuum for the LTNA experiments and to the organic eluent under HPLC conditions is the same.

12. The determination of the geometric parameters of adsorbents by a multiple Headspace-GC method was suggested. Correlation of the surface area, pore volume and pore size distribution measured with the multiple Headspace-GC and with LTNA correlated very well. The advantage of the multiple Headspace-GC technique is that it will permit the measurement of the physical and geometrical characteristics of the HPLC columns, such as the total effective surface area, total pore volume and pore size distribution at any desirable temperature. It allows the ability to study the real thermodynamic adsorption parameters of practically any HPLC system. Also, this proposed method may lead to important breakthroughs in establishing HPLC as a tool for studying molecular surface interactions, which will lead to simplification in targeted development of specific adsorbents for solid phase extraction.